arXiv:0712.2186v4 [astro-ph] 16 Jul 2010

THE AFTERGLOWS OF SWIFT-ERA GAMMA-RAY BURSTS. I. COMPARING PRE-SWIFT AND SWIFT ERA LONG/SOFT (TYPE II) GRB OPTICAL AFTERGLOWS *

D. A. Kann,[1] S. Klose,[1] B. Zhang,[2] D. Malesani,[3] E. Nakar,[4,5] A. Pozanenko,[6] A. C. Wilson,[7] N. R. Butler,[8,9] P. Jakobsson,[10,11] S. Schulze,[1,11] M. Andreev,[12,13] L. A. Antonelli,[14] I. F. Bikmaev,[15] V. Biryukov,[16,17] M. Böttcher,[18] R. A. Burenin,[6] J. M. Castro Cerón,[3,19] A. J. Castro-Tirado,[20] G. Chincarini,[21,22] B. E. Cobb,[23,24] S. Covino,[21] P. D'Avanzo,[22,25] V. D'Elia,[14,26] M. Della Valle,[27,28,29] A. de Ugarte Postigo,[21] Yu. Efimov,[16] P. Ferrero,[1,30] D. Fugazza,[21] J. P. U. Fynbo,[3] M. Gålfalk,[31] F. Grundahl,[32] J. Gorosabel,[20] S. Gupta,[18] S. Guziy,[20] B. Hafizov,[33] J. Hjorth,[3] K. Holhjem,[34,35] M. Ibrahimov,[33] M. Im,[36] G. L. Israel,[14] M. Jelínek,[20] B. L. Jensen,[3] R. Karimov,[33] I. M. Khamitov,[37] Ü. Kiziloğlu,[38] E. Klunko,[39] P. Kubánek,[19] A. S. Kutyrev,[40] P. Laursen,[3] A. J. Levan,[41] F. Mannucci,[42] C. M. Martin,[43] A. Mescheryakov,[6] N. Mirabal,[44] J. P. Norris,[45] J.-E. Ovaldsen,[46] D. Paraficz,[3] E. Pavlenko,[17] S. Piranomonte,[14] A. Rossi,[1] V. Rumyantsev,[17] R. Salinas,[47] A. Sergeev,[12,13] D. Sharapov,[33] J. Sollerman,[3,31] B. Stecklum,[1] L. Stella,[14] G. Tagliaferri,[21] N. R. Tanvir,[48] J. Telting,[33] V. Testa,[14] A. C. Updike,[49] A. Volnova,[50] D. Watson,[3] K. Wiersema,[48,51] D. Xu[3]

ABSTRACT

We have gathered optical photometry data from the literature on a large sample of Swift-era gamma-ray burst (GRB) afterglows including GRBs up to September 2009, for a total of 76 GRBs, and present an additional three pre-Swift GRBs not included in an earlier sample. Furthermore, we publish 840 additional new photometry data points on a total of 42 GRB afterglows, including large data sets for GRBs 050319, 050408, 050802, 050820A, 050922C, 060418, 080413A and 080810. We analyzed the light curves of all GRBs in the sample and derived spectral energy distributions for the sample with the best data quality, allowing us to estimate the host galaxy extinction. We transformed the afterglow light curves into an extinction-corrected $z = 1$ system and compared their luminosities with a sample of pre-Swift afterglows. The results of a former study, which showed that GRB afterglows clustered and exhibited a bimodal distribution in luminosity space, is weakened by the larger sample. We found that the luminosity distribution of the two afterglow samples (Swift-era and pre-Swift) are very similar, and that a subsample for which we were not able to estimate the extinction, which is fainter than the main sample, can be explained by assuming a moderate amount of line-of-sight host extinction. We derived bolometric isotropic energies for all GRBs in our sample, and found only a tentative correlation between the prompt energy release and the optical afterglow luminosity at one day after the GRB in the $z = 1$ system. A comparative study of the optical luminosities of GRB afterglows with echelle spectra (which show a high number of foreground absorbing systems) and those without reveals no indication that the former are statistically significantly more luminous. Furthermore, we propose the existence of an upper ceiling on afterglow luminosities and study the luminosity distribution at early times, which was not accessible before the advent of the Swift satellite. Most GRBs feature afterglows that are dominated by the forward shock from early times on. Finally, we present the first indications of a class of long GRBs which form a bridge between the typical high-luminosity, high-redshift events and nearby low-luminosity events (which are also associated with spectroscopic SNe) in terms of energetics and observed redshift distribution, indicating a continuous distribution overall.

Subject headings: gamma rays: bursts

*BASED IN PART ON OBSERVATIONS OBTAINED WITH THE VERY LARGE TELESCOPE UNDER ESO PROGRAM 075.D-0787, PI TAGLIAFERRI. ALSO BASED PARTLY ON OBSERVATIONS MADE WITH THE ITALIAN TELESCOPIO NAZIONALE GALILEO (TNG) OPERATED ON THE ISLAND OF LA PALMA BY THE FUNDACIÓN GALILEO GALILEI OF THE INAF (ISTITUTO NAZIONALE DI ASTROFISICA) AT THE SPANISH OBSERVATORIO DEL ROQUE DE LOS MUCHACHOS OF THE INSTITUTO DE ASTROFISICA DE CANARIAS UNDER PROGRAM TAC 1238.

[1] Thüringer Landessternwarte Tautenburg, Sternwarte 5, D–07778 Tautenburg, Germany

[2] Department of Physics and Astronomy, University of Nevada, Las Vegas, NV 89154

[3] Dark Cosmology Centre, Niels Bohr Institute, University of Copenhagen, Juliane Maries Vej 30, DK-2100 København Ø, Denmark

[4] Division of Physics, Mathematics, and Astronomy, California Institute of Technology, Pasadena, CA 91125, USA

[5] Raymond and Beverly Sackler School of Physics & Astronomy, Tel Aviv University, Tel Aviv 69978, Israel

[6] Space Research Institute (IKI), 84/32 Profsoyuznaya Str, Moscow 117997, Russia

[7] Department of Astronomy, University of Texas, Austin, TX 78712, USA

[8] Townes Fellow, Space Sciences Laboratory, University of California, Berkeley, CA, 94720-7450, USA

[9] Astronomy Department, University of California, 445 Campbell Hall, Berkeley, CA 94720-3411, USA

[10] Centre for Astrophysics Research, University of Hertfordshire, College Lane, Hatfield, Herts, AL10 9AB, UK

[11] Centre for Astrophysics and Cosmology, Science Institute, University of Iceland, Dunhagi 5, IS 107 Reykjavik, Iceland

[12] Terskol Branch of Institute of Astronomy of RAS, Kabardino-Balkaria Republic 361605 Russian Federation

[13] International Centre of Astronomical and Medico-Ecological Research of NASU, 27 Akademika Zabolotnoho St. 03680 Kyiv, Ukraine

1. INTRODUCTION

The study of the optical afterglows of gamma-ray bursts (GRBs), first discovered over a decade ago (van Paradijs et al. 1997), has taken a great leap forward with the launch of the *Swift* satellite (Gehrels et al. 2004). Its high γ-ray sensitivity and rapid repointing capabilities have ushered in an era of dense early afterglow observations. In the optical regime, one sobering result

is that early afterglows are not as bright as expected, and early optical faintness seems to be the norm rather than the exception (Roming et al. 2006). Furthermore, *Swift*-era optical afterglows are usually observed to have fainter magnitudes than those of the pre-*Swift* era (e.g., Berger et al. 2005a,b; Fiore et al. 2007) (mainly due to even faint afterglows often being discovered thanks to the rapid XRT positions), and also lie at higher redshifts (Jakobsson et al. 2006a; Bagoly et al. 2006), with the most distant up to now at $z = 8.2$ (Tanvir et al. 2009; Salvaterra et al. 2009b). For recent reviews of the impact of *Swift* on GRB research, see Zhang (2007), Mészáros (2006) and Gehrels et al. (2009).

The pre-*Swift* afterglows have been studied extensively, both in terms of their light curve behavior (e.g. Panaitescu & Kumar 2002; Zeh et al. 2006, and references therein), and via their spectral energy distributions (e.g., Stratta et al. 2004; Kann et al. 2006; Starling et al. 2007a), which allow conclusions to be drawn concerning the rest frame line-of-sight extinction and even the dust type in some cases. In our previous study (Kann et al. 2006, henceforth K06), we found that the afterglows that met our selection criteria typically had little line-of-sight extinction, and that the dust properties were best described by Small Magellanic Cloud (SMC) dust, which shows no UV bump and strong FUV extinction (e.g., Pei 1992). These results were confirmed by Starling et al. (2007a), who studied a smaller sample but also incorporated X-ray afterglow data, as well as Schady et al. (2007a, 2010), who also employed joint optical-to-X-ray fits as well as UVOT (and ground-based) data.

Almost six years after the launch of *Swift*, the amount of published data on optical/NIR GRB afterglows have become sufficient to compile a large sample comparable to the pre-*Swift* sample studied by K06, and to determine if some of the afterglows detected by *Swift* are truly fundamentally different to those of the pre-*Swift* era. K06, as well as Liang & Zhang (2006) and Nardini et al. (2006), found a clustering in the optical luminosities after correcting the afterglows for line-of-sight extinction (Galactic and intrinsic) and host contribution, followed by a transformation to a common redshift (such a clustering has also been reported in the host-frame near-infrared bands by Gendre et al. 2008). Therefore, one could speculate that the observationally fainter *Swift* afterglows might be intrinsically fainter too, implying that the clustering of luminosities may be due to a sample selection effect.

Another triumph of *Swift* (and *HETE II*, Villasenor et al. 2005, see Lamb et al. 2004 for more HETE results) was the discovery of optical counterparts to short GRBs (Hjorth et al. 2005b; Fox et al. 2005; Covino et al. 2006a), which, along with X-ray (Gehrels et al. 2005) and radio (Berger et al. 2005c)

[14] INAF, Osservatorio Astronomico di Roma, via Frascati 33, 00040, Monteporzio Catone (RM), Italy
[15] Kazan State University and Academy of Sciences of Tatarstan, Kazan, Russia
[16] Crimean Laboratory of the Sternberg Astronomical Institute, Nauchny, Crimea, 98409, Ukraine
[17] SRI "Crimean Astrophysical Observatory" (CrAO), Nauchny, Crimea, 98409, Ukraine
[18] Astrophysical Institute, Department of Physics and Astronomy, Clippinger 339, Ohio University, Athens, OH 45701, USA
[19] European Space Agency (ESA), European Space Astronomy Centre (ESAC), P.O. Box - Apdo. de correos 78, 28691 Villanueva de la Cañada, Madrid, Spain
[20] Instituto de Astrofísica de Andalucía (IAA-CSIC), Apartado de Correos, 3004, E-18080 Granada, Spain
[21] INAF, Osservatorio Astronomico di Brera, via E. Bianchi 46, 23807 Merate (LC), Italy
[22] Università degli studi di Milano-Bicocca, Dipartimento di Fisica, piazza delle Scienze 3, 20126 Milano, Italy
[23] Department of Astronomy, Yale University, P.O. Box 208101, New Haven, CT 06520, USA
[24] Department of Astronomy, 601 Campbell Hall, University of California, Berkeley, CA 94720–3411
[25] Dipartimento di Fisica e Matematica, Università dell'Insubria, via Valleggio 11, 22100 Como, Italy
[26] ASI-Science Data Centre, Via Galileo Galilei, I-00044 Frascati, Italy
[27] INAF, Osservatorio Astronomico di Capodimonte, Salita Moiariello, 16 80131, Napoli, Italy
[28] European Southern Observatory, Karl Schwarschild Strasse 2, D-85748 Garching bei München, Germany
[29] International Centre for Relativistic Astrophysics Network, Piazzale della Republica 2, Pescara, Abruzzo, Italy
[30] Instituto de Astrofísica de Canarias, C/ Vía Láctea, s/n E38205 - La Laguna (Tenerife). España
[31] Stockholm Observatory, Department of Astronomy, Stockholm University, AlbaNova University Centre, 106 91 Stockholm, Sweden
[32] Department of Physics and Astronomy, University of Aarhus, Ny Munkegade, 8000 Århus C, Denmark
[33] Ulugh Beg Astronomical Institute, Tashkent 700052, Uzbekistan
[34] Nordic Optical Telescope, Apartado 474, Santa Cruz de La Palma, Spain
[35] Argelander-Institut für Astronomie, Universität Bonn, Auf dem Hügel 71, D-53121 Bonn, Germany
[36] Center for the Exploration of the Origin of the Universe (CEOU), Astronomy Program, Dept. of Physics & Astronomy, Seoul National University, 56-1 San, Shillim-dong, Kwanak-gu, Seoul, South Korea
[37] TUBITAK National Observatory, Antalya, Turkey
[38] Middle East Technical University, Ankara, Turkey
[39] Institute of Solar-Terrestrial Physics, Lermontov st., 126a, Irkutsk, 664033 Russia
[40] Observational Cosmology Laboratory, NASA/GSFC, 8800 Greenbelt Rd, Greenbelt, MD 20771-2400, USA
[41] Department of Physics, University of Warwick, Coventry, CV4 7AL, UK
[42] INAF, Osservatorio Astrofisico di Arcetri, largo E. Fermi 5, I-50125 Firenze, Italy
[43] Loyola College, 4501 N. Charles Street, Baltimore, MD 21210, USA
[44] Ramón y Cajal Fellow; Dpto. de Física Atómica, Molecular y Nuclear, Universidad Complutense de Madrid, Spain
[45] Department of Physics and Astronomy, University of Denver, Denver, CO 80208, USA
[46] Institute of Theoretical Astrophysics, University of Oslo, P. O. Box 1029 Blindern, N-0315 Oslo, Norway
[47] Grupo de Astronomía, Facultad de Ciencias Físicas y Matemáticas, Universidad de Concepción, Concepción, Chile
[48] Department of Physics and Astronomy, University of Leicester, University Road, Leicester LE1 7RH, United Kingdom
[49] Department of Physics and Astronomy, Clemson University 118 Kinard Laboratory, Clemson, SC 29634, USA
[50] Sternberg Astronomical Institute, Moscow State University, Universitetsky pr., 13, Moscow 119992, Russia
[51] Astronomical Institute "Anton Pannekoek", University of Amsterdam, Kruislaan 403, 1098 SJ Amsterdam, The Netherlands

afterglows, have placed these GRBs into a cosmological context too, via accurate localization and host galaxy spectroscopy. Further observations, though, have blurred the "classical" short/hard vs. long/soft GRB dichotomy (Kouveliotou et al. 1993; Ford et al. 1995). The first was the discovery of GRBs with light curves consisting of short, hard spikes followed by extended soft emission components which led to $T_{90} \approx 100$ s, such as in the case of GRB 050724, which is unambiguously associated with an early-type galaxy (Barthelmy et al. 2005a; Berger et al. 2005c; Grupe et al. 2006b; Gorosabel et al. 2006; Malesani et al. 2007d). Further complications arose with the discovery of the temporally long, nearby events GRB 060505 and GRB 060614, which lacked SN emission down to very deep levels (Fynbo et al. 2006b; Della Valle et al. 2006b; Gal-Yam et al. 2006; Ofek et al. 2007). The absence of SN emission is a hallmark of short GRBs[1] (e.g., Hjorth et al. 2005a; Fox et al. 2005; Ferrero et al. 2007b), which are thought to derive from the merger of compact objects such as neutron stars and black holes (Blinnikov et al. 1984a,b; Paczyński 1986; Goodman 1986; Eichler et al. 1989). Long GRBs, on the other hand, have been conclusively linked to the explosions of massive stars (Galama et al. 1998; Hjorth et al. 2003; Stanek et al. 2003; Malesani et al. 2004; Pian et al. 2006; Chornock et al. 2010; Starling et al. 2010), showing a photometric SN signature in case the redshift was $z \lesssim 0.7$ and deep searches were carried out (Zeh et al. 2004). The existence of temporally long events which otherwise show signatures of "short" GRBs (e.g., beginning with short, spiky emission and having negligible spectral lag, Norris & Bonnell 2006) led Zhang et al. (2007a, see also Zhang 2006; Gehrels et al. 2006) to introduce an alternative definition. GRBs that have compact-object mergers as progenitors[2] (independent of their duration) are labeled Type I GRBs, while those with massive star progenitors (including X-Ray flashes, XRFs) are Type II GRBs. While this nomenclature has its disadvantages[3], we will adopt it in the following.

In this study, we compile a large amount of optical/NIR photometric data on *Swift*-era Type II GRB afterglows (detected by *Swift*, *INTEGRAL*, *HETE II*, *Fermi* and the *IPN*). We create three samples (see § 2

for details). The "Golden Sample" (§ 2.2.2) follows the quality criteria given in K06. The "Silver Sample" (§ 2.2.3) consists of GRB afterglows with good light curve coverage, but where certain assumptions have to be made to create the SED. The "Bronze Sample" (§ 2.2.4) comprises GRBs with good light curve coverage but where we are not able to derive an SED. For these afterglows, we assume no dust extinction, thus deriving a lower limit on the afterglow luminosity only. Furthermore, we compile the prompt emission parameters of all bursts (including the K06 GRBs) and derive the cosmological corrections and bolometric isotropic energies (§ 2.3). We then undertake a comparison of the GRB afterglows of the pre-*Swift* and the *Swift* era (§ 3). A comparison of the complete Type II GRB afterglow sample with the afterglows of Type I GRBs is presented in a companion paper (Kann et al. 2008, henceforth Paper II). There, we also detail the criteria for separating GRBs into the Type I and Type II samples. The GRBs presented in this paper are those that do not show any indication of being a Type I event, more specifically, following Fig. 8 of Zhang et al. (2009), all GRBs presented in this paper are either classified as Type II GRBs or Type II GRB candidates. This is especially true for the two highest redshift events, GRB 080913 (Greiner et al. 2009b) and GRB 090423 (Tanvir et al. 2009; Salvaterra et al. 2009b), which are intrinsically of short-duration, but are very probably due to collapsars both from their observational properties (Zhang et al. 2009) as well as the basic observability of high-z events with current detectors (Belczynski et al. 2010).

In our calculations we assume a flat universe with a matter density $\Omega_M = 0.27$, a cosmological constant $\Omega_\Lambda = 0.73$, and a Hubble constant $H_0 = 71$ km s^{-1} Mpc^{-1} (Spergel et al. 2003). Errors are given at the 1σ, and upper limits at the 3σ level for a parameter of interest.

2. DATA COLLECTION AND ANALYSIS METHODS
2.1. *Additional photometric observations*

In addition to collecting all available data from the literature, we present further photometric observations of GRB afterglows included in our samples in this paper, many of them published here for the first time, with the rest being revised from preliminary values originally published in the GCN Circulars[4]. Some are identical to GCN magnitudes reported earlier, when these have been deemed to be the final values.

In Appendix A, we present information on observations as well as a table (Table 1) containing 840 data points of 42 GRBs contained in our samples (including the last two pre-*Swift* GRBs of the K06 sample, GRBs 040924 and GRB 041006). Observations have been reduced and analyzed with standard procedures under IRAF[5] and MIDAS[6], magnitudes being derived by aperature and PSF photometry against calibrator stars. See Appendix A for more details on specific calibrators and special analysis techniques in some cases.

---

[1] GRB 060614 and GRB 060505 are discussed in detail in Kann et al. (2008). Still, we wish to point out here that alternative explanations tying these GRBs to the deaths of massive stars have been proposed (Fynbo et al. 2006b; Della Valle et al. 2006b; Gal-Yam et al. 2006; Thöne et al. 2008a; McBreen et al. 2008), with negligible radioactivity-driven emission being either due to fallback black holes (Fryer et al. 2006, 2007) or low energy deposition when the jet penetrates the star (Nomoto et al. 2007; Tominaga et al. 2007). At this time, the available observational information points to GRB 060614, despite its long duration, not being associated with the death of a young, massive star (Gehrels et al. 2006; Zhang et al. 2007a, 2009), while GRB 060505 is, both through analysis of its environment (Thöne et al. 2008a) and due to non-negligible spectral lag (McBreen et al. 2008).

[2] To be more general, those that are not associated with the core collapse of young, massive stars.

[3] Not only does it need multiple observational aspects, which are often not accessible, to associate a GRB with one type or the other (Zhang et al. 2009), but it also links the greater part of all detected GRBs through rather diverse properties (duration and/or spectral lag, for example) to the small sample of events where clear distinctions can be made, such as GRB 050724 (not associated with massive star formation) and GRB 030329 (associated directly with the explosion of a massive star).

[4] http://gcn.gsfc.nasa.gov/gcn3_archive.html

[5] http://iraf.noao.edu/ IRAF is distributed by the National Optical Astronomy Observatories, which are operated by the Association of Universities for Research in Astronomy, Inc., under cooperative agreement with the National Science Foundation.

[6] http://www.eso.org/sci/data-processing/software/esomidas/

2.2. *The Samples*

Further to our own photometry, we compiled optical/NIR afterglow data from public sources (all references can be found in the Appendices) on a total of 79 GRBs with redshifts (three of them photometric, all others spectroscopic) and good light curve coverage (extending to about 1 day in the observer frame if the GRB were at $z = 1$, with a few exceptions) from the *Swift* era (from the end of 2004 to September 2009), a few of which have been localized by missions other than *Swift*, such as *HETE II*, *INTEGRAL*, the *Third Interplanetary Network* (*IPN*) and most recently *Fermi*. This is to be compared with a total of 251 Type II GRB afterglows in the *Swift*-era as of the end of September 2009, of these, 146 have redshifts (122 spectroscopic, 6 photometric, 18 host galaxy-derived)[7]. All the remaining GRBs did not have redshifts and/or sufficient light curve coverage to be included in the sample. Depending on the data quality, we sort the 79 GRB afterglows into three different samples (with one further split temporally). All afterglow data are corrected for Galactic extinction using the maps of Schlegel et al. (1998).

2.2.1. *The pre-*Swift *era "Golden Sample" – An update*

This sample comprises three GRBs. These were all included in the complete sample of K06, but not in their Golden Sample due to the SEDs not conforming to the sample selection criteria. Additional data (GRB 990510) and more diligent analysis (GRB 011211, GRB 030323) have led us to include them in the pre-*Swift* Golden Sample. See Appendix B.1 for more details.

2.2.2. *The* Swift-*era "Golden Sample"*

This sample comprises 48 GRBs. These GRBs fulfill the criteria of the Golden Sample of K06 and are thus directly comparable[8]. The criteria are (K06):

1. The 1σ error in β ($\Delta\beta$) and the 1σ error in $A_{\rm V}$ ($\Delta A_{\rm V}$) should both be ≤ 0.5.

2. $A_{\rm V} + \Delta A_{\rm V} \geq 0$.

3. We do not consider GRBs where all fits (MW, LMC, and SMC) find $A_{\rm V} < 0$, even if the previous criterium is fulfilled[9].

4. $\beta > 0$ (although we do not reject cases with $\beta - \Delta\beta \leq 0$).

5. A known redshift (derived from absorption line spectroscopy in most cases, with some GRBs having redshifts from host galaxy spectroscopy (e.g., XRF 050416A, GRB 061126), and some being photometric redshifts (e.g., GRB 050801, GRB 080916C).

[7] http://www.mpe.mpg.de/∼jcg/grbgen.html
[8] Note that in our case, the derived extinction is always model-dependent, see, e.g., Watson et al. (2006) for a discussion on model-dependent and model-independent extinction estimations.
[9] Such negative extinction is usually found when scatter in the SED results in data points in the blue region being too bright, or an overbright data point creating a "2175 Å emission bump". In such cases, the fitting program determines that the best fit is then "emissive dust" which creates an upward curvature, $A_{\rm V} < 0$ and $\beta > \beta_0$.

Details on the GRB afterglows can be found in Appendix B.2.

2.2.3. *The* Swift-*era "Silver Sample"*

This sample comprises 14 GRBs. These GRBs have well-detected multi-color afterglow light curves but the derived SEDs do not conform to the quality standards of the "Golden Sample". Certain reasonable assumptions are made to derive β and thus $A_{\rm V}$ using the theoretical relations derived from the fireball model (e.g., Zhang & Mészáros 2004). We treated different cases individually, the assumptions are listed for each GRB in Appendix B.3. In some cases, β is derived from the measured pre-break afterglow decay slope α, in other cases, we us the X-ray spectral slope β_X as given on the XRT repository webpage (Evans et al. 2007, 2009), with the assumed optical spectral slope being either $\beta = \beta_X$ or $\beta = \beta_X - 0.5$. Further details on the GRB afterglows can be found in Appendix B.3, see there especially for the case of GRB 071025. Note that all GRBs presented in K06 which were not included in their Golden Sample (an additional 11 GRBs, their Table 1) fit these "Silver Sample" selection criteria (three of these 11 GRBs are now presented in this work and have been added to the pre-*Swift* "Golden Sample").

2.2.4. *The* Swift-*era "Bronze Sample"*

The sample selection criteria used to define the Golden and Silver Samples includes a significant selection bias against dust obscured systems (Fynbo et al. 2009). In limiting ourselves to afterglows that have good multi-color observations (which is usually only the case for observationally bright afterglows), we may be missing out a population of fainter afterglows that would increase the spread of luminosities, in principle possibly bringing Type II GRB afterglows closer to those of Type I GRBs (Paper II). Reducing this selection bias is a complicated task, though. As detailed in Paper II, we expect no significant rest frame dust extinction along the line of sight to Type I GRB afterglows, and only a small spread in redshift, ranging (for now) from $z = 0.1$ to roughly $z = 1$. Both assumptions are invalid for Type II GRBs, which have been detected up to $z = 8.2$ (Tanvir et al. 2009; Salvaterra et al. 2009b), and can be strongly extinguished by dust in their host galaxies (e.g., GRB 051022: Rol et al. 2007; Castro-Tirado et al. 2007; Nakagawa et al. 2006, GRB 060923A: Tanvir et al. 2008a, GRB 061222A, GRB 070521: Perley et al. 2009d, GRB 070306: Jaunsen et al. 2008, GRB 080607: Prochaska et al. 2009 and GRB 090417B: Holland et al. 2010). An unknown redshift can have a strong influence on the magnitude shift (denoted dRc, see § 2.3), that is applied when transforming an afterglow from its observed redshift to a common redshift of $z = 1$. An unknown rest frame extinction can only make the afterglow more luminous if it were corrected for[10]. Therefore we create a third Type II GRB afterglow sample which we denote the "Bronze Sample". The selection criteria are the following: Firstly, the GRB must have a well-constrained redshift. In all

[10] Note that an unknown redshift also implies an additional uncertainty in the host galaxy extinction, but this effect will usually be minor compared to the pure distance effect.

selected GRBs, this is a spectroscopic redshift, but we would not exclude GRBs with well-constrained photometric redshifts. We will not use GRBs that only have pseudo-redshifts (Pélangeon et al. 2006). The knowledge of the redshift removes the strongest uncertainty in the luminosity derivation. Secondly, the redshift must be $z \leq 4$, to keep the R_C band (which is usually the band with the best measurements) unaffected by host galaxy Lyman α absorption or intergalactic Lyman α blanketing. Thirdly, the GRB must have sufficient afterglow data in the R_C band (in some cases, we create composite light curves by shifting other colors to the R_C zero point if sufficient overlap exists) to allow at least a confident extrapolation of the light curve to 0.5 rest frame days after the corresponding burst, where we determine the optical luminosity (§ 2.3). This final criterion removes many GRBs that only have very early detections published, usually *Swift* UVOT observations. In total, we find 14 additional GRBs that fulfill these selection criteria. Clearly a selection bias against very faint afterglows still applies, but if one sets the sample selection threshold even lower (e.g., including also optically dark GRBs with no afterglow detection and no redshift), hardly any useful information can be gleaned. Furthermore, an analysis of all *Swift* afterglow upper limits in the optical/NIR bands is beyond the scope of this paper.

In Appendix B.4, we list the GRBs of the "Bronze Sample". We took data from the references given, constructed the afterglow light curve, and shifted it to a common redshift of $z = 1$ assuming, identical to the Type I GRB sample (Paper II), a spectral index in the optical/NIR bands of $\beta = 0.6$ and a host galaxy extinction of $A_V = 0$ (a single exception is GRB 060605, where an extrapolation of the X-ray slope finds that the optical slope must be identical, and also that the R_C band is unaffected by Lyman α absorption, Ferrero et al. 2009). A value of $\beta = 0.6$ was found to be the mean value for pre-*Swift* afterglows (see, e.g., K06), and we find a similar value for the *Swift*-era Golden Sample (§ 3.2). Most likely, in many cases, these afterglows suffer from host frame extinction as well, even if it is likely to be only a small amount (K06 found a mean extinction of $A_V = 0.2$ in their sample, see also § 3.2), so the derived luminosities are lower limits only. If the host extinction were known, and we would correct for it, the afterglows would always become more luminous. Therefore, the mean absolute magnitude of this sample is a lower limit only.

2.3. *Methods*

With knowledge of the redshift z, the extinction-corrected spectral slope β and the host galaxy rest frame extinction A_V, we can use the method described in K06 to shift all afterglows to a common redshift of $z = 1$, corrected for extinction along the line of sight. The dRc values of the "Silver" (Appendix B.3) and "Bronze" (Appendix B.4) samples are only estimations and lower limits, respectively. After shifting, we derive for all afterglows the apparent magnitude at one day after the GRB (0.5 days in the source frame). In addition, for those GRBs where the light curves extend far enough, we also derive the magnitude at four days. Furthermore, we derive the magnitude in all possible cases at 10^{-3} days (43 seconds in the source frame) to compare the luminosity distribution at very early times. Such an analysis was

not possible in the pre-*Swift* era, as only a few GRBs were detected at such early times.

Our unique sample of afterglow luminosities allows us to look for correlations between the prompt emission and the optical afterglow parameters (see also Paper II). To achieve a comparison with the energies of the GRBs, we compiled the fluences and Band function (or cutoff power law) parameters for all afterglows in K06 and in this paper (Table 2). We denote the low-energy and high-energy power-law indices of the Band function with α_B and β_B respectively, to prevent them from being confused with the afterglow decay slopes $\alpha_{1,2}$ and the optical/NIR spectral index β. Using the given spectral parameters and the redshifts, we derive cosmological corrections for the rest-frame bolometric bandpass from 0.1 to 10000 keV following the method of Bloom et al. (2001). Using the correction, the fluences and the luminosity distances, we then derive the bolometric isotropic energy $E_{\rm iso,bol}$ for all GRBs. Note that if no high energy index β_B is given, we used a cutoff power law instead of a Band function. In the cases of X-Ray flashes (XRFs, no α_B given), we assumed $\alpha_B = -1 \pm 0.3$. As only a small part of the spectral range lies beneath the peak energy in these cases, the choice of the value does not strongly influence the correction. For GRB 000301C, the Band function parameters could not be determined from Konus-Wind data (V. Pal'shin, priv. comm.), and we used mean values (Preece et al. 2000). In rare cases (e.g., GRB 050408) the errors of the correction were not constrained due to missing errors on the input data, and we assumed conservative errors.

3. RESULTS AND DISCUSSION

The energetics, including the bolometric isotropic energies, for the complete sample (including the 19 GRBs from K06) can be found in Table 2. The results of our SED fits with a Milky Way (MW), Large Magellanic Cloud (LMC) and Small Magellanic Cloud (SMC) extinction curve (Pei 1992) are given in Table 3 for the Golden Sample. For the Silver Sample, approximative results can be found in the individual GRB descriptions in Appendix B.3. Apparent and absolute magnitudes at 1 and 4 days after the GRB can be found in Table 5. The magnitudes of a selected sample of GRBs with early observations and/or well-defined peaks in the afterglow evolution can be found in Table 6.

3.1. *Observed Light Curves of* Swift-*era GRB Afterglows*

In Fig. 1 we show, analogous to Fig. 7 in K06, the observed light curves of afterglows of *Swift*-era GRBs (after correcting for Galactic extinction and also host galaxy contribution, if the latter is possible), in comparison with the Golden Sample of K06. The most immediate result is that the rapid and precise localization capabilities of *Swift*, as well as the proliferation of rapid-slewing autonomous robotic telescopes, have strongly increased the number of afterglows that are detected at early times, typically starting within the first minutes after the GRB trigger. A strong spread in early magnitudes is also evident. Only a few GRBs of the *Swift* era are observationally as bright as the brightest pre-*Swift* afterglows. At early times, the prompt optical flash of the "naked-eye" GRB 080319B (Racusin et al. 2008; Bloom et al. 2009;
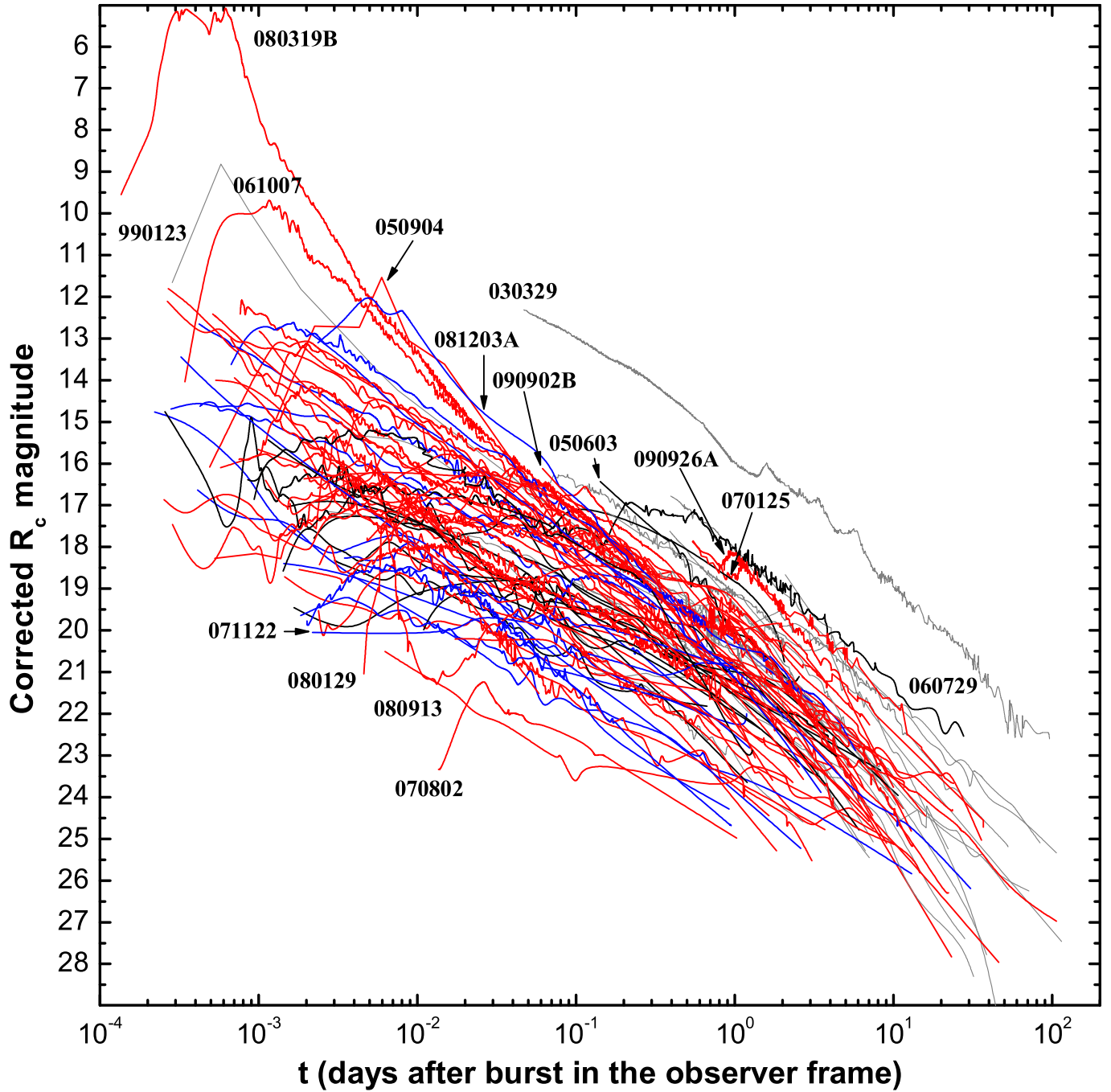
FIG. 1.— The afterglows of Type II GRBs in the observer frame. All data have been corrected for Galactic extinction (Schlegel et al. 1998) and, where possible, the contribution of the host galaxy has been subtracted. Thin gray lines are Type II GRBs from the pre-*Swift* era, taken from K06 (three further GRBs are presented in this paper but are added to the pre-*Swift* sample). Thick red lines are the *Swift*-era Golden Sample. The Silver Sample is blue, and the Bronze Sample is black. The large number of early afterglow detections is evident. Clearly, there are several afterglows that are significantly fainter than the pre-*Swift* sample. At late times, the non-breaking afterglow of GRB 060729 (Grupe et al. 2007a) is brighter than any other except for GRB 030329. At very early times, the prompt flash of the "naked-eye" GRB 080319B (Racusin et al. 2008; Woźniak et al. 2009; Beskin et al. 2009) reaches four magnitudes brighter than the previous record-holder, GRB 990123. GRB 061007 comes close to the magnitude of the optical flash of GRB 990123, making it the third-brightest afterglow ever detected. At late times, the afterglow of the nearby GRB 030329 still remains brighter than any other afterglow discovered since.

Woźniak et al. 2009; Beskin et al. 2009) lies several magnitudes above all other afterglows. Otherwise, only the afterglow of GRB 061007 is comparable[11] to the opti-

cal flash of GRB 990123 (Akerlof et al. 1999). Several

which is included in our sample), had an early afterglow light curve (Jelínek et al. 2006b) which is almost identical in magnitude and evolution to the afterglow of GRB 061007. It was very close to the Sun at trigger time and could not be observed spectroscopically, therefore, it is not included in our sample.
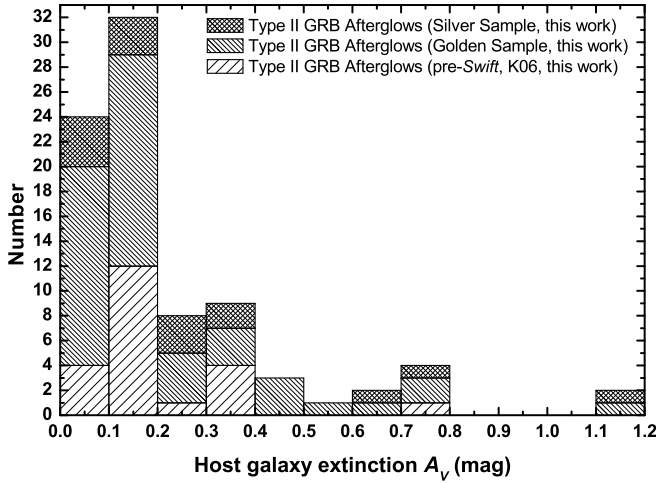
[11] We note that GRB 060117, the burst with the second highest peak photon flux in the complete *Swift* sample (after GRB 090424,

FIG. 2.— Distribution of the derived host galaxy visual extinction A_V in the source frame for the bursts of the Golden Sample of K06 (plus three additional ones presented in this paper) and the values derived in this work (Golden Sample, Table 3 and Silver Sample, Appendix B.3), updating Fig. 2 in K06. In contrast to the sample presented in K06, we find two bursts with $A_V \geq 0.8$, GRB 070802 with $A_V = 1.18 \pm 0.19$ and GRB 060210 with $A_V = 1.18 \pm 0.10$, the latter case being unsure, though. Most bursts have $A_V \leq 0.2$, just as in the pre-*Swift* sample.

FIG. 3.— Derived host galaxy visual extinction A_V in the source frame for the Golden Sample of K06 bursts (grey circles, plus three additional pre-*Swift* GRBs presented here) and the values derived for the GRBs in this work (Golden Sample, Table 3, red stars, and Silver Sample, Appendix B.3, blue diamonds) plotted as a function of the redshift z. A trend of lower extinctions toward higher redshifts is visible but only weakly supported (Kendall's $\tau = -0.34$, Spearman's $\rho = -0.42$). It is unclear if this is due to a selection effect (highly extinct bursts at high redshift are too faint to yield good data and are thus not included in our sample) or to the evolution of dust properties or quantities. Note that for most Silver Sample GRBs, the errors of the derived extinction are underestimated due to parameter fixing in the fitting process. Several exceptional GRBs are indicated.

further early afterglows reach magnitude ≈ 12. At later times, beyond 0.1 days, the afterglows of GRB 050603, GRB 090926A, GRB 070125 and, at very late times, GRB 060729, are among the brightest observed, the latter due to a long plateau phase and a slow, unbreaking decline (Grupe et al. 2007a). At early times, the faintest afterglows are GRB 071122 (which has a long plateau phase, Cenko et al. 2009b), GRB 080129 (which was undetected down to 23rd magnitude in the beginning before rising to a huge optical flare, Greiner et al. 2009a), GRB 080913 (at very high redshift, assuming a fully transparent universe, Greiner et al. 2009b) and GRB 070802 (which exhibited a late rise and a highly extinguished afterglow, Krühler et al. 2008; Elíasdóttir et al. 2009). After 0.1 days, several further afterglows (GRB 050401, XRF 050416A, GRB 060927, GRB 070419A, GRB 050502A) are considerably fainter than the faintest afterglow in the pre-*Swift* sample, GRB 040924 (K06). This confirms the early reports about the faintness of the afterglows of *Swift* GRBs (Berger et al. 2005a,b; Zheng et al. 2009a).

3.2. *Results from SED Fitting – Low Host Extinctions at High Redshifts*

SMC dust is preferred for most GRBs in our Golden Sample, which strengthens the results of K06. Clear exceptions are GRB 060124 (which features a small 2175 Å bump, Kann et al., in preparation) and GRB 070802 (Krühler et al. 2008; Elíasdóttir et al. 2009, see Appendix B.2 for details), and several other GRBs are better fit, though not with high statistical significance, with LMC or MW dust (see Appendix B.2 for more details on each event). In several cases, especially for MW dust, the fitting process finds unphysical "negative extinction" which we interpret as strong evidence that the corresponding dust extinction curve is ruled out. We find a total of 17 GRBs for which the preference for SMC
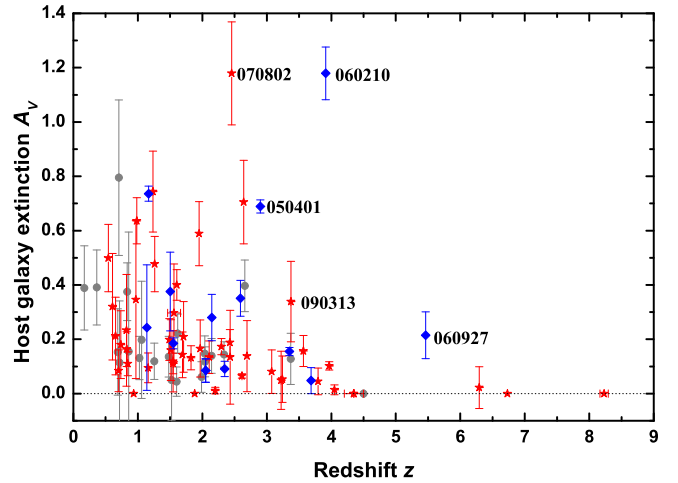
dust is strong, whereas the preference for SMC dust is weak for a further 17 events (cf. K06, which discuss in more detail the dependence of dust model preference on redshift and dust amount). For a total of six afterglows, we find no evidence at all for dust and use the spectral slope without extinction correction (in further cases, the amount of dust is negligible within errors), most of these events (four out of six) lie at high redshift, $z > 4$ (see below). We find a total of seven GRBs with $A_V > 0.5$ within 1σ errors, two of these, GRB 070802 with $A_V = 1.18 \pm 0.19$ and GRB 060210 with $A_V = 1.18 \pm 0.10$ (see Appendix B.3 for caveats on this event, though), lie significantly above the highest value in K06, that of GRB 991208 ($A_V = 0.80 \pm 0.29$). The further GRBs are GRB 050408 ($A_V = 0.74 \pm 0.15$), XRF 071010A ($A_V = 0.64 \pm 0.09$), and GRB 080210 ($A_V = 0.71 \pm 0.15$, though the data are sparse on this event) in the Golden Sample, and GRB 050401 ($A_V = 0.69 \pm 0.02$) and GRB 070208 ($A_V = 0.74 \pm 0.03$) in the Silver Sample, note here that the errors are underestimated due to the spectral slope in the fit not being a variable. Furthermore, evidence for high extinction of an uncommon type is found for GRB 071025, we use the value derived in the work of Perley et al. (2010). Otherwise, all afterglows show very low extinction (Fig. 2). The mean extinction value for the 48 GRB afterglows of the Golden Sample is $\overline{A_V} = 0.21 \pm 0.03$ (FWHM 0.24), identical to the pre-*Swift* sample value of $\overline{A_V} = 0.20 \pm 0.04$ (K06, with the additional three GRBs presented here). Similarly, the mean value for the extinction-corrected spectral slope, $\overline{\beta} = 0.66 \pm 0.04$ (FWHM 0.25), is also in decent agreement within errors with the value from K06, $\overline{\beta} = 0.54 \pm 0.05$. The reason for the larger value in this sample (offset by

1.9σ, which is not yet statistically relevant) is not obvious, though. A possible explanation may be that a higher number of *Swift* GRB afterglows have SEDs which include NIR data, which, being less affected by extinction, allow less flexibility and perhaps overestimation of the extinction. To test this conjecture, we create a subsample of the Golden Sample which contains only SEDs which fulfill the following criteria: 1.) They include NIR data ($YJHK$ as well as *Spitzer* data). 2.) The best fit included a dust model (i.e., no straight power-law fits). 3.) There are at least four SED data points left after removing the NIR points to assure a free fit is possible. A total of 32 afterglow SEDs fulfill these criteria. For the original sample, we find $\overline{\beta} = 0.69 \pm 0.04$ (FWHM 0.24), in full agreement with the complete Golden Sample (48 SEDs). Removing all the NIR data and refitting, we find that more than half the fits are not physically reasonable any more (mostly due to $\beta < 0$), and it is $\overline{\beta} = 0.02 \pm 0.39$ (FWHM 2.19 due to some strong outliers). Generally, this indicates that our conjecture is correct, and points out the need for NIR data to achieve good SED results.

For the Silver Sample, we find a strong preference for SMC dust in some cases (e.g., GRB 051109A and GRB 051111), but even for SMC dust, these fits are still not good and formally rejected. Such strongly curved SEDs were also found for some pre-*Swift* GRB afterglows (e.g., GRB 971214, K06). A free fit to such an SED results in very high extinction and a negative spectral slope β. We find a mean host extinction which is slightly higher than that of both our Golden Samples ($\overline{A_{\rm V}} = 0.32 \pm 0.08$), but we caution that the derived extinctions depend upon fixed spectral index values derived from theoretical relations only.

One big difference between the *Swift*-era sample and the sample of K06 is that there was only one burst (GRB 000131, Andersen et al. 2000) in the pre-*Swift* sample which had $z \geq 3$ (as GRB 030323 [Vreeswijk et al. 2004] has only been included in the pre-*Swift* sample in this work), while in the present Golden Sample, 27% (13 out of 48) of the GRBs lie at such high redshifts (an additional 36%, five out of 14, in the Silver Sample). Like GRB 000131, almost all these high-z GRBs show very small host extinction (Fig. 3). This seems to confirm the initial suspicion in K06 that host extinction declines with higher redshift. Exceptions are GRB 060210 (see above, and Cenko et al. 2009b), GRB 071025 (see Perley et al. 2010), GRB 090313 with a moderate extinction of $A_{\rm V} = 0.34 \pm 0.15$, and possibly GRB 060927, but the result here is unsure. Also, GRB 050401, at $z \approx 3$, clearly shows signs of moderate line-of-sight reddening (see Watson et al. 2006). To check the significance of this possible result, we use two rank correlation tests, Kendall's τ and Spearman's ρ, on the combined Golden Sample bursts of this work and K06. We find $\tau = -0.34$ and $\rho = -0.42$, both results indicate that while there is a (negative, as expected) correlation, it is only weakly significant at best. To estimate the influence of the errors, we do the same tests on the maximum ($A_{\rm V} + \Delta A_{\rm V}$) and minimum possible ($A_{\rm V} - \Delta A_{\rm V}$) values. We find $\tau = -0.14 \cdots - 0.39$ and $\rho = -0.25 \cdots - 0.52$ (with the minimum extinction yielding the lowest rank correlation coefficient, and vice versa). Furthermore, a Kolmogorov-Smirnov (KS) test on two samples (taken from the Golden Samples only), divided by $z < 2$ and $z > 2$, shows that they are likely to be taken from the same distribution ($P = 0.039$). While this low-extinction result might be expected from several evolutionary factors, such as the metallicity evolution of the universe (Lapi et al. 2008; Li 2008, and references therein), different dust depletion patterns at high redshift (see Savaglio 2006, for an overview) or the lack of dust-producing AGB stars (Fiore et al. 2007; Stratta et al. 2007a), we caution that several biases might be involved (as already discussed in K06, see also Fiore et al. 2007) and the evidence is thus not conclusive at all. A higher redshift implies what we see in the optical (and measure with a spectrograph) lies further and further into the rest frame ultraviolet, which is much more affected by dust (especially if it is similar to SMC dust, which is usually found). Therefore, unless rapidly observed, highly extinct high redshift afterglows are much more likely to not be observed successfully spectroscopically, thus excluding them from our sample.

3.3. *Rest-frame Light Curves of* Swift*-era GRB Afterglows*

3.3.1. *On the Rest-Frame Clustering and Redshift-Dependent Bimodality of the Afterglow Distribution in the* Swift*-Era*

It was independently found by three groups (K06; Liang & Zhang 2006; Nardini et al. 2006) studying pre-*Swift* afterglows that the magnitude distribution becomes tighter (clusters) compared to the observed distribution if the afterglows are corrected for host-frame extinction and transformed to a common redshift ($z = 1$ was used). Closer study revealed that this clustering was best described by two populations (a bimodality) which were separated in redshift. Nearby afterglows were, in the mean, less luminous than more distant ones (K06).

In Fig. 4 we show (analogous to figure 8 in K06) the light curves of all optical afterglows shifted to $z = 1$ (for the method, see K06, their Appendix A). The additional 76 afterglows of the *Swift*-era samples seem to confirm the clustering of intrinsic afterglow luminosities. Only three afterglows, those of XRF 050416A, XRF 060512 and GRB 070419A, are fainter than the one of GRB 040924 at one day, but the difference is only large for XRF 050416A, ≈ 1.3 magnitudes. Also, note that XRF 060512 is from the Bronze Sample and thus the luminosity is probably higher, and the low redshift, derived from a galaxy spatially coincident with the optical afterglow, is in dispute, the GRB may be a background event (Oates et al. 2009). Furthermore, also only three afterglows exceed the previously brightest one, GRB 021004, these being GRB 090313, GRB 090926A and especially GRB 080129, which is 0.7 magnitudes brighter. We point out that this was an extremely peculiar afterglow which exhibited a long plateau phase and multiple rebrightenings (Greiner et al. 2009a), and something similar was seen for GRB 090926A (Cenko et al. 2010b; Rau et al. 2010). In K06, a bimodality in the afterglow luminosities was found after dividing the samples into two redshift bins, with $z = 1.4$ as a dividing line. The new afterglows further bolster this finding, with the faintest afterglows at early times (GRB 060729, GRB 060904B, GRB 071122) and at later times (XRF 050416A, XRF
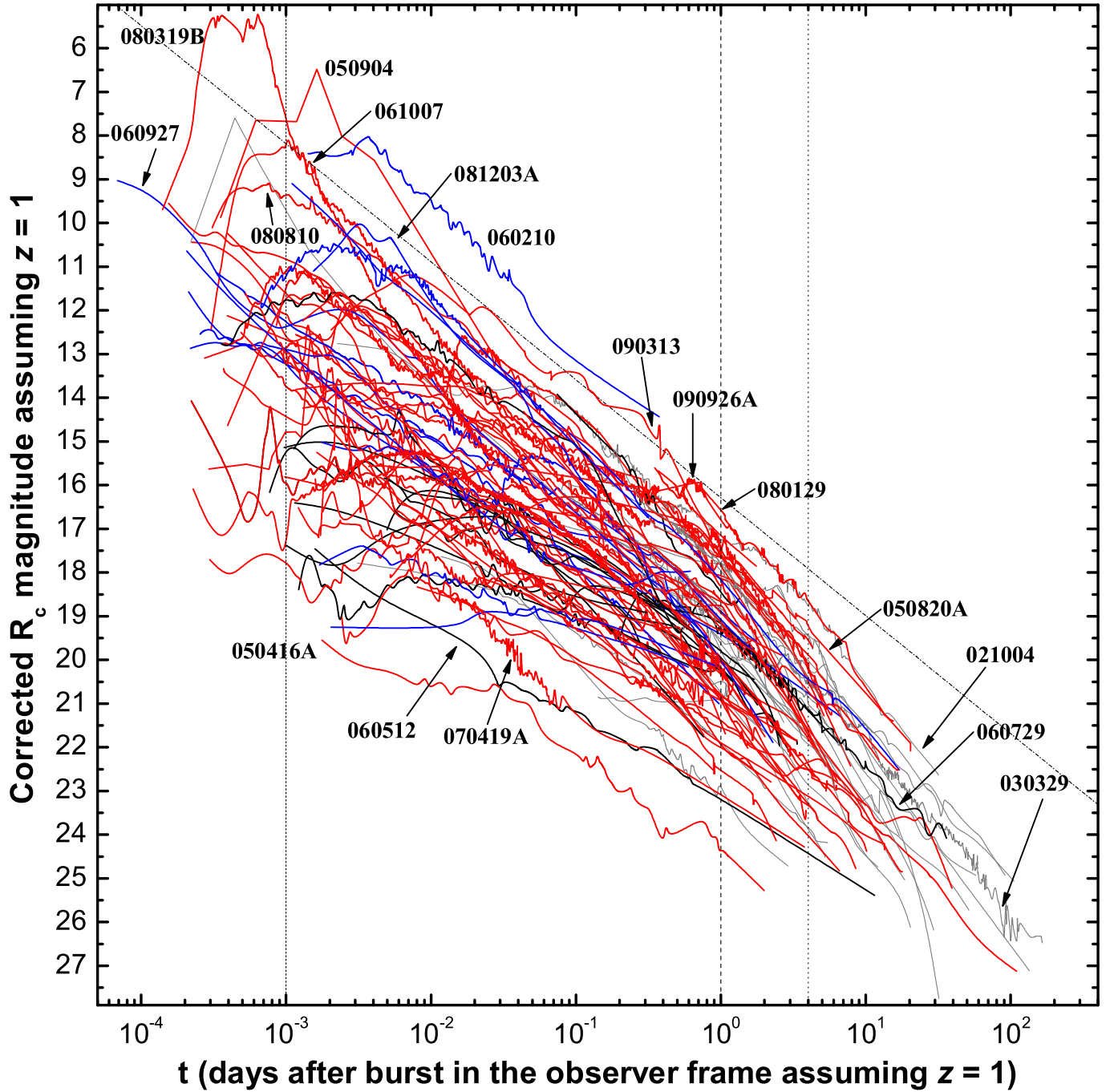
Fig. 4.— The afterglows of Type II GRBs in the observer frame after transforming them to a common redshift of $z = 1$. The labeling is identical to Fig. 1. Note that the Bronze Sample afterglows are lower limits only, as no dust extinction correction could be applied. The vertical lines denote 10^{-3}, 1 and 4 days, times at which the luminosities were determined. All additional *Swift*-era afterglows fit into the tight clustering reported by K06, Liang & Zhang (2006) and Nardini et al. (2006). The width of the distribution expands slightly, with XRF 050416A, XRF 060512 and GRB 070419A being fainter than the faintest afterglow of the pre-*Swift* era, GRB 040924. Note that XRF 060512 is in the Bronze Sample, its luminosity may be underestimated. At very early times, a large spread is visible, as well as several cases of strong variability beyond a simple decay. The brightest bursts at early times are (as in the observer frame) GRBs 080319B, 050904, 061007 and 060210 (the latter an unsure case, the extinction may be overestimated), and several more GRBs (060927, 080413A, 080810, 080721 and 081203A) exceed tenth magnitude. The dot-dashed, slanted line ($\alpha \approx 1$) indicates what may be an upper ceiling for the afterglow luminosity at later times (§ 3.3.3). Similar to the afterglow of GRB 030329 (K06), the afterglow of GRB 060729 is now seen to be of average luminosity at one day, and quite subluminous at early times. Exceptional afterglows, both at the bright and at the faint ends of the distribution, are indicated.

060512, GRB 070419A) all lying at $z \lesssim 1$. A quantitative analysis leads us to be cautious about this result, though. While we find that the total spread of pre-*Swift* afterglows is indeed reduced (7 to 5.7 magnitudes for

those detected at one day), the FWHM of the two samples is identical, though (1.51 vs. 1.54 mags). For the *Swift* era sample, we even find that both the spread (6.9 vs. 7.8 mags) as well as the FWHM (1.48 vs. 1.63 mags)
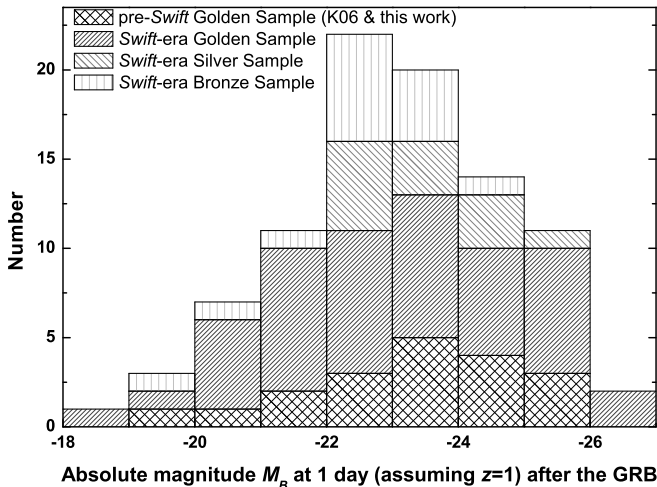
FIG. 5.— The absolute magnitudes of Type II GRB afterglows at one day after the burst assuming $z = 1$. The *Swift*-era Type II GRB afterglows in the Golden Sample analyzed in this paper (mean magnitude $\overline{M_B} = -23.02 \pm 0.27$, FWHM 1.82 mags) are very similar to those of the K06 (plus three additional GRBs presented in this work) sample (mean magnitude $\overline{M_B} = -23.44 \pm 0.36$, FWHM 1.59 mags). The Silver Sample afterglows are identical in luminosity with the pre-*Swift* sample (mean magnitude $\overline{M_B} = -23.69 \pm 0.32$, FWHM 1.11 mags). The Bronze Sample afterglows represent the least luminous afterglows (mean magnitude $\overline{M_B} = -22.53 \pm 0.34$, FWHM 1.25 mags), and the assumption of a small amount of rest frame extinction makes them as bright as the Golden Sample afterglows.

actually *increases*. Only for a complete sample of all afterglows, the range is still reduced (8.9 vs. 7.8 mags) while the FWHM is similar (1.56 vs. 1.61 mags). The effect of the reduced spread is mostly due to a single afterglow, that of the very nearby GRB 030329, whereas the increase in spread in the *Swift*-era data is due to the very faint afterglow of XRF 050416A.

While *Swift* has clearly allowed us to detect afterglows that are observationally fainter (we find $\overline{R_C} = 20.08 \pm 0.36$ for the pre-*Swift* GRBs, and $\overline{R_C} = 21.30 \pm 0.18$ for the *Swift*-era GRBs), are these afterglows also less luminous? In Fig. 5 we show the distribution of afterglow magnitudes measured in the host frame at one day after the GRB assuming a common redshift of $z = 1$ (Table 5). Evidence for the bimodality is not directly evident. Indeed, several recent works (Melandri et al. 2008; Cenko et al. 2009b; Oates et al. 2009), working on small, homogeneous samples derived from single instruments, do not report finding a bimodality. As a whole, the clearer bimodality of the pre-*Swift* sample has disappeared (if one does not do the redshift separation), though see Nardini et al. (2008b). Indeed, while the magnitude distribution is not fit very well with a unimodal distribution (both Gaussian or Lorentzian distributions yield χ^2/d.o.f. > 2 for both the *Swift*-era data set as well as the complete data set [see below]), we were also unable to find a bimodal distribution which significantly improved the fit. We thus, working on a larger sample, find agreement with above-mentioned works (Melandri et al. 2008; Cenko et al. 2009b; Oates et al. 2009), in contrast to the clear bimodality seen by Nardini et al. (2008b).

It is also evident that our four samples are not significantly different from each other. K06 found a mean absolute magnitude of $\overline{M_B} = -23.3 \pm 0.4$ for their Golden Sample, to which we now add three further GRBs (for a total of 19, as three events do not have data at one day), and find $\overline{M_B} = -23.44 \pm 0.36$ (FWHM 1.59 mags). This value is almost identical to our new Golden Sample (a total of 46 GRBs, two not having data at one day), where we find $\overline{M_B} = -23.02 \pm 0.27$ (FWHM 1.82 mags). A KS test shows that both data sets are consistent with being drawn from the same distribution ($P = 0.78$). The Silver Sample (14 GRBs, two do not have data at one day) is slightly more luminous on average, with $\overline{M_B} = -23.69 \pm 0.32$ (FWHM 1.11 mags), whereas the Bronze Sample (14 GRBs) is slightly less luminous on average, with $\overline{M_B} = -22.53 \pm 0.33$ (FWHM 1.25 mags), respectively. The difference is not statistically significant, though, a KS test shows that they are taken from the same distribution as the *Swift*-era Golden Sample ($P = 0.15$ and $P = 0.43$ for the Silver and Bronze Samples, respectively). Furthermore, as no extinction correction has been applied to the Bronze Sample, its mean absolute magnitude is a lower limit only (§ 2.2.4). Assuming $A_V = 0.3$ for all afterglows of this sample, a value just slightly above the mean extinction of the Golden Samples (§ 3.2), we find a mean magnitude $\overline{M_B} = -23.45 \pm 0.38$ (FWHM 1.42 mag), identical with to the Golden Samples of both papers. Therefore, a small amount of host extinction is sufficient to explain the slightly fainter mean magnitude. This is also confirmed by the recent analysis of Schady et al. (2010), who derive A_V values for eight of our Bronze Sample GRB afterglows, and find $A_V \approx 0.3$ or even (significantly) higher for seven of these GRBs, GRB 060729 being the only exception (Appendix B.4).

As the Golden Samples of K06 and this work can be readily compared (Zheng et al. 2009a and Gehrels et al. 2008 also find that the distribution of optical-to-X-ray spectral indices, β_{OX}, is identical in pre-*Swift* and *Swift* GRB afterglows) we create one total Golden Sample and split it along the $z = 1.4$ division used by K06. Here, we find clear evidence for bimodality, it is $\overline{M_B} = -21.89 \pm 0.32$ (FWHM 1.52 mags) for the low-z (22 GRB afterglows) and $\overline{M_B} = -23.78 \pm 0.23$ (FWHM 1.51 mags) for the high-z (43 GRB afterglows) sample. The difference is statistically significant, a KS-test shows that they are probably not taken from the same distribution ($P = 2.9 \times 10^{-4}$). Using the *Swift*-era sample only, and dividing it along the $z = 1.4$ line, we find $P = 8.4 \times 10^{-4}$, further strengthening the result. Non-parametric rank correlation tests find further, albeit relatively weak, evidence for the magnitude increase toward higher redshifts; it is Kendall's $\tau = -0.41$ and Spearman's $\rho = -0.53$ for the *Swift*-era-only sample, and Kendall's $\tau = -0.31$ and Spearman's $\rho = -0.51$ for the complete sample, these very similar values also show that mixing the two samples is not problematic.

While *Swift* has increased the recovery rate of afterglows, and also the percentage of afterglows with successful spectroscopy in follow-up observations, *Swift* GRBs that actually did meet our selection criteria, especially those of the Golden Sample, are quite rare events. These bursts usually not only have a lot of optical follow-up, but are also interesting in such a manner that publica-

tions with data on these bursts are preferred over the many others *Swift* has delivered. For example, GRB 050904 held the record for highest redshift ever discovered for a burst for several years, the afterglow of GRB 060206 showed a very powerful rebrightening, that of GRB 060526 showed a complex optical light curve, and GRB 061007, GRB 070125 and especially GRB 080319B were exceptionally bright, both in gamma-rays and in the optical. GRB 050408, one of the observationally faintest afterglows in our new Golden Sample, was very well observable from both hemispheres, leading to a lot of observations. In other words, our Golden Sample contains mostly GRBs that are not typical of the faint *Swift* era bursts, but more typical of the *Beppo-SAX* era. While the selection criteria of the Silver and especially the Bronze Sample are less stringent, the amount of derived information is also reduced.

Still, it seems clear that for the GRBs in our combined *Swift* sample (i.e., Golden, Silver and Bronze), the larger amount of faint afterglows is an effect based mostly on the increased mean ensemble redshift (Jakobsson et al. 2006a; Bagoly et al. 2006). This is mainly a result of *Swift* BAT's low-energy sensitivity and novel triggering methods, such as image triggers, which find GRBs whose light curves are strongly stretched due to redshift (e.g., Campana et al. 2007; Salvaterra et al. 2007, 2008; Ukwatta et al. 2009). Another factor is the rapid localization capability of *Swift* combined with rapid ground-based follow-up, which is crucial for long-slit spectroscopy of faint high-z targets. But the need for a spectroscopic redshift and decent light curve coverage is, of course, still a strong restriction for inclusion into our sample (see Fiore et al. 2007, for a discussion on these selection effects). There are afterglows which are clearly strongly extinguished by host extinction, such as GRB 051022 (Nakagawa et al. 2006; Rol et al. 2007; Castro-Tirado et al. 2007), GRB 060923A (Tanvir et al. 2008a), GRB 070306 (Jaunsen et al. 2008), GRB 061222A, GRB 070521 (Perley et al. 2009d), GRB 080607 (Prochaska et al. 2009) and GRB 090417B (Holland et al. 2010). In such cases, we are unable to derive the afterglow luminosity (which was probably very high in the case of GRB 051022, since it was an highly energetic burst with a very bright X-ray afterglow; Castro-Tirado et al. 2007). More highly extinguished or intrinsically faint afterglows very probably can be found among those *Swift* afterglows that did not match our selection criteria, even for the Bronze Sample. Therefore, the question if "dark" GRBs are usually optically undetected due to strong host extinction or intrinsic faintness remains unsolved as yet, though several recent works find evidence for dust attenuation being the main factor (Gehrels et al. 2008; Zheng et al. 2009a; Cenko et al. 2009b; Perley et al. 2009d). It therefore remains possible that a population of afterglows would remain that are significantly less luminous than all in our complete sample. In this case, the clustering of afterglow luminosities itself, as inferred by K06, Liang & Zhang (2006) and Nardini et al. (2006) (evidence for which has already been reduced with our larger sample) may be an observational bias, both due to optical sampling criteria (good multicolor light curves and redshift, see, e.g., Coward 2009, for how spectroscopic response time can induce further bias to the redshift distribution, and Fynbo et al.

2009 for other selection effects involving redshift determination) and gamma-ray detection criteria, similar to what has been proposed for the existence of high-energy correlations (e.g., Nakar & Piran 2005b; Band & Preece 2005; Butler et al. 2007). On the other hand, a recent study of pre-*Swift* "dark" GRBs has shown that the bimodal clustering persists even after the inclusion of these events (Nardini et al. 2008a), but we caution that this sample is built upon satellites that were less capable of detecting subluminous GRBs than *Swift*. On the whole, a combination of factors makes the *Swift* afterglow sample less biased than that of the pre-*Swift* era, and thus more representative of the (unknown) true luminosity distribution. That we find only weak evidence for clustering with our less biased sample may indicate that an unknown observational bias has played a role in the pre-*Swift* data. Recent research indicates that a luminosity evolution in the prompt emission of GRBs does exist (e.g., Salvaterra et al. 2009a), and as we find (§ 3.3.5) that bursts with high isotropic energy release are usually also associated with brighter afterglows, this connection, while still involving many insecurities, implies that a true luminosity evolution in the afterglows is also plausible. Recently, Imerito et al. (2009) have also reported that the result of Coward (2009) implies a true evolution in the luminosity function, with afterglows at higher redshifts being more luminous, though their result does not allow a physical interpretation to be derived, nor the true shape of the luminosity function to be discerned.

3.3.2. *Does the high number of* Mg II *foreground absorbers depend on afterglow flux?*

Prochter et al. (2006), studying medium- and high-resolution spectra of bright GRB afterglows, found a high number of strong ($W_r(2796) > 1$ Å) intervening Mg II absorption systems, 4 ± 2 times more than along the lines of sight to quasars studied in the SDSS. Such a discrepancy was not found in intervening C IV systems (Sudilovsky et al. 2007; Tejos et al. 2007), and multiple explanations have been proposed (see, e.g., Porciani et al. 2007, for an overview). Differing beam sizes of quasars and GRBs (Frank et al. 2007) as an explanation can not account for the case of GRB 080319B, where high-S/N multi-epoch data show no temporal variations over several hours (D'Elia et al. 2010, see also Pontzen et al. 2007; Vergani et al. 2009)[12]. Sudilovsky et al. (2009) simulate the effect of dust in the foreground absorbers on quasar detection efficiency and rule out a strong contribution from this factor (see also Cucchiara et al. 2009). Cucchiara et al. (2009) compare properties of foreground Mg II systems along quasar and GRB sightlines and find no significant differences, concluding that the GRB systems are probably not associated with material ejected near the GRB at relativistic velocities (intrinsic origin). Tejos et al. (2009) and Vergani et al. (2009) also study the incidence of weak Mg II systems, and both come to the conclusion that the incidence of weak systems is similar along quasar and

---

[12] Hao et al. (2007) claimed variable equivalent widths of foreground absorber Mg II lines seen in multi-epoch spectra of the GRB 060206 afterglow, but this was later refuted by Thöne et al. (2008c) and Aoki et al. (2009) using high-S/N Subaru and WHT data.

GRB afterglow sightlines, implying that the best expla-
nation is that the GRB afterglows of the echelle sam-
ple have been amplified by gravitational lensing (see also
Wyithe et al. 2010, but see Cucchiara et al. 2009). Both
studies also find that the excess is smaller than originally
deduced from the original small sample by Prochter et al.
(2006), but the significance that the excess is real has in-
creased with increasing sample size and redshift path.

All GRBs in the UVES sample of Vergani et al.
(2009) are included in our Golden Sample (with GRB
021004 being part of the pre-*Swift* Golden Sample,
and GRB 060607A not having any data at 0.5 rest-
frame days, so we will not include it in this dis-
cussion), and two further GRBs with echelle spectra
(Keck HIRES) from the sample of Tejos et al. (2009)
are also part of our Silver Sample. Furthermore, a
GRB with published UVES spectroscopy not included
in the sample of Vergani et al. (2009) is XRF 080330,
which also shows a very strong Mg II foreground ab-
sorber (D'Elia et al. 2009b), and another strong fore-
ground system is seen in the afterglow of GRB 090313,
as measured by X-Shooter (de Ugarte Postigo et al. 2010).
That all of these GRBs are in our samples is not sur-
prising, only very bright afterglows can be successfully
observed with echelle spectrographs, and will therefore
very likely also have extensive photometric follow-up
(and a redshift, of course), allowing inclusion in our
sample (though this situation is now changing with
X-Shooter, see de Ugarte Postigo et al. 2010). While
the telescopes capable of deriving echelle spectra of
GRBs (VLT/UVES+X-Shooter, Magellan/MIKE, and
Keck/HIRES) are all concentrated in one hemisphere
(Chile and Hawaii), and thus some GRBs with bright af-
terglows are missed because they have become too faint
once they are observable (GRB 061007 being a good ex-
ample), the isotropic distribution of GRBs should ensure
that the echelle sample is mostly unbiased.

We first create two samples. The first one, the
"UVES" sample, contains the nine GRBs from the sam-
ple of Vergani et al. (2009) (excluding, as mentioned,
GRB 060607A), furthermore GRB 051111 and GRB
080810 (Tejos et al. 2009, while these are from the Sil-
ver Sample, the extinction correction is small in both
cases, so the insecurity in the luminosity is not large)
XRF 080330 (D'Elia et al. 2009b) and GRB 090313
(de Ugarte Postigo et al. 2010). The "non-echelle" sam-
ple contains all other GRBs from the Golden Samples,
for a total of 54 GRBs. Note that this sample still
includes several GRBs with echelle observations. But
in the cases of GRB 020813 (Fiore et al. 2005), GRB
050502A (Prochaska et al. 2005b) and especially GRB
071003 (Perley et al. 2008d), the resulting spectra had
very low S/N. GRB 081008 was also observed by UVES
(D'Avanzo & Covino 2008), but no information has been
published on whether a foreground system exists or not.
In the case of GRB 030329 (Thöne et al. 2007b), the
GRB is so close that there are no intervening absorbers,
and gravitational lensing is very unlikely. We find the
mean absolute B magnitude of the UVES sample to
be $\overline{M_B} = -23.72 \pm 0.41$, while the other sample has
$\overline{M_B} = -23.05 \pm 0.25$, implying the the UVES sample
is brighter only at the 1.4σ level, which is not statisti-
cally relevant ($P = 0.28$). On the other hand, the UVES

sample can be brighter by, at the 2σ level, up to 1.63
mags, which is a factor of $4.5\times$, which lies above the
amplification of $1.7\times$ inferred by Porciani et al. (2007),
therefore we are not able to rule at such a rather subtle
amplification with any significance either.

A second point is that the sample selection as we are
using it now just gives us information about the af-
terglows which were, or were not, observed with high-
resolution spectrographs, which can be due to nothing
but luck (declination and explosion time). A more pre-
cise analysis needs to compare afterglows with strong
foreground absorbing system with those that definitely
do not have any. We therefore create two subsam-
ples of the UVES sample. The "strong sample" con-
tains GRBs 021004, 050820A, 051111, 060418, 080319B,
080330 and 090313, while the "weak sample" contains
GRBs 050730[13], 050922C, 071031, 080310, 080413A and
080810[14]. We find $\overline{M_B} = -23.65 \pm 0.66$ for the strong
sample, and $\overline{M_B} = -23.80 \pm 0.49$ for the weak sam-
ple, implying they are identical ($P = 0.95$), with the
weak sample actually being marginally brighter (we cau-
tion that we are in the realm of low-number statistics
here). We conclude that if the Mg II statistics are in-
fluenced by lensing, the effect is not statistically rele-
vant, on the other hand, we can also not rule out a
small amplification factor with any significance either.
Clearly, the sample of high-S/N, high-res afterglow spec-
tra must be increased before further conclusions can be
drawn, X-Shooter will make an important contribution
here (de Ugarte Postigo et al. 2010).

We also note that on the issue of dust reddening by
foreground systems, we find no evidence for large absorp-
tion in any of the GRBs in the UVES sample, with the
highest values being found for GRB 060418 ($A_V = 0.20 \pm
0.08$), where one foreground absorbing system may con-
tribute significantly (Ellison et al. 2006; Vergani et al.
2009), and GRB 090313 ($A_V = 0.34 \pm 0.15$). We cau-
tion that the latter value is based on GCN data only so
far, but there is corroborating evidence for dust found in
the spectrum (de Ugarte Postigo et al. 2010).

3.3.3. *Does an Upper Limit on the Forward Shock Luminosity Exist?*

Compared to K06, the luminosity range of our after-
glow sample has slightly expanded, both to lower and
higher luminosities, but this must be seen in the con-
text of a much larger sample. In the K06 sample, the
afterglow of GRB 021004 dominated the luminosity dis-
tribution over a long period of time. In the present
sample, several more GRBs are added which parallel
the evolution of the afterglow of GRB 021004. The
large early luminosity of the afterglow of GRB 050904
has been discussed in Kann et al. (2007a). Its light
curve evolution is clearly anomalous, featuring an early

---

[13] Tejos et al. (2009) find one "Very Strong" foreground ab-
sorber for this event from Magellan MIKE spectroscopy, but
Vergani et al. (2009) give an upper limit for this system below the
$W_r(2796) > 1$ Å cutoff after correcting for sky contamination using
UVES data.
[14] There is tentative evidence for a very weak ($W_r(2796) <
0.07$ Å) Mg II foreground system in the spectrum which was too
weak to even be included in the sample of Tejos et al. (2009) (N.
Tejos, priv. comm.). Of course, this does not influence the fact
that GRB 080810 belongs to the weak sample.

rise, a plateau and a superposed sharp peak. Multiple papers (e.g., Racusin et al. 2008; Woźniak et al. 2009; Beskin et al. 2009; Kumar & Panaitescu 2008; Kumar & Narayan 2009) discuss the extreme prompt optical flash of GRB 080319B. Finally, the derived very high extinction for GRB 060210 is unsure (see Appendix B.3 for more details), implying that the afterglow, which seems to show a standard (not rapid, like GRB 050904 and GRB 080319B) decay after a short plateau and peak, may be much less luminous. Excluding these special events, the early afterglow of GRB 061007 (Mundell et al. 2007b; Schady et al. 2007b) is the most luminous in the sample, although it decays rapidly[15]. Between 0.01 and 0.5 days, the afterglow of GRB 090313 is the most luminous, though we caution that so far, we have only an extensive GCN data set. It is then exceeded by the last strong rebrightening of GRB 080129, which is then followed after about 1.5 days by the afterglow of GRB 090926A, which shows a very similar evolution to that of GRB 021004.

In Fig. 4 we plot as a boundary a power-law decay and attach it to the brightest afterglow detections at times from hours to days (we find $\alpha \approx 1$). At early times, this slope is exceeded, and at least for GRB 990123, GRB 050904 and GRB 080319B, additional emission components dominate over the forward shock afterglow (e.g., Akerlof et al. 1999; Nakar & Piran 2005a; Boër et al. 2006; Wei et al. 2006; Zou et al. 2006; Beskin et al. 2009; Kumar & Panaitescu 2008; Kumar & Narayan 2009). This may also be the case for GRB 061007, although this burst's afterglow showed a remarkable, unbroken broadband (from gamma-rays to optical) power-law decay from very early times onward (Mundell et al. 2007b; Schady et al. 2007b). Beyond ≈ 2 days, the light curves usually become steeper due to jet breaks. This upper boundary may imply that there exists an upper limit for the luminosity of forward-shock generated afterglow emission in the optical bands. Jóhanesson et al. (2007) have studied a large sample of synthetic afterglows created by using the standard fireball model and find that the luminosity function of afterglows (in wavebands from the X-rays to the radio) can be described by a lognormal distribution with an exponential cutoff at high luminosities, which may be considered a theoretical prediction of our result, although they do not explicitly state that. Determining the actual luminosity distribution from the data is clearly non-trivial, especially trying to discern between, e.g., a regular power-law distribution and one that needs an exponential cutoff at high luminosities (as a power-law distribution itself will trend toward zero, just not as sharply as the exponential cutoff). Furthermore, determining the slope of the power-law is complicated by selection effects such as Eddington bias at low luminosities (see, e.g., Teerikorpi 2004 for a discussion in terms of galaxy counts), as well as all the selection effects we have pointed out concerning our optically selected sample.

In the standard afterglow theory (see, e.g., Panaitescu & Kumar 2000, for the equations), the optical flux generally depends on the isotropic kinetic energy $E_{k,iso}$, the ambient density (n for an ISM or A^*

for a wind), and the shock microphysics parameters p (electron spectral index), ε_e (fraction of energy in electrons) and ε_B (fraction of energy in magnetic fields). This upper limit therefore is relevant to a combination of these parameters and cannot be used to pose a limit for each individual parameter. On the other hand, if one makes the assumption that the microphysics parameters do not vary significantly among bursts, this upper limit may suggest that bursts do not have an exceptionally large $E_{k,iso}$ and the fireball is usually not expanding into an ambient medium of very high density. Jóhanesson et al. (2007) also find that variation of the initial energy release is one of the main drivers of the luminosity distribution (the others are the microphysical parameters, but we argue that they should not vary overly much from burst to burst). It may be possible that a very high circumburst density, as one would find within a molecular cloud, is connected to very large gas and dust column densities, and thus to a large line-of-sight extinction, which prevents us from detecting the afterglow or at least adding it to our sample. We note that Jóhanesson et al. (2007) find that a range of circumburst densities has little influence on the afterglow luminosity, but they only vary the density between 0.1 and 10 cm^{-3}. We also note that several of the GRBs that populate the region of the upper limit only reach it due to additional injections of energy into the external shock, e.g. GRB 021004 (de Ugarte Postigo et al. 2005), GRB 060206 (Woźniak et al. 2006; Monfardini et al. 2006), GRB 070125 (Updike et al. 2008b; Chandra et al. 2008), GRB 080129 (Greiner et al. 2009a) and GRB 090926A (Cenko et al. 2010b; Rau et al. 2010). For GRB 050603 and especially GRB 991208 (cf. K06), the lack of early afterglow data makes the situation less clear. The afterglow of GRB 050820A has a relatively slow decay and a very late break. Therefore, several factors may account for the potential existence of this upper luminosity limit, and the afterglow sample will have to increase strongly to reach further conclusions, as these bright events are very rare.

3.3.4. *The Luminosity Distribution at Early Times – Diversity and Clustering*

As mentioned before, many of the *Swift*-era GRBs in our sample have afterglows that have been detected at very early times, when they were for the most part still bright. This allows us to derive the luminosity distribution at early times, an exercise that was not possible in the pre-*Swift* era. We choose 10^{-3} days (86.4 seconds) at $z = 1$, which is equivalent to only 43.2 seconds after the GRB trigger in the source frame (in several cases, GRB prompt high-energy emission is still ongoing at this time). The sample comprises 48 afterglows, with GRB 990123 as the only burst from the pre-*Swift* era[16]. The distribution is presented in Fig. 6. It is, on the one hand, very broad, which was already apparent from Fig. 4. The total width is 11.5 magnitudes, almost twice as wide as the luminosity distribution at one day. On the other hand, 50% of all afterglows (24 out of

---

[15] At one day, it has become so faint that it falls into the faint bin of the bimodal distribution, which could be "expected" from its redshift $z = 1.261 \leq 1.4$.

[16] There is only one other pre-*Swift* afterglow that is detected at such early times, GRB 021211. It is not included here as it did not yield a usable SED (K06). The flat, blue SED and the redshift close to $z = 1$ imply a minimal dRc−shift, though, and it would be $R_C \approx 14$ at 43 seconds in the rest frame.
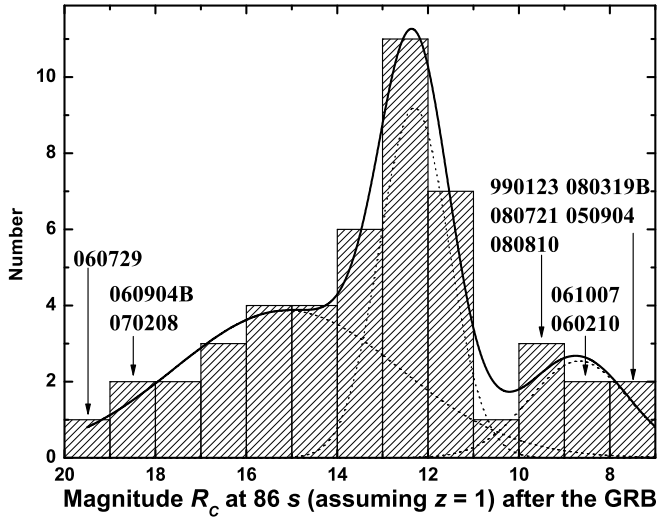
FIG. 6.— The distribution of optical transient magnitudes at 86 seconds (10^{-3} days) after the GRB trigger in the observer frame, after shifting all afterglows to $z = 1$. While the complete spread is very wide (12 magnitudes), there is a strong clustering around 13th magnitude. We interpret these GRB afterglows as those where the forward shock emission dominates already at early times. In some cases, an additional component dominates strongly, making the afterglow even brighter, while many other afterglows suffer from early suppression. The complete distribution is trimodal and well-fit by three overlapping Gaussians. The brightest and faintest afterglows are indicated.

48) cluster within only three magnitudes (a similar tight clustering has been found by Oates et al. 2009 at 100 seconds after the GRB onset in the rest-frame). Eight afterglows (GRBs 080319B, 050904, 061007, 060210, 080810, 080721, 990123 and 080413B) are brighter than this cluster (albeit significantly, in some cases). Most of these are probably dominated by additional emission components at early times (see below), although the unbroken decay from very early times on in the case of GRB 061007 may speak against an additional component (Mundell et al. 2007b; Schady et al. 2007b). GRB 080721 is a similar case (Starling et al. 2009). The strongly clustered afterglows would then be those that are dominated by the forward shock emission already at early times, while the fainter afterglows may suffer from optical supression (Roming et al. 2006) or a late afterglow onset (e.g. Molinari et al. 2007; Nysewander et al. 2009a). In some cases (e.g., GRB 060729, Grupe et al. 2007a), there are also indications that significant long-term energy injection similar to what may cause the shallow decay/plateau phase of the "canonical" X-ray afterglow (Nousek et al. 2006; Zhang et al. 2006; Panaitescu et al. 2006a) occurs, although in most cases the plateau phase in X-rays and the following break to a "classical" afterglow decay is not mirrored in the optical (Panaitescu et al. 2006b). This highlights the possibility that there are afterglows that start at a similar faintness to, e.g., GRB 060729, and then follow a straightforward decay instead of remaining roughly constant. These optical afterglows would be too faint to be included in our sample due to the selection criteria, and might also be much less luminous at 0.5 rest-frame days than the afterglows presented here.

Fitting the complete distribution with a single Gaussian does not yield an acceptable result, it is χ^2/d.o.f.= 1.58, and, more importantly, the fit finds that a constant $y_0 \approx 2$ has to be added, which is unphysical. Instead, following the idea that we are seeing three different types of early behavior, we are able to fit the distribution with three overlapping Gaussians (see Fig. 6). We find a significantly improved fit, it is χ^2/d.o.f.= 0.58, no constant term is needed ($y_0 = 0$), and the three Gaussians are centered at 8.67 ± 0.48 (FWHM 2.20) mags, 12.31 ± 0.09 (FWHM 1.52) mags, and 15.11 ± 1.23 (FWHM 4.95) mags, for the "overluminous", "standard" and "subluminous" types, respectively.

Several caveats apply, however, and the picture is not so simple. Kann et al. (2007a) discussed the possibility of different spectral slopes at early times, in application to the prompt optical emission of GRB 050904. They found that assuming achromaticity (and thus the spectral slope derived from the late-time, forward-shock dominated afterglow), the luminosity of the prompt flash was higher than in the case that spectral slopes more appropriate for early emission were considered (e.g., fast cooling phase, or injection frequency still above the optical band). Therefore, such color evolution may also apply to other afterglows in our early sample, possibly widening the clustering in one photometric band. For some GRBs, early multicolor afterglow data are available, but these yield an inconclusive picture. For example, the prompt optical flare of GRB 061121 (Page et al. 2007) is more pronounced in the V band (*Swift* UVOT) than in unfiltered observations (ROTSE). On the other hand, the color evolution of the afterglow of GRB 061126 (Perley et al. 2008a) goes from redder to bluer, similar to the case of the very-well sampled early afterglow of GRB 080319B (Bloom et al. 2009; Racusin et al. 2008; Woźniak et al. 2009). Several other afterglows show no early color changes at all, e.g. those of GRB 060418 and GRB 060607A (Molinari et al. 2007; Nysewander et al. 2009a) and GRB 061007 (Mundell et al. 2007b; Schady et al. 2007b).

Furthermore, several cases in the "cluster" exist where a detailed study has shown additional emission components. An early reverse shock component has been proposed for GRB 050525A (Klotz et al. 2005a; Shao & Dai 2005), this is also an interpretation for the early steep decay of GRB 061126 (Perley et al. 2008a) and GRB 060908 (Covino et al. 2010). In the case of GRB 051111, an early steep decay is associated with the tail of the prompt emission (Yost et al. 2007a; Butler et al. 2006). Once again, there are counterexamples, e.g. for GRB 060418, early upper limits on the polarization of the optical afterglow point to a weak (or even negligible) reverse shock component (Mundell et al. 2007a; Jin & Fan 2007), in agreement with a dominating forward shock at very early times.

Recently, Panaitescu & Vestrand (2008) have presented a study of early afterglow behavior, investigating different classes and finding a possible correlation between peak luminosity and peak time for afterglows with fast rises (which can be both reverse-shock flashes and forward-shock peaks; from their sample, Oates et al. 2009 find the rises are consistent with forward-shock evolution), which they claim might even be used as a redshift indicator. Our large sample allows us to further study this possible correlation. In total, we find 72 af-
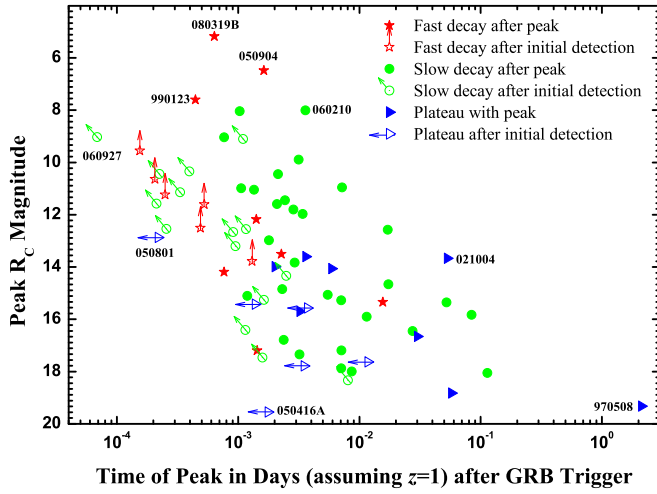
FIG. 7.— The peak magnitudes of 70 afterglows from our samples, as derived from the extinction-corrected $z = 1$ light curves (Fig. 4). We discern between six groups: Those with early peaks followed by rapid decays (possibly of reverse-shock origin, filled red stars), those where the peak is before the earliest detection, but the early decay is also steep (empty red stars with upward-pointing arrows), those with early peaks followed by slower decays (probably of forward-shock origin, filled green discs), those where the peak is before the earliest detection, but the early decay is also slower (green rings with slanted arrows), those with early plateau phases which also show magnitude peaks (very slow rise and decay, filled blue triangles), and those where the early decay is very slow, but the peak lies before the first detection (empty blue triangles with left-pointing arrows). While there is clearly an envelope seen, the scatter is very large. Several outstanding events have been labeled. See text for more details on special cases.

terglows (including several more from the pre-*Swift* era) which have either very early detections, or show later peaks. We have gathered these afterglows in Table 6, where we give the relevant time (peak or earliest detection) and the R_C magnitude in the extinction-corrected $z = 1$ frame (errors are statistical only). We discern between six classes, and indicate additional noteworthy features in the comments to Table 6:

- **Afterglow peak followed by a fast decay:** These afterglows show a fast rise to a peak, followed by a fast decay ($\alpha \approx 1.5 - 2$), which usually becomes flatter later. This behavior is interpreted as an additional component superposed on the forward-shock afterglow, which, due to its rapid decay, quickly becomes less luminous than the forward-shock afterglow, leading to the steep-to-shallow transition. Often, this component is attributed to a reverse-shock flash, with the classical example being GRB 990123 (Mészáros & Rees 1997, 1999; Sari & Piran 1999). In other cases, it is probably tied to optically emissive internal shocks, that is, direct central engine activity, as for GRB 080319B[17] (Racusin et al. 2008; Beskin et al. 2009, but see Kumar & Narayan 2009), GRB 060526 (Thöne et al. 2010), GRB 061121 (Page et al. 2007), and GRB 080129 (Greiner et al. 2009a), making this a diverse class. These afterglows (or,

more correctly, optical transients), are the most luminous among GRB or any other phenomena (Kann et al. 2007a; Bloom et al. 2009). We find seven afterglows (10%) in this category.

- **Initial fast decay:** These afterglows show a similar steep-to-shallow transition as described above, but the observations did not begin until after the peak, implying it must be very early. An example is GRB 090102 (Gendre et al. 2010, see also Stratta et al. 2009). To our knowledge, an early steep decay for GRB 090424 is reported here for the first time. This category contains six afterglows (8%), and the combined fast decay categories make for 18% of all afterglows, in agreement with Klotz et al. (2009c).[18]

- **Afterglow peak followed by a slow decay:** In these cases, after a usually fast rise and a turnover, the decay index is typical for a forward-shock afterglow with constant blastwave energy (aside from the radiative losses, and opposed to a forward shock with energy injection), and there is no further transition between different decay indices. This has been interpreted as the rise of the forward-shock afterglow at deceleration time, with classical examples being GRBs 060418 and 060607A (Molinari et al. 2007; Nysewander et al. 2009a). Panaitescu & Vestrand (2008), from afterglow modeling, also favor this explanation, with a second valid interpretation being non-uniform jets beamed off-axis with respect to the observer. Such an interpretation is favored for late peaks (if the initial Lorentz factor is also a function of angle), as in the case of GRB 080710 (Krühler et al. 2009b). Some special cases also exist, like the extreme rebrightening (following a standard forward-shock decay) of GRB 060206, which has been interpreted as an extreme energy injection event (Woźniak et al. 2006; Monfardini et al. 2006). This group contains the most afterglows, 30 (41%).

- **Initial slow decay:** In these cases, the decay index is typical for a forward-shock dominated afterglow, and no peak is seen. All afterglows in our total sample which we do not discuss here would fit into this category, but have been detected at such late times (e.g., almost all afterglows of the pre-*Swift* era) that no real conclusions can be gathered about their early behavior. Intriguingly, some afterglows with very early detections already feature a typical forward-shock decay from the first detection on. While once seen as the most typical behavior, most forward-shock dominated afterglows peak late enough that their peaks are detected (see above), putting less afterglows in this category, a total of 15 (21%). In total, the early dominance of

[17] Racusin et al. (2008) interpret the intermediately rapid decay in the early light curve of this afterglow as a reverse shock flash component that becomes dominant over the very rapidly fading prompt optical emission.

[18] A reverse shock origin has also been implied for the very early, steeply decaying emission of GRB 060117 (mentioned before, Jelínek et al. 2006b) and GRB 060111B (Stratta et al. 2009), but the latter GRB, which incidentally shows evidence for very high host extinction as well, has no redshift beyond estimates and is also missing from our sample.

the forward shock is found to be the most common case, with 45 afterglows (62%).

- **A plateau with a discernible peak magnitude:** In these cases, a rising-to-decaying transition is seen as well, but the rise and initial decay are very shallow, leading to a plateau phase where the afterglow luminosity barely changes over long times. Such a behavior has often been seen in connection with the spectrally soft X-Ray flashes[19], and may indicate a jet viewed off-axis (e.g., XRF 080310 and XRF 080330, Guidorzi et al. 2009a analyze the latter in detail). Several special cases are included in this category, like GRB 021004, which is dominated by multiple energy injections at early times (de Ugarte Postigo et al. 2005), and the highly peculiar afterglow of GRB 970508, which begins with a very faint plateau followed by a very late, strong rebrightening. This category contains nine afterglows (12%).

- **An early very shallow decay:** Here, the afterglow decays from the first observation onwards, but the decay index is very shallow, less than is expected from a classical forward shock ($\alpha \approx 0-0.4$), creating a plateau phase. A classical example of such behavior is GRB 050801 (Rykoff et al. 2006a; De Pasquale et al. 2007), and it has also been seen in the highest redshift GRB 090423 (Tanvir et al. 2009). These very slow decays are quite rare, with only six afterglows in the sample showing them (8%).

We plot all 73 data points (GRB 060729 has resulted in two measurements) in Fig. 7, discerning between the six classes. Clearly, an envelope is seen which traces the correlation found by Panaitescu & Vestrand (2008), but the scatter is much larger than what they find in their small sample, indicating that the significance of the correlation is much smaller than assumed. Applying rank correlation tests, we find Kendall's $\tau = 0.43$, and Spearman's $\rho = 0.62$, indicating the existence of a correlation with only moderate significance. A similar result was found by Klotz et al. (2009c) using observations of the TAROT robotic telescopes. In magnitudes, the width of the scatter is around ten magnitudes even if we only choose those afterglows which exhibit a fast rise (and fast or slow decay). Intriguingly, those afterglows which are already decaying at first detection cluster more strongly than those with detected peaks (especially those with rapid decays), on the left hand side of the correlation, indicating an extension in this direction and even larger scatter, were the optical follow-up to be even more rapid. All afterglows not included in our sample of 72 would be found in the lower right hand corner, usually beyond 0.1 days and fainter than 16th magnitude.

Oates et al. (2009) find a statistically significant correlation between the early decay index and the magnitude of the afterglow, with bright afterglows decaying more rapidly. This hints both at possible additional early components in the afterglow, as well as pointing

---

[19] Note that some X-ray flashes show a normal, forward-shock-like decay from very early on, e.g., XRF 050406 (Schady et al. 2006) and XRF 050824 (Sollerman et al. 2007).
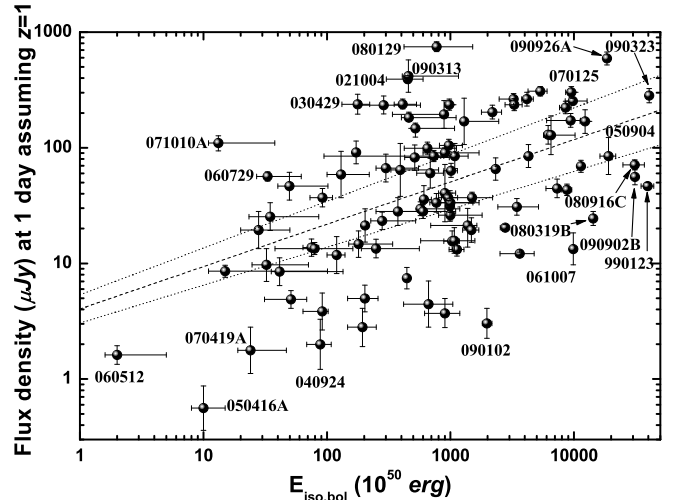
Fig. 8.— The flux density in the R_C band at one day (in the host frame assuming $z = 1$) plotted against the bolometric isotropic energy of the prompt emission for all GRBs in the optically selected sample (except GRB 991208, which was only discovered after several days, and GRBs 060210, 060607A, 060906 and 080319C, where the follow-up does not extend to one day). While no tight correlation is visible, there is a trend of increasing optical luminosity with increasing prompt energy release. This is confirmed by a linear fit (in log-log space), using a Monte Carlo analysis to account for the asymmetric errors. The dashed line shows the best fit, while the dotted line marks the 3σ error region. Several special GRBs are marked.

to the late clustering (a fast-decaying, bright afterglow will be at similar magnitude at one day as a fainter afterglow that decays more slowly, though note the transition time plays an important role as well). Further studies of the early diversity, especially the optically subluminous cases, which must decay slowly or even rebrighten to fit into the late clustering (and are therefore usually found in the two plateau groups mentioned above), are beyond the reach of this work.

3.3.5. Existence of a Correlation between Optical Luminosity and Isotropic Energy?

In Fig. 8 we show the flux density in the R_C band at one day in the host frame assuming $z = 1$ (Fig. 4, Table 5) plotted against the bolometric isotropic energy of the prompt emission (Table 2). This plot is similar to that of Kouveliotou et al. (2004, see also Freedman & Waxman 2001; Liang & Zhang 2006; Amati et al. 2007; Kaneko et al. 2007; Gehrels et al. 2008, and Nakar 2007; Berger 2007 for Type I GRBs), who used the X-ray luminosity at 10 hours (for a detailed discussion, see Granot et al. 2006; Fan & Piran 2006), as well as Nysewander et al. (2009b), who also studied the $R-$band luminosity (as well as the X-ray luminosity) at 11 hours. Similar to the correlations found by the aforementioned authors, a trend is visible in Fig. 8: The optical luminosity increases with increasing prompt energy release. But the scatter is very large, especially in contrast to the often very well constrained flux densities (i.e., the offset from the best fit in units of the individual flux density errors σ_F is much larger than one in many cases, $\frac{|F - F_{Fit}|}{\sigma_F} \gg 1$, with F_{Fit} being the flux density expected from the correlation). This can be clearly seen both in flux density and in isotropic energy. GRB 061007 and GRB 070125 have almost identical isotropic

energy releases, but the flux densities of their optical afterglows differ by a factor of 23^{+12}_{-8}. The span between GRB 080129 and GRB 050502A is even larger, over two orders of magnitude. GRB 990123 has an isotropic energy release roughly 1000 times higher than GRB 060729, but its optical afterglow has a slightly fainter luminosity at one day. The trend is almost non-existent except for three faint bursts: XRF 060512, XRF 050416A and GRB 070419A have been mentioned in § 3.3.1, and here we see that these events are also subenergetic in their prompt emission. The faintest optical afterglow of the K06 sample, GRB 040924, is seen to be among the least energetic GRBs too, but it is still part of the "cloud". In log-log space, we use a linear fit, accounting for the asymmetric error bars with a Monte Carlo simulation. In 30000 runs, we find the following correlation:

$$\frac{F_{opt}\ (\text{at } t = 1 \text{ day})}{1 \mu \text{Jy}} =$$
$$10^{(0.607 \pm 0.041)} \times \left(\frac{E_{iso,bol}}{10^{50}\ erg} \right)^{(0.366 \pm 0.013)} . \quad (1)$$

Using an unweighted fit, we find exactly the same slope and a slightly smaller (though identical within 1σ errors) normalization, indicating that the intrinsic scatter dominates over the errors of the data points. Using Kendall's rank correlation coefficient τ, we check the significance of the correlation. We find $\tau = 0.29$ (significance 4.1σ) for the complete data set. Therefore, the correlation is only of low significance. As would be expected, removing the three subenergetic events reduces the significance even more, it is $\tau = 0.24$ (significance 3.3σ). We conservatively estimate the errors on τ by creating maximally tight and maximally scattered data sets. In the first case, we shift data beneath the best fit closer by $-\delta E_{iso,bol}$ and $+\delta F_{opt}$, and data above the best fit closer by $+\delta E_{iso,bol}$ and $-\delta F_{opt}$. In the latter case, the data are shifted away from the correlation in the reverse way. For the maximally tight data set, we find $\tau = 0.44$ (significance 6.1σ) for the complete data set and $\tau = 0.40$ (significance 5.5σ) when we remove the three subenergetic events. For the maximally scattered data set, the values are $\tau = 0.18$ (significance 2.6σ) and $\tau = 0.13$ (significance 1.8σ), respectively.

Nakar (2007) and Berger (2007) argue that as the cooling frequency is usually beneath the X-ray range (but see Zhang et al. 2007b, who find that 30% (9 of 31) of the X-ray afterglows they studied to still have $\nu_c > \nu_X$ at up to ten hours after the GRB), the X-ray luminosity is independent of the circumburst density and it thus represents an acceptable proxy for the kinetic energy, $L_X \propto \epsilon_e E_K$ (with ϵ_e being the fraction of energy in relativistic electrons). Clearly this is not the case here, as the cooling break lies above the optical bands in most cases (e.g, K06; Panaitescu et al. 2006a,b; Starling et al. 2007a; Schady et al. 2007a; Curran et al. 2010). Therefore, the strong spread in optical luminosities may be explained by the effect of the spread in the circumburst density, which, while typically lying at $1 - 10$ cm^{-3} (cf. Friedman & Bloom 2005), can reach several hundred cm^{-3}, e.g. in the case of GRB 050904 (Frail et al. 2006). Still, the existence of this trend is intriguing, and fur-

ther observations will hopefully reveal more subluminous GRBs. One extension possibility is to do a similar analysis for Type I GRBs, these results are presented in the companion Paper II. Furthermore, using measured jet break times, one could correct for the jet collimation, and step from an "Amati-like" (using E_{iso}) to a "Ghirlanda-like" (using E_Γ) plot, albeit with less events.

3.3.6. *A New Population of Low-Luminosity GRBs at Low Redshifts?*

There is clear evidence for one Type II subpopulation that probably extends the $L_{opt} - E_{iso}$ correlation to significantly lower energy values. These are the so-called low-luminosity SN bursts, GRB 980425, GRB 031203 and XRF 060218 (Pian et al. 2006; Soderberg et al. 2006b; Liang et al. 2007a; Guetta & Della Valle 2007)[20]. In all these three cases, while luminous, basically unreddened SN emission was detected, there were no or only marginal indications of a "classical" optical afterglow (e.g., Galama et al. 1998; Malesani et al. 2004; Campana et al. 2006; Pian et al. 2006; Ferrero et al. 2006; Cobb et al. 2006; Mirabal et al. 2006; Modjaz et al. 2006; Sollerman et al. 2006; Kocevski et al. 2007). On the other hand, the prompt emission energy release of these GRBs is orders of magnitude beneath typical Type II events and thus, they cannot be readily compared with each other. The SN emission and, in the case of GRB 031203, the bright host galaxy (Prochaska et al. 2004; Mazzali et al. 2006; Margutti et al. 2007) prevent us from setting definite limits on afterglow emission, thus, they can not be included in our study.

Recently, systematic photometric and spectroscopic observations of GRB host galaxies[21] (see, e.g., Jakobsson et al. 2006f for a short introduction to the VLT survey, and Perley et al. 2009d for first results from the Keck survey) have started to reveal a population of GRBs that are intermediate in luminosity, both in terms of prompt emission and afterglow, lying between most of the GRBs in our optically selected sample and the local universe low-luminosity events mentioned above. These GRBs are defined by low fluence, usually soft spectra (several are XRFs), usually a simple prompt emission light curve, faint or non-existent afterglows and low redshifts ($z \lesssim 1$)[22]. Recently, the existence of this population was inferred theoretically by comparing the distribution of measured redshifts with what is expected if the GRB rate follows the star formation history of the

---

[20] The recently discovered XRF 100316D (Chornock et al. 2010; Starling et al. 2010) does not yet have enough analyses published to be further included here.

[21] We note that, as many of these events were optically dark, their host galaxies are selected via *Swift* X-ray error boxes. This presents problems similar to Type I GRBs, which up to now have host-galaxy determined redshifts exclusively (see Paper II). Indeed, several host galaxy candidates have been ruled out after a refined X-ray analysis (e.g. Perley et al. 2009d). Also, there is the increased possibility of a chance superposition (Cobb & Bailyn 2008; Campisi & Li 2008).

[22] Note that our sample only overlaps in XRF 060218 with the *Swift* long-lag sample presented by Xiao & Schaefer (2009), which they find is not associated with the Local Supercluster (whereas several of our optically selected GRBs, namely GRB 051111, GRB 060502A and GRB 060607A, are in the sample of those authors). Therefore, a long spectral lag is not a common feature of the sample we present here.

universe (Coward et al. 2008). Several examples are included in our sample (XRF 050416A, XRF 060512, GRB 070419A) and have been mentioned above, although these still have afterglows that are relatively bright observationally. Another example is XRF 050824, although this event has an even brighter optical afterglow. We have searched the literature for further examples of these low-redshift events. Similar to our main Type II sample, we compiled their energetics, which are presented in Table 7. This contains ten events from the *Swift* era and three pre-*Swift* events. Next to GRB 980425 and GRB 031203 we have added XRF 020903. The latter burst did have a faint afterglow and showed a spectroscopic (albeit of low significance) and photometric SN signature (Soderberg et al. 2004, 2005a; Bersier et al. 2006). Due to limited publicly available photometry (or no afterglow detection at all), these GRBs can not be included in our main sample either.

Fiore et al. (2007, see also Kistler et al. 2008) speculate that many bright *Swift* GRBs without optical afterglows could be low-z, dust obscured events. Such events clearly exist, GRB 051022 was mentioned above, and other examples are GRB 060814A and GRB 070508. Both were very bright GRBs with bright X-ray afterglows, but they were optically dark (060814A) or faint (070508) and their afterglows were discovered only in the NIR (060814A, Levan et al. 2006) or were very red (070508, Piranomonte et al. 2007). GRB 060814A lies at $z = 0.84$ (Thöne et al. 2007c), GRB 070508 (probably) at $z = 0.82$ (Jakobsson et al. 2007a, but see Fynbo et al. 2009). But the GRBs listed in Table 7 are clearly a different population, although here too, evidence for dust obscuration does exist, e.g. GRB 060202 (at $z = 0.783$), which had a bright X-ray afterglow, was dark even in the K band (Wang et al. 2006), while the X-ray faint GRB 050223 was situated in a dusty, red galaxy (Pellizza et al. 2006). Intrinsic faintness or dust obscuration is undecided in the other cases, but we point out again that this population has low-luminosity prompt emission. This population may partly be responsible for an excess of dark bursts at low gamma-ray peak fluxes, reported by Dai (2009).

In Fig. 9 we show the distribution of the bolometric isotropic energies for the "optically selected" main sample of this paper (which also includes the K06 bursts), the four SN GRBs/XRFs and the low-z low-luminosity sample. All in all, the isotropic energy releases are distributed over six orders of magnitude without gaps, with only GRB 980425 being over one order of magnitude less energetic than the next faintest event (XRF 020903). Clearly, the three samples are quite distinct from each other. The mean (logarithmic) bolometric isotropic energy of the optically selected sample is $\overline{E_{\rm iso,bol}} = 52.88 \pm 0.09$, it is $\overline{E_{\rm iso,bol}} = 51.30 \pm 0.16$ for the low-z sample and $\overline{E_{\rm iso,bol}} = 49.22 \pm 0.43$ for the "SN" sample. A KS-test finds that the optically selected GRBs and the low-z GRBs do not stem from the same sample with high significance ($P = 2.7 \times 10^{-6}$). This low probability is hardly surprising, as the low-z sample was selected according to the criteria of low fluence and low redshift, necessarily implying a low isotropic energy release. We note that the five faintest GRBs (in terms of prompt energy release) in the optical sample all lie at $z < 1$. Next to XRF
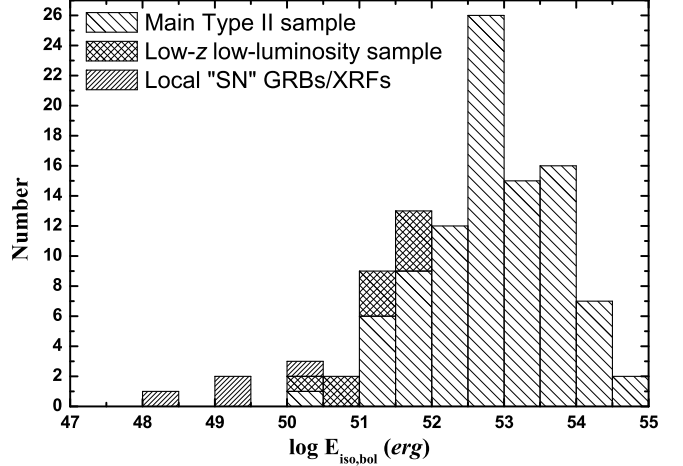
FIG. 9.— The distribution of bolometric isotropic energies for all the GRBs of the "optically selected" main sample of this paper (Table 2) and the low-z low-luminosity events (Table 7) for which we have no optical afterglow information. Here, we also differentiate between the four local "SN" GRBs/XRFs and the new sample which is being uncovered mostly by host galaxy observations. These form an intermediate population between the optically selected sample and the local events with spectroscopic SN signatures.

060512, XRF 050416A, GRB 070419A and XRF 050824 (all mentioned above) this includes XRF 071010A. The latter event, though, has an observationally bright optical afterglow. If we move the first four into the low-z sample, we find $\overline{E_{\rm iso,bol}} = 52.96 \pm 0.08$ for the rest of the optically selected sample and $\overline{E_{\rm iso,bol}} = 51.21 \pm 0.14$ for the larger low-z sample, and the difference becomes even more significant ($P = 7.4 \times 10^{-9}$). On the other hand, the almost continuous distribution of energy releases may indicate that all events are part of a single population that can be described by a single power-law luminosity function. A deeper analysis is beyond the scope of this paper, but it would require an estimation of the true rate of these events, similar to what has been done for the local universe SN events (Pian et al. 2006; Soderberg et al. 2006b; Liang et al. 2007a; Guetta & Della Valle 2007; Virgili et al. 2009).

As pointed out above, most of these low-z events are only now being identified as such due to host galaxy spectroscopy campaigns. These are, of course, biased to low redshift events, both due to host galaxies being observationally brighter and due to effects like the "redshift desert" when the [O II] line moves into the airglow region of the spectrum at $z \gtrsim 1$. Still, it is intriguing that many of the GRBs with new redshift information are not the bright, dust-enshrouded events Fiore et al. (2007) predicted, but a population that falls beneath the "standard energy reservoir" as already pointed out by Kocevski & Butler (2008). These events, being optically dim or even dark, are only observable due to the X-ray localization capabilities of *Swift* (with the flux sensitivity playing a lesser role) which allows discovery of the host galaxy in many cases (although we caution again that the significance some the associations may be questionable). With more host galaxy observation results likely to be published in the future, it is expected that this sample will continue to grow. As most of these redshifts were not found until months after the event, searches for

SN signatures have not been undertaken, so it is as yet unclear if these events are also subluminous (or perhaps superluminous) in terms of their SN explosions (assuming that they truly are related to the deaths of massive stars). But the clear association of events that are even fainter with powerful broad-lined Type Ic SNe indicates that the basic collapsar mechanism will probably also underlie this new population. Future observatories, such as *SVOM* and especially *EXIST*, are predicted to yield much higher detection rates of these subluminous GRBs (Imerito et al. 2008), though we point out that *Fermi* GBM, despite its wide FOV, is not well equipped for this task, as the low localization precision precludes a high identification rate.

4. SUMMARY AND CONCLUSIONS

We have compiled a large amount of optical/NIR photometry of *Swift*-era GRB afterglows, creating a total sample of 76 GRBs (as well as three more pre-*Swift* events), considering events up to the end of September 2009. Following Zeh et al. (2006) and K06, we analyzed the light curves and spectral energy distributions. We also collected data on the energetics of the GRBs. We used this sample to compare the *Swift*-era afterglows to the pre-*Swift* sample taken from K06, and looked for correlations between the optical afterglow luminosity and parameters of the prompt emission. To summarize, we come to the following results.

- As has been found before, observed optical afterglows in the *Swift* era are typically fainter than those of the pre-*Swift* era. The rapid localization and follow-up capabilities available today give us access to this fainter population.

- In terms of luminosity, we find no statistically significant difference between the pre-*Swift* and the *Swift*-era afterglows, the relative faintness of the *Swift*-era afterglows can typically be attributed to a larger mean redshift. But we caution that several selection biases still apply.

- We still find (see also K06) that SMC-like dust is usually preferred and that the line-of-sight extinctions through the GRB host galaxies are usually low. Still, at least one clear case (GRB 070802) of high A_V exists.

- The trend seen in K06 of lower extinction at higher redshifts is confirmed in our new sample, which increases the number of $z > 3$ GRBs from one to 17. We caution though, that the correlation is only weak, and it is still unclear if this is due to a true evolution or to a selection bias.

- The clustering of optical afterglow luminosities at one day reported by K06, Liang & Zhang (2006) and Nardini et al. (2006) is found to be less significant than before, indeed, the spread of magnitudes actually increases in luminosity space due to the discovery of exceptionally over- as well as underluminous events. As the *Swift* sample is less biased than earlier samples, this indicates that the clustering found in pre-*Swift* data may be the result of selection effects only. The bimodal distribution when splitting the afterglows into two redshift bins is confirmed though, but the total sample itself is not found to be bimodally distributed anymore, in agreement with several other recent results.

- Our samples contain all GRBs which have been observed with high-resolution echelle spectroscopy (and have had these results published beyond GCN circulars). Prochter et al. (2006) found a high incidence of strong foreground absorption systems in comparison to a QSO sightline sample. One possible explanation, that these foreground galaxies are gravitationally lensing the afterglow (making them brighter and consequently more accessible to echelle spectroscopy) would imply that the echelle sample is significantly more luminous than other afterglows. We find no evidence for such an increased luminosity, both in comparison between the echelle-observed afterglows and those with low-res spectroscopy only, as well as between those with and without strong foreground absorption systems within the echelle sample. We caution, though, that we are also not able to rule out a low amplification factor.

- We find that an upper boundary on the optical luminosity of a forward-shock driven afterglow seems to exist.

- At very early times, the apparent magnitude spread is much larger than at later times but, intriguingly, half the afterglows strongly cluster within three magnitudes. Basically, there seem to be three classes: optical afterglows with additional early emission components, afterglows dominated by the constant-blastwave-energy forward shock already at early times, and optically faint afterglows that show plateau phases or later rebrightenings (possibly due to energy injections into the forward shock or off-axis viewing geometry). The forward-shock dominated afterglows make up 60% of the sample that had early detections (or late, definite peaks), and the afterglows with additional emission components, which are the most luminous ones, are also the most rare. While there is a trend between the peak time and the peak luminosity of afterglows with fast initial rises, a strong correlation (Panaitescu & Vestrand 2008) is not observed in our larger sample.

- A trend is visible between the isotropic energy release in gamma-rays and the optical luminosity at a fixed late time in the rest frame. The scatter is large, probably due to circumburst density variations, but low-luminosity events support the reality of this trend.

- We propose the existence of a population of low-redshift low-luminosity events that bridge the gap between the Type II GRBs in our main sample (selected due to their optical afterglows) and the "SN" GRBs/XRFs that have been detected in the local universe. These events are optically dim or dark and are being revealed mostly by systematic host galaxy observations which are able to determine that their redshifts are low.

At the time the results of Zeh et al. (2006) and K06 were published, the pre-*Swift* era was a closed chapter and a clear overview of the properties of pre-*Swift* GRB afterglow could be given. The *Swift* era, on the other hand, continues, and with time many more results, larger samples and probably more surprises await us. Therefore, this work and its companion paper (Paper II) can only give a first overview, by nature incomplete, of the less biased sample *Swift* is delivering. And the studies of the properties of dust and the chemical evolution of galaxies in the reionization era, thanks to the high rate of GRBs in the early universe (Yüksel et al. 2008; Kistler et al. 2009; Salvaterra et al. 2009b; Tanvir et al. 2009), has only just begun, and awaits the development of more powerful instruments to study GRB afterglows in the NIR/MIR wavelength regions.

APPENDIX

OBSERVATIONS

- **GRB 040924**: Observations were obtained with the Small and Moderate Aperture Research Telescope System (SMARTS) 1.3m telescope, equipped with the ANDICAM (A Novel Double-Imaging CAMera) detector (only upper limits could be obtained). Detections in R_C were obtained with the 1.5m Russian-Turkish Telescope (RTT150) in Turkey. Calibration was done against Landolt fields.

- **GRB 041006**: Observations were calibrated against comparison stars obtained by Arne Henden[23]. Data were obtained by the 1.5m AZT-22 telescope of the Maidanak observatory in Uzbekistan, equipped with the CCD direct camera, the 0.64m AT-64 telescope of the Crimean Astrophysical Observatory, Ukraine, the 1.34m Schmidt telescope of the Thüringer Landessternwarte Tautenburg (Thuringia State Observatory), Germany, and the RTT150. The results of AT-64 telescope (CrAO) observations were originally presented in Pozanenko et al. (2007).

- **GRB 050315**: Observations were obtained by the SMARTS 1.3m telescope. Imaging was obtained in all possible filters (BVR_CI_CJHK), but the afterglow was only detected in R_C and I_C. The observations were calibrated against Landolt fields.

- **GRB 050319**: We obtained late and deep observations of this afterglow with multiple telescopes. The 2.56m Nordic Optical Telescope, NOT, equipped with the Andalucia Faint Object Spectrograph and Camera (AL-FOSC), the Standby CCD Camera (StanCam) and the NOTCam near-IR camera/spectrograph; the 3.6m Telescope Nazionale Galileo (TNG) equipped with the Low Resolution Spectrograph (LRS) (both telescopes on La Palma in the Canary Islands, Spain); the 1.5m Maidanak and the RTT150. Photometry was obtained using a Henden calibration in the optical. In the K band, we found only a single object (a probable elliptical galaxy) in the small NOTcam FOV which was also significantly detected in the 2MASS K_S band image, but it is too faint to be in the 2MASS catalog. We obtained a zero point of the 2MASS image (standard deviation 0.01 magnitudes) from multiple bright 2MASS sources, measured the single source to be $K_S = 16.07 \pm 0.18$, and used it to derive the zero point of the NOTcam image and determine the afterglow magnitude (adding the statistical errors of the 2MASS and NOTcam magnitudes in quadrature), which is in full agreement with what is expected from the optical afterglow colors.

- **GRB 050401**: Observations (only upper limits could be obtained) were obtained with the SMARTS 1.3m telescope. Calibration was done against Landolt fields.

- **GRB 050408**: Observations were obtained at multiple epochs and in five colors ($UBVR_CI_C$) with the TNG, and a single observation each with the CrAO AT-64 and the Maidanak 1.5m. TNG observations were calibrated against converted magnitudes from the SDSS, while the AT-64 and Maidanak data points used the calibration by Arne Henden.

- **XRF 050416A**: Observations were obtained with the Maidanak 1.5m telescope in BR_C, and have been calibrated against a Henden calibration. Further observations, yielding detections in I_C but only upper limits in J, were obtained with the SMARTS 1.3m, including a late detection of the host galaxy. They were calibrated against Landolt standards.

- **GRB 050502A**: Observations were obtained with the 0.8m IAC80 telescope at Observatorio del Teide, Canary Islands, Spain, the Maidanak 1.5m (shallow upper limit only due to clouds), as well as the 2.5m Isaac Newton Telescope equipped with the Wide Field Camera (WFC) on La Palma. Photometry was performed against a Henden calibration.

- **GRB 050525A**: Observations were obtained with the Southeastern Association for Research in Astronomy (SARA) 0.9m telescope at Kitt Peak National Observatory (KPNO), Arizona, USA, the 0.4m telescope of Ussuriysk Astrophysical Observatory (UAPhO) in the far east of Russia, the CrAO AT-64, the Maidanak 1.5m, the SMARTS 1.3m and the RTT150. Observations were calibrated against Landolt standards (RTT150) and against a calibration by Arne Henden. We detect the afterglow in SMARTS, SARA and RTT150 observations, and obtain upper limits otherwise, with a very deep upper limit from the Maidanak telescope. Some of the results of Maidanak 1.5m and CrAO observations were previously presented in Pozanenko et al. (2007).

- **GRB 050730**: Observations were obtained by the SMARTS 1.3m (only upper limits, detections are presented in Pandey et al. 2006) and the RTT150, from which we obtained detections in the R_C and I_C bands. Observations were calibrated against Landolt standards.

---

[23] The calibration files of Arne Henden have been downloaded at ftp://ftp.aavso.org/public/calib/grb. The files have the names "grb******.dat", where ****** is the date of the GRB, e.g., "grb041006.dat"

- **GRB 050801**: Observations were obtained by the Danish 1.54m telescope at La Silla Observatory, Chile, equipped with the Danish Faint Object Spectrograph and Camera (DFOSC), and with the SMARTS 1.3m. Calibrations in BVI_C were done using five stars each from Ovaldsen et al. (2007), calibration in R_C was done against Landolt field stars observed near the GRB time with the D1.54m, and calibration in JK was done against five 2MASS sources.

- **GRB 050802**: We obtained a large data set on this GRB, the only (beyond the GCN) ground-based observations published so far. Observations were obtained with the 1.5m telescope of the Sierra Nevada Observatory (OSN), Spain, the 2.6m Shajn telescope of the Crimean Astrophysical Observatory, the NOT, the TNG, and the Maidanak 1.5m. Photometry was performed against a Henden calibration.

- **GRB 050820A**: Optical observations were obtained with the UAPhO 0.4m, the Maidanak 1.5m, the Shajn 2.6m and the RTT150. NIR observations were obtained with the TNG and the NICS (Near-Infrared Camera and Spectrometer) detector as well as with the 3.8m United Kingdom Infra-Red Telescope (UKIRT) on Mauna Kea, Hawaii, USA and the University of Wyoming's 2.3m Wyoming Infrared Observatory telescope. Optical data were calibrated against a Henden calibration, while the NIR data were calibrated against 2MASS. WIRO data were strongly affected by weather and detector systematics, while the statistical error are small (≤ 0.06 magnitudes), we added an 0.1 magnitude error in quadrature to account for this; still, some scatter remains. Special care was taken with the late, deep Shajn observation, which was affected strongly by bad seeing, where we used the PSF of a nearby, bright, unsaturated star as a model to subtract the two nearby stars. Still, residuals remain and no significant source could be found at the afterglow position. We place a conservative upper limit of $R_C > 23$ on the afterglow magnitude, which is not constraining.

- **GRB 050908**: A single data point was obtained with the Maidanak 1.5m. Photometry was performed against the USNO A2.0 catalog.

- **GRB 050922C**: We obtained a very large data set, using the Zeiss-600 (0.6m) telescope of the Mt. Terskol observatory, Kabardino-Balkarija, Russia, the 1.3 m McGraw-Hill Telescope at the MDM Observatory, part of KPNO, the 8.2m European Southern Observatory Very Large Telescope (ESO VLT) at Paranal Observatory, Chile, the 4.2m William Herschel Telescope (WHT) on La Palma, the NOT, the D1.54m, and the INT. Data were calibrated using a Henden calibration.

- **GRB 051109A**: A single data point was obtained with the 0.38m K-380 telescope of CrAO. Photometry was performed against the USNO A2.0 catalog, and compares well with the data of Yost et al. (2007a).

- **GRB 051111**: We obtained data with the SARA and Maidanak 1.5m telescopes, and calibrated against the USNOB1.0 catalog. They agree well with other published data.

- **GRB 060206**: We obtained data with the SARA and Maidanak 1.5m telescopes, and calibrated against the USNOB1.0 catalog. They agree well with other published data.

- **GRB 060418**: Observations were obtained by the SMARTS 1.3m and the Maidanak 1.5m telescopes, yielding detections in seven filters (BVR_CI_CJHK). SMARTS observations were calibrated with Landolt stars, while for the Maidanak observations, a Henden calibration was used.

- **XRF 060512**: Observations were obtained with the NOT and NOTcam. They were calibrated against the single 2MASS star in the small FOV.

- **GRB 060607A**: Observations were obtained with the SMARTS 1.3m, yielding detections in all seven filters. Photometry was performed against Landolt standards.

- **GRB 060714**: Observations were obtained with the SMARTS 1.3m. Photometry was performed against 22 USNO-B1.0 stars in the I_C band and six 2MASS stars in the J band. Note that the I_C magnitude is too faint compared with what is expected from the R_C band, this may be due to a systematic offset in the USNO catalog.

- **GRB 060729**: Observations were obtained with the SMARTS 1.3m. Photometry was performed against Landolt standards.

- **GRB 060904B**: Observations were obtained with the RTT150, SNUCAM (Im et al. 2010)on the Maidanak 1.5m and the SMARTS 1.3m. The RTT150 observations were performed starting just eight minutes after the GRB, during dawn twilight, leading to large uncertainties especially in the B and V filters. The observations were calibrated against Landolt stars (RTT150, SMARTS) and the USNO A2.0 catalog, the latter agrees well.

- **GRB 060908**: A single observation was obtained with the Zeiss-2000 (2.0m) telescope of the Mt. Terskol observatory, under very bad seeing conditions, leading to a marginal detection which nonetheless agrees well with other data. Two observations obtained with the Maidanak telescope yielded upper limits only. We also present one UKIRT K-band detection which is not included in Covino et al. (2010). Images were calibrated against comparison stars provided by S. Covino, and UKIRT data against 2MASS stars.

- **GRB 060927**: A single observation (upper limit only) was obtained with the 1.25m AZT-11 telescope of the Crimean Astrophysical Observatory. The observation were calibrated against the USNO A2.0 catalog.

- **GRB 061007**: Observations were obtained with the SMARTS 1.3m. They were calibrated against comparison stars taken from Mundell et al. (2007b) in the optical and against 2MASS stars in the NIR.

- **GRB 061121**: Observations were obtained with the SMARTS 1.3m and the Shajn 2.6m telescope. SMARTS observations were calibrated against Landolt standards, while Shajn observations were calibrated against a set of stars provided by D.M.

- **GRB 070125**: Observations were obtained with the SMARTS 1.3m. In $BVRI$, we calibrated the afterglow against eight standard stars from Updike et al. (2008b), in JHK, we used four 2MASS stars.

- **GRB 070208**: A single data point was obtained with the AZT-33IK (1.5m) telescope of the Sayan Observatory, Mondy, Siberia, Russia. The observation was calibrated against the SDSS catalog and agrees well with other data. A nearby galaxy was removed via mask-subtraction. Analysis of the photometric redshift of this galaxy (from SDSS data) obtained with HyperZ code (Bolzonella et al. 2000) reveals two minima, at $z = 0.52$ ($\chi_\nu^2 = 0.47$) and $z = 0.07$ ($\chi_\nu^2 = 0.98$), indicating that this is clearly not the host galaxy but a foreground absorber. It did not fall in the slit during the spectroscopy reported by Cucchiara et al. (2007a), and no absorption lines from this system are reported either.

- **GRB 070419A**: Two observations were obtained with the SARA 0.9m telescope, resulting in a shallow limit and a marginal detection, as well as an upper limit from the Sayan telescope. Data were calibrated against the USNOB1.0 catalog.

- **GRB 071020**: Observations were obtained with the SARA 0.9m, the 0.7m AZT-8 telescope of the Crimean Astrophysical Observatory, and the 0.6m Zeiss-600 telescope of the Maidanak observatory. The observations were calibrated against the SDSS.

- **XRF 071031**: Observations were obtained with the SMARTS 1.3m. They were calibrated against Landolt standards, and in some cases shifted slightly in zero-point to bring them into agreement with the data set of Krühler et al. (2009a).

- **GRB 080129**: Observations were obtained with the SMARTS 1.3m. This GRB was highly extinct, and no detections were achieved. The observations were calibrated with Landolt standards.

- **GRB 080210**: A single data point was obtained with the Sayan 1.5m telescope. The observation was calibrated against the SDSS catalog. It implies a possible rebrightening in the light curve.

- **XRF 080310**: Observations were obtained with the SMARTS 1.3m. They were calibrated against Landolt standards.

- **XRF 080330**: Observations were obtained with the SMARTS 1.3m and the Terskol 2m. They were calibrated against Landolt standards (SMARTS) and SDSS standards transformed to the Johnson-Cousins R_C band (Terskol).

- **GRB 080413A**: Observations were obtained with the SMARTS 1.3m. They were calibrated against Landolt standards.

- **GRB 080810**: Observations were obtained with the Maidanak, Sayan, AZT-8, Z-600 and RTT150 (TFOSC in the first and second epochs, and the Andor CCD in the third epoch) telescopes. They were calibrated against SDSS standards, except for the RTT150 data, which was calibrated against a Landolt standard star, and slightly adjusted to agree with the zero point of Page et al. (2009).

- **GRB 081008**: Observations were obtained with the SMARTS 1.3m. They were calibrated against Landolt standards (VI_C), 2MASS (JHK) and the USNOB1.0 catalog (BR_C) Additionally, the B data were made brighter by 0.25 mags to bring it into accordance with the zero point for Yuan et al. (2010).

- **GRB 090323**: Observations were obtained with the RTT150, the Shajn telescope, the TLS 1.34m (upper limit not used in McBreen et al. 2010) and the NOT, and calibrated against SDSS standards, either directly (RTT150) or transformed to the Johnson-Cousins bands.

- **GRB 090424**: Observations were obtained with the TLS 1.34m, the Maidanak 1.5m, and with the 1.23m Spanish telescope and the 2.2m telescope of the Centro Astronómico Hispano-Alemán (CAHA), Spain. They were calibrated against SDSS standards transformed to the Johnson-Cousins bands.

TABLE 1
Afterglow Photometry

GRB	Days after trigger (midtime)	Magnitude	Filter	Telescope
040924	0.754109	> 21.20	B	SMARTS
	0.754109	> 20.80	V	SMARTS
	0.373410	21.76 ± 0.09	R_C	RTT150
	0.390927	21.96 ± 0.10	R_C	RTT150
	0.406554	22.06 ± 0.11	R_C	RTT150
	0.422177	21.93 ± 0.09	R_C	RTT150
	0.439080	22.05 ± 0.10	R_C	RTT150
	0.454699	22.12 ± 0.10	R_C	RTT150
	0.470325	22.16 ± 0.09	R_C	RTT150
	0.485950	22.03 ± 0.08	R_C	RTT150
	0.501575	22.27 ± 0.09	R_C	RTT150
	0.517200	22.40 ± 0.10	R_C	RTT150
	0.532824	22.35 ± 0.10	R_C	RTT150
	0.548449	22.53 ± 0.12	R_C	RTT150
	0.564073	22.45 ± 0.11	R_C	RTT150
	0.579696	22.26 ± 0.10	R_C	RTT150
	0.595326	22.31 ± 0.09	R_C	RTT150
	0.610963	22.43 ± 0.16	R_C	RTT150
	0.754109	> 21.10	R_C	SMARTS
	1.498760	23.47 ± 0.21	R_C	RTT150
	2.700000	23.80 ± 0.67	R_C	RTT150
	0.754109	> 20.30	I_C	SMARTS
	0.754109	> 18.30	J	SMARTS
	0.754109	> 17.40	J	SMARTS
	0.754109	> 19.80	K	SMARTS
041006	0.162080	19.93 ± 0.03	B	Maidanak
	0.175120	20.08 ± 0.03	B	Maidanak
	1.182500	> 20.00	B	Maidanak
	0.158010	19.78 ± 0.04	V	Maidanak
	0.165840	19.74 ± 0.05	V	Maidanak
	0.179050	19.75 ± 0.05	V	Maidanak
	1.186460	> 21.00	V	Maidanak
	0.147850	19.23 ± 0.05	R_C	Maidanak
	0.151600	19.23 ± 0.05	R_C	Maidanak
	0.168990	19.19 ± 0.06	R_C	Maidanak
	0.183240	19.52 ± 0.06	R_C	Maidanak
	0.188080	19.44 ± 0.11	R_C	Maidanak
	0.297400	$19.80^{+0.33}_{-0.26}$	R_C	AT-64
	1.178480	> 21.00	R_C	Maidanak
	1.337000	> 20.40	R_C	AT-64
	1.444000	22.06 ± 0.23	R_C	TLS
	4.298870	$23.30^{+0.35}_{-0.27}$	R_C	Maidanak
	6.330470	> 23.30	R_C	Maidanak
	7.276300	> 23.00	R_C	Maidanak
	8.468400	23.80 ± 0.25	R_C	RTT150
	12.41340	24.10 ± 0.20	R_C	RTT150
	0.154190	18.89 ± 0.07	I_C	Maidanak
	0.171910	19.11 ± 0.11	I_C	Maidanak
	1.190430	> 21.00	I_C	Maidanak
050315	0.496574	> 21.50	B	SMARTS
	0.496574	> 21.10	V	SMARTS
	0.496574	20.90 ± 0.2	R_C	SMARTS
	1.491458	> 21.10	R_C	SMARTS
	2.506655	22.0 ± 0.1	R_C	SMARTS
	0.496574	20.70 ± 0.3	I_C	SMARTS
	1.491458	> 20.00	I_C	SMARTS
	0.496574	> 17.40	J	SMARTS
	1.491458	> 17.50	J	SMARTS
	2.506655	> 19.60	J	SMARTS
	0.496574	> 17.40	H	SMARTS
	0.496574	> 16.80	K	SMARTS
050319	0.331	21.09 ± 0.08	B	Maidanak
	0.498	21.42 ± 0.07	B	Maidanak
	0.662	21.81 ± 0.16	B	NOT
	3.645	> 22.50	B	NOT
	10.36	> 22.60	B	Maidanak
	11.334	> 22.70	B	Maidanak
	4.636	22.99 ± 0.12	V	TNG
	0.337	19.96 ± 0.03	R_C	Maidanak
	0.379504	20.09 ± 0.04	R_C	RTT150
	0.447	20.18 ± 0.06	R_C	Maidanak
	0.646	20.43 ± 0.05	R_C	NOT
	1.482	20.90 ± 0.13	R_C	NOT
	1.512	21.22 ± 0.09	R_C	Maidanak
	1.615763	> 21.10	R_C	RTT150

TABLE 1 — *Continued*

GRB	Days after trigger (midtime)	Magnitude	Filter	Telescope
	2.353264	> 21.10	R_C	RTT150
	2.478	21.31 ± 0.09	R_C	Maidanak
	3.383	21.77 ± 0.13	R_C	Maidanak
	3.660	21.83 ± 0.2	R_C	NOT
	4.717	22.38 ± 0.12	R_C	NOT
	5.636	22.32 ± 0.25	R_C	NOT
	7.600	23.41 ± 0.15	R_C	NOT
	9.336	> 20.5	R_C	Maidanak
	10.33	> 23.50	R_C	Maidanak
	11.305	> 23.40	R_C	Maidanak
	11.506	24.30 ± 0.3	R_C	TNG
	19.52	> 24.70	R_C	NOT
	0.670	20.19 ± 0.05	I_C	NOT
	3.675	21.61 ± 0.11	I_C	NOT
	4.685	21.93 ± 0.05	I_C	TNG
	6.545	20.17 ± 0.27	K	NOT
050401	0.683773	> 22.30	I_C	SMARTS
	0.683773	> 19.90	J	SMARTS
050408	0.3177	22.90 ± 0.22	U	TNG
	0.3224	22.50 ± 0.14	U	TNG
	0.3333	23.06 ± 0.05	B	TNG
	0.3413	23.07 ± 0.05	B	TNG
	0.3457	22.32 ± 0.06	V	TNG
	0.3482	22.37 ± 0.06	V	TNG
	0.1908	21.38 ± 0.05	R_C	TNG
	0.1931	21.41 ± 0.04	R_C	TNG
	0.1953	21.41 ± 0.04	R_C	TNG
	0.2641	21.50 ± 0.02	R_C	TNG
	0.2667	21.47 ± 0.02	R_C	TNG
	0.2692	21.52 ± 0.02	R_C	TNG
	0.2718	21.52 ± 0.03	R_C	TNG
	0.2743	21.54 ± 0.03	R_C	TNG
	0.2769	21.51 ± 0.03	R_C	TNG
	0.2794	21.58 ± 0.03	R_C	TNG
	0.2819	21.57 ± 0.03	R_C	TNG
	0.2845	21.55 ± 0.03	R_C	TNG
	0.2871	21.52 ± 0.03	R_C	TNG
	0.2897	21.61 ± 0.03	R_C	TNG
	0.2922	21.60 ± 0.03	R_C	TNG
	0.2948	21.58 ± 0.02	R_C	TNG
	0.2973	21.55 ± 0.03	R_C	TNG
	0.2999	21.54 ± 0.03	R_C	TNG
	0.3024	21.60 ± 0.03	R_C	TNG
	0.3049	21.66 ± 0.03	R_C	TNG
	0.3075	21.59 ± 0.03	R_C	TNG
	0.3101	21.64 ± 0.03	R_C	TNG
	0.3127	21.66 ± 0.03	R_C	TNG
	0.3515	21.71 ± 0.03	R_C	TNG
	0.3540	21.79 ± 0.03	R_C	TNG
	0.4887	22.15 ± 0.08	R_C	TNG
	0.4926	22.21 ± 0.11	R_C	TNG
	1.145	22.55 ± 0.35	R_C	Maidanak
	1.333	23.25 ± 0.11	R_C	TNG
	3.2225	23.95 ± 0.10	R_C	TNG
	9.3041	> 24.19	R_C	TNG
	10.4397	> 23.33	R_C	TNG
	0.09038	> 19.9	CR	AT-64
	0.3573	21.13 ± 0.04	I_C	TNG
	0.3598	21.12 ± 0.04	I_C	TNG
050416A	0.219560	22.93 ± 0.17	B	Maidanak
	0.239560	23.29 ± 0.24	B	Maidanak
	0.190819	21.84 ± 0.10	R_C	Maidanak
	0.198459	21.74 ± 0.08	R_C	Maidanak
	0.207778	22.01 ± 0.11	R_C	Maidanak
	0.257384	22.09 ± 0.08	R_C	Maidanak
	0.268833	22.11 ± 0.11	R_C	Maidanak
	0.329733	22.54 ± 0.13	R_C	Maidanak
	0.341181	22.33 ± 0.10	R_C	Maidanak
	0.353243	22.34 ± 0.13	R_C	Maidanak
	0.365339	22.46 ± 0.13	R_C	Maidanak
	0.377389	22.95 ± 0.21	R_C	Maidanak
	1.271000	> 21.70	R_C	Maidanak
	0.705156	21.90 ± 0.1	I_C	SMARTS
	13.672101	22.40 ± 0.3	I_C	SMARTS
	0.705156	> 19.80	J	SMARTS
	13.672101	> 19.60	J	SMARTS

TABLE 1 — *Continued*

GRB	Days after trigger (midtime)	Magnitude	Filter	Telescope
050502A	0.0309	18.62 ± 0.07	R_C	IAC80
	0.0385	18.78 ± 0.10	R_C	IAC80
	0.0463	19.04 ± 0.08	R_C	IAC80
	0.700	> 16.52	R_C	Maidanak
	1.8347	25.31 ± 0.35	R_C	INT
050525A	0.214768	19.76 ± 0.13	B	SMARTS
	0.214768	19.05 ± 0.11	V	SMARTS
	1.017721	21.17 ± 0.23	V	RTT150
	0.19262	18.60 ± 0.09	R_C	SARA
	0.19985	18.62 ± 0.08	R_C	SARA
	0.2071	18.73 ± 0.09	R_C	SARA
	0.21434	18.75 ± 0.11	R_C	SARA
	0.214768	18.71 ± 0.07	R_C	SMARTS
	0.22159	18.78 ± 0.10	R_C	SARA
	0.22883	18.77 ± 0.09	R_C	SARA
	0.23608	18.77 ± 0.09	R_C	SARA
	0.24332	18.83 ± 0.10	R_C	SARA
	0.25119	18.83 ± 0.09	R_C	SARA
	0.25844	18.94 ± 0.10	R_C	SARA
	0.26568	19.00 ± 0.10	R_C	SARA
	0.27293	19.06 ± 0.12	R_C	SARA
	0.28380	19.51 ± 0.11	R_C	SARA
	0.580637	> 15.90	R_C	UAPhO
	0.816053	> 19.50	R_C	AT-64
	1.063808	21.76 ± 0.18	R_C	RTT150
	6.002	> 24.10	R_C	Maidanak
	0.214768	18.34 ± 0.07	I_C	SMARTS
	2.269375	> 21.4	I_C	SMARTS
	0.214768	17.23 ± 0.09	J	SMARTS
	0.214768	16.57 ± 0.13	H	SMARTS
	0.214768	15.62 ± 0.16	K	SMARTS
050730	0.96308	> 23.03	B	RTT150
	0.96618	> 22.91	V	RTT150
	11.189595	> 21.2	V	SMARTS
	0.95858	21.70 ± 0.17	R_C	RTT150
	0.97138	20.47 ± 0.05	I_C	RTT150
	0.118067	> 16.60	I_C	SMARTS
	10.165579	> 22.10	I_C	SMARTS
	11.189595	> 20.80	I_C	SMARTS
	10.165579	> 19.90	J	SMARTS
	11.189595	> 18.90	J	SMARTS
	11.189595	> 17.20	K	SMARTS
050801	0.227426	21.96 ± 0.05	B	D1.54
	0.231018	21.17 ± 0.05	V	SMARTS
	0.242648	21.19 ± 0.07	V	D1.54
	0.250137	21.26 ± 0.05	V	D1.54
	0.219763	20.77 ± 0.05	R_C	D1.54
	0.234904	20.85 ± 0.04	R_C	D1.54
	1.242030	23.06 ± 0.12	R_C	D1.54
	2.265063	> 23.70	R_C	D1.54
	0.231018	20.36 ± 0.05	I_C	SMARTS
	3.271133	> 21.1	I_C	SMARTS
	0.231018	18.87 ± 0.13	J	SMARTS
	3.271133	> 18.8	J	SMARTS
	0.231018	17.36 ± 0.27	K	SMARTS
	3.271133	> 17.0	K	SMARTS
050802	0.3690	21.36 ± 0.08	B	Shajn
	0.3847	21.45 ± 0.08	B	Shajn
	0.3955	21.66 ± 0.08	B	Shajn
	0.4077	21.60 ± 0.08	B	Shajn
	0.4288	21.63 ± 0.08	B	Shajn
	0.495	21.51 ± 0.12	B	OSN
	0.499	21.56 ± 0.14	B	OSN
	0.506	21.72 ± 0.05	B	TNG
	1.519	23.37 ± 0.53	B	NOT
	2.495461	> 23.30	B	Shajn
	0.3606	20.94 ± 0.08	V	Shajn
	0.3652	20.93 ± 0.08	V	Shajn
	0.3702	21.01 ± 0.08	V	Shajn
	0.3753	21.14 ± 0.08	V	Shajn
	0.4011	21.10 ± 0.06	V	Shajn
	0.4087	21.21 ± 0.06	V	Shajn
	0.4191	21.06 ± 0.06	V	Shajn
	0.4259	21.32 ± 0.06	V	Shajn
	0.4355	21.20 ± 0.06	V	Shajn
	0.478	21.30 ± 0.14	V	OSN

TABLE 1 — *Continued*

GRB	Days after trigger (midtime)	Magnitude	Filter	Telescope
	0.483	21.35 ± 0.17	V	OSN
	0.501	21.55 ± 0.09	V	TNG
	1.484	22.98 ± 0.11	V	TNG
	2.3648	23.24 ± 0.18	V	Shajn
	0.23764	20.06 ± 0.15	R_C	Maidanak
	0.24139	20.22 ± 0.13	R_C	Maidanak
	0.24709	20.14 ± 0.10	R_C	Maidanak
	0.25079	20.18 ± 0.09	R_C	Maidanak
	0.25543	20.35 ± 0.11	R_C	Maidanak
	0.25912	20.29 ± 0.10	R_C	Maidanak
	0.26331	20.26 ± 0.10	R_C	Maidanak
	0.26712	20.29 ± 0.10	R_C	Maidanak
	0.27336	20.40 ± 0.11	R_C	Maidanak
	0.27855	20.40 ± 0.11	R_C	Maidanak
	0.28256	20.51 ± 0.12	R_C	Maidanak
	0.28735	20.40 ± 0.11	R_C	Maidanak
	0.29116	20.49 ± 0.12	R_C	Maidanak
	0.3618	20.76 ± 0.10	R_C	Shajn
	0.3663	20.61 ± 0.10	R_C	Shajn
	0.3713	20.58 ± 0.10	R_C	Shajn
	0.3763	20.58 ± 0.10	R_C	Shajn
	0.4029	20.91 ± 0.08	R_C	Shajn
	0.4105	20.64 ± 0.08	R_C	Shajn
	0.4128	20.71 ± 0.08	R_C	Shajn
	0.4205	20.80 ± 0.08	R_C	Shajn
	0.4275	20.81 ± 0.08	R_C	Shajn
	0.4373	20.87 ± 0.08	R_C	Shajn
	0.467	20.98 ± 0.15	R_C	NOT
	0.498	21.12 ± 0.07	R_C	TNG
	0.559	21.12 ± 0.16	R_C	NOT
	1.275671	22.50 ± 0.19	R_C	Maidanak
	1.529	22.64 ± 0.22	R_C	NOT
	2.244421	> 23.10	R_C	Maidanak
	2.4188	> 23.0	R_C	Shajn
	2.462	23.15 ± 0.22	R_C	NOT
	2.547	23.19 ± 0.27	R_C	Shajn
	3.247893	> 23.10	R_C	Maidanak
	212.729	25.51 ± 0.46	R_C	NOT
	0.3628	20.20 ± 0.13	I_C	Shajn
	0.3674	20.36 ± 0.13	I_C	Shajn
	0.3731	20.33 ± 0.13	I_C	Shajn
	0.3772	19.95 ± 0.13	I_C	Shajn
	0.4052	20.33 ± 0.10	I_C	Shajn
	0.4222	20.35 ± 0.10	I_C	Shajn
	0.4291	20.55 ± 0.10	I_C	Shajn
	0.4314	20.56 ± 0.10	I_C	Shajn
	0.4394	20.55 ± 0.10	I_C	Shajn
	0.487	20.75 ± 0.19	I_C	OSN
	0.491	20.70 ± 0.20	I_C	OSN
	0.493	20.56 ± 0.13	I_C	TNG
	1.526	22.13 ± 0.19	I_C	TNG
	1.544	22.38 ± 0.30	I_C	NOT
	2.4058	22.87 ± 0.32	I_C	Shajn
050820A	1.705417	21.00 ± 0.06	B	RTT150
	2.682917	22.24 ± 0.06	B	RTT150
	3.64875	22.57 ± 0.08	B	RTT150
	0.49479	> 15.30	R_C	UAPhO
	0.49733	18.78 ± 0.14	R_C	Maidanak
	0.56417	19.11 ± 0.23	R_C	Maidanak
	0.6349	19.44 ± 0.10	R_C	Maidanak
	0.64389	19.38 ± 0.14	R_C	Maidanak
	0.65423	19.19 ± 0.12	R_C	Maidanak
	0.66078	19.46 ± 0.12	R_C	Maidanak
	0.66841	19.33 ± 0.13	R_C	Maidanak
	0.752083	19.48 ± 0.01	R_C	RTT150
	1.58598	20.41 ± 0.35	R_C	Maidanak
	1.725833	20.38 ± 0.05	R_C	RTT150
	2.55723	20.96 ± 0.38	R_C	Maidanak
	2.684583	21.02 ± 0.03	R_C	RTT150
	3.655	21.30 ± 0.04	R_C	RTT150
	4.56812	21.12 ± 0.14	R_C	Maidanak
	5.53013	21.24 ± 0.20	R_C	Maidanak
	7.677083	22.14 ± 0.10	R_C	RTT150
	13.5247	> 23.00	R_C	Shajn
	1.73125	19.83 ± 0.07	I_C	RTT150
	2.68875	20.46 ± 0.05	I_C	RTT150
	3.659167	20.87 ± 0.09	I_C	RTT150

Kann et al.

TABLE 1 — *Continued*

GRB	Days after trigger (midtime)	Magnitude	Filter	Telescope
	0.070425	16.01 ± 0.10	J	WIRO
	0.081250	16.39 ± 0.02	J	UKIRT
	0.087207	16.30 ± 0.10	J	WIRO
	0.093731	16.50 ± 0.11	J	WIRO
	0.105986	17.04 ± 0.12	J	WIRO
	0.118947	16.62 ± 0.10	J	WIRO
	0.126404	16.67 ± 0.10	J	WIRO
	0.137795	16.69 ± 0.10	J	WIRO
	0.153087	16.74 ± 0.10	J	WIRO
	0.164213	16.87 ± 0.10	J	WIRO
	0.174285	16.94 ± 0.10	J	WIRO
	0.186502	16.76 ± 0.10	J	WIRO
	0.198318	16.74 ± 0.10	J	WIRO
	0.207129	16.66 ± 0.10	J	WIRO
	0.923065	18.48 ± 0.08	J	TNG
	2.052929	18.68 ± 0.10	J	WIRO
	2.304583	19.55 ± 0.16	J	UKIRT
	0.083750	15.88 ± 0.02	H	UKIRT
	0.938955	17.71 ± 0.05	H	TNG
	2.300000	19.25 ± 0.17	H	UKIRT
	0.085833	15.33 ± 0.06	K	UKIRT
	0.119583	15.51 ± 0.02	K	UKIRT
	0.255833	16.26 ± 0.02	K	UKIRT
	0.818750	17.03 ± 0.06	K	UKIRT
	0.950885	16.97 ± 0.21	K	TNG
	1.187500	17.45 ± 0.05	K	UKIRT
	2.289167	18.18 ± 0.09	K	UKIRT
	3.805000	19.32 ± 0.18	K	UKIRT
050908	0.669086	21.88 ± 0.25	R_C	Maidanak
050922C	0.0864	18.66 ± 0.02	B	NOT
	0.0958	18.75 ± 0.02	B	NOT
	0.3348	20.48 ± 0.02	B	MDM
	0.3527	20.53 ± 0.05	B	D1.54
	0.3542	20.50 ± 0.03	B	MDM
	0.4340	20.90 ± 0.04	B	MDM
	0.4722	20.92 ± 0.04	B	MDM
	1.1802	22.34 ± 0.05	B	VLT
	1.3148	22.50 ± 0.07	B	MDM
	2.3118	23.35 ± 0.15	B	MDM
	2.3596	23.14 ± 0.12	B	MDM
	1.1713	22.00 ± 0.02	V	VLT
	0.0086180	15.98 ± 0.04	R_C	Terskol06
	0.0093124	16.05 ± 0.05	R_C	Terskol06
	0.0100184	16.08 ± 0.05	R_C	Terskol06
	0.0107129	16.12 ± 0.05	R_C	Terskol06
	0.0114073	16.11 ± 0.06	R_C	Terskol06
	0.0121018	16.22 ± 0.05	R_C	Terskol06
	0.0127962	16.26 ± 0.05	R_C	Terskol06
	0.0134907	16.23 ± 0.06	R_C	Terskol06
	0.0141851	16.36 ± 0.07	R_C	Terskol06
	0.0148796	16.43 ± 0.07	R_C	Terskol06
	0.0155740	16.35 ± 0.06	R_C	Terskol06
	0.0169629	16.44 ± 0.07	R_C	Terskol06
	0.0176573	16.39 ± 0.06	R_C	Terskol06
	0.0183518	16.46 ± 0.07	R_C	Terskol06
	0.0190462	16.29 ± 0.15	R_C	Terskol06
	0.0197407	16.52 ± 0.08	R_C	Terskol06
	0.0204351	16.48 ± 0.07	R_C	Terskol06
	0.0211296	16.52 ± 0.07	R_C	Terskol06
	0.0218356	16.51 ± 0.08	R_C	Terskol06
	0.0225300	16.62 ± 0.08	R_C	Terskol06
	0.0232245	16.66 ± 0.08	R_C	Terskol06
	0.0239189	16.62 ± 0.09	R_C	Terskol06
	0.0246134	16.65 ± 0.08	R_C	Terskol06
	0.0253078	16.67 ± 0.09	R_C	Terskol06
	0.0280856	16.75 ± 0.11	R_C	Terskol06
	0.0287800	16.86 ± 0.10	R_C	Terskol06
	0.0294745	16.94 ± 0.11	R_C	Terskol06
	0.0301689	16.88 ± 0.09	R_C	Terskol06
	0.0308634	16.75 ± 0.08	R_C	Terskol06
	0.0315578	16.95 ± 0.13	R_C	Terskol06
	0.0322522	17.08 ± 0.13	R_C	Terskol06
	0.0329467	16.90 ± 0.11	R_C	Terskol06
	0.0336527	16.99 ± 0.13	R_C	Terskol06
	0.0343472	16.89 ± 0.12	R_C	Terskol06
	0.0350416	16.87 ± 0.10	R_C	Terskol06

TABLE 1 — *Continued*

GRB	Days after trigger (midtime)	Magnitude	Filter	Telescope
	0.0357360	16.87 ± 0.10	R_C	Terskol06
	0.0364305	17.07 ± 0.12	R_C	Terskol06
	0.0371249	16.98 ± 0.11	R_C	Terskol06
	0.0378194	17.26 ± 0.17	R_C	Terskol06
	0.0380	17.08 ± 0.02	R_C	NOT
	0.0385138	17.10 ± 0.13	R_C	Terskol06
	0.0392083	17.05 ± 0.13	R_C	Terskol06
	0.0399027	16.98 ± 0.11	R_C	Terskol06
	0.0405972	17.03 ± 0.11	R_C	Terskol06
	0.0412916	16.97 ± 0.12	R_C	Terskol06
	0.0419860	17.31 ± 0.15	R_C	Terskol06
	0.0426805	17.05 ± 0.13	R_C	Terskol06
	0.0433749	17.11 ± 0.12	R_C	Terskol06
	0.0440694	17.21 ± 0.14	R_C	Terskol06
	0.0447754	17.06 ± 0.13	R_C	Terskol06
	0.0454698	17.19 ± 0.14	R_C	Terskol06
	0.0461643	17.32 ± 0.16	R_C	Terskol06
	0.0468587	17.03 ± 0.11	R_C	Terskol06
	0.0475532	17.19 ± 0.12	R_C	Terskol06
	0.0482476	17.09 ± 0.13	R_C	Terskol06
	0.0489421	17.22 ± 0.16	R_C	Terskol06
	0.0496365	17.36 ± 0.16	R_C	Terskol06
	0.0503310	17.45 ± 0.17	R_C	Terskol06
	0.0510254	17.00 ± 0.11	R_C	Terskol06
	0.0517198	17.40 ± 0.19	R_C	Terskol06
	0.0524143	17.33 ± 0.20	R_C	Terskol06
	0.0531087	17.33 ± 0.17	R_C	Terskol06
	0.0538032	17.22 ± 0.13	R_C	Terskol06
	0.0544976	17.43 ± 0.19	R_C	Terskol06
	0.0551921	17.62 ± 0.22	R_C	Terskol06
	0.0558981	17.61 ± 0.25	R_C	Terskol06
	0.0565925	17.29 ± 0.19	R_C	Terskol06
	0.0572870	17.80 ± 0.27	R_C	Terskol06
	0.0579814	17.69 ± 0.23	R_C	Terskol06
	0.0586759	17.68 ± 0.24	R_C	Terskol06
	0.0593703	17.51 ± 0.19	R_C	Terskol06
	0.0600647	17.78 ± 0.31	R_C	Terskol06
	0.0607592	17.43 ± 0.19	R_C	Terskol06
	0.0614536	17.45 ± 0.22	R_C	Terskol06
	0.0621481	17.73 ± 0.27	R_C	Terskol06
	0.0628425	17.27 ± 0.17	R_C	Terskol06
	0.0635370	17.13 ± 0.24	R_C	Terskol06
	0.0642314	17.55 ± 0.22	R_C	Terskol06
	0.0649259	17.67 ± 0.31	R_C	Terskol06
	0.0656203	17.50 ± 0.28	R_C	Terskol06
	0.0663147	17.30 ± 0.25	R_C	Terskol06
	0.0677152	17.56 ± 0.67	R_C	Terskol06
	0.0684097	17.57 ± 0.29	R_C	Terskol06
	0.0691041	17.72 ± 0.56	R_C	Terskol06
	0.0697985	17.80 ± 0.53	R_C	Terskol06
	0.3212	19.63 ± 0.03	R_C	MDM
	0.3425	19.66 ± 0.03	R_C	MDM
	0.3631	19.80 ± 0.06	R_C	D1.54
	0.3784	19.80 ± 0.06	R_C	D1.54
	0.3931	19.85 ± 0.06	R_C	D1.54
	0.4001	19.92 ± 0.06	R_C	D1.54
	0.4184	19.88 ± 0.03	R_C	MDM
	0.4495	19.98 ± 0.03	R_C	MDM
	1.0146	21.22 ± 0.04	R_C	NOT
	1.0319	21.20 ± 0.05	R_C	INT
	1.1753	21.57 ± 0.05	R_C	VLT
	1.1915	21.52 ± 0.05	R_C	NOT
	1.3392	21.67 ± 0.06	R_C	MDM
	2.0392	22.28 ± 0.08	R_C	INT
	2.2915	22.54 ± 0.29	R_C	MDM
	2.3379	22.74 ± 0.11	R_C	MDM
	3.0405	22.97 ± 0.13	R_C	INT
	4.0328	23.56 ± 0.08	R_C	NOT
	7.0140	24.54 ± 0.14	R_C	WHT
	0.0909	17.40 ± 0.02	I_C	NOT
	0.1004	17.50 ± 0.02	I_C	NOT
	0.3668	19.27 ± 0.04	I_C	D1.54
	1.0350	20.74 ± 0.05	I_C	INT
	1.1746	21.05 ± 0.04	I_C	NOT
051109A	0.6463	20.70 ± 0.2	R_C	K-380
051111	0.5245	> 19.00	B	Maidanak

TABLE 1 — *Continued*

GRB	Days after trigger (midtime)	Magnitude	Filter	Telescope
	0.04873	17.81 ± 0.18	R_C	SARA
	0.05334	17.72 ± 0.17	R_C	SARA
	0.05796	17.94 ± 0.23	R_C	SARA
	0.5139	19.78 ± 0.14	R_C	Maidanak
	5.42038	> 20.50	R_C	Maidanak
060206	0.11591	17.13 ± 0.03	R_C	SARA
	0.12300	17.16 ± 0.03	R_C	SARA
	0.13006	17.32 ± 0.04	R_C	SARA
	0.13713	17.38 ± 0.05	R_C	SARA
	0.14420	17.38 ± 0.06	R_C	SARA
	0.15127	17.50 ± 0.08	R_C	SARA
	0.15835	17.39 ± 0.08	R_C	SARA
	0.16543	17.39 ± 0.05	R_C	SARA
	0.17250	17.46 ± 0.04	R_C	SARA
	0.17957	17.50 ± 0.05	R_C	SARA
	0.18664	17.62 ± 0.05	R_C	SARA
	0.19372	17.62 ± 0.05	R_C	SARA
	0.21785	17.70 ± 0.06	R_C	SARA
	0.24759	17.88 ± 0.06	R_C	SARA
	0.25466	17.87 ± 0.06	R_C	SARA
	0.26175	18.00 ± 0.06	R_C	SARA
	0.27235	18.01 ± 0.07	R_C	SARA
	0.28295	18.01 ± 0.07	R_C	SARA
	0.29355	18.18 ± 0.08	R_C	SARA
	0.30417	18.29 ± 0.09	R_C	SARA
	1.782459	20.80 ± 0.08	R_C	Maidanak
	1.793243	20.65 ± 0.05	R_C	Maidanak
	1.804627	20.75 ± 0.05	R_C	Maidanak
	1.819764	20.81 ± 0.05	R_C	Maidanak
060418	0.053808	18.88 ± 0.04	B	SMARTS
	0.102083	19.77 ± 0.05	B	SMARTS
	0.728000	22.38 ± 0.10	B	Maidanak
	0.053808	18.03 ± 0.03	V	SMARTS
	0.102083	19.19 ± 0.05	V	SMARTS
	0.145393	19.49 ± 0.02	V	SMARTS
	0.192986	20.01 ± 0.04	V	SMARTS
	0.247211	20.61 ± 0.10	V	SMARTS
	0.053808	17.63 ± 0.02	R_C	SMARTS
	0.102083	18.51 ± 0.03	R_C	SMARTS
	0.724000	21.14 ± 0.05	R_C	Maidanak
	0.053808	16.97 ± 0.02	I_C	SMARTS
	0.102083	17.83 ± 0.03	I_C	SMARTS
	0.145393	18.37 ± 0.02	I_C	SMARTS
	0.192986	18.84 ± 0.03	I_C	SMARTS
	0.247211	19.37 ± 0.06	I_C	SMARTS
	0.726000	20.66 ± 0.03	I_C	Maidanak
	0.805000	20.35 ± 0.02	I_C	Maidanak
	1.040498	20.97 ± 0.10	I_C	SMARTS
	0.053808	15.75 ± 0.06	J	SMARTS
	0.102083	16.65 ± 0.07	J	SMARTS
	0.145393	17.10 ± 0.05	J	SMARTS
	0.192986	17.63 ± 0.07	J	SMARTS
	0.247211	18.22 ± 0.10	J	SMARTS
	1.040498	19.65 ± 0.17	J	SMARTS
	0.053808	14.90 ± 0.06	H	SMARTS
	0.102083	15.92 ± 0.07	H	SMARTS
	0.053808	14.17 ± 0.08	K	SMARTS
	0.102083	15.02 ± 0.09	K	SMARTS
	0.145393	15.51 ± 0.08	K	SMARTS
	0.192986	15.84 ± 0.08	K	SMARTS
	0.247211	16.16 ± 0.09	K	SMARTS
060512	0.148588	18.90 ± 0.09	J	NOT
	0.160289	18.96 ± 0.09	J	NOT
	0.171794	19.09 ± 0.10	J	NOT
	0.183275	19.14 ± 0.11	J	NOT
060607A	0.170521	20.63 ± 0.1	B	SMARTS
	3.194479	> 21.2	B	SMARTS
	0.170521	19.81 ± 0.08	V	SMARTS
	3.194479	> 20.8	V	SMARTS
	0.170521	19.46 ± 0.07	R_C	SMARTS
	3.194479	> 20.9	R_C	SMARTS
	0.170521	19.04 ± 0.07	I_C	SMARTS
	3.194479	> 20.6	I_C	SMARTS
	0.170521	18.2 ± 0.3	J	SMARTS
	3.194479	> 17.7	J	SMARTS
	0.170521	17.7 ± 0.2	H	SMARTS

TABLE 1 — *Continued*

GRB	Days after trigger (midtime)	Magnitude	Filter	Telescope
	3.194479	> 17.5	H	SMARTS
	0.170521	16.6 ± 0.2	K	SMARTS
	3.194479	> 17.2	K	SMARTS
060714	0.420972	20.70 ± 0.16	I_C	SMARTS
	0.420972	19.71 ± 0.14	J	SMARTS
060729	4.621215	19.99 ± 0.06	I_C	SMARTS
	13.623878	> 21.0	I_C	SMARTS
	4.621215	> 18.90	J	SMARTS
	13.623878	> 19.30	J	SMARTS
060904B	0.014985	18.68 ± 0.42	B	RTT150
	0.017565	18.81 ± 0.25	B	RTT150
	0.014464	17.98 ± 0.21	V	RTT150
	0.015494	18.76 ± 0.50	V	RTT150
	0.164653	20.01 ± 0.07	V	SMARTS
	0.248148	20.55 ± 0.06	V	SMARTS
	4.210961	> 22.10	V	SMARTS
	0.005994	16.79 ± 0.15	R_C	RTT150
	0.006803	16.90 ± 0.03	R_C	RTT150
	0.007602	17.03 ± 0.03	R_C	RTT150
	0.008413	17.08 ± 0.04	R_C	RTT150
	0.009223	17.25 ± 0.05	R_C	RTT150
	0.010033	17.34 ± 0.06	R_C	RTT150
	0.010831	17.47 ± 0.09	R_C	RTT150
	0.011642	17.57 ± 0.09	R_C	RTT150
	0.012440	17.66 ± 0.11	R_C	RTT150
	0.013378	17.63 ± 0.13	R_C	RTT150
	0.016015	18.12 ± 0.33	R_C	RTT150
	0.894104	21.63 ± 0.18	R_C	Maidanak
	1.888104	22.40 ± 0.30	R_C	Maidanak
	0.164653	18.82 ± 0.05	I_C	SMARTS
	0.248148	19.45 ± 0.05	I_C	SMARTS
	4.210961	> 21.70	I_C	SMARTS
	0.164653	17.83 ± 0.09	J	SMARTS
	0.248148	18.11 ± 0.06	J	SMARTS
	4.210961	> 19.60	J	SMARTS
	0.164653	15.90 ± 0.07	K	SMARTS
	0.248148	16.35 ± 0.05	K	SMARTS
	4.210961	> 17.90	K	SMARTS
060908	0.503829	21.40 ± 0.8	R_C	Terskol2
	0.555000	> 20.60	R_C	Maidanak
	0.849930	> 20.40	I_C	Maidanak
	0.117685	18.28 ± 0.07	K	UKIRT
060927	0.160856	> 21.5	R_C	AZT-11
061007	0.874607	22.37 ± 0.27	V	SMARTS
	0.874607	21.95 ± 0.19	R_C	SMARTS
	0.874607	21.53 ± 0.19	I_C	SMARTS
	4.770683	> 21.90	I_C	SMARTS
	0.874607	20.00 ± 0.17	J	SMARTS
	4.770683	> 19.20	J	SMARTS
	0.874607	19.03 ± 0.08	H	SMARTS
	0.874607	18.37 ± 0.26	K	SMARTS
061121	0.642592	> 20.0	V	SMARTS
	2.694711	22.4 ± 0.2	V	SMARTS
	0.487973	19.97 ± 0.26	R_C	Shajn
	1.463343	21.50 ± 0.05	R_C	Shajn
	1.492244	21.60 ± 0.06	R_C	Shajn
	2.441402	22.13 ± 0.07	R_C	Shajn
	0.642592	> 19.8	I_C	SMARTS
	0.674340	20.15 ± 0.08	I_C	SMARTS
	2.694711	22.0 ± 0.2	I_C	SMARTS
	0.674340	> 19.0	J	SMARTS
	2.694711	> 19.6	J	SMARTS
	2.694711	> 17.9	K	SMARTS
070125	1.883345	20.77 ± 0.15	B	SMARTS
	1.883345	20.21 ± 0.09	V	SMARTS
	1.883345	19.61 ± 0.06	R_C	SMARTS
	1.883345	19.00 ± 0.06	I_C	SMARTS
	2.879178	19.80 ± 0.07	I_C	SMARTS
	7.880382	> 19.70	I_C	SMARTS
	1.883345	18.07 ± 0.16	J	SMARTS
	2.879178	18.95 ± 0.21	J	SMARTS
	7.880382	> 19.10	J	SMARTS
	1.883345	17.44 ± 0.09	H	SMARTS
	1.883345	17.03 ± 0.19	K	SMARTS
070208	0.403070	21.70 ± 0.3	R_C	Sayan
070419A	0.025584	> 17.80	R_C	SARA

Kann et al.

TABLE 1 — *Continued*

GRB	Days after trigger (midtime)	Magnitude	Filter	Telescope
	0.048696	20.80 ± 0.71	R_C	SARA
	0.234000	> 19.8	R_C	Sayan
071020	0.702722	> 20.11	B	Z-600
	0.728000	> 21.30	B	AZT-8
	0.058742	19.92 ± 0.07	R_C	SARA
	0.702511	> 20.70	R_C	Z-600
	0.730000	20.10 ± 0.30	I_C	AZT-8
071031	0.027465	19.59 ± 0.08	B	SMARTS
	0.027465	18.77 ± 0.07	V	SMARTS
	0.076574	19.50 ± 0.03	V	SMARTS
	0.127662	20.12 ± 0.03	V	SMARTS
	0.170810	20.19 ± 0.03	V	SMARTS
	0.210787	20.36 ± 0.04	V	SMARTS
	0.254305	20.50 ± 0.11	V	SMARTS
	0.027465	18.43 ± 0.05	R_C	SMARTS
	0.027465	17.91 ± 0.06	I_C	SMARTS
	0.076574	18.75 ± 0.04	I_C	SMARTS
	0.127662	19.17 ± 0.04	I_C	SMARTS
	0.170810	19.47 ± 0.04	I_C	SMARTS
	0.210787	19.72 ± 0.04	I_C	SMARTS
	0.254305	20.14 ± 0.08	I_C	SMARTS
	2.162697	> 22.0	I_C	SMARTS
	0.027465	17.15 ± 0.2	J	SMARTS
	0.076574	18.35 ± 0.2	J	SMARTS
	0.127662	18.35 ± 0.2	J	SMARTS
	0.170810	18.55 ± 0.2	J	SMARTS
	0.210787	> 18.7	J	SMARTS
	0.254305	> 18.1	J	SMARTS
	2.162697	> 19.0	J	SMARTS
	0.027465	> 16.0	H	SMARTS
	0.027465	15.4 ± 0.2	K	SMARTS
	0.076574	16.8 ± 0.2	K	SMARTS
	0.127662	> 17.1	K	SMARTS
	0.170810	> 17.0	K	SMARTS
	0.210787	> 17.3	K	SMARTS
	0.254305	> 16.9	K	SMARTS
080129	0.969468	> 21.90	I_C	SMARTS
	0.969468	> 19.70	J	SMARTS
080210	0.602300	21.7 ± 0.5	R_C	Sayan
080310	0.024838	18.09 ± 0.07	B	SMARTS
	0.024838	17.61 ± 0.07	V	SMARTS
	0.024838	17.19 ± 0.06	R_C	SMARTS
	0.865104	> 21.20	R_C	SMARTS
	0.017836	16.57 ± 0.05	I_C	SMARTS
	0.020868	16.65 ± 0.05	I_C	SMARTS
	0.024838	16.74 ± 0.05	I_C	SMARTS
	0.028970	16.85 ± 0.05	I_C	SMARTS
	0.031852	16.94 ± 0.05	I_C	SMARTS
	0.865104	> 20.70	I_C	SMARTS
	0.998738	20.98 ± 0.11	I_C	SMARTS
	1.885243	21.20 ± 0.11	I_C	SMARTS
	2.846551	> 22.20	I_C	SMARTS
	0.024838	15.85 ± 0.07	J	SMARTS
	0.865104	> 17.9	J	SMARTS
	0.998738	> 19.8	J	SMARTS
	1.885243	> 19.9	J	SMARTS
	2.846551	> 20.0	J	SMARTS
	0.024838	15.08 ± 0.06	H	SMARTS
	0.865104	> 17.30	H	SMARTS
	0.024838	14.37 ± 0.06	K	SMARTS
	0.865104	> 17.10	K	SMARTS
080330	0.025150	18.27 ± 0.04	B	SMARTS
	0.025150	17.90 ± 0.04	V	SMARTS
	0.025150	17.59 ± 0.04	R_C	SMARTS
	0.575000	21.05 ± 0.10	R_C	Terskol2
	0.654000	21.28 ± 0.10	R_C	Terskol2
	4.634803	> 23.30	R_C	Terskol2
	0.017732	16.89 ± 0.03	I_C	SMARTS
	0.022118	16.99 ± 0.03	I_C	SMARTS
	0.025150	17.09 ± 0.03	I_C	SMARTS
	0.030104	17.22 ± 0.03	I_C	SMARTS
	0.032581	17.34 ± 0.04	I_C	SMARTS
	0.997442	21.65 ± 0.09	I_C	SMARTS
	2.009155	> 22.20	I_C	SMARTS
	0.025150	16.36 ± 0.07	J	SMARTS
	0.997442	> 20.10	J	SMARTS

TABLE 1 — *Continued*

GRB	Days after trigger (midtime)	Magnitude	Filter	Telescope
	2.009155	> 19.90	J	SMARTS
	0.025150	15.76 ± 0.07	H	SMARTS
	0.025150	15.14 ± 0.07	K	SMARTS
080413A	0.130498	20.88 ± 0.1	B	SMARTS
	0.174676	21.21 ± 0.08	B	SMARTS
	0.212257	21.75 ± 0.1	B	SMARTS
	1.166887	> 21.50	B	SMARTS
	0.130498	19.95 ± 0.11	V	SMARTS
	0.174676	20.22 ± 0.08	V	SMARTS
	0.212257	20.58 ± 0.09	V	SMARTS
	1.166887	> 20.80	V	SMARTS
	0.130498	19.25 ± 0.05	R_C	SMARTS
	0.174676	19.87 ± 0.07	R_C	SMARTS
	0.212257	20.02 ± 0.07	R_C	SMARTS
	1.166887	> 20.70	R_C	SMARTS
	0.130498	18.84 ± 0.06	I_C	SMARTS
	0.174676	19.26 ± 0.07	I_C	SMARTS
	0.212257	19.57 ± 0.06	I_C	SMARTS
	1.141458	> 21.30	I_C	SMARTS
	1.166887	> 20.30	I_C	SMARTS
	0.130498	17.80 ± 0.2	J	SMARTS
	0.174676	> 17.80	J	SMARTS
	0.212257	> 18.0	J	SMARTS
	1.141458	> 19.0	J	SMARTS
	1.166887	> 17.70	J	SMARTS
	0.130498	17.10 ± 0.2	H	SMARTS
	0.174676	17.60 ± 0.2	H	SMARTS
	0.212257	> 17.60	H	SMARTS
	1.166887	> 17.20	H	SMARTS
	0.130498	16.20 ± 0.1	K	SMARTS
	0.174676	16.60 ± 0.2	K	SMARTS
	0.212257	17.10 ± 0.2	K	SMARTS
	1.166887	> 16.30	K	SMARTS
080810	0.159900	> 19.26	B	Sayan
	0.369734	20.45 ± 0.22	B	RTT150
	0.375289	20.33 ± 0.22	B	RTT150
	0.382210	20.45 ± 0.22	B	RTT150
	0.394259	20.67 ± 0.22	B	RTT150
	0.415984	20.84 ± 0.22	B	RTT150
	0.435347	20.83 ± 0.22	B	RTT150
	0.452199	20.86 ± 0.22	B	RTT150
	0.470023	20.77 ± 0.22	B	RTT150
	0.487535	20.80 ± 0.22	B	RTT150
	0.522581	20.81 ± 0.22	B	RTT150
	0.541400	20.78 ± 0.22	B	RTT150
	0.545347	20.85 ± 0.22	B	RTT150
	0.370891	19.79 ± 0.16	V	RTT150
	0.377014	19.69 ± 0.16	V	RTT150
	0.383946	19.67 ± 0.16	V	RTT150
	0.395417	19.81 ± 0.16	V	RTT150
	0.416632	19.83 ± 0.16	V	RTT150
	0.419907	19.71 ± 0.16	V	RTT150
	0.436331	19.94 ± 0.16	V	RTT150
	0.453194	19.81 ± 0.16	V	RTT150
	0.471018	20.21 ± 0.16	V	RTT150
	0.488125	20.30 ± 0.16	V	RTT150
	0.523565	20.19 ± 0.16	V	RTT150
	0.542384	20.29 ± 0.16	V	RTT150
	0.546354	20.18 ± 0.16	V	RTT150
	1.535651	21.40 ± 0.16	V	RTT150
	2.516073	21.92 ± 0.16	V	RTT150
	0.178600	17.98 ± 0.13	R_C	Sayan
	0.202600	18.10 ± 0.17	R_C	Sayan
	0.346412	19.34 ± 0.11	R_C	RTT150
	0.349108	19.28 ± 0.11	R_C	RTT150
	0.352176	19.17 ± 0.11	R_C	RTT150
	0.354479	19.15 ± 0.11	R_C	RTT150
	0.358356	19.24 ± 0.11	R_C	RTT150
	0.360833	19.40 ± 0.11	R_C	RTT150
	0.364096	19.26 ± 0.11	R_C	RTT150
	0.366955	19.22 ± 0.11	R_C	RTT150
	0.368576	19.27 ± 0.11	R_C	RTT150
	0.372048	19.17 ± 0.11	R_C	RTT150
	0.378750	19.34 ± 0.11	R_C	RTT150
	0.386249	19.25 ± 0.11	R_C	RTT150
	0.396562	19.36 ± 0.11	R_C	RTT150

Kann et al.

TABLE 1 — *Continued*

GRB	Days after trigger (midtime)	Magnitude	Filter	Telescope
	0.417870	19.34 ± 0.11	R_C	RTT150
	0.433100	19.02 ± 0.05	R_C	AZT-8
	0.437315	19.47 ± 0.11	R_C	RTT150
	0.454190	19.64 ± 0.11	R_C	RTT150
	0.455980	19.28 ± 0.16	R_C	Z-600
	0.472002	19.50 ± 0.11	R_C	RTT150
	0.489664	19.55 ± 0.11	R_C	RTT150
	0.524537	19.73 ± 0.11	R_C	RTT150
	0.543391	19.60 ± 0.11	R_C	RTT150
	0.547592	19.68 ± 0.11	R_C	RTT150
	1.520598	20.83 ± 0.11	R_C	RTT150
	2.315000	21.36 ± 0.09	R_C	Maidanak
	2.499909	21.65 ± 0.11	R_C	RTT150
	4.326000	> 22.30	R_C	Maidanak
	0.373206	18.71 ± 0.09	I_C	RTT150
	0.380486	18.65 ± 0.09	I_C	RTT150
	0.387986	18.66 ± 0.09	I_C	RTT150
	0.397720	18.72 ± 0.09	I_C	RTT150
	0.418842	18.72 ± 0.09	I_C	RTT150
	0.438310	18.80 ± 0.09	I_C	RTT150
	0.455185	19.03 ± 0.09	I_C	RTT150
	0.472998	19.08 ± 0.09	I_C	RTT150
	0.490625	19.06 ± 0.09	I_C	RTT150
	0.525764	19.33 ± 0.09	I_C	RTT150
	0.544363	19.56 ± 0.09	I_C	RTT150
	1.512531	20.02 ± 0.09	I_C	RTT150
081008	0.163113	19.66 ± 0.12	B	SMARTS
	0.209930	19.98 ± 0.12	B	SMARTS
	0.267280	20.51 ± 0.14	B	SMARTS
	0.163113	19.22 ± 0.08	V	SMARTS
	0.209930	19.68 ± 0.09	V	SMARTS
	0.267280	20.03 ± 0.10	V	SMARTS
	1.223449	> 21.5	V	SMARTS
	0.163113	18.45 ± 0.2	R_C	SMARTS
	0.209930	18.89 ± 0.21	R_C	SMARTS
	0.267280	19.3 ± 0.21	R_C	SMARTS
	0.163113	18.27 ± 0.09	I_C	SMARTS
	0.209930	18.62 ± 0.09	I_C	SMARTS
	0.267280	18.94 ± 0.10	I_C	SMARTS
	1.223449	> 20.6	I_C	SMARTS
	1.274908	> 21.0	I_C	SMARTS
	0.163113	17.13 ± 0.10	J	SMARTS
	0.209930	17.76 ± 0.15	J	SMARTS
	0.267280	17.92 ± 0.15	J	SMARTS
	1.223449	> 19.1	J	SMARTS
	1.274908	> 18.9	J	SMARTS
	0.163113	16.52 ± 0.10	H	SMARTS
	0.209930	16.91 ± 0.15	H	SMARTS
	0.267280	17.38 ± 0.15	H	SMARTS
	0.163113	16.08 ± 0.10	K	SMARTS
	0.209930	16.02 ± 0.15	K	SMARTS
	0.267280	16.33 ± 0.15	K	SMARTS
	1.223449	> 17.80	K	SMARTS
090323	2.064670	21.25 ± 0.04	r'	RTT150
	5.993400	23.10 ± 0.20	R_C	Shajn
	6.157552	23.19 ± 0.06	R_C	NOT
	6.998807	> 22.70	R_C	TLS
	6.899000	> 22.70	I_C	Shajn
090424	0.292726	21.13 ± 0.08	B	CAHA1
	0.263674	20.03 ± 0.03	V	CAHA1
	0.230028	19.22 ± 0.06	R_C	TLS
	0.235306	19.46 ± 0.04	R_C	TLS
	0.240607	19.37 ± 0.04	R_C	TLS
	0.244041	19.29 ± 0.10	R_C	CAHA1
	0.245897	19.40 ± 0.04	R_C	TLS
	0.251198	19.42 ± 0.05	R_C	TLS
	0.256487	19.50 ± 0.04	R_C	TLS
	0.261811	19.55 ± 0.05	R_C	TLS
	0.267124	19.56 ± 0.04	R_C	TLS
	0.272402	19.43 ± 0.03	R_C	TLS
	0.277680	19.56 ± 0.04	R_C	TLS
	4.18686	21.62 ± 0.03	R_C	Maidanak
	11.322604	21.48 ± 0.08	R_C	CAHA1
	12.361112	21.84 ± 0.24	R_C	CAHA1
	18.358958	21.88 ± 0.08	R_C	CAHA1
	21.336192	21.89 ± 0.05	R_C	CAHA1

TABLE 1 — *Continued*

GRB	Days after trigger (midtime)	Magnitude	Filter	Telescope
	24.355694	22.25 ± 0.15	R_C	CAHA1
	39.380393	22.06 ± 0.24	R_C	CAHA1
	0.250966	18.96 ± 0.16	I_C	CAHA1
	12.424919	21.44 ± 0.09	I_C	CAHA2

Note. — SMARTS is the 1.3m Small and Moderate Aperture Research Telescope System telescope at the Cerro Tololo Interamerican Observatory in Chile. AT-64 is the 0.64m telescope of the Crimean Astrophysical Observatory (CrAO) in the Ukraine. TLS is the 1.34m Schmidt telescope of the Thüringer Landessternwarte Tautenburg (Thuringia State Observatory) in Germany. RTT150 is the 1.5m Russian-Turkish Telescope in Turkey. Maidanak is the 1.5m telescope of the Maidanak observatory in Uzbekistan. NOT is the 2.56m Nordic Optical Telescope on the island of La Palma, the Canary Islands, Spain. TNG is the 3.6m Telescope Nazionale Galileo, also on La Palma. IAC80 is the 0.8m telescope of the Observatorio del Teide, on the Canary Islands. INT is the 2.5m Isaac Newton Telescope, on La Palma. SARA is the 0.9m telescope of the Southeastern Association for Research in Astronomy at Kitt Peak National Observatory, Arizona, USA. UAPhO is the 0.4m telescope of Ussuriysk Astrophysical Observatory (UAPhO) in the far east of Russia. Shajn is the 2.6m Shajn telescope of CrAO. D1.54 is the Danish 1.54m telescope at La Silla Observatory, Chile. OSN is the 1.5m telescope of the Sierra Nevada Observatory, Spain. WIRO is the 2.3m Wyoming Infrared Observatory telescope in Wyoming, USA. UKIRT is the 3.8m United Kingdom Infrared Telescope on Mauna Kea, Hawaii, USA. MDM is the 1.3 m McGraw-Hill Telescope at the MDM Observatory at KPNO. VLT is the 8.2m Very Large Telescope at the European Southern Observatory Paranal Observatory, Chile. Terskol06 is the Zeiss-600 (0.6m) telescope of the Terskol observatory, Kabardino-Balkarija, Russia. WHT is the 4.2m William Herschel Telescope on La Palma. K-380 is the 0.38m telescope of CrAO. Terskol2 is the Zeiss-2000 (2.0m) telescope of Terskol Observatory. AZT-11 is the 1.25m telescope at CrAO. Sayan is the AZT-33IK (1.5m) telescope at Sayan Observatory, Mondy, Russia. Maidanak06 is the Zeiss-600 (0.6m) telescope at Maidanak Observatory. AZT-8 is the 0.7m telescope at CrAO. CAHA1 is the 1.23m Spanish telescope of the Centro Astronómico Hispano-Alemán (CAHA), Spain. CAHA2 is the 2.2m telescope of CAHA.

DETAILS ON THE GRB AFTERGLOW SAMPLES

In this appendix, we describe the GRBs and their afterglows in our different samples on a case-by-case basis. We give the GRB redshifts (references can be found in the caption of Table 3) and cite the sources we took our data from. For many GRBs, we report additional light curve analysis results. We compare the results we derive from our SED analyses with those given by other sources in the literature. In some cases, we give further miscellaneous results and comments.

We followed Zeh et al. (2006) in terms of parameter designations. The parameter m_k is the magnitude normalization, which is either the magnitude of the light curve fit at one day (if fit by a single power law), or the magnitude at the light curve break time t_b assuming a break smoothness parameter $n = \infty$. In many cases, the break smoothness parameter needs to be fixed. By eye, most light curves (if they have breaks) show sharp breaks, here, we fix $n = 10$ (or -10 in the case of steep-to-shallow transitions). In a few cases, the break is much smoother, and we choose $n = 1$. α_1 and α_2 are the decay slopes of the pre-break and post-break power laws, respectively, and m_h is the constant host galaxy magnitude. Often, no host galaxy has been reported, and the final data points show no indication of an upturn due to an emerging host. We fix the magnitude to a value significantly fainter than the the last data point.

Details on the pre-Swift Golden Sample extension

All in all, three GRBs described in K06 have been added to the Golden Sample due to additional data or improved analysis.

GRB 990510, $z = 1.6187 \pm 0.0015$. — We constructed the light curve and the SED with data from the following sources: Israel et al. (1999), Stanek et al. (1999), Harrison et al. (1999), Beuermann et al. (1999), Vreeswijk et al. (1999), Galama et al. (1999), Pietrzynski & Udalski (1999a), Pietrzynski & Udalski (1999b), Hjorth et al. (1999), Fruchter et al. (1999), Bloom (2000), and Curran et al. (2008). This GRB has a densely sampled, very smooth light curve and is known for its very smooth "rollover" break which led to the introduction of the Beuermann equation (Beuermann et al. 1999). The GRB was not included in the Golden Sample of K06 because the short span of the SED (BVR_CI_C) led to large uncertainties. The addition of newly published JHK data (Curran et al. 2008) has strongly reduced these errors. We find a blue but curved SED, SMC dust is strongly preferred, and the extinction-corrected spectral slope, $\beta = 0.17 \pm 0.15$, is very flat. From a combined fit with all colors, we find the following parameters, which update and supersede those presented in Zeh et al. (2006): $\alpha_1 = 0.77 \pm 0.03$, $\alpha_2 = 2.45 \pm 0.12$, $t_b = 1.80 \pm 0.18$ days, $n = 0.81 \pm 0.16$, and $m_h = 29$ was fixed.

GRB 011211, $z = 2.1418 \pm 0.0018$. — We constructed the light curve and the SED with data from the following sources: Holland et al. (2002), Jakobsson et al. (2003), Jakobsson et al. (2004a), and Covino et al. (2002). This afterglow shows early-time small-scale variability which has been attributed to a "patchy shell" model (Jakobsson et al. 2004a). A refined analysis has taken this variability into careful account, especially for the NIR data, and has yielded a significantly improved SED. We find that SMC dust is strongly preferred and there is a small, typical amount of extinction present.

GRB 030323, $z = 3.3718 \pm 0.0005$. — We constructed the light curve and the SED with data from the following sources: Vreeswijk et al. (2004), Gilmore et al. (2003), Smith & Rykoff (2003), Masi et al. (2003), and Wood-Vasey et al. (2003). Similar to GRB 011211, this GRB contains small-scale variability which was not taken into account in K06. A refined analysis yields a significant improvement of the SED. The only band we do not add is the K band which is too bright for unknown reasons. We find an SED best fit by SMC dust (MW dust is ruled out, and LMC dust yields an unrealistically flat intrinsic spectral slope) and a small amount of extinction.

Details on the Swift-era Golden Sample

GRB 050319, $z = 3.2425$. — We constructed the light curve and the SED with data from the following sources: Woźniak et al. (2005a), Mason et al. (2006), Quimby et al. (2006), Huang et al. (2007), Kamble et al. (2007), Torii (2005a), as well as our own extensive data set (NOT, TNG, Maidanak, RTT150). We do not add the $J-$band data from George et al. (2006). If this NIR flare is real, it is a quite mysterious event, as a contemporaneous $V-$band detection (Huang et al. 2007) shows no sign of flaring activity. Initially, the light curve shows a transition from a moderately steep to a shallower decay: $m_k = 18.80 \pm 0.14$ mag, $\alpha_1 = 0.93 \pm 0.026$, $\alpha_2 = 0.46 \pm 0.022$, $t_b = 0.031 \pm 0.006$ days, and $m_h = 28$ mag, $n = -10$ fixed. Another break is found in the late light curve, this is a good jet break candidate with a smooth transition: $m_k = 21.11 \pm 0.12$ mag, $\alpha_1 = 0.46 \pm 0.020$, $\alpha_2 = 2.23 \pm 0.25$, $t_b = 3.47 \pm 0.42$ days, and $m_h = 28$ mag, $n = 1$ fixed. The B band is already affected by Lyman absorption (Huang et al. 2007), leaving us with a VR_CI_CK SED. A fit without extinction yields $\beta_0 = 1.00 \pm 0.06$, in full agreement with Huang et al. (2007). Due to the sparsity of colors and the large error in the K band, we are not able to discern between extinction laws (the 2175 Å feature lies in the z band), and the derived errors of the SED parameters are quite large. Since it yields viable fits to most other GRB afterglows, we use the SMC values of $\beta = 0.74 \pm 0.42$ and $A_V = 0.05 \pm 0.09$, showing that extinction is negligible. Oates et al. (2009) find $A_V = 0.06$ from UVOT data only (using an XRT-UVOT joint fit), in excellent agreement. Schady et al. (2010) find that a cooling break between optical and X-rays is preferred at low significance, but can only derive upper limits for this case, their upper limit of $A_V < 0.09$ for SMC dust agrees very well with our result.

GRB 050408, $z = 1.2357 \pm 0.0002$. — We constructed the light curve and the SED with data from the following sources: Foley et al. (2006a), de Ugarte Postigo et al. (2007), Wiersema et al. (2005), Milne et al. (2005a), Kahharov et al. (2005) and Flasher et al. (2005a), as well as our own data set (TNG, Maidanak, AT-64 upper limit). From our $UBVR_CI_CZJHK$ SED, we derive results that are in full agreement with de Ugarte Postigo et al. (2007). We find that SMC dust is preferred and derive $\beta = 0.28 \pm 0.27$ ($\beta = 0.28 \pm 0.33$ in de Ugarte Postigo et al. 2007) and $A_{\rm V} = 0.74 \pm 0.15$ ($A_{\rm V} = 0.73 \pm 0.18$ in de Ugarte Postigo et al. 2007). Thus, this is one of the highest line-of-sight extinctions found so far for a GRB with a detected afterglow (cf. the sample of K06). We concur that the rebrightening feature observed by de Ugarte Postigo et al. (2007) is very unlikely to be a supernova rebrightening, as we derive a peak luminosity $k = 1.65 \pm 0.55$ (in units of the SN 1998bw peak luminosity in the same band at the same redshift, Zeh et al. 2004) and a stretching factor $s = 0.22 \pm 0.05$, which is much faster than any known GRB-SN (Ferrero et al. 2006), although we note that the shape of the rebrightening can be well approximated by a strongly compressed SN 1998bw light curve. Also, employing the extinction correction as described in Ferrero et al. (2006), we derive $k = 3.27^{+0.87}_{-0.68}$, which is also much brighter than any GRB-SN in the sample of Ferrero et al. (2006). Excluding the rebrightening from the fit, we find the light curve parameters $m_k = 21.96 \pm 0.44$ mag, $\alpha_1 = 0.48 \pm 0.10$, $\alpha_2 = 2.06 \pm 0.46$, $t_b = 0.92 \pm 0.32$ days and $m_h = 24.56 \pm 0.15$ mag. We fix $n = 1$, as in this case there is a smooth transition between slopes.

XRF 050416A, $z = 0.6528 \pm 0.0002$. — We constructed the light curve and the SED with data from the following sources: Holland et al. (2007), Soderberg et al. (2007), and Perley et al. (2009d), as well as our own data set (Maidanak, ANDICAM). Similar to GRB 050401, observations in different filters are taken with little overlap. The light curve evolution is not entirely clear, but we concur with Soderberg et al. (2007) that there is an early break. We find the following results for a broken power law fit of the composite, host-subtracted light curve ($\chi^2 = 52.7$ for 47 degrees of freedom): $m_k = 19.94 \pm 0.16$ mag, $\alpha_1 = 0.25 \pm 0.07$, $\alpha_2 = 0.97 \pm 0.05$, $t_b = 0.025 \pm 0.005$ days, and $n = 10$ fixed. The late decay slope is slightly steeper than what Soderberg et al. (2007) find ($\alpha_{opt/NIR} \approx 0.75$), possibly due to our use of a brighter host galaxy magnitude (Perley et al. 2009d). We were not able to reproduce the SN results reported by Soderberg et al. (2007). We obtain a broad SED ($UVW2\,UVM2\,UBVR_CI_Cz'K_S$), which has some scatter, but yields a small amount of dust for all extinction laws. While we can not rule out MW and LMC dust, we find no evidence for a 2175 Å bump, which falls into the U band.

GRB 050502A, $z = 3.793$. — We constructed the light curve and the SED with data from the following sources: Guidorzi et al. (2005), Yost et al. (2005), and Durig (2005), as well as our own data (IAC80, INT, as well as an unused upper limit from the Maidanak telescope). We fit the R-band light curve (excepting the last two points), which also contains the $ROTSE\,C_R$ data points, with a broken power-law. We find $m_k = 19.55 \pm 0.39$ mag, $\alpha_1 = 1.06 \pm 0.043$, $\alpha_2 = 1.45 \pm 0.028$, $t_b = 0.067 \pm 0.017$ days, $m_h = 28$ mag is fixed. The data quality is high enough to leave the break smoothness parameter free, we find $n = 149.3 \pm 6.1$, i.e., a very sharp break is required. This is an astonishing result, as no other afterglow light curve where it was possible to let n be a free parameter of the fit showed $n > 10$ (Zeh et al. 2006). Our results compare well with Yost et al. (2005), who find $\alpha_1 = 1.13 \pm 0.023$, $\alpha_2 = 1.44 \pm 0.022$ and $t_b = 0.066 \pm 0.009$ days. Yost et al. (2005) interpret the break as the passage of the cooling frequency ν_c through the R band. We note that Zeh et al. (2006) found a similarly sharp break for the cooling frequency passage of the afterglow of GRB 030329 (Sato et al. 2003). Also, that break was a bit stronger ($\Delta\alpha = 0.33 \pm 0.01$) than the theoretical prediction $\Delta\alpha = 0.25$ (Panaitescu & Kumar 2001), similar to this case ($\Delta\alpha = 0.31 \pm 0.03$). The final deep INT data point shows that a second break must have occurred. Fitting all data from 0.07 days onward, we find $\alpha_2 = 1.39 \pm 0.031$, $\alpha_3 = 1.82 \pm 0.20$, $t_b = 0.34 \pm 0.13$ days, and $n = 10$, $m_h = 28$ mag are fixed. The SED is well-fit by a small amount of SMC dust, but the preference is weak only. If the cooling break lies redward of the optical, p derived from the intrinsic spectral slope ($p = 1.52 \pm 0.32$) is in agreement with the value derived from the post-break decay slope ($p = 1.82 \pm 0.20$), but no X-ray data exist to further examine this possibility.

GRB 050525A, $z = 0.606$. — We constructed the light curve and the SED with data from the following sources: Klotz et al. (2005a), Blustin et al. (2006), Della Valle et al. (2006a), Heng et al. (2008), Rykoff et al. (2009), Yanagisawa et al. (2005), Kaplan et al. (2005), and Flasher et al. (2005b), as well as our own data set (SARA, ANDICAM, RTT150, as well as upper limits from several Russian telescopes). Excluding the early data before the rebrightening (Klotz et al. 2005a), we find $m_k = 18.87 \pm 0.13$ mag, $\alpha_1 = 1.09 \pm 0.032$, $\alpha_2 = 1.77 \pm 0.024$, $t_b = 0.30 \pm 0.023$ days, $m_h = 24.96 \pm 0.04$ mag, and $n = 10$ was fixed. This agrees very well with Della Valle et al. (2006a), who find $\alpha_1 = 1.1$, $\alpha_2 = 1.8$ and $t_b = 0.3$ days. The SN parameters we find are reported in Ferrero et al. (2006). We find that SMC dust is preferred (although the SED shows scatter even for SMC dust, resulting in a high χ^2/d.o.f.), $A_{\rm V} = 0.32 \pm 0.20$. This is in agreement with Blustin et al. (2006), who also find SMC dust and $A_{\rm V} = 0.23 \pm 0.15$. Schady et al. (2007a) also find that SMC dust is preferred, and for a solution with a cooling break between the optical and X-rays, they derive $A_{\rm V} = 0.26 \pm 0.04$, also in agreement with our result. Heng et al. (2008) use *Spitzer Space Telescope* detections to extend the SED all the way to $24\mu m$. Deriving the intrinsic SED from a fit to the X-ray and MIR data, they find $A_{\rm V} \approx 0.02 - 0.41$ for different models (e.g., amount of host contribution to the MIR data), with the most realistic model yielding $A_{\rm V} = 0.15 \pm 0.06$, smaller than our result due to the larger assumed intrinsic $\beta = 0.87$. Oates et al. (2009) find $A_{\rm V} = 0.06$ from UVOT data only (using an XRT-UVOT joint fit), a significantly smaller value. Schady et al. (2010) find, similar to Schady et al. (2007a), the need for a cooling break and the preference of SMC dust, but derive $A_{\rm V} = 0.16 \pm 0.02$, comparable to Heng et al. (2008) and still in agreement within errors with our value.

GRB 050730, $z = 3.96855 \pm 0.00005$. — We constructed the light curve and the SED with data from the following sources: Pandey et al. (2006), Perri et al. (2007), Blustin et al. (2005), Klotz et al. (2005b), Damerdji et al. (2005), Holman et al. (2005), Haislip et al. (2005a), Jacques & Pimentel (2005), and Kannappan et al. (2005), as well as our own data set (RTT150 and ANDICAM upper limits not given in Pandey et al. 2006). No host galaxy is found down to deep limits (Chen et al. 2009). The light curve of this burst is highly variable (Pandey et al. 2006; Perri et al. 2007), and the SED was evaluated carefully. We fit the light curve with a broken power law and find $m_k = 18.20 \pm 0.10$ mag, $\alpha_1 = 0.56 \pm 0.008$, $\alpha_2 = 1.69 \pm 0.085$, $t_b = 0.17 \pm 0.026$ days, and $m_h = 27$ mag, $n = 10$ were fixed. This is concurrent with the results of Pandey et al. (2006): $\alpha_1 = 0.60 \pm 0.07$, $\alpha_2 = 1.71 \pm 0.06$ and $t_b = 0.1$ days. The SED results, on the other hand, differ quite strongly between different works. Chen et al. (2005) find a steep $\beta = 1.88 \pm 0.01$ from the continuum fitting of an echelle spectrum. Starling et al. (2005), also fitting a spectrum, find $\beta = 1.34 \pm 0.21$. Pandey et al. (2006), using only I, J and K data, find $\beta = 0.56 \pm 0.06$. Our result, for an $i'I_CJK$ SED, is $\beta_0 = 0.82 \pm 0.041$ (β_0 being the spectral slope without any extinction correction) and $\beta = 0.52 \pm 0.045$, $A_V = 0.10 \pm 0.015$ for the preferred SMC dust. Starling et al. (2005) find $A_V \approx 0.01$ from spectral fitting. Oates et al. (2009) find $A_V = 0.15$ from UVOT data only (using an XRT-UVOT joint fit), a value comparable to ours. Schady et al. (2010) find that no dust model is able to fit the SED well, and derive $A_V \approx 0.16 - 0.39$ for their different models, mostly in excess of our value.

GRB 050801, $z = 1.56 \pm 0.1$. — We constructed the light curve and the SED with data from the following sources: Rykoff et al. (2006a), De Pasquale et al. (2007), Monard (2005), as well as our own data set (ANDICAM, Danish 1.54m). No host was detected down to deep limits by Ovaldsen et al. (2007). This GRB has a photometric redshift only, but it is precise enough for our analysis, $z = 1.56 \pm 0.10$ (De Pasquale et al. 2007) (Oates et al. 2009 find a slightly different value, $z = 1.38 \pm 0.07$). The light curve shows an early, almost flat plateau phase before breaking sharply to a typical power law decay (Rykoff et al. 2006a). Fitting the light curve with a broken power law, we find: $m_k = 14.85 \pm 0.05$ mag, $\alpha_1 = 0.13 \pm 0.03$, $\alpha_2 = 1.19 \pm 0.01$, $t_b = 247 \pm 11$ seconds, and $n = 10$, $m_h = 28$ were fixed. If we use all data, the SED of this afterglow does not yield a reasonable result, with the UVOT data (De Pasquale et al. 2007) being much brighter. Therefore, we use only the late-time ground-based data presented in this work, and derive a red SED which is well-fit by a moderate amount of SMC dust. This result is different from those based on UVOT data exclusively, De Pasquale et al. (2007) find that the optical-to-X-ray SED is described by a single slope, and Oates et al. (2009) find no evidence for any extinction (using an XRT-UVOT joint fit).

GRB 050802, $z = 1.7102$. — We constructed the light curve and the SED with data from the following sources: Oates et al. (2007) and our own extensive data set (OSN, NOT, TNG, Maidanak, Shajn). The two main data sets (*Swift* UVOT, Oates et al. 2007, and ground-based, ours), hardly overlap. Creating a composite light curve, we find that the light curve is well described by a broken power law with the following parameters: $m_k = 21.31 \pm 0.53$ mag, $\alpha_1 = 0.84 \pm 0.022$, $\alpha_2 = 1.43 \pm 0.25$, $t_b = 0.63 \pm 0.31$ days, $m_h = 25.36 \pm 0.46$ mag, and $n = 10$ fixed. If this is a jet break, the post-break slope is very shallow, but this has been seen before (e.g., GRB 010222 and GRB 041006, Zeh et al. 2006). We are able to derive a very smooth SED ($UBVR_CI_C$, the UV filters are all affected by Lyman damping), but the rather large errors of the data points lead to large uncertainties in the values of β and A_V. LMC dust is marginally preferred, following the shape of the SED much better than MW or SMC dust, and we find $\beta = 0.36 \pm 0.26$ and $A_V = 0.21 \pm 0.13$. This is lower than the result of Oates et al. (2007), who find $E(B-V) = 0.18$ ($A_V = 0.56$) for MW dust (they only fit with MW and SMC dust). A similar value is found by Nardini et al. (2010). Oates et al. (2009), on the other hand, find $A_V = 0.11$ from UVOT data only (using an XRT-UVOT joint fit), which compares well with our result. Schady et al. (2010) find a marginal preference for MW dust and a cooling break between the optical and the X-rays, and derive $A_V \approx 0.15$ for this case, in agreement with our value. At 210 days after the GRB, a faint host galaxy is detected.

GRB 050820A, $z = 2.6147$. — We constructed the light curve and the SED with data from the following sources: Vestrand et al. (2006), Cenko et al. (2006b) and references therein, Macomb et al. (2005), as well as our own large data set (UAPhO, Maidanak, Shajn, RTT150, UKIRT, TNG, WIRO). Due to the complicated light curve structure (Cenko et al. 2006b), special care is taken in deriving the SED. Similar to Cenko et al. (2006b), we find that the optical afterglow is composed of four parts, a moderately steep decay, a shallow rebrightening phase, then another phase with an identical decay slope as the first phase, and finally a steep decay that is probably due to a jet break. As our late data are taken almost exclusively from Cenko et al. (2006b), our parameter results are identical within errors. Fixing the decay smoothness to $n = -10$ and the host galaxy magnitude $m_h = 27$, we find $m_k = 17.49 \pm 0.094$ mag, $\alpha_1 = 1.07 \pm 0.011$, $\alpha_2 = 0.54 \pm 0.051$, $t_b = 0.073 \pm 0.007$ days for the steep to shallow transition from 0.006 to 0.22 days. For the shallow to steep transition (0.09 to 7.7 days) we find (fixing $n = 10$, $m_h = 27$ mag): $m_k = 18.22 \pm 0.088$ mag, $\alpha_1 = 0.50 \pm 0.051$, $\alpha_2 = 1.04 \pm 0.016$, $t_b = 0.27 \pm 0.025$ days. Clearly, the fit finds identical values for the shallow phase from both fits, and the steep phases are also almost identical within errors (1.9σ). Finally, fitting the data from 0.75 days onward, we follow Cenko et al. (2006b) and fix $\alpha_2 = p = 2.34$, and find $m_k = 22.94 \pm 0.11$ mag, $\alpha_1 = 1.04 \pm 0.015$, $t_b = 18.19 \pm 1.28$ days, again in agreement with Cenko et al. (2006b). For the SED, we derive a steeper unextinct slope than Cenko et al. (2006b), $\beta_0 = 0.96 \pm 0.028$, and find no conclusive evidence for color evolution. We find a very low host extinction $A_V = 0.065 \pm 0.008$, in agreement with Cenko et al. (2006b), who find $A_V = 0$ for all dust extinction curves. Schady et al. (2010) find strong evidence for a cooling break between the optical and the X-rays, but are not able to distinguish the dust models beyond this, and find a higher value, $A_V \approx 0.14 - 0.32$, in comparison to ours.

XRF 050824, $z = 0.8281 \pm 0.004$. — We constructed the light curve and the SED with data from the following sources: Sollerman et al. (2007), Schady et al. (2005), and Lipunov et al. (2005). The full light curve analysis (which also finds evidence for a rapid supernova) can be found in Sollerman et al. (2007). The addition of *Swift* UVOT data (Schady et al. 2005) allows us to create a more detailed SED than that presented by Sollerman et al. (2007). From a fit without extinction, we find $\beta_0 = 0.65 \pm 0.07$, in accordance, within errors, with the value found by Sollerman et al. (2007), $\beta_0 = 0.56 \pm 0.04$. These authors are unable to discern MW, LMC and SMC extinction, and find $A_V = 0.4 \pm 0.2$ mag for SMC dust, albeit with $\beta \approx 0$. From our SED, we find a weak preference for SMC dust (with MW dust being ruled out, as the fit finds negative extinction), with $A_V = 0.14 \pm 0.13$ mag and $\beta = 0.45 \pm 0.18$, in accordance with the limit $A_V \leq 0.5$ mag from Sollerman et al. (2007). Schady et al. (2007a) find that SMC dust is weakly preferred, and are not able to discern between a scenario with and one without a cooling break between the X-rays and the optical. In the former case, they find $A_V = 0.12 \pm 0.04$, in the latter $A_V = 0.16^{+0.06}_{-0.04}$, in excellent agreement with our value.

GRB 050904, $z = 6.295 \pm 0.002$. — The complete analysis of this GRB is presented in Kann et al. (2007a). For Figure 1 in Paper II, we added the dRc value derived in Kann et al. (2007a) to the $z = 1$ light curve and transformed the time back to the observer frame. This is what the observed light curve in the R band would have looked like in a hypothetical fully ionized universe (no Lyman dropout). Liang & Li (2009) report higher extinction than we found using the "Drude" model of Li et al. (2008c). They claim to find a 2175 Å bump as well as an evolution in the characteristics of the extinction. Stratta et al. (2007a) claim the existence of non-standard "high-z SN dust" (Maiolino et al. 2004) and a larger extinction value than we derive. Recently, these results have been refuted by a careful analysis of Zafar et al. (2010), who concur with the analysis of Kann et al. (2007a), finding no evidence for dust or evolution.

GRB 050922C, $z = 2.1992 \pm 0.0005$. — We constructed the light curve and the SED with data from the following sources: Rykoff et al. (2009), Ofek et al. (2005), Durig & Price (2005), Henych et al. (2005), Novak (2005), Hunsberger et al. (2005), and Li et al. (2005), as well as our own extensive data set (Terskol, NOT, MDM, Danish 1.54, INT, WHT, VLT). No host galaxy is found down to deep limits (Ovaldsen et al. 2007; Chen et al. 2009). The composite light curve shows some small variations in the early UVOT data (Li et al. 2005; Hunsberger et al. 2005) but is otherwise a smooth broken power law with a soft rollover. We find $m_k = 17.70 \pm 0.089$ mag, $\alpha_1 = 0.76 \pm 0.016$, $\alpha_2 = 1.39 \pm 0.023$, $t_b = 0.11 \pm 0.008$ days, $n = 3.36 \pm 0.69$ and $m_h = 28$ mag was fixed. If this is due to a jet break, it is very early and the post-break slope is very shallow (see Zeh et al. 2006, for pre-*Swift* values). The SED shows essentially no signs of dust extinction, and no dust model can be preferred. Oates et al. (2009) find $A_V = 0.08$ from UVOT data only (using an XRT-UVOT joint fit), a comparably small value. Schady et al. (2010) are also unable to prefer any dust model (or make a statement concerning the location of the cooling break), but find a comparably low $A_V = 0.07 \pm 0.02$ for SMC dust and no cooling break (but higher values up to $A_V \approx 0.28$ for other models).

GRB 060124, $z = 2.297 \pm 0.001$. — We constructed the light curve and the SED with data from the following sources: Misra et al. (2007), Deng et al. (2006) and D. A. Kann et al., in preparation (paper on the GRB 060124 afterglow). Preliminary analyses of the data set of Kann et al. have been published by Curran et al. (2006) and Covino et al. (2006b). The afterglow of this extremely long GRB (Romano et al. 2006) is very luminous and well-described by an achromatic broken power law, with a contemporary break seen in the X-rays. The SED is best fit with a MW dust law, as there is evidence for a small 2175 Å bump. Schady et al. (2010) also find marginal evidence for a preference of MW dust, but derive an extinction value ($A_V = 0.52 \pm 0.13$) much in excess of our own ($A_V = 0.17 \pm 0.03$).

GRB 060206, $z = 4.04795 \pm 0.0002$. — We constructed the light curve and the SED with data from the following sources: Woźniak et al. (2006), Stanek et al. (2007), Monfardini et al. (2006), Curran et al. (2007b), Ofek et al. (2006), Lin et al. (2006), Milne & Williams (2006), Alatalo et al. (2006), Terada et al. (2006), Boyd et al. (2006), Greco et al. (2006a), LaCluyze et al. (2006), Reichart et al. (2006), and Thöne et al. (2008c) (host galaxy detection) as well as our own data set (SARA, Maidanak). The light curve is very complex, showing an extreme rebrightening feature (Woźniak et al. 2006; Monfardini et al. 2006), and special care was taken in determining the SED. Excluding the early rebrightening feature ($t < 0.09$ days), we fit the light curve with a broken power law and find $m_k = 17.79 \pm 0.049$ mag, $\alpha_1 = 0.80 \pm 0.031$, $\alpha_2 = 1.42 \pm 0.021$, $t_b = 0.26 \pm 0.008$ days, $n = 7.73 \pm 2.48$ and $m_h = 24.91 \pm 0.26$ mag (note that the actual host is several magnitudes fainter, but can only be separated from a very nearby galaxy by the HST, Thöne et al. 2008c; Chen et al. 2009). These results differ quite strongly from Stanek et al. (2007), who find $\alpha_1 = 0.7$, $\alpha_2 = 2.0$, and $t_b = 0.6$ days. There are small-scale variations present in the densely sampled data of Stanek et al. (2007), and it is possible that the light curve parameters and especially the break time are very sensitive to which data are actually included in the fit. As the final deep data points (Curran et al. 2007b) are overestimated in our fit, this may be indicative of another break and a following, steeper decay. These authors use only data after 0.2 days, and we are able to exactly reproduce their results if we use the same interval, we find $m_k = 18.87 \pm 0.11$ mag, $\alpha_1 = 1.13 \pm 0.016$, $\alpha_2 = 1.64 \pm 0.035$, $t_b = 0.57 \pm 0.044$ days, $n = 10$, $m_h = 24.9$ fixed. This afterglow is a good example of why dense sampling can be very important. From the SED, we find that MW dust is ruled out, but the preference for SMC dust is only weak. We find almost negligible extinction, in concurrence with Oates et al. (2009), who use UVOT data only (using an XRT-UVOT joint fit). Schady et al. (2010) also find (low) upper limits only on the extinction.

GRB 060418, $z = 1.49010 \pm 0.0001$. — We constructed the light curve and the SED with data from the following sources: Molinari et al. (2007), Melandri et al. (2008), Cenko et al. (2010a), Falcone et al. (2006), Nysewander et al.

(2006a), Jelínek et al. (2006a), Schady & Falcone (2006), Chen et al. (2006), Huang et al. (2006a), D. Malesani et al., in preparation (paper on the GRB 060418 afterglow), as well as our own data set (ANDICAM, Maidanak). As reported by several groups, the light curve shows a strong initial rise, which then rolls over into a power-law decay (Molinari et al. 2007; Nysewander et al. 2006a; Jelínek et al. 2006a). Shifting all data to the R_C zero point, we find no evidence for color evolution, in accordance with Molinari et al. (2007). The composite light curve is well fit with a broken power law and we find $m_k = 11.92 \pm 0.18$ mag, $\alpha_R = -5.89 \pm 1.38$, $\alpha_1 = 1.19 \pm 0.003$, $t_b = 80.7 \pm 10.8$ seconds, $n = 0.42 \pm 0.11$ and $m_h = 24.97 \pm 0.14$ mag (Cenko et al. 2010a, find no host underlying the direct afterglow position, but a very nearby galaxy complex would influence any ground-based imaging). We find no evidence for a jet break out to at least 10 days, in accordance with Cenko et al. (2010a), who detect a break only in late, very deep HST imaging. A host-corrected light curve confirms that the HST data lies more than a magnitude under the extrapolation of the earlier decay. These fit values are in similar to those found by Molinari et al. (2007), though we find a smoother rollover and a steeper early rise (which is sparsely sampled). The SED has been derived from a joint fit to all bands. We derive a very broad SED in 11 filters, and find that while no dust model can be strongly preferred, LMC dust yields the best result, with $A_V = 0.20 \pm 0.08$. This is interesting, as Ellison et al. (2006) find clear evidence of a 2175 Å bump deriving from a dusty foreground absorber at $z = 1.1$ in an echelle spectrum of the afterglow. While we fit at the redshift of the burst ($z = 1.49$, Prochaska et al. 2006), the low resolution of the SED may lead to the bump also affecting our SED. The extinction we derive is therefore probably a superposition of extinction in the host frame and in the foreground absorbers. Our extinction results are marginally consistent to those derived by Schady et al. (2007a), who derive higher values, but also prefer LMC dust. Oates et al. (2009) find $A_V = 0.08$ from UVOT data only (using an XRT-UVOT joint fit), a smaller value. Schady et al. (2010) find marginal preference for SMC dust and a value similar to Oates et al. (2009), $A_V \approx 0.09$.

GRB 060526, $z = 3.211 \pm 0.001$. — The complete analysis of this GRB is presented in Thöne et al. (2010). Those authors find that the complex, highly variable light curve can be modeled with multiple energy injections, as well as jet break (see also Dai et al. 2007). The SED is fit well by SMC dust and a small amount of extinction. Oates et al. (2009) find no evidence for dust from UVOT data only (using an XRT-UVOT joint fit). Schady et al. (2010) derive mostly low upper limits and two low detections and are not able to discern between dust models.

GRB 060607A, $z = 3.0749$. — We constructed the light curve and the SED with data from the following sources: Molinari et al. (2007), Nysewander et al. (2009a), Ziaeepour et al. (2008), and Fynbo et al. (2009) as well as our own ANDICAM data set. No host is detected down to deep levels (Chen et al. 2009). The afterglow shows an early rise and several achromatic bumps (Molinari et al. 2007; Nysewander et al. 2009a; Ziaeepour et al. 2008). As the last detection is at 0.2 days in the observer frame, no statement can be made about the magnitude at one day. The SED shows very little dust, the SMC fit is weakly preferred, but the extinction is 0 within errors. This is comparable to Oates et al. (2009), who find $A_V = 0.05$ from UVOT data only (using an XRT-UVOT joint fit). Schady et al. (2010) similarly derive low upper limits only and are not able to discern between any models.

GRB 060904B, $z = 0.7029$. — We constructed the light curve and the SED with data from the following sources: Klotz et al. (2008c), Rykoff et al. (2009), Fynbo et al. (2009), de Ugarte Postigo et al. (2006b), Skvarc (2006), Oates & Grupe (2006), Greco et al. (2006b), Prymak et al. (2006), Soyano et al. (2006), and Huang et al. (2006b), as well as our own data set (ANDICAM, RTT150, Maidanak). This GRB features strong early variability during the prompt emission (Rykoff et al. 2009). In agreement with Klotz et al. (2008c), we find a peaking afterglow from 0.001 to 0.012 days, with parameters $m_k = 16.347 \pm 0.031$ mag, $\alpha_R = -0.665 \pm 0.085$ (rising slope), $\alpha_F = 1.143 \pm 0.069$ (falling slope), $t_b = 546 \pm 20$ s and $n = 10$ fixed. At $t_{b2} = 1213 \pm 110$ s, the decay goes over into a slow decay/plateau phase with $\alpha_P = 0.145 \pm 0.077$, before resuming, at $t_{b3} = 4281 \pm 314$ s, a smooth decay with $\alpha = 1.170 \pm 0.026$. As the slopes before and after the plateau are identical, this may indicate a "step" due to an energy injection (see Klotz et al. 2008c). The SED is very broad, and includes 10 filters from $UVW2$ to K. The SED is relatively steep but also flat, and we only find a small amount of dust. This is indicative of a cooling break redward of the optical. SMC dust is (weakly) preferred, and the bright detections in UB clearly rule out a 2175 Å bump. Schady et al. (2010) find no good fit for any dust model (with fits without a cooling break between optical and X-rays being even less likely), but derive low extinction in all cases, in agreement with our result.

GRB 060908, $z = 1.8836$. — We constructed the light curve and the SED with data from the following sources: Covino et al. (2010), Cenko et al. (2009b), Fynbo et al. (2009), Nysewander et al. (2006b), as well as a single data point published here. The light curve is adequately fit with a single power law: $m_k = 22.66 \pm 0.03$ mag and $\alpha = 1.08 \pm 0.007$ (for our fits, we use host-subtracted data). But there are significant deviations from the power law, $\chi^2 = 192$ for 117 degrees of freedom. The earliest data points show a steeper decay, removing these yields a significant improvement ($\chi^2 = 115$ for 109 degrees of freedom), and the parameters $m_k = 22.52 \pm 0.03$ and $\alpha = 1.04 \pm 0.007$. Two data points at one day lie significantly (≈ 0.5 mag) below the extrapolation of the early decay, indicating that a break may have occurred (we note that a further P60 data point at four days is overluminous and has not been included). Due to the sparsity of the data, the break time and post-break decay slope are unconstrained in a free fit, but fixing $\alpha_2 = 1.6$ (from the SED, see below), we find $t_b = 0.44 \pm 0.12$ days. The SED is broad, from B to K. We find a very flat SED ($\beta_0 = 0.30 \pm 0.06$, which implies $p = 1.6$ for ν_c blueward of the optical bands, in excellent agreement with the hard X-ray slope $\Gamma = 1.798$) and no evidence for dust. MW and LMC fits yield negative extinction and are ruled out. The SMC fit yields a small amount of dust (albeit 0 within errors) but makes the SED even more blue. Therefore, we use

β_0. The flat SED strongly resembles that of GRB 021211 (Kann et al. 2006). Oates et al. (2009) also find very low extinction, $A_V = 0.02$ from UVOT data only (using an XRT-UVOT joint fit). Similarly, Schady et al. (2010) derive low upper limits for all models only, they marginally prefer a cooling break between the optical and the X-rays.

GRB 061007, $z = 1.2622$. — We constructed the light curve and the SED with data from the following sources: Mundell et al. (2007b), Schady et al. (2007b), and Rykoff et al. (2009), as well as our own ANDICAM data, which includes the only NIR detections of this GRB that we are aware of. We confirm the rebrightening feature (Mundell et al. 2007b). Excluding this feature, we can fit the data with a single power law with $m_k = 22.32 \pm 0.033$ (note that in this case this is the R magnitude at 1 day after the GRB) and $\alpha = 1.71 \pm 0.009$. We fix $m_h = 26$ mag. This is fully consistent with Mundell et al. (2007b), who find $\alpha = 1.72 \pm 0.10$, and also consistent with Schady et al. (2007b), who find $\alpha = 1.64 \pm 0.01$. Furthermore, consistent with Mundell et al. (2007b) and Schady et al. (2007b), we find that the afterglow, notwithstanding its extreme brightness, is moderately extinct. While there is only weak evidence for the 2175 Å feature, we find that LMC is the preferred dust model, since both MW and SMC dust lead to much smaller extinction and intrinsic spectral slopes that are too steep for the standard fireball model. We find $\beta = 1.07 \pm 0.19$ and $A_V = 0.48 \pm 0.10$, which is among the highest values in comparison with the sample of K06. Mundell et al. (2007b) derive $\beta = 1.02 \pm 0.05$ and $A_V = 0.48 \pm 0.19$ for SMC dust and a joint optical to X-ray fit, in excellent agreement with our value. From a similar fit, Schady et al. (2007b) find $\beta = 0.90 \pm 0.005$ and $A_V = 0.39 \pm 0.01$ for SMC dust but they also prefer LMC dust, where they find $\beta = 0.98 \pm 0.007$ and $A_V = 0.66 \pm 0.02$. Oates et al. (2009) also find a high value, $A_V = 0.66$, from UVOT data only (using an XRT-UVOT joint fit). Schady et al. (2010) also find high extinction values, they strongly rule out MW dust and prefer LMC dust, where, for a fit with no cooling break between the optical and the X-rays, they find $A_V = 0.75 \pm 0.02$. Similar to the SED of GRB 050525A, there is scatter while the errors themselves are small, leading to a high χ^2/d.o.f.

GRB 061126, $z = 1.1588 \pm 0.0006$. — We constructed the light curve and the SED with data from the following sources: Perley et al. (2008a), and Gomboc et al. (2008). The light curve analysis is presented in the latter paper. We confirm the early color evolution found by Perley et al. (2008a), and thus exclude this data from the SED construction. We find a rather steep but very straight broad SED (U to K_S, the *Swift* UVOT UV filters lie beyond Lyman α and are not included.). Fitting with dust, we find that SMC dust gives the best fit, with a very low amount of line-of-sight extinction, $A_V = 0.095 \pm 0.055$. This is fully in agreement with Perley et al. (2008a), who find no "classical" dust but imply the need for strong gray extinction to explain the optical subluminosity in contrast with the bright X-ray afterglow (see also Li et al. 2008a). Gomboc et al. (2008) find higher extinction values from joint X-ray-to-optical fits, as well as variable extinction, which stems from the fact that the X-ray afterglow decays more rapidly than the optical afterglow, reducing the offset Perley et al. (2008a) first detected. At 40 ks, Gomboc et al. (2008) find $A_V \lesssim 0.13$ mag, in agreement with our result. Nardini et al. (2010) interpret the light curve as being dominated at late times by "late prompt" emission, and also find no need for any extinction. Schady et al. (2010) find marginal preference for SMC dust and a strong preference for a cooling break between the optical and the X-rays, and find $A_V = 0.10 \pm 0.04$, in excellent agreement with our result.

GRB 070125, $z = 1.5477 \pm 0.0001$. — We constructed the light curve and the SED with data from the following sources: Updike et al. (2008b), Chandra et al. (2008), Dai et al. (2008), Yoshida et al. (2007a), Uemura et al. (2007a), Durig & Gary (2007), and Sposetti (2007a), as well as our own ANDICAM data set. By shifting data to the R-band zero point, we find an achromatic evolution (except for very early UVOT observations, which have a different $B-V$ color than later on), and construct a cleaned composite light curve. In accordance with Updike et al. (2008b), we find an early rebrightening. Fitting the data up to 0.95 days (before the plateau and rebrightening), we find $m_k = 18.806 \pm 0.014$ mag and $\alpha_1 = 1.460 \pm 0.063$. The following rebrightening episodes are described in detail in Updike et al. (2008b). Using all data from beyond 1.5 days, we find clear evidence for a break in the light curve, in accordance with Updike et al. (2008b), Chandra et al. (2008), and Dai et al. (2008). We derive the following parameters: $m_k = 21.442 \pm 0.303$ mag, $\alpha_1 = 1.793 \pm 0.014$, $\alpha_2 = 2.875 \pm 0.200$, $t_b = 5.309 \pm 0.810$ days, and $n = 10$ fixed. We followed Cenko et al. (2008) and assume an extremely faint "host galaxy" (e.g., tidal tail starburst). The SED, reaching from $UVW2$ to K, consists of 14 filters (the UVOT UV filters are affected by Lyman damping and are not included in the fit). We find a very good fit with SMC dust, which is strongly preferred.

GRB 070419A, $z = 0.9705$. — We constructed the light curve and the SED with data from the following sources: Melandri et al. (2009), Cenko et al. (2009b), Dai et al. (2008), Fynbo et al. (2009), Iizuka et al. (2007), Wren et al. (2007b), Swan et al. (2007b), and Landsman & Stamatikos (2007), and we also publish SARA data (one upper limit and one marginal detection) and an unused upper limit from the 1.5m Sayan telescope. The complex light curve, featuring an early rise, a broken power-law decay, and a late flattening, is analyzed in Melandri et al. (2009). At very late times, there is a possible supernova bump (Dai et al. 2008). We derive the SED from a joint fit to the broken power-law portion, and find $\alpha_1 = 0.54 \pm 0.08$, $\alpha_2 = 1.42 \pm 0.04$, $t_b = 0.0158 \pm 0.0014$ days and $n = 10$ fixed (no host galaxy). These values are in good agreement with Melandri et al. (2009). For the SED, we use UVOT v data, as the V data from Melandri et al. (2009) is too bright, probably due to the NOMAD calibration (A. Melandri, priv. comm.). The SED shows some scatter. We find the best fit is achieved with MW dust, though the preference is weak, our value ($A_V = 0.32 \pm 0.27$) is in excellent agreement with that of Melandri et al. (2009) ($A_V = 0.37 \pm 0.19$ from a joint optical-X-ray fit), but only marginally in agreement with Cenko et al. (2009b), who find $A_V = 0.70^{+0.31}_{-0.10}$.

GRB 070802, z = 2.4541. — We constructed the light curve and the SED with data from the following sources: Krühler et al. (2008), and Elíasdóttir et al. (2009). The afterglow of this faint GRB features an early peak/flare peaking at 0.027 days (Krühler et al. 2008). Late detections are sparse, and we need to extrapolate to determine the magnitude at one day after the GRB. The afterglow is highly reddened ($\beta_0 \approx 3$) and shows a clear 2175 Å dust feature, the most distant detected so far except for the also highly extinct GRB 080607 (Prochaska et al. 2009). In agreement with Krühler et al. (2008) and Elíasdóttir et al. (2009), we find that the SED is best fit (among the three dust laws we use) by a large amount of LMC dust. We find $A_V = 1.18 \pm 0.19$, in combination with an intrinsic spectral slope $\beta = 1.07 \pm 0.31$, which is in perfect agreement with the X-ray spectrum ($\beta_X = 1.02^{+0.17}_{-0.15}$, Elíasdóttir et al. 2009), implying that both lie on the same slope and the derived extinction is actually the lowest possible amount (from an optical/NIR only spectrum, using the complete broadband spectrum can actually lead to lower values, see Elíasdóttir et al. 2009). The high $\chi^2_\nu = 2.84$ of the fit indicates that even LMC dust is not able to model the SED perfectly. This is a good candidate for the advanced dust model ("Drude" model) of Li et al. (2008c), and Elíasdóttir et al. (2009) find that the best fits are obtained from the spectrum and a Fitzpatrick-Massa parametrization. Liang & Li (2009) have used the "Drude" model and find that the extinction curve consists of a 2175 Å bump similar to that of the MW combined with a UV extinction similar to the LMC. We use our SED (excluding the H band, so we have eleven filters) and derive a very peculiar result: $\chi^2 = 6.62$ for 4 d.o.f., $F_0 = 5022677 \pm 30347844$, $\beta = -11.83 \pm 10.95$, $A_V = 12.22 \pm 7.61$, $c_1 = 0.41 \pm 3.78$, $c_2 = -0.82 \pm 4.46$, $c_3 = -1.68 \pm 2.75$, $c_4 = 0.0031 \pm 0.0019$ (F_0 is the normalization. β and A_V are identical in usage to this paper, and the constants $c_{1...4}$ determine the specific shape of the "Drude" functions, see Li et al. 2008c for details). By eye, the fit is excellent, but clearly this result is unphysical, and reveals two fundamental problems of the "Drude" approach: Firstly, the function is too flexible, and can achieve good fitting results which are nonsensical in terms of the resulting parameters. Secondly, and related, the parameters are almost all unconstrained. This is mainly due to parts of the function being "anchored" by only very few data points at the blue and red ends of the SED. Fixing $\beta = 1.02$, we find $\chi^2 = 10.15$ for 5 d.o.f., $F_0 = 590 \pm 1112$, $A_V = 1.35 \pm 2.04$, $c_1 = 0.22 \pm 22.6$, $c_2 = -0.60 \pm 31.8$, $c_3 = -1.94 \pm 6.14$, $c_4 = 0.033 \pm 0.054$. These values are roughly comparable with those of Liang & Li (2009), but they are all unconstrained. Liang & Li (2009) do not publish the errors of their values. This is, next to the more unsure extinction of GRB 060210, the largest extinction found in the sample, clearly exceeding all values from the pre-*Swift* era (K06), though still much less than some very dark GRBs described in Perley et al. (2009d) or the case of GRB 080607 (Prochaska et al. 2009).

GRB 071003, z = 1.60435. — We constructed the light curve and the SED with data from the following sources: Perley et al. (2008d), and Guidorzi et al. (2007b). This very energetic GRB is discussed in detail in Perley et al. (2008d). The early light curve features a small chromatic flare, and at 0.04 days, the afterglow decay turns over into a large (but only sparsely sampled) rebrightening. The late decay is probably smooth but most measurements are low S/N due to a nearby bright star. Very late NIR AO observations reveal no underlying galaxy to deep levels (Perley et al. 2008d). Construction of the SED of this GRB was complicated, as observations in different filters often do not occur simultaneously. We assume an achromatic evolution (excepting the small early flare) but can not conclusively show that this is the case. The SED is well-fit by SMC dust and moderately high extinction, in agreement with Perley et al. (2008d).

XRF 071010A, z = 0.985 ± 0.005. — We constructed the light curve and the SED with data from the following sources: Covino et al. (2008c), and Cenko et al. (2009b). Covino et al. (2008c) present a detailed analysis of this XRF and its optical/NIR afterglow, which features an early rise, an energy injection at about 0.6 days and a late, steep decay, very probably post-jet break. We find the following parameters from a compound light curve: $\alpha_{rise} = -0.94 \pm 0.10$, $t_{peak} = 0.005 \pm 0.0002$ days, $\alpha_1 = 0.73 \pm 0.01$. After the energy injection, we find: $\alpha_{EI} = 1.01 \pm 0.22$, $t_b = 1.08 \pm 0.10$ days, and $\alpha_2 = 2.14 \pm 0.04$. These values are in full agreement with Covino et al. (2008c). We furthermore confirm that this GRB afterglow is moderately highly extinct, for the strongly preferred SMC dust, we find $A_V = 0.64 \pm 0.09$, one of the highest values and clearest detections (7.5σ) in the sample.

XRF 071031, z = 2.6918. — We constructed the light curve and the SED with data from the following sources: Krühler et al. (2009a), Fynbo et al. (2009), Haislip et al. (2007), Stroh et al. (2007) as well as our own ANDICAM data set. The early afterglow of this XRF shows a complex evolution, with an early rise and several superposed flares which show color evolution (Krühler et al. 2009a). We derive the SED from data after 0.07 days, where the afterglow is mostly achromatic. We find an intrinsically blue SED with a small amount of SMC dust, which is strongly preferred. The magnitude at one day can only be derived via extrapolation and thus has a large error associated with it. ANDICAM limits at two days are not deep enough to allow any assertions about the existence of a break in the light curve.

GRB 071112C, z = 0.8227. — We constructed the light curve and the SED with data from the following sources: Fynbo et al. (2009), Yuan et al. (2007b), Wang et al. (2007), Klotz et al. (2007), Burenin et al. (2007), Chen et al. (2007a,b), Dintinjana et al. (2007), Oates & Stratta (2007), Ishimura et al. (2007b), Greco et al. (2007), Sposetti (2007b), Yoshida et al. (2007c), Uemura et al. (2007b), Minezaki et al. (2007), and Huang et al. (2008a). This GRB afterglow was rapidly observed by many observatories on the western Pacific rim. It shows a plateau phase early on (Yuan et al. 2007b; Huang et al. 2008a), after 0.003 days, we find a decay slope of $\alpha = 0.93 \pm 0.02$ in the R_C band. The SED is broad ($UVW1$ to K), shows slight curvature, is well fit by a small amount of SMC dust and shows a strong dropout in $UVM2$ and $UVW2$, in agreement with the low redshift (z=0.8227, Fynbo et al. 2009).

GRB 080129, z = 4.349 ± 0.002. — We constructed the light curve and the SED with data from the following sources: Greiner et al. (2009a), and Perley & Bloom (2008) (we also present ANDICAM upper limits). This faint high-z event had a remarkable light curve, the most striking feature being a huge optical/NIR flare that peaks at about 0.006 days after the GRB, a phenomenon that has not been seen in any other optical/NIR light curve. This flare is followed by a slow rise and a very long plateau phase extending up to 2 days after the GRB, where a steep decay sets in (Greiner et al. 2009a). Even at late times, the afterglow exhibits small-scale variations, e.g. a flare at 0.82 days for which we find a clear spectral hardening. The early flare shows clear color evolution (Greiner et al. 2009a), and we derive the SED from a joint fit of data after 0.78 days, where the afterglow is mostly achromatic. From this fit, we find parameters $\alpha_1 = -0.15 \pm 0.06$, $\alpha_2 = 2.15 \pm 0.23$, $t_b = 2.03 \pm 0.13$ days, and $n = 10$ fixed (no host galaxy). The burst lay in the Galactic plane, with high foreground extinction ($E(B - V) \approx 1$), after correcting for this, we find a straight SED with no sign of dust extinction. The very long plateau phase combined with the high redshift leads to this afterglow being the most luminous ever discovered at 0.5 days after the GRB in the host frame, even though especially the early afterglow is significantly fainter than most afterglows in the sample.

GRB 080210, z = 2.6419. — We constructed the light curve and the SED with data from the following sources: Fynbo et al. (2009), Klotz et al. (2008a), Küpcü Yoldas et al. (2008), Brennan et al. (2008), Updike et al. (2008a), Perley et al. (2008b), Grupe et al. (2008), as well as one data point from the 1.5m Sayan telescope. Data on this GRB is rather sparse. It seems to show an early peak, after which the light curve decays with $\alpha = 1.06 \pm 0.02$ (though the Sayan observation indicates a rebrightening feature). The SED is broad, encompassing ten filters from GROND g to GROND K, very red and shows a spectral "plateau" in the GROND i and GROND z bands which may indicate the presence of a 2175 Å bump. Indeed, while there is still some deviation from the model, the best fit is achieved by a quite large ($A_V = 0.7$) amount of LMC dust. SMC dust shows strong residuals, and MW dust undercorrects the extinction. We caution that this fit is based on preliminary data from GROND only. The VLT spectrum also indicates significant reddening (Fynbo et al. 2009). The large extinction leads to a large dRc, making it this a very bright afterglow at early times.

XRF 080310, z = 2.4274. — We constructed the light curve and the SED with data from the following sources: Cenko et al. (2009b), Chornock et al. (2008), Covino et al. (2008a,b), Milne & Williams (2008), Chen et al. (2008), Hoversten & Cummings (2008), Woźniak et al. (2008), Perley et al. (2008c), Garnavich et al. (2008a,b), Yoshida et al. (2008a), Yuan et al. (2008a), Urata et al. (2008), Wegner et al. (2008), and Hill et al. (2008) as well as our own ANDICAM data set. This XRF has a complex optical light curve, with an early plateau phase which smoothly rolls over into a steeper decay, and a second flat phase from 1 to 2 days after the trigger, after which the light curve decays steeply. From a joint fit of the data up to 0.5 days, we find $\alpha_1 = -0.12 \pm 0.05$, $\alpha_2 = 1.64 \pm 0.11$, $t_b = 0.049 \pm 0.0041$ days, $n = 0.83 \pm 0.18$, and $m_h = 27$ fixed. The SED is broad and well-sampled, from B to K bands, and is well-fit with SMC dust and a small amount of extinction.

GRB 080319B, z = 0.9371. — We constructed the light curve and the SED with data from the following sources: Bloom et al. (2009), Racusin et al. (2008), Woźniak et al. (2009), Tanvir et al. (2008b), Cenko et al. (2009b), Pandey et al. (2009), Swan et al. (2008), Hentunen et al. (2008), and Cenko et al. (2010a). GRB 080319B is optically the most extreme GRB ever observed. Observationally, the prompt optical flash (Racusin et al. 2008; Bloom et al. 2009; Swan et al. 2008) reached 5th magnitude, earning it the moniker "naked-eye GRB". Due to the proximity of GRB 080319A which happened just 27 minutes earlier and 14 degrees away on the sky, it was observed even before the trigger by wide-field sky monitors (Racusin et al. 2008; Woźniak et al. 2009), allowing, for the first time, a sub-second sampling of the prompt optical light curve (Beskin et al. 2009). The event also had the highest fluence of any GRB in the *Swift* era including IPN GRBs which were not localized and followed up. In the last 20 years, only GRB 021206 has had a higher fluence (Wigger et al. 2008). The extremely bright early afterglow combined with favorable observing conditions lead to the second-best afterglow sampling ever (after GRB 030329), but at one day already, the afterglow is not especially luminous anymore. Concurrent with Bloom et al. (2009) and Racusin et al. (2008), we find a very flat spectrum (determined from 0.04 to 0.4 days after the GRB, there is strong color evolution earlier on, Bloom et al. 2009; Racusin et al. 2008; Woźniak et al. 2009) and no sign of any dust extinction. The early prompt flash is the most luminous source ever observed, and exceeds GRB 050904 (Kann et al. 2007a) by over a magnitude (Bloom et al. 2009). The afterglow evolution is complex, with evidence for a late jet break (Racusin et al. 2008) as well as an underlying supernova (Bloom et al. 2009; Tanvir et al. 2008b).

GRB 080319C, z = 1.9492. — We constructed the light curve and the SED with data from the following sources: Cenko et al. (2009b), Fynbo et al. (2009), Williams & Milne (2008), Li & Fillipenko (2008), Wren et al. (2008a), Pagani et al. (2008), and Perley et al. (2009d). Due to GRB 080319B, this burst does not have extensive follow-up. At 0.004 days, it shows an optical flare also seen in the X-rays (Perley et al. 2009d). These authors also report on an intrinsically luminous host galaxy. Starting at 0.01 days, the afterglow decays quite steeply ($\alpha = 1.47 \pm 0.08$). As the data around one day at $z = 1$ (Cenko et al. 2009b) are already strongly dominated by the host galaxy, we are unable to firmly deduce a magnitude at one day. We find moderately high extinction and a strong preference for SMC dust, in accordance with Cenko et al. (2009b) and Perley et al. (2009d).

XRF 080330, z = 1.5115. — We constructed the light curve and the SED with data from the following sources: Guidorzi et al. (2009a), Yuan et al. (2008b), Schaefer & Guver (2008), Bloom & Starr (2008), Im et al. (2008), Wang et al. (2008), Schubel et al. (2008), Wren et al. (2008b), Block & Templeton (2008), and additional Seeing In

The Dark Internet Telescope data (A. Block, priv. comm.) as well as our own data set (ANDICAM, Terskol 2m). The light curve of this X-ray flash is complex (and similar to that of XRF 080310), with initial rapid variability (Yuan et al. 2008b; Wren et al. 2008b), followed by a plateau phase, and then a gradual steepening of the decay. Finally, another break (possibly a jet break) may occur (Guidorzi et al. 2009a). Fitting the data from 0.04 to 1 days, we find: $\alpha_1 = 0.09 \pm 0.02$, $\alpha_2 = 1.127 \pm 0.005$, $t_b = 0.021 \pm 0.0005$ days, n $= 3.60 \pm 0.36$ (no host galaxy). We note a small amplitude optical flare from 0.2 to 1 day. The SED spans from U to K and consists of 15 data points. We find weak evidence for a preference of Milky Way type dust, but all three dust models fit well with a small amount of dust. Intrinsically, the afterglow is not very luminous.

GRB 080413A, $z = 2.4330$. — We constructed the light curve and the SED with data from the following sources: Yuan et al. (2008b), Klotz et al. (2008b), Antonelli et al. (2008), Fukui et al. (2008), as well as our own ANDICAM data set. We are able to jointly fit all afterglow data with a broken power-law with parameters $\alpha_1 = 0.64 \pm 0.03$, $\alpha_2 = 1.58 \pm 0.04$, $t_b = 0.013 \pm 0.002$ days, and $n = 2.5$ fixed, and no host galaxy. We find a strong preference for SMC dust (MW and LMC dust yield negative extinction) and low extinction (equal to 0 within errors).

GRB 080710, $z = 0.8454$. — We constructed the light curve and the SED with data from the following sources: Krühler et al. (2009b), Li et al. (2008b), D'Avanzo et al. (2008), Bersier & Gomboc (2008), Landsman & Sbarufatti (2008), Weaver et al. (2008), Perley & Melis (2008), and Yoshida et al. (2008b). This afterglow showed a slow rise and multiple breaks (Krühler et al. 2009b) and is one of the observationally brightest afterglows ever observed around 0.05 days. The low redshift of $z = 0.8454$ (Fynbo et al. 2009) and the small amount of dust extinction imply that it is much fainter intrinsically, though. Using data beyond the light curve peak at 0.03 days, a joint fit finds $\alpha_1 = 0.54 \pm 0.04$, $\alpha_2 = 1.60 \pm 0.01$, $t_b = 0.110 \pm 0.003$ days, $n = 3.68 \pm 0.82$, and we assumed no host galaxy. These values are in agreement with Krühler et al. (2009b). A fit to the broad SED ($UVM2$ to K_G, 14 filters) shows that only a small amount of extinction is needed. While we can not discern between SMC and LMC dust, there is no evidence of a 2175 Å bump.

GRB 080913, $z = 6.733$. — We constructed the light curve and the SED with data from the following sources: Greiner et al. (2009b). This very high redshift GRB (the record holder until the recent GRB 090423 at $z = 8.2$, Tanvir et al. 2009; Salvaterra et al. 2009b) has been extensively analyzed in Greiner et al. (2009b). The light curve shows a strong late-time rebrightening. In accordance with these authors, we find no evidence for dust. Intrinsically, the afterglow is fainter than the mean at early times, but the rebrightening causes it to become more luminous than the mean at late times.

GRB 080916C, $z = 4.35 \pm 0.15$. — We constructed the light curve and the SED with data from the following sources: Greiner et al. (2009c). This extremely energetic GRB was detected by Fermi GBM/LAT and extensively discussed by Abdo et al. (2009a). The optical observations are sparse and only a photo-z (albeit with good precision) is known (Greiner et al. 2009c). We find no evidence for any dust along the sightline. The afterglow decays with $\alpha = 1.40 \pm 0.10$. Both results are in perfect agreement with Greiner et al. (2009c). The afterglow, despite the extremely energetic prompt emission, is not overly luminous and comparable to most afterglows in the sample. We note that if the LAT emission of this GRB is dominated by external shock emission (Kumar & Barniol Duran 2009), the isotropic energy release may be overestimated, on the other hand, the bolometric bandpass should be dominated by the true prompt emission, implying that the correction, if any, is small. This changes if the energetics are computed up to 10 GeV in the rest frame, though (Amati et al. 2009).

GRB 080928, $z = 1.6919$. — We constructed the light curve and the SED with data from the following sources: Rossi et al. (2010), Fynbo et al. (2009), and Ferrero et al. (2008b) (see Rossi et al. 2010 for further details). The light curve evolution and the SED analysis are reported in Rossi et al. (2010), who find a strongly variable early light curve with multiple peaks and a steep late decay, as well as a rather red SED which is best fit by a small amount of MW dust; the underlying spectral slope is still steep, and in full agreement with the X-ray spectral slope.

GRB 081008, $z = 1.9685$. — We constructed the light curve and the SED with data from the following sources: Yuan et al. (2010), as well as our own ANDICAM data set. Yuan et al. (2010) report an initially rising afterglow with small-scale variability (probably linked to central engine activity) superposed, which then goes over into a smooth decay which later shows a break. From a multicolor joint fit, we find $\alpha_1 = 0.931 \pm 0.006$, $\alpha_2 = 1.132 \pm 0.008$, $t_b = 0.048 \pm 0.004$ days, $n = 10$ fixed, and a faint host galaxy assumed. Our decay slopes agree very well with Yuan et al. (2010), but we find an earlier break. Late upper limits hint that a further break may have occurred. The SED shows a bit of scatter, we find it is best fit by a small amount of SMC dust and an intrinsically blue slope. Yuan et al. (2010) find a break in the optical SED, with a larger amount of dust and $\beta \approx 0$, we can not confirm this.

GRB 090102, $z = 1.547$. — We constructed the light curve and the SED with data from the following sources: Gendre et al. (2010), de Ugarte Postigo et al. (2009a,b), Curran et al. (2009), Cenko et al. (2009a), Malesani et al. (2009), and Levan et al. (2009). We set T_0 as 14 seconds before the Swift trigger. This GRB shows an early steep decay, which may be due to a reverse shock flash, caught in high time resolution by TAROT (Gendre et al. 2010). Note that this refined analysis comes to a very different result from Klotz et al. (2009a), who found a rapid rise to a peak. The reverse shock flash interpretation is further supported by the recent report of significant polarization in the early optical afterglow (Steele et al. 2009). Gendre et al. (2010) fit the complete, well-sampled light curve with a

steep-to-shallow broken power law. Using a similar fit, we find $\alpha_1 = 1.79 \pm 0.09$, $\alpha_2 = 1.10 \pm 0.02$, $t_b = 0.004 \pm 0.00075$ days, $n = -10$ fixed, in decent agreement with the values from Gendre et al. (2010): $\alpha_1 = 1.50 \pm 0.06$, $\alpha_2 = 0.97 \pm 0.03$, $t_b \approx 0.012$ days. But there are clear residuals seen between 0.01 and 0.1 days, and we find the light curve can be fit by a total of four power law segments: $\alpha_1 = 1.92 \pm 0.03$, $t_{b1} = 0.0060 \pm 0.0016$ days, $\alpha_2 = 1.54 \pm 0.13$, $t_{b2} = 0.0167 \pm 0.0064$ days, $\alpha_3 = 0.86 \pm 0.05$, $t_{b3} = 0.200 \pm 0.027$ days, $\alpha_4 = 1.38 \pm 0.04$ ($n = -10$ or $n = 10$ fixed), $m_h = 24.2 \pm 0.12$ mags. Gendre et al. (2010) have already noted that the afterglow behavior does not agree with the standard fireball model, if this more complex evolution is correct, the problem becomes even more persistent. We furthermore confirm no (jet) break out to several days. Both afterglow behavior and the SED are comparable to those of GRB 061126, according to Gendre et al. (2010), and we also confirm this in terms of the SED. The moderately red, well-sampled SED is best fit by a small amount of SMC dust (with LMC dust yielding similar results), with an intrinsic spectral slope in good agreement with the blue X-ray slope (Gendre et al. 2010). But Gendre et al. (2010) find a $\beta_{OX} = 0.53$ which makes this almost a dark burst, implying either very gray extinction or an additional emissive component in the X-rays. They find higher extinction values for MW and LMC dust, but their SMC result is in agreement with our value within errors. Note that the redshift of this GRB is almost identical to that of GRB 070125.

GRB 090313, $z = 3.3736 \pm 0.0004$. — We constructed the light curve and the SED with data from the following sources: Updike et al. (2009a), Guidorzi et al. (2009b), Nissinen (2009), de Ugarte Postigo et al. (2009c,d), Morgan et al. (2009), Vaalsta & Coward (2009), Perley (2009a), Klotz et al. (2009b), Perley et al. (2009b), Cobb (2009a), and Maiorano et al. (2009). This moderately high redshift *Swift* GRB has an exceptionally luminous afterglow. The afterglow evolution is complex, with an early rise and a possible long plateau phase (Perley et al. 2009a; de Ugarte Postigo et al. 2009c) and a late steep decay (de Ugarte Postigo et al. 2009d; Cobb 2009a). We find that SMC dust is strongly preferred and the extinction is quite high for a burst at $z > 3$, with $A_V = 0.34 \pm 0.15$. From about 0.02 to 0.5 days (at $z = 1$), this is the most luminous afterglow ever detected.

GRB 090323, $z = 3.568 \pm 0.004$. — We constructed the light curve and the SED with data from the following sources: McBreen et al. (2010), Cenko et al. (2010b), Wang et al. (2009), Perley et al. (2009c); Perley (2009b), Guidorzi et al. (2009c) as well as our own data set (RTT150, NOT, Shajn). We find that until 5 days after the GRB, the decay is described well with a power-law $\alpha = 1.93 \pm 0.02$, before a plateau phase sets in (de Ugarte Postigo et al. 2009e; McBreen et al. 2010), before returning to a similar decay rate as before. McBreen et al. (2010) give evidence that this is a post-jet-break decay slope, this is contested in Cenko et al. (2010b). This burst was extremely energetic (Bissaldi 2010) (within the rest-frame 1 - 10000 keV band, it has the highest isotropic energy in the entire sample, larger even than that of GRB 080916C, see also Amati et al. 2009) and was detected by Fermi LAT up to several kiloseconds after the event (Ohno et al. 2009). We find that the SED is well-fit by a small amount of SMC dust, which is strongly preferred. The afterglow is intrinsically highly luminous, among the brightest in the sample.

GRB 090328, $z = 0.7354 \pm 0.0003$. — We constructed the light curve and the SED with data from the following sources: McBreen et al. (2010), Cenko et al. (2010b), and Allen et al. (2009). McBreen et al. (2010) report the afterglow can be fit with a steep decay and a late-time, achromatic bump before going over into a bright host galaxy. We find that it can be fit equally well with a steep-to-shallow transition, with the following parameters: $\alpha_1 = 2.36 \pm 0.50$, $\alpha_2 = 1.36 \pm 0.26$, $t_b = 2.33 \pm 0.61$ days, $n = -10$ fixed, and host galaxy magnitudes left free for each filter except for K_G and i'. The steep decay is consistent with a post-jet-break decay (but see Cenko et al. 2010b), and there is marginal evidence for a more shallow decay at one day and earlier. The SED is red but straight, and we find that we can not discern between MW, LMC and SMC dust, in full agreement with what was found by McBreen et al. (2010). For SMC dust, we find $\beta = 1.17 \pm 0.17$, $A_V = 0.18 \pm 0.13$, indicating that the cooling break lies redwards of the optical band.

GRB 090423, $z = 8.23^{+0.06}_{-0.07}$. — We constructed the light curve and the SED with data from the following sources: Tanvir et al. (2009), and Yoshida et al. (2009). With a redshift of $z = 8.23^{+0.06}_{-0.07}$ (Tanvir et al. 2009), this is the most distant spectroscopically confirmed source in the universe (see also Salvaterra et al. 2009b). It is only detected in the NIR JHK bands (therefore, we can not do free dust model fits, and the GRB is not listed in Table 3). From a joint fit of all data (excepting the last detections, which show a flare, Tanvir et al. 2009), we find, as Tanvir et al. (2009), an early plateau. It is $\alpha_1 = 0.063 \pm 0.052$, $\alpha_2 = 1.76 \pm 0.31$, $t_b = 0.38 \pm 0.06$ days ($t_b = 0.041 \pm 0.0066$ days in the rest frame), and $n = 10$ was fixed, no host galaxy was assumed. These values are broadly in agreement with those of Tanvir et al. (2009). From the joint fit, we find a flat SED, $\beta_0 = 0.45 \pm 0.13$, also in broad agreement with Tanvir et al. (2009). Chary et al. (2009) report a 2σ detection at 46 days from an ultra-deep $3.6\mu m$ Spitzer observation. We find, from extrapolation of our SED, that the color $J_{Vega} - 3.6\mu m_{AB} = -0.3$ mag, and $J_{Vega} - 3.6\mu m_{AB} = -0.18$ mag from a (long!) extrapolation of the light curve decay. Both values are in good agreement, as Chary et al. (2009) also report, indicating an as yet negligible contribution by the host galaxy, and no jet break until at least 5 days post-burst in the rest frame. There is no evidence for dust. While the latter fact is similar to the two other $z \geq 6$ GRBs, GRB 050904 and GRB 080913, both of those showed straight but red SEDs, with $\beta_0 \approx 1.1$. The flat spectral slope leads to a blue $R_C - J$ color, we find that the composite J-band light curve needs to be dimmed by 0.98 magnitudes to derive the R_C light curve for the case of a hypothetically fully ionized universe (see Kann et al. 2007a). The dRc correction is also smaller than for the two closer GRBs mentioned above, and at $z = 1$, we find the light curve to be quite unremarkable,, though it is brighter than most GRBs at one day due to the optical flare. A later deep upper limit (Tanvir et al. 2009) indicates that this flare is not similar to the strong rebrightenings experienced by the afterglow

of GRB 080913 (Greiner et al. 2009b), though. All in all, in terms of duration, isotropic energy release and optical luminosity, GRB 080913 and GRB 090423 are similar, in stark contrast to the very powerful GRB 050904.

GRB 090424, $z = 0.544$. — We constructed the light curve and the SED with data from the following sources: Yuan (2009), Xin et al. (2009), Schady & Cannizzo (2009), Guidorzi et al. (2009d), Urata et al. (2009), Olivares et al. (2009), Nissinen & Hentunen (2009), Im et al. (2009), Roy et al. (2009), Mao et al. (2009), Cobb (2009b), and Rumyantsev et al. (2009), as well as our own TLS, CAHA and Maidanak data. This was, in terms of peak photon flux (Sakamoto et al. 2009), the brightest burst *Swift* has detected so far, mainly due to it lying at a comparatively low redshift (Chornock et al. 2009), with a host galaxy that has been pre-imaged in the SDSS (Evans & Holland 2009). We find from fitting a composite light curve that the early afterglow may show the signature of a reverse shock flash: $\alpha_1 = 2.12 \pm 0.16$, $\alpha_2 = 0.92 \pm 0.006$, $t_b = 0.002 \pm 0.0001$ days, $m_h = 22.77 \pm 0.12$, $n = -10$ was fixed. From the available data, we find no evidence for a jet break, which was suggested by Im et al. (2009). We derive a very broad ($UVW1$ to K) SED which is clearly reddened ($\beta_0 = 1.58 \pm 0.03$). The best fit is achieved with LMC dust and a moderate extinction of $A_V = 0.50 \pm 0.12$ mag. The intrinsic SED is still red ($\beta = 0.97 \pm 0.15$) and in excellent agreement with the X-ray spectrum (from the *Swift* XRT repository, Evans et al. 2007, 2009), indicating that the cooling break lies redward of the optical.

GRB 090902B, $z = 1.8229 \pm 0.0004$. — We constructed the light curve and the SED with data from the following sources: McBreen et al. (2010), Pandey et al. (2010), and Cenko et al. (2010b). This extremely energetic GRB has the third-highest fluence of all GRBs in the *Swift* era, featured the highest observed energy ever for a GeV photon, and shows a high-energy spectrum consisting of a superposition of a Band function and a power-law rising to GeV energies which also dominates below 50 keV (Abdo et al. 2009b). It is the first *Fermi* GRB for which the afterglow was detected (by ROTSE) before the LAT position (or a *Swift* XRT position) was published, by mosaicing the GBM ground position. This detection shows the afterglow was probably dominated in the first hours by a reverse shock flash (Pandey et al. 2010). We find $\alpha_{RS} > 1.8$, $\alpha_1 = 0.96 \pm 0.02$, $t_b < 0.46$ days. Fitting only data after 0.5 days, we find $\alpha_1 = 0.95 \pm 0.03$, $\alpha_2 = 1.37 \pm 0.17$, $t_b = 10.97 \pm 3.91$ days, $n = 10$ fixed, and a faint host galaxy assumed. This late break is probably a jet break (McBreen et al. 2010; Cenko et al. 2010b); while the post-break decay slope is very shallow, it is derived from only a few data points (the GRB became unobservable), so it is entirely possible that we are seeing a smooth break which has not reached its asymptotic decay value yet. This very late break makes the GRB hyper-energetic according to McBreen et al. (2010), though note that Cenko et al. (2010b) find evidence for a very low circumburst density which reduces the energy requirements. The SED disfavors MW dust, but we can not discern between LMC and SMC dust (we work with the latter). The very slow decay puts the afterglow among the most luminous ones at late times (McBreen et al. 2010).

GRB 090926A, $z = 2.1062 \pm 0.0004$. — We constructed the light curve and the SED with data from the following sources: Rau et al. (2010) and Cenko et al. (2010b). This was another high-fluence *Fermi* LAT/GBM GRB. The afterglow is observationally very bright, and began a powerful rebrightening phase (Rau et al. 2010; Cenko et al. 2010b) just as ground-based observations started. In this way, it strongly resembles GRB 070125 (Updike et al. 2008b). Fitting data from 0.8 to 2 days, we find $\alpha_1 = -2.27 \pm 0.13$, $\alpha_2 = 1.64 \pm 0.01$, $t_b = 0.947 \pm 0.003$ days, $n = 10$ fixed. The afterglow then undergoes two further rebrightenings, the first which is also found by Rau et al. (2010). As the decay slopes after each rebrightening are identical within errors, this is a classical example of multiple energy injections into the forward shock. Joining the two large data sets from Rau et al. (2010) and Cenko et al. (2010b), we concur with Cenko et al. (2010b) (in disagreement with Rau et al. 2010) that the late afterglow shows another break; using only data after the last rebrightening (4.8 days after the GRB), we find: $\alpha_3 = 1.53 \pm 0.32$, $\alpha_4 = 2.09 \pm 0.17$, $t_b = 7.96 \pm 4.20$ days, $n = 10$ fixed. This is probably a jet break, together with that of GRB 090902B one of the latest discovered, again implying that this is a hyper-energetic event (Rau et al. 2010; Cenko et al. 2010b). Concerning the SED, we note that there seems to be a discrepancy between the calibrations from Cenko et al. (2010b) (unextincted slope for their data only: $\beta_0 = 1.53 \pm 0.08$) and Rau et al. (2010) (unextincted slope for their data only: $\beta_0 = 0.89 \pm 0.05$, in agreement with their result). Joining all data yields a usable SED, but a high χ^2 due to the scatter, we find it is best fit by a small amount of SMC dust, in general agreement with Rau et al. (2010). After shifting it to $z = 1$, the afterglow is seen to be among the most luminous ever detected at any time during its observations.

Details on the *Swift-era Silver Sample*

GRB 050401, $z = 2.8992 \pm 0.0004$. — We constructed the light curve and the SED with data from the following sources: Rykoff et al. (2005a), De Pasquale et al. (2006), Watson et al. (2006), Kamble et al. (2009) and Chen et al. (2009) (we also publish upper limits from ANDICAM in this work). We note that the three magnitude values given in Kamble et al. (2009) are about one magnitude too bright. For the SED, we derive the $V - R_C$ and $R_C - I_C$ colors from the Kamble et al. (2009) data only, as the colors are in agreement with the rest of the SED. Construction of the SED is hampered by the fact that the NIR data (JHK) are for the most part not contemporaneous with the densely sampled part of the R_C light curve. The SED we derive yields negative β for a free fit (LMC and SMC), or strongly unphysical results (MW). While being very red ($\beta_0 = 1.88 \pm 0.11$), the curvature is too strong to be explained even by SMC dust. As already noted earlier (Rykoff et al. 2005a; Watson et al. 2006), the light curve is reasonably well fitted ($\chi^2 = 35.2$ for 28 degrees of freedom) with a simple power law, we find $\alpha = 0.84 \pm 0.02$. We point out that if one fits only the later R_C data, without the early ROTSE points (Rykoff et al. 2005a), a broken power law gives a

significantly improved fit ($\chi^2 = 12.5$ for 21 degrees of freedom). We find the following results: $m_k = 22.43 \pm 0.52$ mag, $\alpha_1 = 0.58 \pm 0.11$, $\alpha_2 = 0.96 \pm 0.04$, $t_b = 0.32 \pm 0.17$ days, and $n = 10$, $m_h = 27$ were fixed (the host galaxy magnitude is given in Chen et al. 2009). The early time (2 hours in the rest frame) and the small $\Delta\alpha = 0.38 \pm 0.12$, close to the expected value $\Delta\alpha = 0.25$ may indicate that this is a cooling break. This would also mean that the early light curve shows a more complicated evolution than a single power law. We find no evidence for a jet break at late times, in agreement with Watson et al. (2006). Using this α value (what is labeled α_2 in our fit represents the pre-break decay slope α_1), and assuming a wind environment and a cooling frequency above the optical band, we derive $\beta = 0.30$. While this is untypically shallow, the X-ray spectrum is also quite hard ($\Gamma = 1.85 - 1.89$, Watson et al. 2006), yielding a similar spectral slope ($0.35 - 0.39$, from $\beta = \Gamma - 1 - 0.5$) to what we derive from the decay slope. Using this fixed value, we find $A_V = 0.69 \pm 0.02$ (we caution that this strongly underestimates the error, see K06). This is close to the result Watson et al. (2006) derive, they fix $\beta = 0.39$ and find $A_V = 0.67$ from the spectrum. This is a rare GRB at high redshift where significant extinction has been detected.

GRB 051109A, z = 2.346. — We constructed the light curve and the SED with data from the following sources: Yost et al. (2007a), Holland et al. (2005), Bloom et al. (2005), Milne et al. (2005b), Haislip et al. (2005b), Huang et al. (2005), Woźniak et al. (2005b), Li (2005b), Misra et al. (2005), and Kinugasa & Torii (2005), as well as our own data (one point from the 0.38m K-380 telescope). While this GRB had one of the densest early multi-color follow-ups ever obtained, most of this data are as yet unpublished, therefore our analysis is preliminary. The R_C light curve is well fit with a broken power law with the following parameters: $m_k = 19.99 \pm 0.099$ mag, $\alpha_1 = 0.64 \pm 0.006$, $\alpha_2 = 1.88 \pm 0.17$, $t_b = 1.44 \pm 0.16$ days, $m_h = 23.37 \pm 0.15$ mag, and $n = 1$ (smooth rollover) fixed. This is one of the best examples of an optical light curve with a probable jet break in the *Swift* era. Data in other colors is sparse. We derive a broad SED ($VR_C I_C JHK_S$), but it is strongly curved, free fits yield negative β (LMC, SMC) or unphysical results (MW). A fit without extinction yields $\beta_0 = 0.61 \pm 0.057$. Deriving β from α, we find that the only physical solution is found for an ISM-BLUE model, with $\beta = 0.42$. For this case, $p = 1.85 \pm 0.012$, identical to $p = 1.88 \pm 0.17$ derived from $p = \alpha_2$. SMC dust gives the significantly best fit, we find $A_V = 0.09 \pm 0.03$. Oates et al. (2009) find $A_V = 0.01$ from UVOT data only (using an XRT-UVOT joint fit), a smaller value. Schady et al. (2010) find strong evidence for a cooling break between the optical and the X-rays, but are not able to discern between the extinction models beyond that, they derive low upper limits on any extinction, in agreement with our result.

GRB 051111, z = 1.54948 \pm 0.00001. — We constructed the light curve and the SED with data from the following sources: Yost et al. (2007a), Butler et al. (2006), Guidorzi et al. (2007a), Milne et al. (2005c), Poole et al. (2005), Nanni et al. (2005), and Penprase et al. (2006, host galaxy), as well as our own data set (SARA, Maidanak). Similar to GRB 051109A, this GRB was observed in multiple colors at early times, and the R_C light curve is very well sampled. Basically, it can be described by a broken power law with the following parameters: $m_k = 19.64 \pm 0.34$ mag, $\alpha_1 = 0.91 \pm 0.006$, $\alpha_2 = 2.32 \pm 0.80$, $t_b = 0.55 \pm 0.18$ days, $m_h = 25.6$ mag and $n = 10$ fixed. The late slope indicates the existence of a jet break, but there are few late data points, and the error on α_2 is very large. Furthermore, the light curve residuals show significant variability ($\chi^2 = 542$ for 118 degrees of freedom), e.g., the earliest data points follow a steeper decay (cf. Yost et al. 2007a). Butler et al. (2006) also present an early, shallow break. Another similarity to GRB 051109A is that this SED is also strongly curved. Only SMC dust yields an acceptable result, but the fit finds negative β. Assuming a constant density environment and a cooling break bluewards of the optical yields $\beta = 0.61$, fixing this value, we find $A_V = 0.19 \pm 0.02$. This is fully in agreement with the result of Butler et al. (2006), who find $A_V = 0.23 \pm 0.07$ for SMC dust, which they find is clearly preferred.

GRB 060210, z = 3.9133. — We constructed the light curve and the SED with data from the following sources: Stanek et al. (2007), Curran et al. (2007a), Cenko et al. (2009b), Perley et al. (2009d), Fynbo et al. (2009), Li (2006), Williams & Milne (2006), and Hearty et al. (2006a). This GRB at a moderately high redshift was rapidly observed by several ground-based telescopes, yielding a dense early light curve coverage. At early times, the afterglow shows a plateau, which is followed by a small rebrightening (Li 2006), before it decays achromatically with $\alpha = 1.29 \pm 0.02$ (fully in agreement with, e.g., Stanek et al. 2007). Note that this GRB shows rather strong pre-trigger activity (Curran et al. 2007a), and we shifted all afterglow data by 230 seconds. With the exception of a quite bright host galaxy (Perley et al. 2009d), a bright detection which is is in conflict with surrounding upper limits (Misra 2006) and the late K_S observation (Hearty et al. 2006a), there are no reported detections after ≈ 0.1 days. The K_S data point can only be added to the SED if one does a long extrapolation of the initial light curve decay, assuming achromaticity (we also assume $K_S = 22$ for the host galaxy, but note that Hearty et al. 2006a report possible blending with an extended source). In such a case, one finds a large $R_C - K_S = 5$ mag, but this is still ≈ 2 magnitudes lower than what is expected from the fit only to the optical data (see the following). Dai & Stanek (2006) report the detection of a light curve break at 7.9 hours in the XRT light curve, which, if achromatic, would imply a larger $R_C - K_S$ color. Due to these insecurities, we therefore choose not to use the K_S point in the SED, and point out that there may also be a problem with the photometric calibration of the P60 data of Cenko et al. (2009b), as their i' magnitudes are already significantly brighter (instead of slightly fainter, as expected) than I_C data from Curran et al. (2007a) and Li (2006). As already found by Cenko et al. (2009b), the SED is extremely red ($\beta_0 = 7.09 \pm 0.52$, in agreement with Cenko et al. 2009b), this cannot be attributed to the redshift. Spanning only from R_C to z', a free fit results in negative β for the SMC or too little correction for LMC and MW dust. We can rule out MW dust from the bright z' detection, but can not discern between SMC and LMC dust as no NIR data has been published. We choose SMC dust as this is most often found in GRB hosts (and also needs less extinction). From the optical decay slope, and assuming an ISM environment with the cooling break

blueward of the optical, we infer $\beta = 0.76$ and a very high extinction $A_V = 1.18 \pm 0.10$. This is fully in agreement with the result of Cenko et al. (2009b), $A_V = 1.21^{+0.16}_{-0.12}$. This result is remarkable, not only is there only one other GRB in the sample for which a similarly high extinction was found (GRB 070802), but the high redshift leads to the highest correction in the whole sample, $dRc \approx 10$. If this value is correct, then GRB 060210 has not only one of the most luminous early afterglows ever discovered (Fig. 4), it also becomes, by 0.005 days after the GRB, the most luminous of all afterglows, roughly one magnitude brighter than the upper boundary now given by GRBs 090313 and 080129. This either implies that afterglows, even at times when prompt flashes like those of GRBs 050904 and 080319B have significantly decayed, can be much more luminous than is known now, or that there is a problem with the data. Indeed, Cenko et al. (2009b) state that they did not derive an independent photometric calibration of the field, which may lead to especially the z' magnitudes to be too bright. Though as long as no additional data are published, especially NIR data, there is no way to discern between the two scenarios.

GRB 060502A, $z = 1.5026$. — We constructed the light curve and the SED with data from the following sources: Cenko et al. (2009b), Fynbo et al. (2009), Poole & La Parola (2006), and Jakobsson et al. (2006b). Data on this afterglow is sparse. From a joint fit, we find a shallow decay, $\alpha = 0.56 \pm 0.17$. The SED is red ($\beta_0 = 1.99 \pm 0.35$, in agreement with Cenko et al. 2009b). Free fits result in negative β. We take $\beta = 1.01$ from the X-ray spectrum (from the *Swift* XRT repository, Evans et al. 2007, 2009) and find, with SMC dust, $A_V = 0.38 \pm 0.15$. If we assume a cooling break redward of the optical, we derive $\beta = 0.71$ and $A_V = 0.50 \pm 0.15$, comparable to Cenko et al. (2009b), who derive $A_V = 0.53 \pm 0.13$. Schady et al. (2010) strongly rule out MW dust, and marginally prefer SMC dust and a cooling break between the optical and the X-rays, for this model, they derive an extinction identical to our result.

GRB 060906, $z = 3.685 \pm 0.002$. — We constructed the light curve and the SED with data from the following sources: Cenko et al. (2009b), Fynbo et al. (2009), and Li & Bloom (2006). This moderately high redshift GRB has a peculiar early afterglow featuring a strong optical rebrightening (Cenko et al. 2009b). Only three colors are given, as the Gunn g band is affected by Lyman absorption. From the X-ray spectrum (from the *Swift* XRT repository, Evans et al. 2007, 2009) and under the assumption of a cooling break between the X-rays and the optical (the uncorrected optical slope is already bluer than the X-ray slope), we use $\beta = 0.61$ and find only a very small amount ($A_V = 0.05 \pm 0.05$) of SMC dust. This value is smaller than what was found by Cenko et al. (2009b), $A_V = 0.20^{+0.01}_{-0.12}$.

GRB 060927, $z = 5.4636$. — We constructed the light curve and the SED with data from the following sources: Ruiz-Velasco et al. (2007), Torii (2006), and Zheng et al. (2009b) (we also publish an unused upper limit). This GRB has the fourth highest spectroscopic redshift determined to date, and incidentally, it also had the most rapid follow-up observation ever (Ruiz-Velasco et al. 2007), excepting the coincidental observations of GRB 080319B. Similar to GRB 050904, observations in most colors yielded only upper limits due to Lyman dropout. After a strong rebrightening at 0.01 days (Ruiz-Velasco et al. 2007), the light curve follows a simple power law, we find $m_k = 23.394 \pm 0.118$ and $\alpha = 1.235 \pm 0.033$ ($m_h = 28$ fixed), in agreement with Ruiz-Velasco et al. (2007). We construct the R_C light curve following the method Kann et al. (2007a) used for GRB 050904. Only three colors are unaffected by Lyman damping. From the decay slope, we derive $\beta = 0.823$ from a model where the cooling break lies redward of the optical (the unextinct slope is quite steep, $\beta = 1.297$), and find $A_V = 0.209 \pm 0.084$ for SMC dust. This is also in agreement with the simultaneous optical/X-ray fits presented in Ruiz-Velasco et al. (2007). The additional extinction correction makes this GRB afterglow have an even larger dRc shift than found for GRB 050904 (Kann et al. 2007a).

GRB 070208, $z = 1.165$. — We constructed the light curve and the SED with data from the following sources: Melandri et al. (2008), Cenko et al. (2009b), Bloom (2007), Halpern & Mirabal (2007), Wren et al. (2007a), Sato et al. (2007), Swan et al. (2007a), as well as one data point from the Sayan telescope. This GRB had a faint afterglow which exhibited an early rise (Wren et al. 2007a; Melandri et al. 2008) and a slow decay, we find $\alpha = 0.55 \pm 0.02$ from a joint fit. The SED is red ($\beta_0 = 2.27 \pm 0.12$, in agreement with Cenko et al. 2009b), and, under the assumption of a cooling break between the X-rays and the optical, the X-ray spectrum (from the *Swift* XRT repository, Evans et al. 2007, 2009) yields $\beta = 0.66$ and we derive $A_V = 0.74 \pm 0.03$ with SMC dust. Similar values are found if we assume a cooling break redward of the optical and derive the spectral index from the optical decay slope. Cenko et al. (2009b) derive a slightly higher value, $A_V = 0.96 \pm 0.09$.

GRB 071020, $z = 2.1462$. — We constructed the light curve and the SED with data from the following sources: Cenko et al. (2009b), Fynbo et al. (2009), Schaefer et al. (2007), Yuan et al. (2007a), Bloom et al. (2007), Xin et al. (2007), Im et al. (2007), Hentunen (2007), and Ishimura et al. (2007a), as well as our own data set (SARA, Z-600 and AZT-8). This very bright GRB had a bright early afterglow (Schaefer et al. 2007) and featured a strong rebrightening or plateau phase after about 0.2 days (Im et al. 2007). Excluding the very first ROTSE point, we find the afterglow decays with $\alpha = 1.11 \pm 0.07$, and, after ≈ 0.2 days, rises with $\alpha_R \approx -0.4$. Yuan et al. (2007a) report a steeper early decay slope of $\alpha = 1.52$, which may point to an additional component from a reverse shock flash. The X-ray spectrum (from the *Swift* XRT repository, Evans et al. 2007, 2009) is hard, with $\beta \approx 0.8$. Assuming no cooling break between the X-rays and the optical, we find, with SMC dust, $A_V = 0.28 \pm 0.09$. The uncorrected SED is moderately reddened, it is $\beta_0 = 1.47 \pm 0.21$.

GRB 071025, $z = 4.8 \pm 0.4$. — We constructed the light curve and the SED with data from the following sources: Perley et al. (2010), and Jiang et al. (2007). This afterglow has been extensively discussed in Perley et al. (2010). No spectroscopic redshift is know, but photometric constraints as well as the trace of a very low-S/N Keck HIRES

spectrum (Fynbo et al. 2009) indicate $z = 4.4 - 5.2$, and Perley et al. (2010) use $z = 5$ in their discussion, which we adopt. They find a complex, double-peaked light curve. Fitting the two peaks separately (but using all available filters in each case), we find $\alpha_1 = -1.39 \pm 0.18$, $\alpha_2 = 1.89 \pm 0.30$, $t_b = 0.0073 \pm 0.0008$ days, $n = 1$ fixed, and $\alpha_3 = -5.10 \pm 0.58$, $\alpha_4 = 1.42 \pm 0.02$, $t_b = 0.0138 \pm 0.0002$ days, $n = 1$ fixed, for the first and second peak, respectively. These values are in rough agreement with those found by Perley et al. (2010). Those authors find that the SED, which is well-determined in the NIR, shows a plateau phase between the J and H bands, which we fully confirm from both our early and late SED (which also show a different color, like Perley et al. 2010 find). They are unable to fit the SED with any typical dust model (which we also confirm), but find that it can be fit well with SN-synthesized dust (Maiolino et al. 2004). To correctly derive the intrinsic luminosity of the afterglow, we used the dust extinction in the individual filters A_λ (it is $A_{I_C} = 1.98$ mag, $A_Y = 1.29$ mag, $A_J = 1.14$ mag, $A_H = 1.18$ mag, and $A_K = 0.95$ mag, D. A. Perley, priv. com.). Correcting for these values, we find a straight SED with $\beta = 0.93 \pm 0.05$, in accordance with Perley et al. (2010), who find $\beta = 0.96 \pm 0.14$. Extrapolating this to the R_C band, we find $A_{R_C} = 3.74$ mag, note that this is a combined effect of Lyman α absorption as well as dust reddening, the two can not be disentangled due to insecurities in the dust model (D. A. Perley, priv. com.). We find $dR_C = 4.20$ mag from $\beta = 0.93 \pm 0.05$, $z = 5$ and no dust, for a total shift of $dR_c = 7.94$. This large correction makes the afterglow of GRB 071025 one of the most luminous known at early times.

GRB 071122, $z = 1.14$. — We constructed the light curve and the SED with data from the following sources: Cenko et al. (2009b), and Brown et al. (2007). This GRB had a faint afterglow which exhibited a slow rise and long plateau phase (Cenko et al. 2009b). There are not enough filters to freely fit the SED. The X-ray spectrum (from the *Swift* XRT repository, Evans et al. 2007, 2009) is hard (though this may be influenced by a flare, Stamatikos et al. 2007), with $\beta = 0.66$. Assuming no cooling break between the X-rays and the optical, we find, with SMC dust, $A_V = 0.22 \pm 0.23$, significantly less than Cenko et al. (2009b), who derive $A_V = 0.58 \pm 0.05$. This is puzzling, as our uncorrected slope ($\beta_0 = 0.99 \pm 0.43$) is in agreement with their value ($\beta_0 = 1.3 \pm 0.6$).

GRB 080721, $z = 2.591 \pm 0.001$. — We constructed the light curve and the SED with data from the following sources: Starling et al. (2009), and Huang et al. (2008b). This very energetic GRB, which also had a very bright afterglow, is discussed in detail in Starling et al. (2009). We confirm that the data up to 30 days can be fit with a single power-law with neither a (jet) break nor host galaxy contribution. Our value ($\alpha = 1.239 \pm 0.005$) agrees with that of Starling et al. (2009) ($\alpha = 1.256 \pm 0.010$). There is some scatter involved in the data, leading to a high χ^2 (97 for 25 degrees of freedom). We note that all data after three days lies systematically beneath the fit. Fixing $n = 10$ and fitting with a broken power law, we find $\alpha_1 = 1.217 \pm 0.008$, $\alpha_2 = 1.446 \pm 0.071$ and $t_b = 1.32 \pm 0.88$ days, and an improvement in the fit ($\chi^2 = 69$ for 23 degrees of freedom, $\Delta\chi^2 = 28$ for 2 additional parameters). If real, this is a very shallow break, and $\Delta\alpha = 0.23 \pm 0.07$ may indicate that it is a cooling break. While the SED data has large errors (see Starling et al. 2009), we find a red slope ($\beta_0 = 2.36 \pm 0.30$), and, using $\beta = 0.86$ from the X-rays (no cooling break between X-rays and optical, Starling et al. 2009), we find $A_V = 0.35 \pm 0.07$. Correcting for this extinction, the afterglow of GRB 080721 is seen to be one of the most luminous known at early times, in accordance with its extreme energetics (Starling et al. 2009).

GRB 080810, $z = 3.35104$. — We constructed the light curve and the SED with data from the following sources: Page et al. (2009) Ikejiri et al. (2008), Uemura et al. (2008), Okuma et al. (2008), and Yoshida et al. (2008c), as well as our own data set (RTT150 and several Russian telescopes). This complex, moderate redshift GRB had a very luminous afterglow featuring early variability contemporaneous with the γ-ray emission (Page et al. 2009). After about 0.004 days, the afterglow can be fit by a single power-law decay, with $\alpha = 1.153 \pm 0.003$, in agreement with Page et al. (2009), who find $\alpha = 1.22 \pm 0.09$. There is marginal evidence for late steepening, which was already noted by Galeev et al. (2008) and Thöne et al. (2008d), this may be a candidate for an optical jet break, but the post-break decay is not measured long enough to make a significant case for a break (see also Page et al. 2009). The SED shows a bit of scatter, and free fits do not yield good results. The uncorrected SED is moderately red ($\beta_0 = 1.24 \pm 0.08$), indicating possible additional dust along the line of sight. The spectral slope of the X-ray spectrum ($\beta = 1.00 \pm 0.09$, for the late data, Page et al. 2009) is in agreement with the spectral slope ($\beta = 0.44$) derived from the optical decay assuming an ISM environment and a cooling break blueward of the optical (as found by Page et al. 2009), so we use $\beta = 0.5$ and find a typical amount of SMC dust, $A_V = 0.16 \pm 0.02$. Note that Page et al. (2009) find the same slope, but intrinsic, with no need for extinction. The dust models can not be distinguished yet, this will need further NIR data. After correction, the afterglow of GRB 080810 is found to be one of the most luminous ever observed, comparable to GRB 061007 at early times and to GRB 090313 at later times.

GRB 081203A, $z = 2.05 \pm 0.01$. — We constructed the light curve and the SED with data from the following sources: Andreev et al. (2008a,b), De Pasquale & Parsons (2008), Volkov (2008), West et al. (2008), Liu et al. (2008), Mori et al. (2008), Isogai & Kawai (2008), Rumyantsev et al. (2008), and Fatkhullin et al. (2008). We set T_0 as 69 seconds before the Swift trigger. This GRB hat an very bright early afterglow (Kuin et al. 2009; West et al. 2008) observationally and shows a strong early rise and peak. Most of the filters it was detected in lie beyond Lyman α. The SED comprises only five filters ($Bg'VR_CI_C$) and shows strong curvature, which leads to unphysical results in free fits (especially for SMC dust). The X-ray spectrum (from the *Swift* XRT repository, Evans et al. 2007, 2009) gives $\beta = 1.096$, and as the uncorrected spectral slope in the optical is already shallower than this, we assume a cooling break between the two bands and fix $\beta = 0.596$, and the best fit is found with a small amount of SMC dust, $A_V = 0.09 \pm 0.04$. At $z = 1$, this would have been one of the brightest afterglows ever seen at very early times, reaching 10th magnitude.

Details on the Swift-*era Bronze Sample*

GRB 050315, z = 1.9500 ± 0.0008. — Data taken from Berger et al. (2005b), Bersier et al. (2005), Gorosabel et al. (2005) (host galaxy) as well as our own ANDICAM data set.

GRB 050318, z = 1.4436 ± 0.0009. — Data taken from Berger et al. (2005b) and Still et al. (2005). Schady et al. (2010) find SMC dust is preferred for this GRB, and derive a rather high $A_V \approx 0.53$.

GRB 050603, z = 2.821. — Data taken from Berger & McWilliam (2005), Grupe et al. (2006a), and Li et al. (2006).

GRB 050908, z = 3.3467. — Data taken from Cenko et al. (2009b), Torii (2005b), Li (2005a), Kirschbrown et al. (2005), and Durig et al. (2005), as well as a single point from Maidanak.

GRB 060512, z = 0.4428. — Data taken from Melandri et al. (2008), Cenko (2006a), Hearty et al. (2006b), Milne (2006), Tanaka et al. (2006), De Pasquale & Cummings (2006), and Klotz et al. (2006), as well as NOT *J* band data we publish here. Schady et al. (2010) find that no dust model is capable of fitting the SED well, and derive moderate-to-high extinction in all cases ($A_V \approx 0.47 - 0.66$ for the "least bad" SMC dust.)

GRB 060605, z = 3.773 ± 0.001. — Data taken from Ferrero et al. (2009), Rykoff et al. (2009), Zhai et al. (2006), Khamitov et al. (2006a), Khamitov et al. (2006b), Malesani et al. (2006), Sharapov et al. (2006), and Karska & Garnavich (2006). We follow Ferrero et al. (2009) and assume $\beta = 1.06$ in this case. Schady et al. (2010) find that no dust model can be preferred, and find moderate extinction ($A_V \approx 0.25 - 0.35$) for all cases.

GRB 060707, z = 3.425 ± 0.002. — Data taken from de Ugarte Postigo et al. (2006a), Stefanescu et al. (2006a), Schady & Moretti (2006), and Jakobsson et al. (2006c).

GRB 060714, z = 2.711 ± 0.001. — Data taken from Stefanescu et al. (2006b), Jakobsson et al. (2006d), Melandri et al. (2006a), A. Pozanenko, in preparation (paper on the GRB 060714 afterglow), as well as our own ANDICAM data set. Schady et al. (2010) find that no dust model can be preferred significantly, and find moderate extinction ($A_V \approx 0.46$) for the SMC single power-law case.

GRB 060729, z = 0.5428. — Data taken from Grupe et al. (2007a), Rykoff et al. (2009), and Quimby & Rykoff (2006), as well as our own ANDICAM data set. Schady et al. (2010) find that no dust model can be preferred significantly, and find low extinction ($A_V \approx 0.03 - 0.18$) for all cases.

GRB 061121, z = 1.3145. — Data taken from Page et al. (2007), Melandri et al. (2008), Yost et al. (2006), Uemura et al. (2006), Cenko (2006b), Halpern et al. (2006), Halpern & Armstrong (2006a,b), as well as our own data set (ANDICAM, Shajn). Schady et al. (2010) find that a cooling break between the X-ray and the optical bands is preferred, but can not distinguish the dust models significantly beyond this, finding moderate extinction ($A_V \approx 0.28 - 0.55$) for all cases.

GRB 070110, z = 2.3521. — Data taken from Troja et al. (2007) and Malesani et al. (2007a,b). Schady et al. (2010) find that a cooling break between the X-ray and the optical bands is preferred at low significance, but can not distinguish the dust models significantly beyond this, finding moderate extinction ($A_V \approx 0.23 - 0.49$) for all cases.

GRB 070411, z = 2.9538. — Data taken from Ferrero et al. (2008a), Melandri et al. (2008), Jelínek et al. (2007), Berger et al. (2007), Prieto et al. (2007), Perley et al. (2007a), and D. Malesani et al., in preparation (paper on the GRB 070411 afterglow). Schady et al. (2010) are only able to rule out high extinction toward this GRB, with $A_V < 0.21 - 0.47$ depending on the dust different models.

GRB 070612A, z = 0.617. — Data taken from Updike et al. (2007a,b), Cenko et al. (2007a), Mirabal et al. (2007a,b), Yoshida et al. (2007b), Malesani et al. (2007c), D'Avanzo et al. (2007), and Taubenberger et al. (2007).

GRB 070810A, z = 2.17. — Data taken from Chester et al. (2007), Thöne et al. (2007a), Perley et al. (2007b), and Yuan & Rykoff (2007).

REFERENCES

Abdo, A. A., et al. 2009a, Science, 323, 1688
Abdo, A. A., et al. 2009b, ApJ, 706, L138
Akerlof, C., et al. 1999, Nature, 398, 400
Alatalo, K., Perley, D., & Bloom, J. S. 2006, GCN Circ. 4702
Allen, B., et al. 2009, GCN Circ. 9058
Amati, L., et al. 2007, A&A, 463, 913
Amati, L., Frontera, F., & Guidorzi, C. 2009, A&A, 508, 173
Andersen, M. I., et al. 2000, A&A, 364, L54
Andreev, M., Sergeev, A., Babina, J., & Pozanenko, A. 2008a, GCN Circ. 8596
Andreev, M., Sergeev, A., Babina, J., & Pozanenko, A. 2008b, GCN Circ. 8615
Antonelli, L. A., et al. 2006, GCN Circ. 5546
Antonelli, L. A., et al. 2008, GCN Circ. 7597
Aoki, K., et al. 2009, PASJ, 61, 387
Atteia, J.-L., et al. 2005, ApJ, 626, 292

Bagoly, Z., et al. 2006, A&A, 453, 797
Band, D. L., & Preece, R. D. 2005, ApJ, 627, 319
Barthelmy, S. D., et al. 2005a, Nature, 438, 994
Belczynski, K., Holz, D. E., Fryer, C. L., Berger, E., Hartmann, D. H., & O'Shea, B. 2010, ApJ, 708, 117
Bellm, E. C., et al. 2008, ApJ, 688, 491
Bellm, E. C. et al. 2008, GAMMA-RAY BURSTS 2007: Proceedings of the Santa Fe Conference. AIP Conference Proceedings, Volume 1000, pp. 154-157 (2008)
Berger, E. & Becker, G. 2005, GCN Circ. 3520
Berger, E., & McWilliam, A. 2005, GCN Circ. 3511
Berger, E., et al. 2005a, ApJ, 629, 328
Berger, E., et al. 2005b, ApJ, 634, 501
Berger, E., et al. 2005c, Nature, 438, 988
Berger, E., et al. 2007, GCN Circ. 6278
Berger, E. 2007, ApJ, 670, 1254

Bersier, D., & Gomboc, A. 2008, GCN Circ. 7963
Bersier, D., Rhoads, J., Fruchter, A., & Gilbank, D. 2005, GCN Circ. 3103
Bersier, D., et al. 2006, ApJ, 643, 284
Beskin, G., et al. 2009, Science, submitted (arXiv:0905.4431)
Beuermann, K., et al. 1999, A&A, 352, L26
Bissaldi, E., 2010, Proceedings for "The Shocking Universe - Gamma-Ray Bursts and High Energy Shock phenomena", Venice (Italy), September 14-18, 2009 (arXiv:1002.4194)
Blinnikov, S. I., Novikov, I. D., Perevodchikova, T. V., & Polnarev, A. G. 1984, SvAL, 10, 177
Blinnikov, S. I., Novikov, I. D., Perevodchikova, T. V., & Polnarev, A. G. 1984, PHAz, 10, 422
Block, A., & Templeton, M. 2008, GCN Circ. 7580
Bloom, J. S., & Starr, D. L. 2008, GCN Circ. 7542
Bloom, J. S., et al. 1998, ApJ, 507, L25
Bloom, J. S., Frail, D. A., & Sari, R. 2001, AJ, 121, 2879
Bloom, J. S., Frail, D. A., & Kulkarni, S. R. 2003, ApJ, 594, 674
Bloom, J. S., Blake, C. H., Starr, D., & Alatalo, K. 2005, GCN Circ. 4216
Bloom, J. S., Foley, R. J., Kocevski, D. & Perley, D. 2006, GCN Circ. 5217
Bloom, J. S., Perley, D. A., & Starr, D. L. 2007, GCN Circ. 6953
Bloom, J. S., et al. 2009, ApJ, 691, 723
Bloom, J. S., 2000, GCN Circ. 756
Bloom, J. S. 2005, GCN Circ. 3990
Bloom, J. S. 2007, GCN Circ. 6079
Blustin, A. J., Holland, S. T., Cucchiara, A., White, N., & Hinshaw, D. 2005, GCN Circ. 3717
Blustin, A. J., et al. 2006, ApJ, 637, 901
Boër, M., et al. 2006, ApJ, 638, L71
Bolzonella, M., Miralles, J.-M., & Pelló, R. 2000, A&A, 363, 476
Boyd, P., Morris, D., Marshall, F., & Gehrels, N. 2006, GCN Circ. 4722
Brennan, T., et al. 2008, GCN Circ. 7284
Brown, P. J., Chester, M. M., Starling, R. L. C., & Stamatikos, M. 2007, GCN Circ. 7131
Burenin, R. et al. 2007, GCN Circ. 7066
Butler, N. R., et al. 2006, ApJ, 652, 1390
Butler, N. R., Kocevski, D., Bloom, J. S., & Curtis, J. L. 2007, ApJ, 671, 656
Butler, N. R. 2007, ApJ, 656, 1001
Campana, S., et al. 2006, Nature, 442, 1008
Campana, S., et al. 2007, A&A, 464, L25
Campisi, M. A., & Li, L.-X. 2008, MNRAS, 391, 935
Castro, S., et al. 2003, ApJ, 586, 128
Castro-Tirado, A. J., et al. 2001, A&A, 370, 398
Castro-Tirado, A. J., et al. 2007, A&A, 475, 101
Castro-Tirado, A. J., et al. 2010, A&A, in press (arXiv:1004.1131)
Cenko, S. B., & Fox, D. B. 2007, GCN Circ. 6306
Cenko, S. B., et al. 2006b, ApJ, 652, 480
Cenko, S. B., Ofek, E. O., & Fox, D. B. 2007a, GCN Circ. 6525
Cenko, S. B., et al. 2007b, GCN Circ. 6556
Cenko, S. B., et al. 2008, ApJ, 677, 441
Cenko, S. B., Rau, a., & Salvato, M. et al. 2009a, GCN Circ. 8773
Cenko, S. B., et al. 2009b, ApJ, 693, 1484
Cenko, S. B., et al. 2010a, ApJ, 711, 641
Cenko, S. B., et al. 2010b, ApJ, submitted (arXiv:1004.2900v2)
Cenko, S. B. 2006a, GCN Circ. 5125
Cenko, S. B. 2006b, GCN Circ. 5844
Chandra, P., et al. 2008, ApJ, 683, 924
Chary, R., Surace, J., Carey, S., Berger, E., & Fazio, G. 2009, GCN Circ. 9582
Chen, H.-W., Prochaska, J. X., Bloom, J. S., & Thompson, I. B. 2005, ApJ, 634, L25
Chen, B. A., Lin, C. S., Huang, K. Y., Ip, W. H., & Urata, Y. 2006, GCN Circ. 4982
Chen, I. C., Huang, K. Y., & Urata, Y. 2007a, GCN Circ. 7067
Chen, I. C., Huang, K. Y., & Urata, Y. 2007b, GCN Circ. 7067
Chen, T. W., Huang, L. C., Huang, K. Y., & Urata, Y. 2008, GCN Circ. 7395
Chen, H.-W., et al. 2009, ApJ, 691, 152
Chester, M. M., Marshall, F. E., & Cummings, J. R. 2007, GCN Circ. 6735
Chevalier, R. A., & Li, Z.-Y. 1999, ApJ, 520, L29
Chornock, R., Foley, R. J., Li, W., & Fillipenko, A. V. 2008, GCN Circ. 7383
Chornock, R., Perley, D. A., Cenko, S. B., Bloom, J. S. 2009, GCN Circ. 9243
Chornock, R., et al., ApJ, submitted (arXiv:1004.2262)
Cobb, B. E., & Bailyn, C. D. 2008, ApJ, 677, 1157
Cobb, B. E., Bailyn, C. D., van Dokkum, P. G., & Natarajan, P. 2006, ApJ, 645, L113
Cobb, B. E. 2009a, GCN Circ. 9008
Cobb, B. E. 2009b, GCN Circ. 9313
Connaughton, V., et al. 2009, GCN Circ. 9230
Covino, S., et al. 2002, GCN Circ. 1214

Covino, S., et al. 2005, GCN Circ. 4046
Covino, S., et al. 2006a, A&A, 447, L5
Covino, S., et al. 2006b, Il Nuovo Cimento B, vol. 121, Issue 10, p.1171-1176
Covino, S., et al. 2008a, GCN Circ. 7385
Covino, S., et al. 2008b, GCN Circ. 7393
Covino, S., et al. 2008c, MNRAS, 388, 347
Covino, S., et al. 2010, A&A, submitted
Coward, D. M., Guetta, D, Burman, R. R., & Imerito, A. 2008, MNRAS, 386, 111
Coward, D. M. 2009, MNRAS, 393, L65
Cucchiara, A., Fox, D. B., Cenko, S. B., & Price, P. A., et al. 2007a, GCN Circ. 6083
Cucchiara, A., Fox, D. B., & Cenko, S. B. 2007b, GCN Circ. 7128
Cucchiara, A., Jones, T., Charlton, J. C., Fox, D. B., Einsig, D., & Narayanan, A. 2009, ApJ, 697, 345
Curran, P. A., Kann, D. A., Ferrero, P., Rol, E., & Wijers, R. A. M. J. 2006, Il Nuovo Cimento B, vol. 121, Issue 12, p.1461-1462
Curran, P. A., et al. 2007, A&A, 467, 1049
Curran, P. A., et al. 2007b, MNRAS, 381, L65
Curran, P. A., Wijers, R. A. M. J., Heemskerk, M. H. M., Starling, R. L. C., Wiersema, K., & van der Horst, A. J. 2008, A&A, 490, 1047
Curran, P. A., Mangano, V., & Holland, S. T. 2009, GCN Circ. 8770
Curran, P. A., Evans, P. A., Page, M. J., de Pasquale, M., & van der Horst, A. J. 2010, ApJ, 716, L135
Dai, X., & Stanek, K. Z. 2006, GCN Circ. 5147
Dai, X., et al. 2007, ApJ, 658, 509
Dai, X., et al. 2008, ApJ, 682, L77
Dai, X. 2009, ApJ, 697, L68
Damerdji, Y., Klotz, A., Boër, M., & Atteia, J. L. 2005, GCN Circ. 3741
D'Avanzo, P. Covino, S. 2008, GCN Circ. 8350
D'Avanzo, P., et al. 2007, GCN Circ. 6588
D'Avanzo, P., et al. 2008, GCN Circ. 7960
De Pasquale, M., & Cummings, J. 2006, GCN Circ. 5130
De Pasquale, D., & Parsons, A. 2008, GCN Circ. 8603
De Pasquale, M. 2006, MNRAS, 365, 1031
De Pasquale, M., et al. 2007, MNRAS, 377, 1638
de Ugarte Postigo, A., et al. 2004, A&A, 443, 841
de Ugarte Postigo, A. et al. 2006a, GCN Circ. 5290
de Ugarte Postigo, A., French, J., & Kubanek, P. 2006b, GCN Circ. 5510
de Ugarte Postigo, A., et al. 2007, A&A, 462, L57
de Ugarte Postigo, A., Jakobsson, P., Malesani, D., Fynbo, J. P. U., Simpson, E., & Barros, S. 2009a, GCN Circ. 8766
de Ugarte Postigo, A., Blanco, L., & Castro-Tirado, A. J. 2009b, GCN Circ. 8772
de Ugarte Postigo, A., Gorosabel, J., Sota, A., & Castro-Tirado, A. J. 2009c, GCN Circ. 8992
de Ugarte Postigo, A., et al. 2009d, GCN Circ. 8999
de Ugarte Postigo, A., et al. 2009e, GCN Circ. 9051
de Ugarte Postigo, A., et al. 2010, A&A, 513, A42
D'Elia, V., et al. 2009a, ApJ, 694, 332
D'Elia, V., et al. 2009b, A&A, 503, 437
D'Elia, V., et al. 2010, MNRAS, 401, 385
Della Valle, M., et al. 2006a, ApJ, 642, L103
Della Valle, M., et al. 2006b, Nature, 444, 1050
Deng, J., Zheng, W., Zhai, M., Qiu, Y., Wei, J., & Hu, J. 2006, Il Nuovo Cimento B, vol. 121, Issue 12, p.1469-1470
Dintinjana, B., Maticic, S., Mikuz, H. & Skvarc, J. 2007, GCN Circ. 7078
Durig, D. T., & Gary, B. 2007, GCN Circ. 6048
Durig, D. T., & Price, A. 2005, GCN Circ. 4023
Durig, D. T., McLarty, N. P., & Manning, J. R. 2005, GCN Circ. 3950
Durig, D. T. 2005, GCN Circ. 3340
Efimov, Y., Rumyantsev, V., & Pozanenko, A. 2006a, GCN Circ. 5850
Efimov, Y., Rumyantsev, V., & Pozanenko, A. 2006b, GCN Circ. 5850
Eichler, D., Livio, M., Piran, T., & Schramm, D. N. 1989, Nature, 340, 126
Elíasdóttir, Á., et al. 2009, ApJ, 697, 1725
Ellison, S., et al. 2006, MNRAS, 372, L38
Evans, P. A. & Holland, S. T. 2009, GCN Circ. 9226
Evans, P. A., et al. 2007, A&A, 469, 379
Evans, P. A., et al. 2009, MNRAS, 397, 1177
Falcone, A., et al. 2006, GCN Circ. 4966
Fan, Y., & Piran, T. 2006, MNRAS, 369, 197
Fatkhullin, T., et al. 2008, GCN Circ. 8695
Ferrero, P., et al. 2006, A&A, 457, 857
Ferrero, P., et al. 2007b, AJ, 134, 2118
Ferrero, P., et al. 2008a, GAMMA-RAY BURSTS 2007: Proceedings of the Santa Fe Conference. AIP Conference Proceedings, Volume 1000, pp. 257-260 (2008)

Ferrero, A., French, J., & Melady, G. 2008b, GCN Circ. 8303
Ferrero, P., et al. 2009, A&A, 497, 729
Fiore, F., et al. 2005, ApJ, 624, 853
Fiore, F., Guetta, D., Piranomonte, S., D'Elia, V., & Antonelli, L. A. 2007, A&A, 470, 515
Flasher, J., et al. 2005a, GCN Circ. 3561
Flasher, J., et al. 2005b, GCN Circ. 3567
Foley, R. J., et al. 2006a, ApJ, 645, 450
Foley, S., et al. 2006b, A&A, 447, 891
Ford, L. A., et al. 1995, ApJ, 439, 307
Fox, D. B., et al. 2005, Nature, 437, 845
Frail, D. A. et al. 2006, ApJ, 646, L99
Frank, S., Bentz, M. C., Stanek, K. Z., Mathur, S., Dietrich, M., Peterson, B. M., & Atlee, D. W. 2007, Ap&SS, 312, 325
Freedman, D. L., & Waxman, E. 2001, ApJ, 547, 922
Friedman, A. S., & Bloom, J. S. 2005, ApJ, 627, 1
Fruchter, A., Ferguson, H., Pepper, J., Gibbons, R., Sahu, K., & Pian, E. 1999, GCN Circ. 386
Fryer, C. L., Young, P. A., & Hungerford, A. L. 2006, ApJ, 650, 1028
Fryer, C. L., Hungerford, A. L., & Young, P. A. 2007, ApJ, 662, L55
Fukui, A., Itow, Y., Sumi, T., & Tristam, P. 2008, GCN Circ. 7622
Fynbo, J. P .U., et al. 2006a, A&A, 451, L47
Fynbo, J. P. U., et al. 2006b, Nature, 444, 1047
Fynbo, J. P. U., et al. 2009, ApJS, 185, 526
Galama, T. J., et al. 1998, Nature, 395, 670
Galama, T. J., et al. 1999, GCN Circ. 313
Galeev, A., et al. 2008, GCN Circ. 8102
Gal-Yam, A., et al. 2006, Nature, 444, 1053
Garnavich, P., Prieto, J. L., & Pogge, R. 2008a, GCN Circ. 7409
Garnavich, P., Prieto, J. L., & Pogge, R. 2008b, GCN Circ. 7414
Gehrels, N., et al. 2004, ApJ, 611, 1005
Gehrels, N., et al. 2005, Nature, 437, 851
Gehrels, N., et al. 2006, Nature, 444, 1044
Gehrels, N., et al. 2008, ApJ, 689, 1161
Gehrels, N., Ramirez-Ruiz, E., & Fox, D. B. 2009, ARA&A, 2009, vol. 47: 567-617
Gendre, B., Pelisson, S., Boër, M., Basa, S., & Mazure, A. 2008, A&A, 492, L1
Gendre, B., et al. 2010, MNRAS, 405, 2372
George, K., Banerjee, D. P. K., Chandrasekhar, T., & Ashok, N. M. 2006, ApJ, 640, L13
Gilmore, A., Kilmartin, P., & Henden, A. A. 2003, GCN Circ. 1949
Götz, D., & Mereghetti, S. 2005, GCN Circ. 3329
Golenetskii, S., et al. 2005a, GCN Circ. 3179
Golenetskii, S., et al. 2005b, GCN Circ. 3518
Golenetskii, S., et al. 2005c, GCN Circ. 4030
Golenetskii, S., et al. 2005d, GCN Circ. 4238
Golenetskii, S., et al. 2006a, GCN Circ. 5722
Golenetskii, S., et al. 2006b, GCN Circ. 5837
Golenetskii, S., Aptekar, R., Mazets, E., Pal'shin, V., Frederiks, D., & Cline, T. 2007b, GCN Circ. 6960
Golenetskii, S., et al. 2008b, GCN Circ. 7995
Golenetskii, S., et al. 2008c, GCN Circ. 8611
Golenetskii, S., et al. 2009a, GCN Circ. 8776
Golenetskii, S., et al. 2009b, GCN Circ. 9959
Gomboc, A., et al. 2008, ApJ, 687, 443
Goodman, J. 1986, ApJ, 308, L47
Gorosabel, J., et al. 2005, GCN Circ. 3294
Gorosabel, J., et al. 2006, A&A, 450, 87
Granot, J. Königl, A., Piran, T. 2006, MNRAS, 370, 1946
Greco, G., et al. 2006a, GCN Circ. 4732
Greco, G., et al. 2006b, GCN Circ. 5526
Greco, G. et al. 2007, GCN Circ. 7089
Greiner, J., et al. 2003, ApJ, 599, 1223
Greiner, J. et al. 2009a, ApJ, 692, 1912
Greiner, J. et al. 2009b, ApJ, 693, 1610
Greiner, J. et al. 2009c, A&A, 498, 89
Grupe, D., et al. 2006a, ApJ, 645, 464
Grupe, D., et al. 2006b, ApJ, 653, 462
Grupe, D., et al. 2007a, ApJ, 662, 443
Grupe, D. et al. 2008, GCN Report 114.1
Guetta, D., & Della Valle, M. 2007, ApJ, 657, L73
Guidorzi, C., et al. 2005, ApJ, 630, L121
Guidorzi, C., et al. 2007a, A&A, 463, 539
Guidorzi, C. et al. 2007b, GCN Circ. 6848
Guidorzi, C. et al. 2009a, A&A, 499, 439
Guidorzi, C., et al. 2009b, GCN Circ. 8989
Guidorzi, C., et al. 2009c, GCN Circ. 9039
Guidorzi, C., Bersier, D., & Tanvir, N. 2009d, GCN Circ. 9238
Haislip, J., et al. 2005a, GCN Circ. 3712
Haislip, J., et al. 2005b, GCN Circ. 4220
Haislip, J., et al. 2007, GCN Circ. 7022
Halpern, J. P., & Armstrong, E. 2006a, GCN Circ. 5851

Halpern, J. P., & Armstrong, E. 2006b, GCN Circ. 5853
Halpern, J. P., & Mirabal, N. 2007, GCN Circ. 6082
Halpern, J. P., Mirabal, N., & Armstrong, E. 2006, GCN Circ. 5847
Hao, H., et al. 2007, ApJ, 659, L99
Harrison, F. A., et al. 1999, ApJ, 523, L121
Hearty, F., et al. 2006a, GCN Circ. 4753
Hearty, F., et al. 2006b, GCN Circ. 5126
Heng, K., et al. 2008, ApJ, 681, 1116
Hentunen, V.-P., Oksanen, A., & Kehusmaa, P. 2008, GCN Circ. 7484
Hentunen, V.-P. 2007, GCN Circ. 6981
Henych, T., Kocka, M., Hroch, F., Jelínek, M., & Hudec, R. 2005, GCN Circ. 4026
Hill, J., Ragazzoni, R., Baruffolo, A., & Garnavich, P. 2008, GCN Circ. 7523
Hjorth, J., Burud, I., Pizzella, A., Pedersen, H., Jaunsen, A. O., & Lindgren, B. 1999, GCN Circ. 320
Hjorth, J., et al. 2003, Nature, 423, 847
Hjorth, J., et al. 2005, ApJ, 630, L117
Hjorth, J., et al. 2005b, Nature, 437, 859
Holland, S. T., et al. 2002, AJ, 124, 639
Holland, S. T., Campana, S., Smith, P., Huckle, H., & Gehrels, N. 2005, GCN Circ. 4235
Holland, S. T., et al. 2007, AJ, 133, 122
Holland, S. T., et al. 2010, ApJ, 717, 223
Holman, M., Garnavich, P., & Stanek, K. Z. 2005, GCN Circ. 3727
Hoversten, E. A., & Cummings, J. R. 2008, GCN Circ. 7398
Huang, F. Y., et al. 2005, GCN Circ. 4230
Huang, K. Y., Ip, W. H., & Urata, Y. 2006a, GCN Circ. 4984
Huang, K. Y., Ip, W. H., Lee, Y. S., & Urata, Y. 2006b, GCN Circ. 5549
Huang, K. Y., et al. 2007, ApJ, 654, L25
Huang, K. Y., Schwamb, M. e., Wang, J. H., & Wen, C. Y. 2008a, GCN Circ. 7334
Huang, L.-C., Chen, T.-W., Chen, Y.-T., Huang, K. Y., & Urata, Y. 2008b, GCN Circ. 7999
Hunsberger, S. D., et al. 2005, GCN Circ. 4041
Iizuka, R., Matsuda, K., Naito, H., & Tsumuraya, F. 2007, GCN Circ. 6316
Ikejiri, Y., et al. 2008, GCN Circ. 8081
Im, M., Lee, I. & Urata, Y. 2007, GCN Circ. 6970
Im, M., et al. 2008, GCN Circ. 7546
Im, M., Park, W., Jeon, Y., Lee, I., Jeon, Y.-B., & Urata, Y. 2009, GCN Circ. 9275
Im, M., Ko, J., Cho, Y., Choi, C., Jeon, Y., Lee, I., & Ibrahimov, M. 2010, J. of Korean Astr. Soc.,43, 75
Imerito, A., Coward, D., Burman, R., & Blair, D. G. 2008, MNRAS, 391, 405
Imerito, A., Coward, D., Burman, R., & Blair, D. G. 2009, MNRAS, 399, L108
Ishimura, T., Yatsu, Y., Shimokawabe, T., Kawai, N., & Yoshida, M. 2007a, GCN Circ. 7026
Ishimura, T., et al. 2007b, GCN Circ. 7087
Isogai, M., & Kawai, N. 2008, GCN Circ. 8629
Israel, G. L., et al. 1999, A&A, 348, L5
Jacques, C., & Pimentel, E. 2005, GCN Circ. 3712
Jakobsson, P., et al. 2003, A&A, 408, 941
Jakobsson, P., et al. 2004a, New Astron., 9, 435
Jakobsson, P., et al. 2004b, A&A, 427, 785
Jakobsson, P., et al. 2006a, A&A, 447, 897
Jakobsson, P., et al. 2006b, GCN Circ. 5195
Jakobsson, P., et al. 2006c, GCN Circ. 5298
Jakobsson, P., et al. 2006d, GCN Circ. 5320
Jakobsson, P., et al. 2006e, A&A, 460, L13
Jakobsson, P., Hjorth, J., Fynbo, J. P. U., Gorosabel, J., & Jaunsen, A. O. 2006f, Proceedings of the Eleventh Marcel Grossmann Meeting on General Relativity, eds. H. Kleinert, R. T. Jantzen & R. Ruffini, World Scientific, Singapore, 2007 (astro-ph/0611561)
Jakobsson, P., et al. 2007a, GCN Circ. 6398
Jakobsson, P., et al. 2007b, GCN Circ. 6997
Jaunsen, A. O., et al. 2008, ApJ, 681, 453
Jelínek, M., Kubánek, P, & Prouza, M. 2006a, GCN Circ. 4976
Jelínek, M., et al. 2006b, A&A, 454, L119
Jelínek, M., Caballero, J. A., de la Nuez, A., & Castro-Tirado, A. J. 2007, GCN Circ. 6272
Jensen, B. L., et al. 2001, A&A, 370, 909
Jiang, l., Bian, F., & Fan, X. 2007, GCN Circ. 7003
Jin, Z. P., & Fan, Y. Z. 2007, MNRAS, 378, 1043
Jóhanesson, G., Björnson, G., & Gudmundsson, E. H. 2007, A&A, 472, L29
Kahharov, B., et al. 2005, GCN Circ. 3261
Kamble, A., Resmi, L., & Misra, K. 2007, ApJ, 664, L5
Kamble, A., Misra, K., Bhattacharya, D., & Sagar, R. 2009, MNRAS, 394, 214

Kaneko, Y., et al. 2007, ApJ, 654, 385
Kann, D. A., Klose, S., & Zeh, A. 2006, ApJ, 641, 993 (K06)
Kann, D. A., Masetti, N., Klose, S. 2007a, AJ, 133, 1187
Kann, D. A., et al. 2008, ApJ, submitted (arXiv:0804.1959)
    (Paper II)
Kannappan, S., Garnavich, P., Stanek, K. Z., Christlein, D., &
    Zaritsky, D. 2005, GCN Circ. 3778
Kaplan, D., Garnavich, P., Rosenberg, J., & Stanek, K. Z. 2005,
    GCN Circ. 3507
Karska, A., & Garnavich, P. 2006, GCN Circ. 5260
Kawai, N., et al. 2006, Nature, 440, 184
Khamitov, I. et al. 2006a, GCN Circ. 5224
Khamitov, I. et al. 2006b, GCN Circ. 5235
Kinugasa, K., & Torii, K. 2005, GCN Circ. 4295
Kippen, R. M. 1999, GCN Circ. 224
Kirschbrown, J., et al. 2005, GCN Circ. 3947
Kistler, M. D., Yüksel, H., Beacom, J. F., & Stanek, K. Z. 2008,
    ApJ, 673, 119
Kistler, M. D., Yüksel, H., Beacom, J. F., Hopkins, A. M.,
    Wyithe, J. S. B. 2009, ApJ, 705, L104
Kiziloglu, U., et al. 2005, GCN Circ. 3139
Klotz, A., et al. 2005a, A&A, 439, L35
Klotz, A., Boër, M., & Atteia, J. L. 2005b, GCN Circ. 3720
Klotz, A., Boër, M., & Atteia, J. L. 2006, GCN Circ. 5140
Klotz, A., Boër, M., & Atteia, J. L. 2007, GCN Circ. 7065
Klotz, A., Boër M., & Atteia, J. L. 2008a, GCN Circ. 7280
Klotz, A., Boër M., & Atteia, J. L. 2008b, GCN Circ. 7595
Klotz, A., et al. 2008c, A&A, 483, 847
Klotz, A., Gendre, B., Boër M., & Atteia, J. L. 2009a, GCN Circ.
    8764
Klotz, A., Gendre, B., Boër M., & Atteia, J. L. 2009b, GCN Circ.
    8998
Klotz, A., Boër, M., Atteia, J. L., & Gendre, B. 2009c, AJ, 137,
    4100
Kocevski, D., & Butler, N. R. 2008, ApJ, 680, 531
Kocevski, D., et al. 2007, ApJ, 663, 1180
Kouveliotou, C., et al. 1993, ApJ, 413, L101
Kouveliotou, C., et al. 2004, ApJ, 608, 872
Krühler, T., et al. 2008, ApJ, 685, 376
Krühler, T., et al. 2009a, ApJ, 697, 758
Krühler, T., et al. 2009b, A&A, 508, 593
Krimm, H. A., et al. 2009, ApJ, 704, 1405
Kuin, N. P. M., et al. 2009, MNRAS, 395, L21
Kulkarni, S. R., et al. 1999, Nature, 398, 389
Kumar, P., & Barniol Duran, R. 2009, MNRAS, 400, L75
Kumar, P., & Narayan, R., 2009, MNRAS, 395, 472
Kumar, P., & Panaitescu, A., 2008, MNRAS, 391, L19
Küpcü Yoldas, A., Yoldas, A., Greiner, J., & Klose, S. 2008, GCN
    Circ. 7283
LaCluyze, A., et al. 2006, GCN Circ. 4750
Lamb, D. Q., et al. 2004, New Astronomy Reviews, Volume 48,
    Issue 5-6, p. 423-430
Landsman, W. B., & Sbarufatti, B. 2008, GCN Circ. 7965
Landsman, W., & Stamatikos, M. 2007, GCN Circ. 6340
Lapi, A., et al. 2008, MNRAS, 386, 608
Ledoux, C., et al. 2005, GCN Circ. 3860
Ledoux, C., Vreeswijk, P., Smette, A., Jaunsen, A., & Kaufer, A.
    2006, GCN Circ. 5237
Ledoux, C. et al. 2007, GCN Circ. 7023
Levan, A. J., Tanvir, N. R., Rol, E., Fruchter, A., & Adamson, A.
    2006, GCN Circ. 5455
Levan, A. J., et al. 2009, GCN Circ. 8856
Li, W., & Bloom, J. S. 2006, GCN Circ. 5532
Li, W., & Fillipenko, A. V. 2008, GCN Circ. 7475
Li, W., et al. 2005, GCN Circ. 4095
Li, W., et al. 2006, PASP, 118, 37
Li, Y., Li, A., & Wei, D. M. 2008a, ApJ, 678, 1136
Li, W., Chornock, R., Perley, D. A., & Filippenko, A. V. 2008b,
    GCN Circ. 7959
Li, A., Liang, S. L., Kann, D. A., Wei, D. M., Klose, S., & Wang,
    Y. J. 2008c, ApJ, 685, L1046
Li, W. 2005a, GCN Circ. 3945
Li, W. 2005b, GCN Circ. 4240
Li, W. 2006, GCN Circ. 4727.
Li, L.-X. 2008, MNRAS, 388, 1487
Liang, S. L., & Li, A. 2009, ApJ, 690, L56
Liang, E., & Zhang, B. 2006, ApJ, 638, L67
Liang, E., Zhang, B., Virgili, F., & Dai, Z. G. 2007a, ApJ, 662,
    1111
Liang, E.-W., Zhang, B.-B., & Zhang, B. 2007b, ApJ, 670, 565
Lin, C. S., et al. 2006, GCN Circ. 4696
Lipunov, V., et al. 2005, GCN Circ. 3883
Liu, H., et al. 2008, GCN Circ. 8618
Macomb, D., et al. 2005, GCN Circ. 3843
Maiolino, R., et al. 2004, Nature, 431, 533
Maiorano, E., et al. 2006, A&A, 455, 423
Maiorano, E., et al. 2009, GCN Circ. 9606

Malesani, D., et al. 2004, ApJ, 609, L5
Malesani, D., Fiore, F., Masetti, N., Pedani, M., & Mainella, G.
    2006, GCN Circ. 5225
Malesani, D., Jaunsen, A. O., & Vreeswijk, P. M. 2007a, GCN
    Circ. 6021
Malesani, D., Fynbo, J. P. U., Jaunsen, A. O., & Vreeswijk, P. M.
    2007b, GCN Circ. 6021
Malesani, D., et al. 2007c, GCN Circ. 6555
Malesani, D., et al. 2007d, A&A, 473 ,77
Malesani, D., Fynbo, J. P. U., de Ugarte Postigo, A., Gorosabel,
    J., Barros, S., & Simpson, E. 2009, GCN Circ. 8780
Mannucci, F., Covino, S., & Malesani, D. 2005, GCN Circ. 4045
Mao, J., Cha, G., & Bai, J. 2009, GCN Circ. 9305
Margutti, R., et al. 2007, A&A, 474, 815
Marshall, F. E., et al. 2008 GCN Report Nr. 129
Masi, G., Jensen, B. L., Hjorth, J., & Michelsen, R. 2003, GCN
    Circ. 1960
Mason, K. O., et al. 2006, ApJ, 639, 311
Mazzali, P. A., et al. 2006, ApJ, 645, 1323
McBreen, S., et al. 2008, ApJ, 677, L85
McBreen, S., et al. 2010, A&A, 516, A71
Melandri, A., Tanvir, N., & Guidorzi, C. 2006a, GCN Circ. 5322
Melandri, A., et al. 2008, ApJ, 686, 1209
Melandri, A., et al. 2009, MNRAS, 395, 1941
Mészáros, P., & Rees, M. J. 1997, ApJ, 467, 232
Mészáros, P., & Rees, M. J. 1999, MNRAS, 306, L39
Mészáros, P. 2006, Rep. Prog. Phys., 69, 2259
Milne, P. A., & Williams, G. G. 2006, GCN Circ. 4699
Milne, P. A., & Williams, G. G. 2008, GCN Circ. 7387
Milne, P. A., Williams, G. G., & Park, H.-S. 2005a, GCN Circ.
    3258
Milne, P. A., Williams, G. G., Park, H. S., & Barthelmy, S.
    2005b, GCN Circ. 4218
Milne, P. A., Williams, G. G., Park, H. S., Barthelmy, S., &
    Crist-Lair, J. 2005c, GCN Circ. 4252
Milne, P. A. 2006, GCN Circ. 5127
Minezaki, T., Price, P. A., Yoshii, Y., & Cowie, L. L. 2007, GCN
    Circ. 7135
Mirabal, N., et al. 2002, ApJ, 578, 818
Mirabal, N., Halpern, J. P., An, D., Thorstensen, J. R., &
    Terndrup, D. M. 2006, ApJ, 643, L99
Mirabal, N., McGreer, I. D., Halpern, J. P., Dietrich, M., &
    Peterson, B. M. 2007a, GCN Circ. 6526
Mirabal, N., McGreer, I. D., Halpern, J. P. 2007b, GCN Circ.
    6534
Mirabal, N., Halpern, J. P., & O'Brien, P. T. 2007c, ApJ, 661,
    L127
Misra, K., et al. 2005, GCN Circ. 4259
Misra, K., et al. 2007, A&A, 464, 903
Misra, K., 2006, GCN Circ. 4742
Modjaz, M., et al. 2006, ApJ, 645, L21
Molinari, E., et al. 2007, A&A, 469, L13
Monard, B. 2005, GCN Circ. 3728
Monfardini, A., et al. 2006, ApJ, 648, 1125
Morgan, A. N., Vanden Berk, D. E., Brown, P., & Evans, P. A.
    2006, GCN Circ. 5553
Morgan, A. N., Bloom, J. S., Perley, D. A., & Starr, D. 2009,
    GCN Circ. 8995
Mori, Y. A., et al. 2008, GCN Circ. 8619
Moskvitin, A. S., Fatkhullin, T. A., Komarova, V. N., &
    Burenkov, A. N. 2008, GCN Circ. 7559
Mundell, C. G., et al. 2007a, Science, 315, 1822
Mundell, C. G., et al. 2007b, ApJ, 660, 489
Nakagawa, Y. E., et al. 2006, PASJ, 58, L35
Nakar, E., & Piran, T. 2005a, ApJ, 619, L147
Nakar, E., & Piran, T. 2005b, MNRAS, 360, L73
Nakar, E. 2007, Physics Reports - Bethe Centennial Volume,
    Volume 442, Issue 1-6, p. 166-236. (astro-ph/0701748)
Nanni, D., et al. 2005, GCN Circ. 4298
Nardini, M., et al. 2006, A&A, 451, 821
Nardini, M., Ghisellini, G., & Ghirlanda, G. 2008a, MNRAS, 383,
    1049
Nardini, M., Ghisellini, G., & Ghirlanda, G. 2008b, MNRAS, 386,
    L87
Nardini, M., Ghisellini, G., Ghirlanda, G., & Celotti, A. 2010,
    MNRAS, 403, 1131
Nissinen, M., & Hentunen, V.-P. 2009, GCN Circ. 9246
Nissinen, M. 2009, GCN Circ. 8993
Nomoto, K., et al. 2007, Proceedings of the Conference "SWIFT
    and GRBs: Unveiling the Relativistic Universe", Venice, June
    5-9, 2006. Il Nuovo Cimento, Vol. 121 B, N. 10-11, 1207
Norris, J. P., & Bonnell, J. T. 2006, ApJ, 643, 266
Nousek, J. A., et al. 2006, ApJ, 642, 389
Novak, R. 2005, GCN Circ. 4027
Nysewander, M., et al. 2006a, GCN Circ. 4971
Nysewander, M., et al. 2006b, GCN Circ. 5545
Nysewander, M., et al. 2009a, ApJ, 693, 1417

Nysewander, M., Fruchter, A. S., & Pe'er, A. 2009b, ApJ, 701, 824
Oates, S. R., & Grupe, D. 2006, GCN Circ. 5519
Oates, S. R., & Stratta, G. 2007, GCN Circ. 7080
Oates, S. R., et al. 2007, MNRAS, 380, 270
Oates, S. R., et al. 2009, MNRAS, 395, 490
Ofek, E. O., Lipkin, Y. M., & Dann, J. 2005, GCN Circ. 4018
Ofek, E. O., Cenko, S. B., Soderberg, A. M., & Fox, D. B. 2006, GCN Circ. 4691
Ofek, E. O., et al. 2007, ApJ, 662, 1129
Ohno, M., Cutini, S., McEnery, J., Chiang, J., & Koerding, E. 2009, GCN Circ. 9021
Okuma, Y., Fujimoto, H., Nashimoto, T., Wada, A. Yonetoku, D., & Murakami, T. 2008, GCN Circ. 8091
Olivares, F., Küpcü Yoldaş, A., Greiner, J., Yoldaş, A. 2009, GCN Circ. 9245
Ovaldsen, J. E., et al. 2007, ApJ, 662, 294
Paczyński, B. 1986, ApJ, 308, L43
Pagani, C., Holland, S. T., & Stamatikos, M. 2008, GCN Report Nr. 124.1
Page, K. L., et al. 2007, ApJ, 663, 1125
Page, K. L., et al., 2008, MNRAS, 400, 134
Palmer, D. M., et al. 2008, GCN Circ. 8351
Pal'shin, V., et al. 2008, GCN Circ. 8256
Panaitescu, A., & Kumar, P. 2001, ApJ, 543, 66
Panaitescu, A., & Kumar, P. 2001, ApJ, 554, 667
Panaitescu, A., & Kumar, P. 2002, ApJ, 571, 779
Panaitescu, A. & Vestrand, W. T. 2008, MNRAS, 387, 497
Panaitescu, A., Kumar, P. & Narayan, R. 2001, ApJ, 561, L171
Panaitescu, A., Mészáros, P., Gehrels, N., Burrows, D., & Nousek, J. 2006a, MNRAS, 366, 1357
Panaitescu, A., et al. 2006b, MNRAS, 369, 2059
Pandey, S. B., et al. 2006, A&A, 460, 415
Pandey, S. B., et al. 2009, A&A, 504, 45
Pandey, S. B., et al. 2010, ApJ, 714, 799
Patel, M., Warren, S. J., Mortlock, D. J., & Fynbo, J. P. U. 2010, A&A, 512, L3
Pei, Y. C. 1992, ApJ, 395, 130
Pélangeon, A., Atteia, J.-L., Lamb, D. Q., & the Hete-2 Science Team 2006, GAMMA-RAY BURSTS IN THE SWIFT ERA: Sixteenth Maryland Astrophysics Conference. AIP Conference Proceedings, Volume 836, pp. 149-152 (2006)
Pellizza, L. J., et al. 2006, A&A, 459, L5
Penprase, B. E., et al. 2006, ApJ, 646, 358
Perley, D. A., & Bloom, J. S. 2008, GCN Circ. 7233
Perley, D. A., & Melis, C. 2008, GCN Circ. 7970
Perley, D. A., Bloom, J. S., Foley, R. J., & Kocevski, D. 2007a, GCN Circ. 6350
Perley, D. A., Bloom, J. S., & Thöne, C. C. 2007b, GCN Circ. 6757
Perley, D. A., et al. 2007c, Poster presented at the Santa Fe GRB conference
Perley, D. A., et al. 2008a, ApJ, 672, 449
Perley, D. A., Modjaz, M., Bloom, J. S., Poznanski, D., Miller, A., & Kocevski, D. 2008b, GCN Circ. 7298
Perley, D. A., Bloom, J. S., & Li, W. 2008c, GCN Circ. 7406
Perley, D. A. et al. 2008d, ApJ, 688, 470
Perley, D. A., Li, W., Chornock, R. & Fillipenko, A. V. 2009a, GCN Circ. 8985
Perley, D. A., Cenko, S. B., Bloom, J. S., Li, W., & Cobb, B. E. 2009b, GCN Circ. 9001
Perley, D. A., Klein, C. R., Morgan, A. N., & Petigura, E. 2009c, GCN Circ. 9036
Perley, D. A., et al. 2009d, AJ, 138, 1690
Perley, D. A., et al. 2010, MNRAS, in press (arXiv:0912.2999v2)
Perley, D. A. 2009a, GCN Circ. 8997
Perley, D. A. 2009b, GCN Circ. 9041
Perri, M., et al. 2007, A&A, 471, 83
Pian, E., et al. 2006, Nature, 442, 1011
Pietrzynski, G., & Udalski, A. 1999a, GCN Circ. 316
Pietrzynski, G., & Udalski, A. 1999b, GCN Circ. 319
Piran, T. 2005, Rev. Mod. Phys., 76, 1143
Piranomonte, S., et al. 2007, GCN Circ. 6385
Piranomonte, S., et al. 2008, A&A, 492, 775
Piro, L., et al. 2005, ApJ, 623, 314
Pontzen, A., Hewett, P., Carswell, R., & Wild, V. 2007, MNRAS, 381, L99
Poole, T. S., & La Parola, V. 2006, GCN Circ. 5068
Poole, T. S., Sakamoto, T., Blustin, A. J., Hancock, A., & Kennedy, T. 2005, GCN Circ. 4263
Porciani, C., Viel, M., & Lilly, S. J. 2007, ApJ, 659, 218
Pozanenko, A., et al., 2007, Izv. Krym. Astrofiz. Obs. 103, 3, 48
Preece, R. D., et al. 2000, ApJS, 126, 19
Press, W. H., et al. 1992, Numerical Recipes in C (Cambridge: Cambridge Univ. Press)
Price, P. A., et al. 2002a, ApJ, 573, 85
Price, P. A., et al. 2002b, GCN Circ. 1475
Price, P. A., et al. 2003, ApJ, 589, 838

Prieto, J., et al. 2007, GCN Circ. 6346
Prochaska, J. X., et al. 2004, ApJ, 611, 200
Prochaska, J. X., Bloom, J. S., Chen, H.-W., & Foley, R. J. 2005a, GCN Circ. 3204
Prochaska, J. X., Ellison, S., Foley, R. J., Bloom, J. S., & Chen, H.-W. 2005b, GCN Circ. 3332
Prochaska, J. X., Chen, H.-W., Bloom, J. S., Falco, E., & Dupree, A. K. 2006, GCN Circ. 5002
Prochaska, J. X., et al. 2009, ApJ, 691, L27
Prochter, G. e., et al. 2006, ApJ, 648, L93
Prymak, N., et al. 2006, GCN Circ. 5541
Quimby, R., & Rykoff, E. S. 2006, GCN Circ. 5377
Quimby, R., Fox, D., Hoeflich, P., Roman, B., & Wheeler, J. C. 2005, GCN Circ. 4221
Quimby, R. M., et al. 2006, ApJ, 640, 402
Racusin, J. L., et al. 2008, Nature, 455, 183
Rau, A., et al. 2010, ApJ, in press (arXiv:1004.3261v2)
Reichart, D., LaCluyze, A., Nysewander, M., & Haislip, J. 2006, GCN Circ. 4768
Rol, E., et al. 2007, ApJ, 669, 1098
Romano, P., et al. 2006, A&A, 456, 917
Roming, P. W. A., et al. 2006, ApJ, 652, 1416
Rossi, A., et al. 2010, A&A, submitted (arXiv:1007.0383)
Roy, R., Kumar, B., Pandey, S. B., & Kumar, B. 2009, GCN Circ. 9278
Ruiz-Velasco, A. E., et al. 2007, ApJ, 669, 1
Rumyantsev, V., & Pozanenko, A. 2009, GCN Circ. 9324
Rumyantsev, V., Antonyuk, K., Andreev, M., & Pozanenko, A. 2008, GCN Circ. 8645
Rumyantsev, V., Antoniuk, K., & Pozanenko, A. 2009, GCN Circ. 9320
Rykoff, E. S., et al. 2005a, ApJ, 631, L121
Rykoff, E. S., et al. 2006a, ApJ, 638, L5
Rykoff, E. S., Yuan, F., & MacKay, T. A. 2008, GCN Circ. 8293
Rykoff, E. S., et al. 2009, ApJ, 702, 489
Sakamoto, T., et al. 2004, ApJ, 602, 875
Sakamoto, T., et al. 2008, GCN Circ. 8101
Sakamoto, T., et al. 2009, GCN Circ. 9231
Salvaterra, R., Campana, S., Chincarini, G., Tagliaferri, G., & Covino, S. 2007, MNRAS, 380, L45
Salvaterra, R., Campana, S., Chincarini, G., Covino, S., & Tagliaferri, G. 2008, MNRAS, 385, 189
Salvaterra, R., Guidorzi, C., Campana, S., Chincarini, G., & Tagliaferri, G. 2009, MNRAS, 396, 299
Salvaterra, R., et al. 2009b, Nature, 461, 1258
Sari, R., & Piran, T. 1999, ApJ, 517, L109
Sato, R., Kawai, N., Suzuki, M., et al. 2003, ApJ, 599, L9
Sato, G., et al. 2007, GCN Report 31.1
Savaglio, S. 2006, NJPh, 8, 195
Sazonov, S. Y., Lutovinov, A. A., & Sunyaev, R. A. 2004, Nature, 430, 646
Schady, P., & Cannizzo, J. K. 2009, GCN Circ. 9234
Schady, P., & Falcone, A. D. 2006, GCN Circ. 4978
Schady, P., & Moretti, A. 2006, GCN Circ. 5294
Schady, P., et al. 2005, GCN Circ. 3880
Schady, P., et al. 2006, ApJ, 643, 276
Schady, P., et al. 2007a, MNRAS, 377, 273
Schady, P., et al. 2007b, MNRAS, 380, 1041
Schady, P., et al. 2010, MNRAS, 401, 2773
Schaefer, B. E., & Guver, T. 2008, GCN Circ. 7538
Schaefer, B. E., McKay, T. A., & Yuan, F. 2007, GCN Circ. 6948
Schaefer, B. E. 2007, ApJ, 660, 16
Schlegel, D. J., Finkbeiner, D. P., & Davis, M. 1998, ApJ, 500, 525
Schubel, M., et al. 2008, GCN Circ. 7560
Shao, L., & Dai, Z. G. 2005, ApJ, 633, 1027
Sharapov, D., Augusteijn, T., & Pozanenko, A. 2006, GCN Circ. 5263
Shin, M.-S., et al. 2007, ApJ, submitted (astro-ph/0608327)
Skvarc, J. 2006, GCN Circ. 5511
Smith, D. A., & Rykoff, E. S. 2003, GCN Circ. 1952
Soderberg, A. M., et al. 2004, ApJ, 606, 994
Soderberg, A. M., et al. 2006, ApJ, 627, 877
Soderberg, A. M., Berger, E., & Ofek, E. O. 2005, GCN Circ. 4186
Soderberg, A. M., et al. 2006a, ApJ, 636, 391
Soderberg, A. M., et al. 2006b, Nature, 442, 1014
Soderberg, A. M., et al. 2007, ApJ, 661, 982
Sollerman, J., et al. 2006, A&A, 454, 503
Sollerman, J., et al. 2007, A&A, 466, 839
Soyano, T., Mito, H., & Urata, Y. 2006, GCN Circ. 5548
Spergel, D. N., et al. 2003, ApJS, 148, 175
Sposetti, S., 2007a, GCN Circ. 6067
Sposetti, S. 2007b, GCN Circ. 7090
Stamatikos, M., et al. 2007, GCN Report 107.1
Stanek, K. Z., et al. 1999, ApJ, 522, L39
Stanek, K. Z., et al. 2003, ApJ, 591, L17
Stanek, K. Z., et al. 2007, ApJ, 654, L21

Starling, R. L. C., et al. 2005, A&A, 442, L21
Starling, R. L. C., et al. 2007a, ApJ, 661, 787
Starling, R. L. C. et al. 2009, MNRAS, 400, 90
Starling, R. L. C., et al. 2010, MNRAS, submitted (arXiv:1004.2919)
Steele, I. A., Mundell, C. G., Smith, R. J., Kobayashi, S., & Guidorzi, C. G. 2009, Nature, 462, 767
Stefanescu, A., et al. 2006a, GCN Circ. 5291
Stefanescu, A., et al. 2006b, GCN Circ. 5314
Still, M., et al. 2005, ApJ, 635, 1187
Stratta, G., et al. 2004, ApJ, 608, 846
Stratta, G., Maiolino, R., Fiore, F., & D'Elia, V. 2007a, ApJ, 661, L9
Stratta, G., et al. 2007b, GCN Report 104.2
Stratta, G., et al. 2009, A&A, 503, 783
Stroh, M. C., et al. 2007, GCN Report 99.1
Sudilovsky, V., Savaglio, S., Vreeswijk, P., Ledoux, C., Smette, A., & Greiner, J. 2007, ApJ, 669, 741
Sudilovsky, V., Smith, D., & Savaglio, S. 2009, ApJ, 699, 56
Sugita, S., et al. 2008, GAMMA-RAY BURSTS 2007: Proceedings of the Santa Fe Conference. AIP Conference Proceedings, Volume 1000, pp. 354-357 (2008)
Sugita, S., et al. 2009, PASJ, 61, 527
Swan, H., Smith, I., Skinner, M., & Russel, T. et al. 2007a, GCN Circ. 6090
Swan, H., Smith, I., Akerlof, C., Rykoff, E. S., & Skinner, M. 2007b, GCN Circ. 6339
Swan, H., Yuan, F., & Rujopakarn, W. 2008, GCN Circ. 7470
Tanaka, I., et al. 2006, GCN Circ. 5129
Tanvir, N. R., et al. 2008a, MNRAS, 388, 1743
Tanvir, N. R., et al. 2008b, ApJ, submitted (arXiv:0812.1217)
Tanvir, N. R., et al. 2009, Nature, 461, 1254
Taubenberger, S., et al. 2007, GCN Circ. 6566
Teerikorpi, P. 2004, A&A, 424, 73
Tejos, N., Lopez, S., Prochaska, J. X., Chen, H.-W., & Dessauges-Zavadsky,M. 2007, ApJ, 671, 622
Tejos, N., Lopez, S., Prochaska, J. X., Bloom, J. S., Chen, H.-W., Dessauges-Zavadsky, M., & Maureira, M. J. 2009, ApJ, 706, 1309
Terada, H., Pyo, T.-S., Kobayashi, N., & Kawai, N. 2006, GCN Circ. 4716
Thöne, C. C., et al. 2007a, GCN Circ. 6741
Thöne, C. C., et al. 2007b, ApJ, 671, 628
Thöne, C. C., Perley, D. A., & Bloom, J. S. 2007c, GCN Circ. 6663
Thöne, C. C., et al. 2008a, ApJ, 676, 1151
Thöne, C. C., et al. 2008c, A&A, 489, 37
Thöne, C. C., de Ugarte Postigo, A., & Liebig, C. 2008d, GCN Circ. 8106
Thöne, C. C., et al. 2008d, A&A, submitted (arXiv:0806.1182v2)
Tominaga, N., et al. 2007, ApJ, 657, L77
Torii, K. 2005a, GCN Circ. 3121
Torii, K. 2005b, GCN Circ. 3943
Torii, K. 2006, GCN Circ. 5642
Troja, E., et al. 2007, ApJ, 665, 599
Tueller, J., et al. 2008, GCN Circ. 7402
Uemura, M., Arai, A., & Uehara, T. 2006, GCN Circ. 5828
Uemura, M., Arai, A. & Uehara, T. 2007a, GCN Circ. 6039
Uemura, M., Sasada, M., Arai, A., & Uehara, T. 2007b, GCN Circ. 7094
Uemura, M. 2008, GCN Circ. 8085
Ukwatta, T. N., et al. 2009, GAMMA-RAY BURST: Sixth Huntsville Symposium. AIP Conference Proceedings, Volume 1133, pp. 437-439 (2009)
Ulanov, M. V., et al. 2005, Il Nuovo Cimento, Vol. 28, Nr. 3, 351
Updike, A. C., et al. 2007a, GCN Circ. 6515
Updike, A. C., et al. 2007b, GCN Circ. 6530
Updike, A. C., Williams, G. G., Milne, P. A., & Hartmann, D. H. 2008a, GCN Circ. 7288
Updike, A., et al. 2008b, ApJ, 685, 361
Updike, A. C., Klose, S., Clemens, C., & Greiner, J. 2009a, GCN Circ. 8983
Urata, Y., Chen, T. W., Huang, K. Y., Huang, L. C., Im, M., & Lee, I. 2008, GCN Circ. 7415
Urata, Y., Zhang, Z. W., Wen, C. Y., Huang, K. Y., & Wang, S. Y. 2009, GCN Circ. 9240
Vaalsta, T., & Coward, D. M. 2009, GCN Circ. 8996
van Paradijs, J., et al. 1997, Nature, 386, 686
Vergani, S., D., Petitjean, P., Ledoux, C., Vreeswijk, P., Smette, A., & Meurs, E. V. J. 2009, A&A, 503, 771
Vestrand, W. T., et al. 2006, Nature, 442, 172
Villasenor, J. S., et al. 2005, Nature, 437, 855
Virgili, F. J., Liang, E.-W., & Zhang, B. 2009, MNRAS, 392, 91
Volkov, I. 2008, GCN Circ. 8604
von Kienlin, A. 2009, GCN Circ. 9229
Vreeswijk, P. M., et al. 1999, GCN Circ. 310
Vreeswijk, P. M., et al. 2001, ApJ, 546, 672

Vreeswijk, P. M., et al. 2004, A&A, 419, 927
Vreeswijk, P. M., et al. 2006, A&A, 447, 145
Wang, W.-H., et al. 2006, GCN Circ. 4653
Wang, X. F., et al. 2007, GCN Circ. 7063
Wang, X. F., et al. 2008, GCN Circ. 7550
Wang, X. F., et al. 2009, GCN Circ. 9034
Watson, D., et al. 2006, ApJ, 652, 1011
Weaver, E., et al. 2008, GCN Circ. 7967
Wegner, G., Garnavich, P., Prieto, J. L., & Stanek, K. Z. 2008, GCN Circ. 7423
Wei, D. M., Yan, T., & Fan, Y. Z. 2006, ApJ, 636, L69
West, J. P. et al. 2008, GCN Circ. 8617
Wiersema, K. et al. 2005, GCN Circ. 3200
Wiersema, K., Thöne, C. C., & Rol, E. 2006, GCN Circ. 5552
Wiersema, K., et al., 2008, A&A, 481, 319
Wigger, C., Wigger, O., Bellm, E., & Hajdas, W. 2008, ApJ, 675, 553
Williams, G. G., & Milne, P. A. 2006, GCN Circ. 4730
Williams, G. G., & Milne, P. A. 2008, GCN Circ. 7443
Woźniak, P., et al. 2005a, ApJ, 627, L13
Woźniak, P. R., Vestrand, W. T., Wren, J., White, R., & Evans, S. 2005b, GCN Circ. 4239
Woźniak, P. R., et al. 2006, ApJ, 642, L99
Woźniak, P., Vestrand, W. T., Wren, J., & Davis, H. 2008, GCN Circ. 7403
Woźniak, P. R., Vestrand, W. T., Panaitescu, A. D., Wren, J. A., Davis, H. R., & White, R. R. 2009, ApJ, 691, 495
Wood-Vasey, W. M., et al. 2003, GCN Circ. 1968
Woosley, S. E., Bloom, J. S. 2006, ARA&A, 44, 507
Woosley, S. E. 1993, ApJ, 405, 273
Wren, J., Vestrand, W. T., Woźniak, P. R., White, R., & Pergande, J. 2007a, GCN Circ. 6084
Wren, J., Vestrand, W. T., Woźniak, P. R. White, R., & Pergande, J. 2007b, GCN Circ. 6324
Wren, J., Vestrand, W. T., Woźniak, P. R., & Davis, H. 2008a, GCN Circ. 7477
Wren, J., Vestrand, W. T., Woźniak, P. R., & Davis, H. 2008b, GCN Circ. 7568
Wyithe, J. S. B., Oh, S. P., & Pindor, B. 2010, MNRAS, submitted (arXiv:1004.2081)
Xiao, L., & Schaefer, B. E., 2009, ApJ, 698, 803
Xin, L. P., et al. 2007, GCN Circ. 6956
Xin, L. P., et al. 2009, GCN Circ. 9225
Yanagisawa, K., Toda, H., & Kawai, N. 2005, GCN Circ. 3489
Yoshida, M., Yanagisawa, K., & Kawai, N. 2007a, GCN Circ. 6050
Yoshida, M., Yanagisawa, K., Shimizu, Y., Nagayama, S., & Kawai, N. 2007b, GCN Circ. 6531
Yoshida, M., Yanagisawa, K., Shimizu, Y., Nagayama, S., Toda, H., & Kawai, N. 2007c, GCN Circ. 7091
Yoshida, M., Yanagisawa, K., Shimizu, Y., Nagayama, S., Toda, H., & Kawai, N. 2008a, GCN Circ. 7410
Yoshida, M., et al. 2008b, GCN Circ. 7973
Yoshida, M., et al. 2008c, GCN Circ. 8097
Yoshida, M., et al. 2009, GCN Circ. 9218
Yost, S. A., et al. 2005, ApJ, 636, 959
Yost, S. A., Schaefer, B. E., & Yuan, F. 2006, GCN Circ. 5824
Yost, S., et al. 2007a, ApJ, 657, 925
Yuan, F. & Rykoff, E. S. 2007, GCN Circ. 6761
Yuan, F., Rykoff, E. S., McKay, T. A., Schaefer, B. E., Quimby, R., & Swan, H. 2007a, GCN Circ. 6951
Yuan, F., Rykoff, E. S., Rujopakarn, W., & Swan, H. 2007b, GCN Circ. 7061
Yuan, F., Quimby, R., Swan, H., & Akerlof, C. 2008a, GCN Circ. 7411
Yuan, F., et al. 2008b, 2008 NANJING GAMMA-RAY BURST CONFERENCE. AIP Conference Proceedings, Volume 1065, pp. 103-106 (2008)
Yuan, F., et al. 2010, ApJ, 711, 870
Yuan, F., 2009, GCN Circ. 9224
Yüksel, H., Kistler, M. D., Beacom, J. F., Hopkins, A. M. 2008, ApJ, 683, L5
Zafar, T., et al. 2010, A&A, 515, A94
Zeh, A., Klose, S., & Hartmann, D. H. 2004, ApJ, 609, 952
Zeh, A., Klose, S., & Kann, D. A. 2006, ApJ, 637, 889
Zhai, M., Qiu, Y. L., Wei, J. Y., Hu, J. Y., Deng, J. S., & Zheng, W. K. 2006, GCN Circ. 5230
Zhang, B., & Mészáros, P. 2004, Int.J.Mod.Phys. A19 (2004) 2385
Zhang, B. et al. 2006, ApJ, 642, 354
Zhang, B. et al. 2007a, ApJ, 655, L25
Zhang, B. et al. 2007b, ApJ, 655, 989
Zhang, B., et al. 2009, ApJ, 703, 1696
Zhang, B. 2006, Nature, 444, 1010
Zhang, B. 2007, ChJAA, 7, 1
Zheng, W.-K., Jinsong, D., & Wang, J. 2009a, Research in Astron. Astrophys., 9 (2009), 1103
Zheng, W.-K. et al. 2009b, Chin. J. Astron. Astrophys. Vol. 8 (2008) No.6, 693 (arXiv:0906.2692)

Ziaeepour, H., et al. 2008, MNRAS, 385, 453
Zou, Y. C., Xu, D., & Dai, Z. G. 2006, ApJ, 646, 1098

TABLE 2
ENERGETICS OF THE TYPE II GRB SAMPLE

GRB	Redshift z	Fluence (10^{-7} erg cm^{-2})	Band (keV)	Low-energy index α_B	High-energy index β_B	$E_{\rm p,rest}$ (keV)	log $E_{\rm iso,bol}$ (erg)	References (for Energetics)
970508	0.8349 ± 0.0003	26 ± 3	$20-2000$	-1.71 ± 0.1	-2.2 ± 0.25	168.8 ± 47.7	$51.87^{+0.06}_{-0.07}$	1, 2
990123	1.6004 ± 0.0008	5090 ± 20	$20-2000$	-0.89 ± 0.08	-2.45 ± 0.97	2031 ± 161.0	54.60 ± 0.05	1, 3
990510	1.6187 ± 0.0015	270 ± 50	$20-2000$	-1.23 ± 0.05	-2.7 ± 0.4	423.0 ± 42.0	$53.34^{+0.07}_{-0.09}$	1, 2
991208	0.7063 ± 0.0017	1630 ± 50	$20-2000$	-1.1 ± 0.4	-2.2 ± 0.4	312.3 ± 5.1	$53.43^{+0.05}_{-0.06}$	1, 2, 4
991216	1.02 ± 0.01	2480 ± 120	$20-2000$	-1.23 ± 0.25	-2.18 ± 0.39	763.6 ± 20.2	$53.93^{+0.04}_{-0.05}$	1, 2
000131	4.5 ± 0.015	440 ± 60	$20-2000$	-1.2 ± 0.1	-2.4 ± 0.1	1293 ± 110.0	$54.28^{+0.06}_{-0.07}$	1, 2
000301C	2.0404 ± 0.0008	83 ± 6	$20-2000$	-1.0 ± 0.3	-2.3 ± 0.3	1213 ± 303.0	$52.99^{+0.03}_{-0.04}$	2
000911	1.0585 ± 0.0001	1920 ± 340	$20-2000$	-1.11 ± 0.12	-2.32 ± 0.41	2106 ± 177.0	$53.86^{+0.08}_{-0.09}$	1, 2
000926	2.0387 ± 0.0008	260 ± 40	$20-2000$	-1.1 ± 0.1	-2.43 ± 0.4	306.9 ± 18.2	$53.52^{+0.06}_{-0.08}$	1, 2, 4
010222	1.47688 ± 0.00002	1390 ± 80	$20-2000$	-1.35 ± 0.19	-1.64 ± 0.02	765.4 ± 29.7	54.06 ± 0.03	1, 2
011121	0.362 ± 0.001	2270 ± 250	$20-2000$	-1.1 ± 0.3	-2.1 ± 0.2	1201 ± 126.7	$53.01^{+0.06}_{-0.07}$	2, 5
011211	2.1418 ± 0.0018	50 ± 5	$40-700$	-0.84 ± 0.09	-2.3 ± 0.46	185.0 ± 22.0	$53.01^{+0.05}_{-0.06}$	1
020405	0.68986 ± 0.00004	830 ± 60	$20-2000$	-0.0 ± 0.25	-1.87 ± 0.23	532.3 ± 25.3	$53.17^{+0.06}_{-0.07}$	1, 2
020813	1.254 ± 0.005	1410 ± 130	$20-2000$	-0.94 ± 0.03	-1.57 ± 0.04	710.0 ± 33.8	53.94 ± 0.04	1, 2
021004	2.3304 ± 0.0005	25.5 ± 6	$2-400$	-1.01 ± 0.19	-2.3 ± 0.46	266.0 ± 117.0	$52.65^{+0.12}_{-0.17}$	1
030226	1.98691 ± 0.00015	130 ± 60	$20-2000$	-0.89 ± 0.17	-2.3 ± 0.46	349.5 ± 41.8	$53.17^{+0.17}_{-0.27}$	1, 2
030323	3.3718 ± 0.0005	$12.3^{+3.7}_{-3.4}$	$2-400$	$-0.80^{-0.80}_{+0.83}$	$\cdots$	$192.4^{+393.5}_{-113.7}$	$52.53^{+0.23}_{-0.19}$	1, 6
030328	1.5216 ± 0.0006	369.5 ± 14.1	$2-400$	-1.14 ± 0.03	-2.09 ± 0.4	318.0 ± 34.0	$53.56^{+0.12}_{-0.16}$	1
030329	0.16867 ± 0.00001	1970 ± 70	$20-2000$	-1.26 ± 0.02	-2.28 ± 0.06	121.5 ± 2.3	$52.24^{+0.01}_{-0.02}$	1, 2
030429	2.658 ± 0.005	8.5 ± 1.4	$2-400$	-1.12 ± 0.25	-2.3 ± 0.46	128.0 ± 35.0	$52.25^{+0.10}_{-0.13}$	1
040924	0.858 ± 0.001	27.3 ± 1.2	$20-500$	-1.17 ± 0.23	-2.3 ± 0.46	125.0 ± 11.0	$51.95^{+0.09}_{-0.11}$	1
041006	0.716 ± 0.001	70 ± 7	$30-400$	-1.37 ± 0.27	-2.3 ± 0.46	109.0 ± 22.0	$52.31^{+0.11}_{-0.14}$	1
050315	1.9500 ± 0.0008	43^{+2}_{-6}	$15-350$	$\cdots$	-2.06 ± 0.09	$126.9^{+32.5}_{-123.9}$	$52.76^{+0.32}_{-0.01}$	7
050318	1.4436 ± 0.0009	$14.1^{+1.3}_{-1.0}$	$15-350$	-1.2 ± 0.4	$\cdots$	122.2 ± 24.4	$52.08^{+0.07}_{-0.08}$	7
050319	3.2425	$19^{+0.2}_{-0.3}$	$15-350$	-2 ± 0.2	$\cdots$	$190.8^{+114.5}_{-182.3}$	$52.66^{+0.38}_{-0.06}$	7
050401	2.8992 ± 0.0004	193 ± 4	$20-2000$	-0.99 ± 0.19	-2.51 ± 0.23	458.2 ± 70.2	53.63 ± 0.03	8, 9
050408	1.2357 ± 0.0002	50.54	$25-100$	-1.979	$\cdots$	44.6	$53.03^{+0.17}_{-0.27}$	10
050416A	0.6528 ± 0.0002	3.5 ± 0.3	$15-350$	-1^{-1}_{+2}	$\cdots$	24.8 ± 8.3	$51.00^{+0.18}_{-0.10}$	7
050502A	3.793	14	$20-200$	-1.1 ± 0.4	-2.2 ± 0.4	$445.7^{+263.6}_{-167.8}$	$52.96^{+0.12}_{-0.17}$	4, 11
050525A	0.606	213^{+12}_{-11}	$15-10000$	$-1.02^{+0.10}_{-0.11}$	$-3.12^{+0.50}_{-0.25}$	130.1 ± 4.8	52.38 ± 0.03	12
050603	2.821	341 ± 6	$20-3000$	-0.79 ± 0.06	-2.15 ± 0.09	1334 ± 107.0	53.79 ± 0.01	13
050730	3.96855 ± 0.00005	26 ± 2	$15-350$	-1.4 ± 0.1	$\cdots$	$973.8^{+2797}_{-432.3}$	$52.95^{+0.28}_{-0.18}$	7
050801	1.56 ± 0.1	$3.3^{+0.4}_{-0.6}$	$15-350$	-1.9 ± 0.2	$\cdots$	$104.1^{+111.4}_{-100.0}$	$51.51^{+0.34}_{-0.12}$	7
050802	1.7102	27^{+2}_{-9}	$15-350$	-1.6 ± 0.1	$\cdots$	$268.3^{+623.3}_{-75.9}$	$52.26^{+0.28}_{-0.08}$	7
050820A	2.6147	527^{+158}_{-69}	$20-1000$	-1.12 ± 0.1	$\cdots$	$1327^{+343.4}_{-224.1}$	$53.99^{+0.11}_{-0.06}$	14
050824	0.8281 ± 0.004	3.6 ± 0.6	$15-350$	$\cdots$	-2.9 ± 0.45	$23.8^{+3.7}_{-21.9}$	$51.18^{+0.83}_{-0.13}$	7
050904	6.295 ± 0.002	152^{+43}_{-19}	$15-1100$	-1.15 ± 0.12	$\cdots$	$2291^{+1262}_{-649.3}$	$53.97^{+0.08}_{-0.19}$	7, 15
050908	3.3467	$6.2^{+0.7}_{-1.3}$	$15-350$	-1.7 ± 0.2	$\cdots$	$303.4^{+632.8}_{-91.4}$	$52.11^{+0.23}_{-0.11}$	7
050922C	2.1992 ± 0.0005	73 ± 5	$20-2000$	-1.0 ± 0.3	$\cdots$	$585.2^{+853.9}_{-175.9}$	$52.98^{+0.08}_{-0.05}$	16
051109A	2.346	40^{+3}_{-34}	$20-500$	-1.38 ± 0.33	$\cdots$	$466.8^{+388.1}_{-150.6}$	$52.87^{+0.08}_{-0.89}$	9, 17
051111	1.54948 ± 0.00001	$144^{+40.9}_{-23}$	$15-2000$	-1.23 ± 0.07	$\cdots$	$1328^{+696.0}_{-379.9}$	$52.99^{+0.11}_{-0.08}$	18
060124	2.297 ± 0.001	320^{+40}_{-30}	$0.5-2000$	1.48 ± 0.02	$\cdots$	$636.3^{+257.2}_{-128.6}$	$53.62^{+0.05}_{-0.04}$	19
060206	4.04795 ± 0.0002	$10.4^{+1}_{-0.8}$	$15-350$	-1.2 ± 0.3	-2.9 ± 0.45	$419.0^{+176.7}_{-80.8}$	$52.61^{+0.11}_{-0.07}$	7
060210	3.9133	142^{+8}_{-39}	$15-350$	-1.18 ± 0.18	$\cdots$	$1017^{+520.8}_{-568.5}$	$53.79^{+0.06}_{-0.15}$	7, 18
060418	1.49010 ± 0.0001	224^{+77}_{-44}	$15-10000$	-1.52 ± 0.07	$\cdots$	$1554^{+1671}_{-597.6}$	$53.15^{+0.13}_{-0.10}$	12
060502A	1.5026	$58^{+32.9}_{-19.2}$	$15-2000$	-1.29 ± 0.16	$\cdots$	$705.7^{+1119}_{-310.3}$	$52.57^{+0.20}_{-0.18}$	18
060512	0.4428	$2.0^{+0.7}_{-0.3}$	$15-350$	0^{-2}_{+4}	$\cdots$	$33.2^{+15.9}_{-28.9}$	$50.30^{+0.40}_{-0.10}$	7
060526	3.211 ± 0.001	18 ± 3	$15-350$	-1.9 ± 0.3	$\cdots$	$307.4^{+635.9}_{-303.2}$	$52.72^{+0.32}_{-0.03}$	7
060605	3.773 ± 0.001	$6.1^{+1.7}_{-0.9}$	$15-350$	$-0.3^{-0.7}_{+0.9}$	$\cdots$	$677.8^{+1714}_{-238.7}$	$52.40^{+0.35}_{-0.12}$	7
060607A	3.0749	37^{+5}_{-4}	$15-350$	-1.0 ± 0.3	$\cdots$	$428.4^{+889.9}_{-167.4}$	$52.95^{+0.25}_{-0.11}$	7
060707	3.425 ± 0.002	19^{+7}_{-2}	$15-350$	-0.7 ± 0.8	$\cdots$	$283.2^{+110.6}_{-62.0}$	$52.79^{+0.06}_{-0.01}$	7
060714	2.711 ± 0.001	43^{+3}_{-4}	$15-350$	-1.9 ± 0.1	$\cdots$	$196.7^{+348.8}_{-181.8}$	$52.89^{+0.30}_{-0.05}$	7
060729	0.5428	43 ± 3	$15-350$	-1.8 ± 0.1	$\cdots$	$103.2^{+352.7}_{-38.5}$	$51.52^{+0.27}_{-0.09}$	7
060904B	0.7029	$37^{+12.4}_{-14.3}$	$15-2000$	-1.16 ± 0.16	$\cdots$	$563.7^{+897.4}_{-241.8}$	$51.71^{+0.13}_{-0.21}$	18
060906	3.685 ± 0.002	36^{+3}_{-4}	$15-350$	2.0 ± 0.1	$\cdots$	$220.2^{+117.1}_{-210.8}$	$53.11^{+0.28}_{-0.03}$	7
060908	1.8836	$68^{+38.1}_{-24.9}$	$15-2000$	-1.05 ± 0.22	$\cdots$	$470.2^{+421.0}_{-135.5}$	52.82 ± 0.20	18
060927	5.4636	$13.2^{+3.6}_{-1}$	$15-350$	-0.8 ± 0.4	$\cdots$	$472.1^{+148.7}_{-77.6}$	$52.95^{+0.09}_{-0.05}$	7
061007	1.2622	2490^{+170}_{-120}	$20-10000$	-0.7 ± 0.04	-2.61 ± 0.18	$902.1^{+43.0}_{-40.7}$	$54.00^{+0.03}_{-0.02}$	20
061121	1.3145	577^{+30}_{-50}	$20-5000$	$-1.32^{-0.04}_{+0.05}$	$\cdots$	$1402^{+208.3}_{-166.6}$	$53.45^{+0.02}_{-0.04}$	21

TABLE 2 — *Continued*

GRB	Redshift z	Fluence (10^{-7} erg cm^{-2})	Band (keV)	Low-energy index α_B	High-energy index β_B	$E_{\rm p,rest}$ (keV)	log $E_{\rm iso,bol}$ (erg)	References (for Energetics)
061126	1.1588 ± 0.0006	300 ± 40	$15 - 2000$	-1.06 ± 0.07	$\cdots$	$1338^{+474.9}_{-345.4}$	53.06 ± 0.06	22
070110	2.3521	25^{+2}_{-8}	$15 - 350$	-1.5 ± 0.1	$\cdots$	$372.1^{+1036}_{-90.5}$	$52.48^{+0.26}_{-0.08}$	7
070125	1.5477 ± 0.0001	1750^{+130}_{-140}	$20 - 10000$	$-1.14^{-0.09}_{+0.08}$	$-2.11^{-0.10}_{+0.16}$	$1095^{+206.3}_{-155.4}$	$53.98^{+0.04}_{-0.05}$	23
070208	1.165	$5.7^{+1.4}_{-0.9}$	$15 - 350$	0^{-1}_{+2}	$\cdots$	$142.9^{+387.5}_{-71.4}$	$51.45^{+0.25}_{-0.15}$	7
070411	2.9538	42^{+2}_{-3}	$15 - 350$	-1.7 ± 0.1	$\cdots$	$474.5^{+2198}_{-154.2}$	$53.00^{+0.26}_{-0.10}$	7
070419A	0.9705	$5.4^{+1.2}_{-0.6}$	$15 - 350$	0 ± 2	$\cdots$	$53.2^{+31.5}_{-37.4}$	$51.38^{+0.29}_{-0.10}$	7
070612A	0.617	90 ± 18.6	$15 - 2000$	-0.70 ± 0.18	$\cdots$	$346.0^{+67.9}_{-51.7}$	$51.96^{+0.08}_{-0.10}$	18
070802	2.4541	$3.96^{+0.70}_{-1.66}$	$15 - 350$	$-1.82^{-0.29}_{+0.27}$	$\cdots$	$190.0^{+922.5}_{-124.4}$	$51.70^{+0.31}_{-0.09}$	24
070810A	2.17	$5.7^{+1.3}_{-0.4}$	$15 - 350$	$-0.83^{-0.75}_{+0.70}$	$\cdots$	$132.2^{+26.8}_{-22.7}$	$51.96^{+0.05}_{-0.16}$	24
071003	1.60435	$403^{+15.2}_{-93.3}$	$15 - 2000$	-1.22 ± 0.05	$\cdots$	$3183^{+1133}_{-768.3}$	$53.51^{+0.03}_{-0.12}$	18
071010A	0.985 ± 0.005	$4.7^{+1.1}_{-1.8}$	$15 - 350$	$\cdots$	$-2.11^{-0.44}_{+0.39}$	$73.0^{+97.7}_{-69.9}$	$51.12^{+0.46}_{-0.08}$	24
071020	2.1462	$77.1^{+3.9}_{-47.6}$	$20 - 2000$	$-0.65^{-0.27}_{+0.32}$	$\cdots$	$1013^{+251.6}_{-166.7}$	$52.95^{+0.02}_{-0.42}$	25
071025	4.8 ± 0.4	110 ± 3	$15 - 350$	1.67 ± 0.06	$\cdots$	$989.2^{+2996}_{-366.2}$	$53.81^{+0.19}_{-0.06}$	24
071031	2.6918	$11.0^{+1.63}_{-1.43}$	$15 - 350$	$\cdots$	$-2.27^{-0.32}_{+0.29}$	$45.23^{+22.85}_{-41.54}$	$52.59^{+0.31}_{-0.08}$	24
071112C	0.8227	37.5 ± 5	$15 - 150$	-1.09 ± 0.07	$\cdots$	$768.6^{+251.7}_{-189.6}$	$52.29^{+0.11}_{-0.12}$	26, 27
071122	1.14	$10.4^{+2.5}_{-3.6}$	$15 - 350$	$-1.57^{-0.36}_{+0.37}$	$\cdots$	$236.5^{+1123.7}_{-143.0}$	$51.54^{+0.39}_{-0.17}$	24
080129	4.349 ± 0.002	$19.2^{+3.1}_{-2.7}$	$15 - 350$	$-1.22^{-0.24}_{+0.25}$	$\cdots$	$1338^{+2635}_{-822.4}$	$52.89^{+0.29}_{-0.26}$	24
080210	2.6419	$27.4^{+1.86}_{-1.76}$	$15 - 350$	-1.75 ± 0.12	$\cdots$	$329.4^{+1719}_{-132.8}$	$52.71^{+0.28}_{-0.08}$	24
080310	2.4274	$26.9^{+2.0}_{-4.2}$	$15 - 350$	$\cdots$	$-2.35^{-0.18}_{+0.16}$	$75.4^{+72.0}_{-30.8}$	$52.77^{+0.45}_{-0.08}$	24
080319B	0.9371	6130 ± 130	$20 - 7000$	$-0.855^{-0.014}_{+0.013}$	$-3.59^{-0.32}_{+0.62}$	1308 ± 42.6	54.16 ± 0.01	28
080319C	1.9492	201 ± 10.4	$15 - 2000$	-1.34 ± 0.07	$\cdots$	3979^{+1787}_{-1133}	53.37 ± 0.03	18
080330	1.5115	$4.41^{+0.92}_{-0.77}$	$15 - 350$	$\cdots$	$-2.38^{-0.45}_{+0.41}$	$50.68^{+16.52}_{-48.17}$	$51.62^{+0.51}_{-0.07}$	24
080413A	2.4330	$85^{+14.3}_{-41.9}$	$15 - 2000$	-1.29 ± 0.12	$\cdots$	$614.5^{+350.2}_{-154.5}$	$53.14^{+0.07}_{-0.30}$	18
080710	0.8454	$32.4^{+5.50}_{-4.82}$	$15 - 350$	-1.26 ± 0.24	$\cdots$	$554.3^{+1018}_{-375.5}$	$51.90^{+0.31}_{-0.32}$	24
080721	2.591 ± 0.001	838^{+62}_{-60}	$20 - 5000$	$-0.933^{-0.106}_{+0.084}$	$-2.43^{-0.24}_{+0.42}$	1742^{+241}_{-212}	$54.09^{+0.03}_{-0.04}$	29
080810	3.35104	170^{+20}_{-10}	$15 - 1000$	-1.2 ± 0.1	2.5	2523^{+3698}_{-1131}	$53.73^{+0.05}_{-0.10}$	30
080913	6.733	$8.5^{+6.0}_{-2.2}$	$15 - 1000$	$-0.89^{-0.46}_{+0.65}$	$\cdots$	$1008^{+1731}_{-369.4}$	$52.81^{+0.23}_{-0.19}$	31
080916C	4.35 ± 0.15	2400 ± 100	$10 - 10000000$	-0.91 ± 0.02	-2.08 ± 0.06	2268 ± 128	$54.49^{+0.08}_{-0.10}$	32
080928	1.6919	$39.6^{+2.99}_{-2.81}$	$15 - 350$	$-1.73^{-0.13}_{+0.12}$	$\cdots$	$199.4^{+654.1}_{-69.7}$	$52.45^{+0.27}_{-0.09}$	24
081008	1.9685	53.4 ± 8.89	$15 - 350$	$-1.30^{-0.33}_{+0.27}$	$\cdots$	$261.7^{+489.9}_{-53.8}$	$52.84^{+0.10}_{-0.11}$	33
081203A	2.05 ± 0.01	305^{+140}_{-89}	$20 - 3000$	$-1.33^{-0.27}_{+0.20}$	$\cdots$	$1763^{+7314}_{-884.5}$	$53.54^{+0.18}_{-0.15}$	34
090102	1.547	309^{+29}_{-25}	$20 - 2000$	$-0.86^{-0.13}_{+0.14}$	$\cdots$	$1149^{+185.9}_{-147.7}$	53.30 ± 0.04	35
090313	3.3736 ± 0.0004	$21.5^{+3.94}_{-3.46}$	$15 - 350$	$-1.89^{-0.32}_{+0.29}$	$\cdots$	$240.1^{+885.4}_{-223.5}$	$52.66^{+0.41}_{-0.05}$	24
090323	3.568 ± 0.004	1120 ± 20	$8 - 1000$	-1.05 ± 0.02	$-2.7^{-0.2}_{+0.4}$	$2701^{+164.5}_{-150.8}$	54.61 ± 0.01	36
090328	0.7354 ± 0.0003	509 ± 4	$8 - 1000$	-1.07 ± 0.02	$\cdots$	$1291^{+86.8}_{-81.5}$	52.99 ± 0.01	37
090423	$8.23^{+0.06}_{-0.07}$	11 ± 3	$8 - 1000$	-0.77 ± 0.35	$\cdots$	759.3 ± 138.9	$53.04^{+0.11}_{-0.14}$	37
090424	0.544	520 ± 10	$8 - 1000$	-0.90 ± 0.02	-2.9 ± 0.1	273.3 ± 4.6	52.65 ± 0.01	38
090902B	1.8829 ± 0.0004	3740 ± 30	$50 - 10000$	-0.61 ± 0.01	$-3.8^{-0.2}_{+0.3}$	2049 ± 22.6	54.49 ± 0.01	39
090926A	2.1062 ± 0.0004	1800^{+80}_{-70}	$20 - 10000$	-0.76 ± 0.03	$-2.59^{-0.13}_{+0.10}$	997.1 ± 37.3	54.27 ± 0.02	40

NOTE. — References for z: GRB 970508: Bloom et al. (1998), GRB 990123: Kulkarni et al. (1999), GRB 990510: Vreeswijk et al. (2001), GRB 991208: Castro-Tirado et al. (2001), GRB 991216: Vreeswijk et al. (2006), GRB 000131: Andersen et al. (2000), GRB 000301C: Jensen et al. (2001), GRB 000911: Price et al. (2002a), GRB 000926: Castro et al. (2003), GRB 010222: Mirabal et al. (2002), GRB 011121: Greiner et al. (2003), GRB 011211: Vreeswijk et al. (2006), GRB 020405: Price et al. (2003), GRB 020813: Price et al. (2002b), GRB 021004: Castro-Tirado et al. (2010), GRB 030226: Shin et al. (2007), GRB 030323: Vreeswijk et al. (2004), GRB 030329: Maiorano et al. (2006), GRB 030429: Thöne et al. (2007b), GRB 030429: Jakobsson et al. (2004b), GRB 040924: Wiersema et al. (2008), GRB 041006: Soderberg et al. (2006a), GRB 050315: Berger et al. (2005b), GRB 050318: Berger et al. (2005b), GRB 050319, GRB 050802, GRB 050820A, GRB 050908, 060210, GRB 060502A, GRB 060607A, GRB 060729, GRB 060904B, GRB 060908, GRB 060927, GRB 061007, GRB 061121, GRB 070110, GRB 070411, GRB 070419A, GRB 071020, XRF 071031, GRB 071112C, GRB 080210, GRB 080310, GRB 080413A, GRB 080710, GRB 080928: all from Fynbo et al. (2009), GRB 050401: Watson et al. (2006), GRB 050408: Prochaska et al. (2005a), XRF 050416A: Soderberg et al. (2007), GRB 050502A: Prochaska et al. (2005b), GRB 050525A: Della Valle et al. (2006a), GRB 050603: Berger & Becker (2005), GRB 050730: Chen et al. (2005), GRB 050801: De Pasquale et al. (2007), XRF 050824: Sollerman et al. (2007), GRB 050904: Kawai et al. (2006), GRB 050922C: Piranomonte et al. (2008), GRB 051109A: Quimby et al. (2005), GRB 051111: Penprase et al. (2006), GRB 060206: Fynbo et al. (2006a), GRB 060418: Prochaska et al. (2006), XRF 060512: Bloom et al. (2006), GRB 060526, GRB 060707, GRB 060714 GRB 060906: all four from Jakobsson et al. (2006e), GRB 060605: Ferrero et al. (2009), GRB 070125: Cenko et al. (2008), GRB 070208: Cucchiara et al. (2007a), GRB 070612A: Cenko et al. (2007b), GRB 070810A: Thöne et al. (2007a), GRB 071003: Perley et al. (2008d), GRB 071010A: Covino et al. (2008c), GRB 071122: Cucchiara et al. (2007b), GRB 080129: Greiner et al. (2009a), GRB 080319B: D'Elia et al. (2009a), XRF 080330: D'Elia et al. (2009b), GRB 080721: Starling et al. (2009), GRB 080810: Page et al. (2009), GRB 080913: Patel et al. (2010), GRB 080916C: Greiner et al. (2009c), GRB 081008: D'Avanzo & Covino (2008), GRB 081203A: Kuin et al. (2009), GRB 090102: de Ugarte Postigo et al. (2009a), GRB 090313: de Ugarte Postigo et al. (2010), GRB 090323: Cenko et al. (2010b), GRB 090328: McBreen et al. (2010), GRB 090423: Tanvir et al. (2009), GRB 090424: Chornock et al. (2009), GRB 090902B: Cenko et al. (2010b), GRB 090926A: Rau et al. (2010), References for energetics (Fluence, Band, E_p, Band function parameters): (1) Friedman & Bloom (2005), (2) Ulanov et al. (2005), (3) Kippen (1999), (4) Schaefer (2007), (5) Piro et al. (2005), (6) Atteia et al. (2005), (7) Butler et al. (2007), (8) Golenetskii et al. (2005a), (9) Sugita et al. (2008), (10) http://space.mit.edu/HETE/Bursts/GRB050408/, (11) Götz & Mereghetti (2005), (12) Bellm et al. (2008), (13) Golenetskii et al. (2005b), (14) Cenko et al. (2006b), (15) Sugita et al. (2009), (16) Golenetskii et al. (2005c), (17) Golenetskii et al. (2005d), (18) Krimm et al. (2009), (19) Romano et al. (2006), (20) Golenetskii et al. (2006a), (21) Perley et al. (2008a), (23) Bellm et al. (2008), (24) this work, (25) Golenetskii et al. (2007b), (26) Stratta et al. (2007b), (27) $E_{\rm p,rest}$ computed according to equ. (3) of Liang et al. (2007b) (28) Racusin et al. (2008), (29) Golenetskii et al. (2008b), (30) Sakamoto et al. (2008), (31) Pal'shin et al. (2008), (32) Abdo et al. (2009a), (33) Palmer et al. (2008), (34) Golenetskii et al. (2008c), (35) Golenetskii et al. (2009a), (36) Bissaldi (2010), (37) von Kienlin (2009), (38) Connaughton (2009), (39) Abdo et al. (2009b), (40) Golenetskii et al. (2009b).

TABLE 3
RESULTS OF THE SED FITTING FOR THE GOLDEN SAMPLE – PART I

GRB	Filters	No Extinction		MW Dust		
		χ^2_{dof}	β_0	χ^2_{dof}	β	A_V
990510	$BVR_ci^GI_cJHK_S$	1.83	0.61 ± 0.04	1.95	0.69 ± 0.09	-0.06 ± 0.06
011211	BVR_cI_cJK	1.57	0.72 ± 0.04	1.3	0.84 ± 0.09	-0.09 ± 0.06
030323	R_cI_cJH	0.94	0.85 ± 0.03	0	1.22 ± 0.27	-0.35 ± 0.25
050319	VR_CI_CK	0.38	1.00 ± 0.06	0.71	0.94 ± 0.33	0.06 ± 0.31
050408	$UBVR_cI_cZJHK$	3.12	1.61 ± 0.14	3.27	1.17 ± 0.60	0.33 ± 0.44
050416A	$U_3U_2UBVR_CI_cz'K_S$	0.39	1.15 ± 0.17	0.91	1.20 ± 0.45	0.11 ± 0.38
050502A	$R_ci'JHK_s$	0.76	0.95 ± 0.06	0.39	0.46 ± 0.22	0.40 ± 0.18
050525A	$U_1UBVR_cJHKS_{3.6}S_{4.5}S_{8.0}S_{24.0}$	12.7	1.02 ± 0.03	13.7	1.12 ± 0.07	-0.11 ± 0.06
050730	$i'I_cJK$	0.71	0.82 ± 0.04	0.89	0.88 ± 0.09	-0.08 ± 0.10
050801	BVR_CI_CJK	3.53	1.28 ± 0.10	4.43	1.40 ± 0.17	-0.07 ± 0.07
050802	$UBVR_CI_C$	0.9	0.78 ± 0.05	1.01	0.76 ± 0.06	0.05 ± 0.07
050820A	$g'VR_cI_cz'JHK$	1.09	0.96 ± 0.03	1.12	0.98 ± 0.04	0.02 ± 0.02
050824	$U_1UBVR_CI_CK$	0.79	0.65 ± 0.07	0.97	0.70 ± 0.29	-0.05 ± 0.19
050904	$YJHK$	0.05	1.00 ± 0.09	0.01	0.99 ± 0.10	0.02 ± 0.08
050922C	BVR_cI_c	0.02	0.56 ± 0.01	0.04	0.56 ± 0.01	0.00 ± 0.01
060124	BVR_cI_c	15.13	0.54 ± 0.11	0.9	0.57 ± 0.03	0.17 ± 0.03
060206	$R_cI_ci'z'JHK_s$	0.25	0.77 ± 0.01	0.24	0.81 ± 0.04	-0.03 ± 0.03
060418	$UBVr'R_ci'I_cz'JHK$	2.11	0.98 ± 0.02	2.06	0.88 ± 0.07	0.07 ± 0.05
060526	$r'R_ci'I_cJHK_s$	0.08	0.65 ± 0.06	0.07	0.70 ± 0.18	-0.05 ± 0.16
060607A	$g'Vr'R_ci'I_cJHK$	0.88	0.98 ± 0.08	0.98	0.85 ± 0.26	0.10 ± 0.18
060904B	$U_2U_1UBVR_cI_cJK$	1.14	1.21 ± 0.03	1.04	1.31 ± 0.13	-0.11 ± 0.13
060908	$BVr'R_Ci'I_Cz'JHK$	0.17	0.30 ± 0.06	0.18	0.33 ± 0.15	-0.02 ± 0.08
061007	$UBVR_Ci'JHK$	9.08	1.93 ± 0.03	10.4	1.87 ± 0.05	0.05 ± 0.03
061126	$UBVR_cI_cJHK_S$	3.57	0.97 ± 0.03	4.16	0.96 ± 0.11	0.01 ± 0.08
070125	$UBg'Vr'R_ci'I_cJHK$	1.88	0.86 ± 0.02	2.12	0.85 ± 0.03	0.00 ± 0.02
070419A	$Bg^GVr'R_Ci'I_Cz'JHK$	1.52	1.01 ± 0.10	1.5	0.60 ± 0.36	0.35 ± 0.29
070802	$Bg_GVr_GR_ci_GI_cz_Gz^GJ_GH_GK_G$	6.88	2.98 ± 0.04	4.78	2.24 ± 0.16	0.52 ± 0.11
071003	$g'VR_ci'I_cz'K_S$	1.09	1.09 ± 0.09	1.14	1.32 ± 0.27	-0.18 ± 0.20
071010A	$UBVR_cI_cJHK$	20.4	1.51 ± 0.07	15.08	0.88 ± 0.40	0.52 ± 0.32
071031	$Vr_GR_ci_GI_cz_GJJ_GH_GKK_G$	0.37	0.66 ± 0.06	0.25	0.76 ± 0.11	-0.08 ± 0.07
071112C	$U_1UBVR_CI_CJHK_S$	1.04	0.94 ± 0.08	0.75	0.05 ± 0.56	0.79 ± 0.49
080129	$i_Gz_GJ_GH_GK_G$	0.81	0.69 ± 0.05	1.21	0.68 ± 0.09	0.01 ± 0.07
080210	$Bg_Gg'Vr_GR_Ci_Gz_GJ_GH_GK_G$	6.25	1.90 ± 0.08	5.91	1.53 ± 0.15	0.35 ± 0.12
080310	$Bg^GVr'R_ci'I_cz'JHK$	2.67	0.87 ± 0.03	2.48	1.00 ± 0.08	-0.10 ± 0.05
080319B	$UBVr'R_ci'I_cz'JHK_S$	0.73	0.21 ± 0.03	0.72	0.14 ± 0.08	0.05 ± 0.06
080319C	$UBVR_ci'z'$	7.4	3.10 ± 0.08	2.68	3.64 ± 0.16	-0.29 ± 0.06
080330	$UBg'Vr'R_ci'I_cz'JJ_GHH_GKK_G$	0.46	0.75 ± 0.04	0.43	0.53 ± 0.16	0.16 ± 0.11
080413A	VR_cI_cJHK	0.28	0.81 ± 0.08	0.21	0.91 ± 0.17	-0.08 ± 0.12
080710	$U_2U_1Bg_GVr_GR_Ci_GI_Cz_GJJ_GH_GK_G$	0.77	0.99 ± 0.03	0.83	1.11 ± 0.14	-0.10 ± 0.12
080913	$JJ_GH_GK_G$	0.41	1.16 ± 0.17	0.05	1.13 ± 0.17	0.08 ± 0.09
080916C	$i_Gz_GJJ_GHH_GK_SK_G$	0.45	0.38 ± 0.10	0.52	0.36 ± 0.12	0.03 ± 0.10
080928	$UBgg_GVr_GR_Ci_Gz_GJ_GH_GK_G$	0.49	1.30 ± 0.07	0.19	1.08 ± 0.14	0.14 ± 0.08
081008	$Bg_GVr_GR_Ci_Gz_GJJ_GH_GKK_G$	1.30	0.73 ± 0.06	0.98	1.01 ± 0.14	-0.22 ± 0.10
090102	$UBg_GVR_Ci_Gz_GJ_GH_GHK_G$	0.44	0.97 ± 0.05	0.49	1.04 ± 0.41	-0.06 ± 0.34
090313	$r'R_ci'I_cz'JHK_S$	1.69	1.65 ± 0.08	0.87	2.05 ± 0.18	-0.33 ± 0.13
090323	$i'i_Gz_GJ_GH_GK_G$	2.88	1.14 ± 0.02	1.60	1.28 ± 0.06	-0.13 ± 0.05
090328	$Ug_Gr_Gi_Gi'z_GJ_GH_GK_G$	1.25	1.41 ± 0.04	1.26	1.26 ± 0.14	0.12 ± 0.11
090424	$U_1UBg_GVr_Gr'R_Ci_GI_Cz_GJJ_GH_GKK_G$	2.65	1.58 ± 0.03	1.92	1.10 ± 0.15	0.42 ± 0.13
090902B	$Ug_GVr_Gr'i_Gi'z_GJJ_GH_GK_GK$	2.18	0.87 ± 0.04	2.16	0.96 ± 0.07	-0.06 ± 0.04
090926A	$Bg_Gg'Vr_Gr'R_Ci_GI_Cz_GJJ_GH_GK_G$	2.64	1.07 ± 0.05	2.15	1.28 ± 0.09	-0.18 ± 0.06

NOTE. — Filters that are not used for the fit (e.g, due to Lyman α dampening) are not included. The degrees of freedom of the fit are always number of filters minus three for the fits with extinction, and minus two for the fit without extinction. β_0 is the spectral slope without extinction correction. $U_{1,2,3}$ denote the *Swift* UVOT UVW1, UVM2 and UVW2 filters, respectively. $S_{3.6,4.5,8.0,24.0}$ denote *Spitzer Space Telescope* IRAC 3.6μm, 4.5μm, 8.0μm and MIPS 24.0μm filters, respectively. A superscript G denotes a Gunn filter. A subscript G denotes *GROND* dichroic filters. The results on GRB 050904 are taken from Kann et al. (2007a), the results on GRB 060526 are from Thöne et al. (2010).

TABLE 4
RESULTS OF THE SED FITTING FOR THE GOLDEN SAMPLE – PART II

GRB	LMC Dust			SMC Dust		
	χ^2_{dof}	β	$A_{\rm V}$	χ^2_{dof}	β	$A_{\rm V}$
990510	1.81	0.36 ± 0.18	0.16 ± 0.11	0.21	0.17 ± 0.15	0.22 ± 0.07
011211	1.82	0.51 ± 0.24	0.13 ± 0.14	0.45	0.41 ± 0.15	0.14 ± 0.06
030323	0.03	0.15 ± 0.51	0.35 ± 0.26	0.03	0.46 ± 0.28	0.13 ± 0.09
050319	0.17	0.64 ± 0.52	0.12 ± 0.17	0.31	0.74 ± 0.42	0.05 ± 0.09
050408	1.1	0.01 ± 0.47	1.06 ± 0.31	0.59	0.28 ± 0.27	0.74 ± 0.15
050416A	0.56	0.84 ± 0.38	0.33 ± 0.24	0.46	0.92 ± 0.30	0.21 ± 0.14
050502A	0.35	0.43 ± 0.22	0.24 ± 0.10	0.16	0.76 ± 0.16	0.05 ± 0.05
050525A	11.27	0.53 ± 0.10	0.42 ± 0.08	8.42	0.52 ± 0.08	0.36 ± 0.05
050730	0.5	0.45 ± 0.28	0.21 ± 0.16	0.03	0.52 ± 0.05	0.10 ± 0.02
050801	4.7	1.29 ± 0.25	-0.01 ± 0.13	3.69	0.69 ± 0.34	0.30 ± 0.18
050802	0.06	0.36 ± 0.26	0.21 ± 0.13	0.74	0.39 ± 0.35	0.10 ± 0.10
050820A	0.67	0.91 ± 0.03	0.04 ± 0.02	0.06	0.72 ± 0.03	0.07 ± 0.01
050824	0.76	0.44 ± 0.24	0.17 ± 0.19	0.59	0.45 ± 0.18	0.14 ± 0.13
050904	0.03	0.92 ± 0.35	0.05 ± 0.20	0.03	1.31 ± 1.20	-0.10 ± 0.40
050922C	0.03	0.53 ± 0.05	0.02 ± 0.02	0.02	0.51 ± 0.05	0.01 ± 0.01
060124	13.48	0.13 ± 0.38	0.19 ± 0.17	29	0.30 ± 1.13	0.05 ± 0.26
060206	0.31	0.75 ± 0.09	0.01 ± 0.05	0.27	0.73 ± 0.05	0.01 ± 0.02
060418	1.54	0.69 ± 0.11	0.20 ± 0.08	1.74	0.78 ± 0.09	0.12 ± 0.05
060526	0.04	0.35 ± 0.62	0.16 ± 0.33	0.05	0.51 ± 0.32	0.05 ± 0.11
060607A	0.85	0.65 ± 0.30	0.15 ± 0.13	0.87	0.72 ± 0.27	0.08 ± 0.08
060904B	1.08	1.13 ± 0.12	0.07 ± 0.12	0.93	1.11 ± 0.10	0.08 ± 0.08
060908	0.19	0.29 ± 0.28	0.01 ± 0.15	0.18	0.24 ± 0.20	0.03 ± 0.10
061007	6.19	1.07 ± 0.19	0.48 ± 0.10	9.5	1.62 ± 0.14	0.13 ± 0.05
061126	3.52	0.84 ± 0.12	0.09 ± 0.09	2.77	0.82 ± 0.09	0.10 ± 0.06
070125	1.77	0.73 ± 0.08	0.07 ± 0.04	0.96	0.59 ± 0.10	0.11 ± 0.04
070419A	1.5	0.46 ± 0.47	0.46 ± 0.39	1.54	0.48 ± 0.48	0.42 ± 0.37
070802	2.84	1.07 ± 0.31	1.18 ± 0.19	6.44	2.31 ± 0.21	0.34 ± 0.11
071003	0.99	0.45 ± 0.52	0.43 ± 0.35	0.1	0.35 ± 0.11	0.40 ± 0.06
071010A	2.78	0.37 ± 0.21	0.90 ± 0.16	1.61	0.61 ± 0.12	0.64 ± 0.09
071031	0.36	0.89 ± 0.37	-0.14 ± 0.22	0.27	0.34 ± 0.30	0.14 ± 0.13
071112C	0.92	0.41 ± 0.42	0.44 ± 0.34	1	0.63 ± 0.29	0.23 ± 0.21
080129	1.22	0.72 ± 0.35	-0.02 ± 0.18	1.18	0.76 ± 0.26	-0.03 ± 0.09
080210	4.36	0.44 ± 0.32	0.71 ± 0.15	6.16	1.19 ± 0.29	0.21 ± 0.08
080310	1.95	0.34 ± 0.19	0.30 ± 0.10	0.92	0.42 ± 0.12	0.19 ± 0.05
080319B	0.72	0.11 ± 0.11	0.07 ± 0.08	0.76	0.13 ± 0.10	0.05 ± 0.07
080319C	8.87	4.20 ± 0.68	-0.43 ± 0.25	0.8	0.98 ± 0.42	0.59 ± 0.12
080330	0.33	0.27 ± 0.20	0.32 ± 0.13	0.35	0.42 ± 0.15	0.19 ± 0.08
080413A	0.37	0.87 ± 0.74	-0.04 ± 0.46	0.17	0.52 ± 0.37	0.13 ± 0.17
080710	0.47	0.75 ± 0.12	0.17 ± 0.08	0.29	0.80 ± 0.09	0.11 ± 0.04
080913	0.04	0.79 ± 0.45	0.21 ± 0.24	0.05	3.02 ± 2.17	-0.58 ± 0.67
080916C	0.45	0.08 ± 0.47	0.16 ± 0.24	0.52	0.23 ± 0.51	0.05 ± 0.16
080928	0.31	0.90 ± 0.29	0.23 ± 0.17	0.55	1.32 ± 0.22	-0.01 ± 0.10
081008	1.41	0.86 ± 0.36	-0.09 ± 0.22	1.19	0.38 ± 0.23	0.17 ± 0.11
090102	0.38	0.63 ± 0.36	0.23 ± 0.24	0.35	0.74 ± 0.22	0.12 ± 0.11
090313	1.98	1.36 ± 0.60	0.16 ± 0.32	0.96	0.74 ± 0.40	0.34 ± 0.15
090323	3.84	1.11 ± 0.32	0.02 ± 0.18	1.35	0.74 ± 0.15	0.16 ± 0.06
090328	1.18	1.20 ± 0.17	0.17 ± 0.14	1.10	1.17 ± 0.17	0.18 ± 0.13
090424	1.49	0.97 ± 0.15	0.50 ± 0.12	1.56	1.12 ± 0.12	0.35 ± 0.09
090902B	2.04	0.58 ± 0.16	0.15 ± 0.08	1.49	0.52 ± 0.12	0.13 ± 0.04
090926A	2.86	1.07 ± 0.27	0.00 ± 0.15	2.43	0.72 ± 0.17	0.13 ± 0.06

NOTE. — Filters that are not used for the fit (e.g, due to Lyman α dampening) are not included. The degrees of freedom of the fit are always number of filters minus three for the fits with extinction, and minus two for the fit without extinction. β_0 is the spectral slope without extinction correction. $U_{1,2,3}$ denote the *Swift* UVOT UVW1, UVM2 and UVW2 filters, respectively. $S_{3.6,4.5,8.0,24.0}$ denote *Spitzer Space Telescope* IRAC 3.6μm, 4.5μm, 8.0μm and MIPS 24.0μm filters, respectively. A superscript G denotes a Gunn filter. A subscript G denotes *GROND* dichroic filters. The results on GRB 050904 are taken from Kann et al. (2007a), the results on GRB 060526 are from Thöne et al. (2010).

TABLE 5
CORRECTED APPARENT AND ABSOLUTE MAGNITUDES OF TYPE II
AFTERGLOWS

GRB[a]	dRc[b]	R_C (at 1 day[c])	M_B (at 1 day[c])	R_C (at 4 days[c])	M_B (at 4 days[c])	Type[d]
990510	-1.60	17.95 ± 0.15	-24.73 ± 0.16	20.83 ± 0.16	-21.85 ± 0.16	B
011211	-2.18	$19.22^{+0.14}_{-0.16}$	$-23.53^{+0.15}_{-0.16}$	21.92 ± 0.32	-20.83 ± 0.32	B
030323	-3.38	$17.80^{+0.19}_{-0.20}$	$-24.96^{+0.20}_{-0.22}$	20.80 ± 0.24	-21.96 ± 0.25	B
050319	-3.20	$18.09^{+0.08}_{-0.12}$	$-24.77^{+0.14}_{-0.16}$	$20.41^{+0.18}_{-0.20}$	$-22.43^{+0.21}_{-0.23}$	B
050408	-2.00	$20.73^{+0.27}_{-0.28}$	$-21.99^{+0.28}_{-0.29}$	$22.40^{+0.29}_{-0.30}$	$-20.32^{+0.30}_{-0.31}$	A
050416A	$+0.83$	24.35 ± 0.48	-18.54 ± 0.49	$\cdots$	$\cdots$	A
050502A	-3.56	$22.30^{+0.31}_{-0.32}$	$-20.55^{+0.31}_{-0.32}$	$\cdots$	$\cdots$	B
050525A	$+0.73$	20.40 ± 0.36	-22.39 ± 0.37	23.15 ± 0.40	-19.64 ± 0.41	A
050730	-3.75	$18.83^{+0.10}_{-0.11}$	$-23.95^{+0.10}_{-0.11}$	$\cdots$	$\cdots$	B
050801	-1.82	$21.05^{+0.36}_{-0.35}$	$-21.38^{+0.38}_{-0.36}$	$\cdots$	$\cdots$	B
050802	-1.77	$20.80^{+0.29}_{-0.28}$	$-21.94^{+0.30}_{-0.29}$	$\cdots$	$\cdots$	B
050820A	-2.64	17.71 ± 0.05	-25.13 ± 0.05	19.21 ± 0.05	-23.63 ± 0.05	B
050824	$+0.19$	21.39 ± 0.13	-21.37 ± 0.13	22.60 ± 0.13	-20.16 ± 0.13	A
050904	-5.05	18.13 ± 0.15	-24.78 ± 0.15	21.50 ± 0.20	-21.41 ± 0.20	B
050922C	-1.91	19.80 ± 0.06	-22.98 ± 0.06	22.24 ± 0.30	-20.54 ± 0.30	B
060124	-2.55	17.67 ± 0.15	-25.13 ± 0.15	19.55 ± 0.20	-23.25 ± 0.20	B
060206	-3.54	$17.78^{+0.10}_{-0.11}$	$-25.06^{+0.10}_{-0.11}$	$20.45^{+0.19}_{-0.20}$	$-22.39^{+0.19}_{-0.20}$	B
060418	-1.45	19.91 ± 0.21	$-22.63^{+0.21}_{-0.22}$	21.80 ± 0.20	$-21.03^{+0.20}_{-0.19}$	B
060526	-3.00	$18.30^{+0.19}_{-0.11}$	$-24.48^{+0.21}_{-0.14}$	$21.80^{+0.22}_{-0.16}$	$-20.98^{+0.24}_{-0.18}$	B
060607A	-3.14	$\cdots$	$\cdots$	$\cdots$	$\cdots$	B
060904B	$+0.84$	22.00 ± 0.20	-20.95 ± 0.19	23.40 ± 0.40	-19.55 ± 0.40	A
060908	-1.44	22.50 ± 0.50	-20.62 ± 0.50	$\cdots$	$\cdots$	B
061007	-1.58	$20.91^{+0.34}_{-0.35}$	$-22.02^{+0.34}_{-0.35}$	$\cdots$	$\cdots$	A
061126	-0.57	20.92 ± 0.14	-21.94 ± 0.14	23.43 ± 0.32	-19.43 ± 0.32	A
070125	-1.33	17.52 ± 0.12	-25.28 ± 0.12	20.20 ± 0.21	-22.60 ± 0.21	B
070419A	-0.50	23.10 ± 0.51	-19.70 ± 0.51	24.33 ± 0.51	-18.44 ± 0.50	A
070802	-5.88	19.55 ± 0.30	-23.38 ± 0.31	$\cdots$	$\cdots$	B
071003	-2.07	17.67 ± 0.12	-25.07 ± 0.12	19.97 ± 0.30	-22.77 ± 0.30	B
071010A	-1.10	$18.62^{+0.17}_{-0.16}$	$-24.18^{+0.17}_{-0.16}$	$21.72^{+0.17}_{-0.16}$	$-21.08^{+0.17}_{-0.16}$	A
071031	-2.73	19.20 ± 0.57	-23.53 ± 0.58	$\cdots$	$\cdots$	B
071112C	$+0.11$	$22.60^{+0.42}_{-0.41}$	$-20.21^{+0.43}_{-0.42}$	$\cdots$	$\cdots$	A
080129	-3.59	$16.54^{+0.10}_{-0.11}$	$-26.29^{+0.10}_{-0.11}$	19.60 ± 0.30	-23.23 ± 0.30	B
080210	-4.35	$18.93^{+0.28}_{-0.27}$	$-23.83^{+0.29}_{-0.28}$	$\cdots$	$\cdots$	B
080310	-2.67	18.67 ± 0.13	$-24.08^{+0.13}_{-0.14}$	21.62 ± 0.22	-21.13 ± 0.22	B
080319B	$+0.15$	20.25 ± 0.15	-22.45 ± 0.15	22.35 ± 0.20	-20.35 ± 0.20	A
080319C	-3.44	$\cdots$	$\cdots$	$\cdots$	$\cdots$	B
080330	-1.37	21.40 ± 0.30	-21.38 ± 0.30	$\cdots$	$\cdots$	B
080413A	-2.56	$20.40^{+0.47}_{-0.37}$	$-22.38^{+0.48}_{-0.38}$	$\cdots$	$\cdots$	B
080710	$+0.26$	20.90 ± 0.13	-21.96 ± 0.13	23.30 ± 0.11	-19.56 ± 0.11	A
080913	-5.25	18.73 ± 0.13	-24.22 ± 0.14	20.30 ± 0.40	-22.65 ± 0.40	B
080916C	-3.26	19.09 ± 0.11	-23.65 ± 0.11	21.20 ± 0.50	-21.54 ± 0.50	B
080928	-1.82	20.30 ± 0.19	-22.63 ± 0.19	$\cdots$	$\cdots$	B
081008	-2.03	19.27 ± 0.32	-23.47 ± 0.33	$\cdots$	$\cdots$	B
090102	-1.39	$22.52^{+0.32}_{-0.33}$	$-20.32^{+0.33}_{-0.34}$	$\cdots$	$\cdots$	B
090313	-4.58	17.17 ± 0.35	-25.67 ± 0.37	$\cdots$	$\cdots$	B
090323	-3.92	$17.59^{+0.16}_{-0.15}$	-25.25 ± 0.16	20.25 ± 0.21	-22.59 ± 0.27	B
090328	$+0.58$	19.98 ± 0.33	-22.98 ± 0.33	22.50 ± 0.30	$-20.46^{+0.37}_{-0.38}$	A
090423	-4.64	18.90 ± 0.27	-23.86 ± 0.27	21.58 ± 0.40	-21.18 ± 0.40	B
090424	$+0.95$	21.54 ± 0.23	-21.36 ± 0.23	23.13 ± 0.30	-19.77 ± 0.30	A
090902B	-1.80	19.35 ± 0.17	-23.43 ± 0.17	20.71 ± 0.17	-22.07 ± 0.17	B
090926A	-2.27	16.79 ± 0.14	-26.04 ± 0.15	18.62 ± 0.18	$-24.21^{+0.18}_{-0.19}$	B
050401	-5.06	18.90 ± 0.25	-23.82 ± 0.25	20.25 ± 0.35	-22.47 ± 0.35	B
051109A	-2.08	18.90 ± 0.12	-23.85 ± 0.12	$\cdots$	$\cdots$	B
051111	-1.52	20.10 ± 0.15	-22.70 ± 0.15	$\cdots$	$\cdots$	B
060210	-9.85	$\cdots$	$\cdots$	$\cdots$	$\cdots$	B
060502A	-1.99	20.10 ± 0.30	-22.81 ± 0.30	$\cdots$	$\cdots$	B
060906	-3.37	18.15 ± 0.50	-24.31 ± 0.50	$\cdots$	$\cdots$	B
060927	-5.74	19.70 ± 0.62	-23.16 ± 0.62	$\cdots$	$\cdots$	B
070208	-1.82	20.50 ± 0.40	-22.32 ± 0.40	$\cdots$	$\cdots$	A
071020	-2.80	18.00 ± 0.30	-24.86 ± 0.30	$\cdots$	$\cdots$	B
071025	-7.94	18.45 ± 0.42	-24.44 ± 0.42	$\cdots$	$\cdots$	B
071122	-0.80	20.21 ± 0.30	-22.61 ± 0.30	$\cdots$	$\cdots$	A
080721	-3.68	$18.15^{+0.26}_{-0.25}$	$-24.72^{+0.26}_{-0.25}$	$20.43^{+0.28}_{-0.27}$	$-22.44^{+0.28}_{-0.27}$	B
080810	-3.52	17.50 ± 0.10	-25.28 ± 0.10	20.50 ± 0.50	-22.28 ± 0.50	B
081203A	-2.00	20.00 ± 0.18	-22.80 ± 0.18	22.90 ± 0.33	-19.90 ± 0.33	B
050315	-1.64	20.04 ± 0.15	-22.76 ± 0.15	$\cdots$	$\cdots$	B
050318	-0.91	21.04 ± 0.40	-21.76 ± 0.40	$\cdots$	$\cdots$	B

Kann et al.

TABLE 5 — *Continued*

GRB[a]	dRc[b]	R_C (at 1 day[c])	M_B (at 1 day[c])	R_C (at 4 days[c])	M_B (at 4 days[c])	Type[d]
050603	−2.51	18.44 ± 0.20	$−24.36 \pm 0.20$	⋯	⋯	B
050908	−2.90	19.30 ± 0.50	$−23.50 \pm 0.50$	⋯	⋯	B
060512	+2.03	23.20 ± 0.20	$−19.60 \pm 0.20$	⋯	⋯	A
060605	−3.61	20.90 ± 0.20	$−22.03 \pm 0.20$	⋯	⋯	B
060707	−2.96	19.84 ± 0.30	$−22.96 \pm 0.30$	⋯	⋯	B
060714	−2.42	19.91 ± 0.20	$−22.89 \pm 0.20$	⋯	⋯	B
060729	+1.54	19.34 ± 0.10	$−23.46 \pm 0.10$	21.15 ± 0.10	$−21.65 \pm 0.10$	A
061121	−0.68	20.45 ± 0.07	$−22.35 \pm 0.07$	22.02 ± 0.20	$−20.78 \pm 0.20$	A
070110	−2.08	19.16 ± 0.30	$−23.64 \pm 0.30$	21.15 ± 0.30	$−21.65 \pm 0.30$	B
070411	−2.62	20.18 ± 0.10	$−22.62 \pm 0.10$	22.78 ± 0.50	$−20.02 \pm 0.50$	B
070612A	+1.21	19.80 ± 0.20	$−23.00 \pm 0.20$	23.21 ± 0.50	$−19.59 \pm 0.50$	A
070810A	−1.89	22.26 ± 0.40	$−20.54 \pm 0.40$	⋯	⋯	B

[a] First block: Additional pre-*Swift* Golden Sample; second block: Golden Sample; third block: Silver Sample; fourth block: Bronze Sample.
[b] Magnitude shift, see K06.
[c] After the GRB, assuming $z=1$.
[d] Type A: $z < 1.4$; Type B: $z \geq 1.4$. See K06 for more information on the two types.

TABLE 6
EARLY AFTERGLOW PEAK OR LIMIT MAGNITUDES

Type[a]	GRB	Time[b]	R_C Magnitude[c]
Peak + Fast Decay	990123	0.0004440	7.60 ± 0.02
	080319B[d]	0.0006359	5.18 ± 0.02
	061121[e]	0.0007647	14.19 ± 0.16
	060526[f]	0.0014088	12.18 ± 0.14
	060729[g]	0.0014365	17.20 ± 0.14
	050904[h]	0.0016318	6.48 ± 0.24
	080129[i]	0.0022666	13.51 ± 0.10
	070802[j]	0.0155854	15.34 ± 0.07
Limit + Fast Decay	080413A[k]	0.0001546	9.55 ± 0.08
	071020	0.0002060	10.64 ± 0.05
	061126	0.0002495	11.23 ± 0.01
	060908	0.0004103	12.51 ± 0.04
	090102	0.0005246	11.61 ± 0.20
	090424	0.0013043	13.78 ± 0.10
Peak + Slow Decay	080810[l]	0.0007660	9.04 ± 0.12
	061007	0.0010277	8.04 ± 0.13
	060607A	0.0010565	10.98 ± 0.05
	060714[m]	0.0011901	15.10 ± 0.27
	081008	0.0013476	11.04 ± 0.03
	060418	0.0017900	12.98 ± 0.05
	060605	0.0020854	11.59 ± 0.10
	071025	0.0021328	10.45 ± 0.06
	070810A[n]	0.0023068	14.84 ± 1.00
	071112C[o]	0.0023744	16.79 ± 0.10
	080210[p]	0.0024286	11.44 ± 0.30
	050730[q]	0.0028513	11.80 ± 0.30
	080319C[r]	0.0029180	13.83 ± 0.02
	081203A[s]	0.0031460	9.89 ± 0.01
	070208	0.0032076	17.35 ± 0.20
	050820A[t]	0.0033973	11.97 ± 0.02
	060210[u]	0.0035812	8.00 ± 0.08
	071010A	0.0054710	15.06 ± 0.10
	071031	0.0070640	15.27 ± 0.07
	070419A	0.0070725	17.87 ± 0.15
	060904B[u]	0.0071057	17.19 ± 0.09
	090313	0.0071958	10.95 ± 0.05
	060729[v]	0.0086297	18.00 ± 0.10
	060707[n]	0.0114726	15.90 ± 0.17
	060206[w]	0.0171000	12.57 ± 0.03
	080928[n]	0.0172837	14.56 ± 0.28
	080710	0.0274666	16.45 ± 0.05
	060906[y]	0.0521760	15.35 ± 0.18
	030429	0.0841990	15.83 ± 0.08
	070612A[n]	0.1133787	18.05 ± 0.20
Limit + Slow Decay	060927[y]	0.0000685	9.03 ± 0.20
	050401	0.0002119	11.57 ± 0.29
	050502A[z]	0.0002242	10.44 ± 0.11
	051109A	0.0002554	12.54 ± 0.20
	051111[aa]	0.0003312	11.14 ± 0.03
	071003[ab]	0.0003949	10.34 ± 0.02
	050319[ac]	0.0009090	12.94 ± 0.14
	050525A[ad]	0.0009513	13.20 ± 0.24
	080721	0.0010968	9.10 ± 0.01
	060502A	0.0011465	16.41 ± 0.07
	050922C	0.0011617	12.55 ± 0.03
	060512	0.0015863	17.46 ± 0.17
	080913	0.0016264	15.25 ± 0.03
	050802	0.0024857	14.33 ± 0.25
	050824	0.0080368	18.33 ± 0.35
Plateau + Peak	080310	0.0020151	13.99 ± 0.07
	080330[ae]	0.0032251	15.70 ± 0.13
	060124	0.0036178	13.61 ± 0.11
	070411	0.0059173	14.07 ± 0.10
	070110[af]	0.0300253	16.66 ± 0.26
	021004[ag]	0.0529879	13.67 ± 0.12
	071122	0.0575405	18.82 ± 0.38
	970508[ah]	2.1210965	19.33 ± 0.10
Limit + Plateau	050801	0.0002186	12.87 ± 0.05
	050908	0.0013855	15.42 ± 0.10
	050416A	0.0017643	19.55 ± 0.30
	041006	0.0034965	17.78 ± 0.10
	090423	0.0037297	15.57 ± 0.11
	040924	0.0117394	17.63 ± 0.10

TABLE 6 — *Continued*

Type[a]	GRB	Time[b]	R_C Magnitude[c]

m

[a] See text for more details on the basic types.

[b] Days after the GRB trigger in $z = 1$ frame, either peak time or earliest detection.

[c] In $z = 1$ frame, either peak magnitude or magnitude of earliest detection. Errors do not include error of dRc.

[d] Complex multi-peaked structure during prompt GRB emission, last and brightest peak given. Followed by very steep decay, probably due to curvature effect radiation, then a less steep decay of a probable reverse shock (Racusin et al. 2008; Beskin et al. 2009; Bloom et al. 2009; Woźniak et al. 2009).

[e] Peak associated with the main prompt emission peak (Page et al. 2007).

[f] Associated with a bright prompt emission flare, also seen as a giant X-ray flare (Thöne et al. 2010).

[g] First of three peaks, fast rise and decline.

[h] Comes after plateau phase, possibly associated with the prompt emission, but steep decay typical of a reverse shock later.

[i] Extremely fast optical flare, possibly associated with the prompt emission (Greiner et al. 2009a).

[j] Steep rise and decay, but seems superposed on a forward shock peak (Krühler et al. 2008).

[k] The situation for this afterglow is somewhat unclear. While the first point lies on an extrapolation of the late decay (which has a typical value for a forward shock), the second point is significantly fainter, and it is followed by a small optical flare associated with a prompt emission peak, implying a steep decay between the first and second data point (Yuan et al. 2008b).

[l] The decay after the peak is very slow, forming a plateau before breaking into a typical forward-shock decay.

[m] There is a second peak after the first one reaching almost the same magnitude level.

[n] Data situation is sparse and the given value may not represent the true peak.

[o] The very earliest data point implies a very early steep decay. The peak is followed by a plateau.

[p] The very earliest data points imply a very early steep decay.

[q] Followed by an early optical flare, possibly an energy injection.

[r] The peak is possibly followed by a steep decay, but Kuin et al. (2009) do not publish the data shown in their figure, and the *Swift* observations stop at a critical point.

[s] Preceded and partially superposed by flares linked to the prompt emission (Vestrand et al. 2006).

[t] The peak is preceded by an early plateau phase.

[u] Value given for the second peak. There is a very early complex variability (Rykoff et al. 2009), and the second flare is followed by a plateau probably due to an energy injection.

[v] Second of three peaks, followed by a plateau phase, a decay, and another optical rebrightening (Grupe et al. 2007a).

[w] Late, very bright peak probably due to a strong energy injection (Woźniak et al. 2006).

[x] Late peak after an early plateau and a decay (Cenko et al. 2009b).

[y] Possibly a peak, as decay is slower between the first two points than later. Followed by a strong rebrightening (Ruiz-Velasco et al. 2007).

[z] Possible very early plateau or peak, as there is hardly any decay between the first two points (Yost et al. 2005).

[aa] The early decay is slightly steeper than later, probably due to a tail component associated with the prompt emission Yost et al. (2007a); Butler et al. (2006).

[ab] Followed by a small chromatic bump and a later, strong rebrightening (Perley et al. 2008d).

[ac] Followed by a plateau phase (Quimby et al. 2006).

[ad] Later followed by a plateau phase (Klotz et al. 2005a).

[ae] Long, slow rollover preceded by early complex variability.

[af] Follows an early, sparsely sampled decay, goes over into a long rollover.

[ag] Complex evolution, early plateau, then decay to second plateau, then rise to the peak given here.

[ah] Very faint ($R_C \approx 20.9$) early plateau starting < 0.15 days after the GRB, which goes over into a very strong, late rebrightening.

TABLE 7
Energetics of the Low-Redshift Type II GRB Sample

GRB	Redshift z	Fluence $(10^{-7}\ \mathrm{erg\ cm^{-2}})$	Band (keV)	Low-energy index α	High-energy index β	$E_{\mathrm{p,rest}}$ (keV)	$\log E_{\mathrm{iso,bol}}$ (erg)	References
980425	0.00867 ± 0.00004	38.7 ± 3.9	$20 - 2000$	-1.27 ± 0.25	-2.3 ± 0.46	$119.0^{+24.2}_{-24.2}$	$48.03^{+0.07}_{-0.08}$	1
020903	0.2506 ± 0.0003	$0.98^{+0.67}_{-0.36}$	$2 - 400$	-1 ± 0.3	$-2.6^{-0.4}_{+0.5}$	$3.25^{+1.75}_{-1.00}$	$49.29^{+0.23}_{-0.21}$	2
031203	0.10536 ± 0.00007	20 ± 4	$20 - 200$	-1.63 ± 0.06	$\cdots$	159.2 ± 50.8	$50.06^{+0.08}_{-0.10}$	3, 4
050223	0.584 ± 0.005	$8.8^{+0.9}_{-3}$	$15 - 350$	-1.7 ± 0.2	$\cdots$	$106.1^{+179.0}_{-36.4}$	$50.85^{+0.23}_{-0.07}$	5
050826	0.296 ± 0.001	10^{+2}_{-3}	$15 - 350$	-1.2 ± 0.3	$\cdots$	$440.6^{+1023.8}_{-272.2}$	$50.48^{+0.37}_{-0.48}$	5
051016B	0.9364	$1.4^{+0.2}_{-0.3}$	$15 - 350$	-1 ± 0.3	-2.1 ± 0.3	$71.6^{+36.8}_{-69.7}$	$50.57^{+0.40}_{-0.08}$	5
060202	0.783	38^{+3}_{-4}	$15 - 350$	-1.7 ± 0.1	$\cdots$	$156.9^{+613.4}_{-46.4}$	$51.85^{+0.27}_{-0.07}$	5
060218	0.03342 ± 0.00002	173^{+18}_{-78}	$0.5 - 150$	-1.44 ± 0.06	-2.54 ± 0.07	4.83 ± 1.19	$49.50^{+0.05}_{-0.26}$	6, 7
060319	1.15	2.4 ± 0.3	$15 - 350$	-1 ± 0.3	-2.2 ± 0.3	$53.0^{+10.4}_{-50.9}$	$51.31^{+0.34}_{-0.09}$	5, 8
060602A	0.787	35^{+4}_{-8}	$15 - 350$	-1.3 ± 0.2	$\cdots$	$536.9^{+985.5}_{-311.0}$	$51.98^{+0.16}_{-1.18}$	5, 8
061028	0.76	16^{+3}_{-6}	$15 - 350$	-1.7 ± 0.3	$\cdots$	$137.1^{+766.6}_{-65.8}$	$51.36^{+0.36}_{-0.12}$	5, 8
061110A	0.7578	20^{+2}_{-6}	$15 - 350$	-1.6 ± 0.1	$\cdots$	$186.3^{+527.4}_{-70.3}$	$51.45^{+0.30}_{-0.10}$	5

Note. — References for z: GRB 980425: Foley et al. (2006b), XRF 020903: Bersier et al. (2006), GRB 031203: Margutti et al. (2007), GRB 050223: Pellizza et al. (2006), GRB 050826: Mirabal et al. (2007c), XRF 051016B: Soderberg et al. (2005b), GRB 060202: Butler (2007), XRF 060218: Pian et al. (2006), XRF 060319: Perley et al. (2007c), GRB 060602A: Jakobsson et al. (2007b), GRB 061028: Kocevski & Butler (2008), GRB 061110A: Fynbo et al. (2009). References for energetics (Fluence, Band, E_p, Band function parameters): (1) Friedman & Bloom (2005), (2) Sakamoto et al. (2004), (3) Sazonov et al. (2004), (4) Ulanov et al. (2005), (5) Butler et al. (2007), (6) Kaneko et al. (2007), (7) Campana et al. (2006), (8) this work.